Developmental and Host Effects from the Oxylipome of *Aspergillus fumigatus*

By

Gregory John Fischer

A dissertation submitted in partial fulfillment of

the requirements for the degree of

Doctor of Philosophy

(Genetics)

at the

UNIVERSITY OF WISCONSIN-MADISON

2016

Date of final oral examination: 8/22/2016

The dissertation is approved by the following members of the Final Oral Committee:
Nancy Keller, Professor, Medical Microbiology & Immunology & Bacteriology
Audrey Gasch, Associate Professor, Genetics
Allen Laughon, Professor, Genetics
James Gern, Professor, Pediatrics & Medicine
Gregory Gauthier, Associate Professor, Medicine

THESIS ABSTRACT

Aspergillus fumigatus is an opportunistic human pathogen associated with human disease in individuals of both the hypo- and hyper-immune states. Infection within the lung begins with the inhalation of dormant spores that can either cause hyper-immune responses such as Allergic Bronchopulmonary Aspergillosis (ABPA), a severe form of asthma, or invasive growth (Invasive Aspergillosis, IA) in the hypo-immune due to insufficient host recognition, neutralization, and/or clearance of spores. The signals governing germination or invasive growth which are paramount to the development of these diseases are poorly understood.

Oxylipins are cross-kingdom signaling molecules with documented roles in mammalian immune responses, plant defense, and fungal development. Oxylipins produced by human cyclooxygenases and lipoxygenases are well-characterized and modulate many immunological responses associated with allergy and asthma. While *A. fumigatus* encodes three cyclooxygenase and two lipoxygenase homologs, their role in fungal development and modulation of host immune responses has not been thoroughly investigated. This thesis finds that disruption of an *A. fumigatus* lipoxygenase results in a significant germination defect in the presence of the polyunsaturated fatty acid, arachidonic acid (AA), likely due to the lack of of an AA-derived oxylipin signal that promotes spore germination in the presence of AA. Overexpression of this lipoxygenase (*OE::loxB)* accelerates germination, but yields a more allergenic strain as extracts from the *OE::loxB* strain cause an increase in airway hyperresponsiveness, macrophage and eosinophil recruitment, and serum IgE levels in a murine model of asthma. Investigation

of an *A. fumigatus* cyclooxygenase homolog (PpoA) reveals its cognate oxylipin products play a critical role in asexual spore development, production of immuno-modulatory metabolites, and hyphal branching. Collectively, the following chapters provide novel insight into 1.) host recognition of *A. fumigatus* spores and 2.) the pivotal role of two fungal oxygenases. Specifically germination, secondary metabolite production, and hyphal branching are examined which are lucrative drug targets for the control of human fungal disease.

ACKNOWLEDGEMENTS

It takes several years and many failed experiments to earn a PhD, and it takes several people to guide you through the experience. To Jean Abreu and Rick Koenig who showed me at a very young age how amazing the world of biology is through their passion in the classroom. To Dr. Julie Anderson, who not only taught me the fundamentals about molecular biology and genetics, but also helped me realize my true potential and was influential in my decision to pursue a doctoral degree. You are an amazing professor, life coach, and friend.

I would also like to acknowledge my Keller lab colleagues who have been wonderful co-workers and great friends. Special thanks to Dr. Philipp Wiemann and Dr. Ali Soukup for all of the scientific discussion, technique training, and extra-curricular learning. I would also like to thank my mentor, Dr. Nancy Keller, for helping me realize my passion for fungal genetics and host interactions while pushing me to become a better writer, scientist, and thinker.

Finally, I would like to thank my family. To my parents Patsy and John who have supported everything I have wanted to pursue from the very beginning. The work ethic you have taught me is the main reason I have been able to earn a PhD. To my aunt Beverly and late uncle David, for always making my support network that much stronger. It is because of all of you that I have become the individual and scientist I am today.

TABLE OF CONTENTS

CHAPTER 1: Production of cross-kingdom oxylipins by pathogenic fungi: An update on their role in development and pathogenicity

This work has been accepted for publication as:
Fischer GJ & Keller NP. (2016) Production of cross-kingdom oxylipins by pathogenic fungi: An update on their role in development and pathogenicity. *Jour. Microbiol* 54(3):254-264.

1.1 Introduction

Communication is key in all aspects of life processes. Organisms must be able to sense their surrounding environment and adapt accordingly depending on appropriate cues. It is becoming increasingly clear that plants, animals, and fungi all utilize oxygenated polyunsaturated fatty acids (oxylipins) as a common communication currency to elicit biological responses. In recent years, it has become apparent that fungi not only produce oxylipins to coordinate their developmental program, but to modify plant and mammalian host responses.

Oxylipins are produced by the incorporation of molecular oxygen into polyunsaturated fatty acids (PUFAs), and occasionally monounsaturated fatty acids, by the action of oxygenases. PUFAs vary by the length of the carbon chain and by the location/number of double bonds within the carbon chain. A list of unsaturated fatty acids and their corresponding oxylipin classes are listed in Table 1. C_{18} PUFAs such as linoleic, α-linolenic, and the monounsaturated oleic acid are classified as omega-6 fatty acids and are the predominant oxygenase substrates used in plants and fungi, specifically basidiomycetes and ascomycetes (1). A C_{20} PUFA known as arachidonic acid (AA) is utilized by mammals to produce a class of oxylipins known uniquely as the eicosanoids (Figure 1A). Most fungi only produce minor amounts of AA, however the zygomycete *Mortierella alphina* synthesizes large quantities of AA (2, 3). Those fungi that do not produce significant amounts of AA readily utilize and oxygenate AA from environmental sources (1) to generate various bioactive oxylipins implicated in disease development (4).

Oxygenases are predominantly classified into three major categories in plants, animals and fungi: cyclooxygenases, including the α-dioxygenases which share common catalytic features with cyclooxygenases (5), lipoxygenases, and monooxygenases. The cyclooxygenase and lipoxygenase classes are well-known for their role in the synthesis of the AA-derived eicosanoids (Figure 1A) that are regulators of mammalian immune responses, particularly with inflammation and allergy (6). Eicosanoids are potent and short-lived, usually being synthesized *de novo* and exerting their effects locally at nanomolar concentrations (7, 8). Monooxygenases are a broader class of specialized cytochrome P450 enzymes that are responsible for downstream processing of many oxylipins, particularly in plants (e.g. allene oxide synthases, hydroperoxide lyases, divinyl ether synthases, and peroxygenases, 9). While knowledge of oxylipin function in plants and animals has been known for several decades, the idea that host-pathogen "cross-talk" occurs and contributes to infection has only emerged in the last ten years since discovering that many microbes, including some fungi, produce prostaglandins and prostaglandin-like molecules (6). As a result, examples of inter-kingdom signaling molecules that are perceived between animals, plants, and fungi are now well documented (Table 2).

Here we present a summary of the oxylipins produced by each class of oxygenase in fungi, focusing on oxylipins that also have functions in plants and mammals. Recent examples of fungi responding to plant oxylipin defense molecules are provided as well as cases where the fungal oxylipins affect the mammalian host. Understanding what fungal species produce oxylipins and the mechanism by which they are perceived as cross-

kingdom signaling molecules will have implications on both human health and global food production as fungi are intimately linked with both topics.

1.2 Fungal oxygenases and their corresponding oxylipins.

Sequencing of fungal genomes has revealed putative homologs of canonical oxylipin-producing enzymes found in plants and mammals (10). In some cases, biochemical analyses have determined oxylipins produced by particular oxygenases, some of which are already known to regulate biological responses in plants and animals. For example, eicosanoids derived from environmental or host AA have been identified in several pathogenic species of *Candida*, *Cryptococcus neoformans, Paracoccidioides brasiliensis, Epidermophyton floccosum, Fusarium dimerim, Microsporum audiouinii, Microsporum canis, Trichophyton rubrum, Sporotrix schenkii, Absidia corymbifera, Histoplasma capsulatum, Blastomyces dermatitidis, Penicillium* spp., *Rhizopus* spp., *Rhizomucor pusillus* and numerous *Aspergillus* species (6, 11, 12).

1.2.1 Fungal Cyclooxygenases.

Prostaglandins were first identified in environmental yeasts of the Lipomycetaceae family (*Dipodascopsis*, *Lipomyces*, *Zygozyma*, and *Myxozyma*) and *Saccharomyces cerevisiae* in the early 1990s (6, 13). Since then, prostaglandins have been identified in *Cryptococcus neoformans,* several pathogenic species of *Candida, Paracoccidioides brasiliensis,* and several *Aspergillus* spp. (11, 14–16).

The psi factor-producing oxygenases (Ppo proteins), first described in the genus *Aspergillus* but found in most fungi, are a well characterized class of cyclooxygenase-like enzymes. These enzymes and their cognate oxylipins were initially investigated in the fungus *A. nidulans* with regard to their impact on asexual or sexual spore development (17–20).

Aspergillus species contain between 3-4 Ppo enzymes (19–24). Although chemical characterization has been assessed primarily with linoleic acid as a substrate, additional work suggest that Ppo proteins also oxidize oleic, linolenic, and arachidonic acids (16, 18, 25, 26) and may synthesize certain prostaglandins (16, 22).

PpoA in *A. nidulans* is well-characterized and contains two heme domains each of which catalyze specific reactions (27). The N-terminal heme peroxidase domain predominantly oxidizes linoleic acid to 8R-hydroperoxyoctadecadienoic acid (8R-HPODE) which can be reduced to 8-hydroxyoctadecadienoic acid (8R-HODE), or further isomerized by the C-terminal P450 heme thiolate domain to 5,8-dihydroxyoctadecadieonic acid (5,8-diHODE) (27–29). Studies with GFP-tagged forms of PpoA reveal that PpoA localizes to lipid bodies within the reproductive structures of *A. nidulans,* including the metulae of the asexual conidiophore and the Hülle cells and young cleistothecia of the sexual structures. Bioinformatic analysis of PpoA confirmed the presence of a proline knot motif essential for targeting proteins to lipid bodies (30). Thus, PpoA is localized within the reproductive tissues of *A. nidulans* (such as phialides, metulae, cleistothecia, and Hülle cells) with large quantities of fatty acid substrate in close proximity for conversion to oxylipins.

Other Ppo proteins are also involved in sporulation processes as determined by overexpression of, or deletion of, *ppo* genes or exogenous application of the oxylipins and their substrate produced by these (and host) enzymes affects sporulation in *Aspergillus* spp. (20, 31). Detailed work with *A. nidulans* showed deletion of either *ppoA* or *ppoB* results in increased production of asexual spores with a corresponding decrease in sexual spore production whereas loss of *ppoC* yields the opposite phenotype (19, 20, 30). In *A. flavus* where there are four *ppo* genes, disruption of both *ppoA* and *ppoC* resulted in decreased asexual sporulation whereas disruption of *ppoD* resulted in increased asexual sporulation in a density-dependent fashion (22). In *A. fumigatus* deletion of *ppoC* significantly reduced spore numbers but resulted in enlarged spore size (32). In addition to sporulation processes, Ppo proteins have an impact on diverse processes such as production of toxic secondary metabolites and degradative enzymes as will be discussed in greater detail in the fungal/plant interaction section below.

Several studies have focused on characterizing Ppo homologs (also known as linoleate diol synthases, linoleate dioxygenases, or LDSs) in fungi other than aspergilli. LDS-encoding genes have been identified in both pathogenic and non-pathogenic fungi including *Magnaporthe oryzae* (33, 34)*, Cercospora zeae-maydis* (35)*, Ustilago maydis* (36)*,* and the cereal pathogen *Fusarium verticillioides* (37)*. Fusarium verticillioides* contains an LDS termed Fv*lds1* that produces oxylipins that regulates fungal development. Oxylipin profiling of a Fv*lds1* deletion strain identified reduced levels of 11-

HPODE, 12,13-diHOME, 12-epoOME (epoxy-octadecenoic acid), 9,10-diHOME, 9-epoOME, 8,13-diHODE, 8-HPODE, and 8-HODE (37).

The dimorphic fungus *Cryptococcus neoformans* produces prostaglandin E_2 (PGE_2) that is identical to human PGE_2 even though a canonical cyclooxygenase is not present in the genome (Figure 2). Mass spectrometry of *C. neoformans* lysate with exogenous AA identified PGE_2 production which could not be inhibited by the additions of aspirin or indomethacin, known inhibitors of cyclooxygenase enzymes (38). Further studies identified that a *C. neoformans* laccase (*lac1)* was necessary to synthesize PGE_2 from exogenous AA. Recombinant Lac1 did not convert AA to PGE_2, but could convert a prostaglandin intermediate PGG_2 to PGE_2 and 15-keto-PGE_2, suggesting additional enzymes participate in *C. neoformans* prostaglandin production (39).

1.2.2 Fungal Lipoxygenases.

Reports of fungal lipoxygenase activity were published as early as the 1950s. The first partially purified lipoxygenase was reported in *Fusarium oxysporum* in 1975 through the detection of linoleic acid-derived hydroperoxides with similar R*f* values to linoleic acid hydroperoxides from a soybean lipoxygenase (40). Since, LOX activity has been documented in the fungus *Pityrosporum orbiculare* (the causative agent of the skin disorder, pityriasis versicolor) (41, 42), *Gaeumannomyces graminis* (the causative agent of take-all root rot disease) (43), *A. fumigatus* (44)*,* and *A. flavus* (21)*.*

The most recent comprehensive analysis of fungal lipoxygenases has been carried out by Heshof, *et al* (44) who phylogenetically describe the relation of fungal LOXs with respect to their ability to be secreted (signal peptide sequence), their carboxy-terminal amino acid, oxylipin stereochemistry, and metal ion cofactor. Heshof *et al* divided fungal LOXs into two groups: those that encode a C-terminal isoleucine (Ile-group) or valine (Val-group). The Ile-group LOXs all contain a conserved WRYAK motif whereas the Val-group contain a conserved WL-L/F-AK sequence found in plant and mammalian lipoxygenases. The Val-group LOXs have signal peptide sequences suggesting the proteins are expressed extracellularly. Biochemical analysis of a Val-group LOX from *A. fumigatus* identified manganese as the cofactor and the predominant oxylipin product to be 13-HPODE, derived from linoleic acid (44).

In the plant pathogen *A. flavus,* the sole lipoxygenase (Lox) along with the Ppo proteins is involved in quorum sensing (Figure 2). Disruption of either Lox or PpoC alters the density-dependent production of sclerotia and conidia: specifically, an increase in sclerotia and a decrease in conidia at high cell densities (>10^5 spores/plate) compared to increased conidia and decreased sclerotia in wild type (21, 22). Mutants where all four *ppo* genes and *lox* were down-regulated together resulted in up to a 500-fold increase in the sexual stage and 100-fold decrease in the asexual stage (22).

1.2.3 Fungal Monooxygenases.

Monooxygenases are much more prevalent in fungi than lipoxygenase or cyclooxygenase homologs. Only recently has a monooxygenase been definitively linked to oxylipin production in fungi, specifically with the production of 12-OH-jasmonic acid (12-OH-JA) in the rice blast fungus, *M. oryzae* (Figure 1B) (45). A possible connection has been inferred with the dimorphic fungus *Candida albicans.* Lipidomic studies of *C. albicans* cultures show that the fungus is capable of producing Resolvin E1, a potent anti-inflammatory oxylipin identified in mammals and derived from the modification of eicosapentaneoic acid (EPA) (46) by a cytochrome P450 monooxygenase (CYP450s) and neutrophil 5-lipoxygenase in mammals (46, 47). *Candida albicans* grown in the presence of EPA produces significant amounts of Resolvin E1 (Figure 2). Furthermore, canonical mammalian LOX inhibitors, such as esculetin (12/15-LOX) and zileuton (5-LO inhibitor) inhibit the production of *C. albicans* RvE1 by 91% and 53%, respectively yet no lipoxygenase is not present in the genome of the fungus. However, the genome encodes at least fifteen CYP450s that the authors speculate participate in one or multiple biosynthetic steps in Resolvin E1 production (48).

1.3 Oxylipin Perception.

In mammals, eicosanoid oxylipins are detected by different G-protein coupled receptors (GPCRs) which vary depending on the cell type (6, 7). Nine prostaglandin receptors have been identified in humans and mice: four of the receptors (EP_1-EP_4) bind PGE_2, two (DP_1 and DP_2) bind PGD_2, and PGF_2, PGI_2, and TxA_2 via FP, IP, and TP, respectively. Most of the prostaglandin receptors are localized at the plasma membrane, but some are also

found in the nuclear envelope (7, 49). Cysteinyl leukotrienes are also perceived via two subtypes of GPCRs, $CysLT_1$ which is expressed on smooth muscle cells and vascular endothelial cells, and $CysLT_2$ which is expressed on spleen, Purkinje fibers of the heart, and regions of the adrenal gland. $CysLT_1$ activation promotes bronchoconstriction and up-regulation of cell adhesion molecules whereas the role of $CysLT_2$ is less clear. G2A is a GPCR expressed in lymphoid tissues that induces cell cycle arrest during the G_2/M transition and on macrophages near atherosclerotic lesions. Oxylipins derived from linoleic and arachidonic acid including 9(S)-HPODE, 13(S)-HPODE, 5-HETE, 8-HETE, 8-HETE, 11-HETE, 12-HETE, 15-HETE, and 9(S)-HODE) are recognized by G2A (50).

Interestingly, two of the G2A ligands, 13(S)-HPODE and 9(S)-HPODE, affect sporulation and mycotoxin production in *Aspergillus* (31, 51), suggesting that fungal GPCR receptors might also recognize and respond to these oxylipins. To query this possibility, Affeldt *et al* (52), characterized 10 *A. nidulans* GPCR disruption mutants and found that GprD was responsible for perception of 13(S)-HPODE, 9(S)-HPODE, 13(S)-HODE, and 9(S)-HODE (52). Since then, a deletion library for GPCRs was developed in *A. flavus* and responses to PUFAs and oxylipins characterized (53). Strains where *gprA, gprB, gprF, gprG, gprM, gprO, gprP,* or *gprR* are deleted are non-responsive to exogenous methyl jasmonate – a potent plant defense oxylipin (Figure 1B and Table 2). Mutants where *gprA, gprC, gprD, gprF, gprG, gprJ, gprO,* or *gprP* are disrupted still sporulate in response to linoleic acid, but are non-responsive to the sporulation inducing oxylipin 13(S)-HPODE, suggesting that the lack of sporulation is specific to the inability to detect 13(S)-HPODE (53).

1.4 Oxylipin signaling in fungal/host interactions

1.4.1 Fungi and plants.

Jasmonic acid (JA) is a plant signaling molecule that is involved in plant responses to desiccation, ozone, UV, osmotic, cold, and light stresses and regulation of seasonal and circadian rhythms (54) (Table 2). Upon wounding, α-linolenic acid is liberated from chloroplast membranes via phospholipase A1 and is oxygenated by a 13-lipoxygenases (13-LOX), modified by a 13-allene oxide synthase (AOS) and allene oxide cyclase (AOC), and undergoes β-oxidation in peroxisomes to yield JA (Figure 1B) (54). JA is only active when conjugated to an amino acid (valine, leucine, or isoleucine (55, 56) or methylated (9). Jasmonyl-isoleucine is formed specifically upon wounding or attack by fungi, leading to the production of toxic compounds that deter further damage and initiate plant defense responses. JA may impact aflatoxin production, a mycotoxin produced by *A. flavus*, during fungal invasion of seed although the literature supports cases for JA inhibition (57), JA induction (58), and no impact of JA (51) on aflatoxin synthesis (Figure 2).

Disrupting JA biosynthesis in *Arabidopsis* and in rice increases susceptibility to *F. oxysporum* and *Magnaporthe oryzae* infection, respectively (59, 60). Specifically, the loss of allene oxide cyclase increases rice susceptibility to *M. oryzae* strains that are normally unable to cause virulence (60). A recent investigation by Patkar *et al* (45) identified a *M. oryzae* monooxygenase (referred to as antibiotic biosynthesis monooxygenase, or *abm*) that specifically modifies JA in rice. *M. oryzae* strains that lack *abm* grow like wild type with respect to appressorium formation, vegetative growth, and asexual development.

However, the strains are severely attenuated in their ability to penetrate the rice cell wall. Only 35% of appressoria penetrate the rice sheath when *abm* is disrupted, compared to 70% in the wild type. When appressoria formation is induced artificially on a glass surface, extracellular fluid from the wild type and the Δ*abm* strains reveals a striking difference in the jasmonates produced by *M. oryzae*: wild type extracellular fluid contained JA and a hydroxylated derivative 12-OH-JA (Figure 2), whereas Δ*abm* fluid only contained JA and methyl-jasmonate (MeJA). Interestingly, addition of increasing concentrations of exogenous MeJA to the wild type strain reduce the number of invading appressoria in a dose-dependent fashion. Alternately, exogenous 12-OH-JA *increases* the number of Δ*abm* invading appressoria in a dose-dependent fashion. The authors went on to identify that Abm is secreted from both the biotrophic interfacial complex (BIC) and the appressorium of *M. oryzae* during pathogenic growth, providing evidence that Abm hydroxylates not only *M. oryzae* JA, but plant-derived JA as well (45).

As mentioned earlier, *A. flavus* contains a single lipoxygenase that produces oxylipin products that influence host responses in maize and peanut. Lipidomic approaches to characterize the oxylipin profile of wild type and *lox* mutants on maize kernels show increased levels of diHODES and HPODE oxylipins in maize inoculated with the Δ*lox* strain, suggesting that *A. flavus* LOX produces compounds that suppress maize kernel oxylipin production. Furthermore, the *lox* (also called ΔAf*lox1*) disruption strain is unable to produce aflatoxin in axenic culture under inducing conditions, but produces slightly more aflatoxin when grown on maize kernels (61). The LOX product, 13-HPODE and its stable surrogate, 13-HODE have been well characterized as an important mediator of

mammalian, plant, and fungal biological responses (Table 2). Seeds produce 13-HPODE and 9-HPODE, both lipoxygenase products, when subjected to abiotic or biotic stresses such as fungal infection. Both oxylipins alter secondary metabolism in *Aspergillus parasiticus and A. nidulans* (51, 62), increase levels of asexual spores in *A. flavus* and *A. nidulans*, and increase cAMP levels in *A. nidulans* (Figure 2) (31, 52). Experiments done with *F. verticillioides* infection of maize have revealed similar results: when inoculated on maize, LOX-derived products from linoleic acid (9- and 13-HODE) and linolenic acid (9- and 13-Hydroxyoctadecatrienoic acid or HOTE) were significantly up-regulated when compared to levels found in *F. verticillioides* or maize grown independently (63).

Aspergillus infection alters plant *LOX* gene expression in corn (64) and in peanut (65, 66) through the action of *ppo* genes (Figure 2) (67). Infection of peanut seeds with *A. nidulans* strains with defects in one or more *ppo* genes decreases peanut *13-LOX* (*pnlox2 and* pnlox3) expression, specifically when inoculated with *ΔppoAC* and *ΔppoABC* strains (67). A *ppo* homolog in *Fusarium verticillioides* (Fv*lds1*) influences plant *LOX* expression as well. Virulence assays on maize cobs revealed that a Fv*lds1* deletion strain is more virulent than wild type, and does not trigger the expression of *ZmLOX3* and *ZmPR4* as vigorously in maize as wild type (37). *ZmLOX3* is a maize lipoxygenase that is induced upon interaction with mycotoxin-producing fungi (68) and *ZmPR4* is a chitinase that helps degrade the invading fungal cell wall (69). Interestingly, *ZmPR4* is known to be regulated through the action of ethylene- and jasmonic acid pathways in *Arabidopsis* (70). Maize strains where lipoxygenases are deleted (*lox3-4)* are more susceptible to *A. flavus* and

A. nidulans infection. These fungi produced more spores and increased amounts of mycotoxins when maize *lox3-4* are disrupted (71).

1.4.2 Fungi and mammals.

Higher eukaryotes rely heavily on oxylipins to respond to environmental factors and cue responses. Eicosanoids are derived from AA and include leukotrienes and prostanoids (prostaglandins, thromboxanes, and prostacyclins) (Figure 1A). Leukotrienes (LTs including LTB_4 LTC_4, LTD_4, and LTE_4) are lipoxygenase derived and play an important signaling role in inflammation and bronchial smooth muscle contraction (72, 73) (for review, see 74). Prostaglandins are cyclooxygenase-derived and have widespread roles in numerous diseases, with implications in bronchodilation, pain signaling, innate and adaptive immune responses, arthritis, atherosclerosis, and cancer (75, 76)

Paracoccidioides brasiliensis evades dendritic cell recognition by inhibiting the production of PGE2 by immature dendritic cells, as their maturation is PGE2-dependent (Figure 2) (77). A potent derivative of PGE_2, 3-hydroxy-PGE_2, is produced by the yeast *Dipodascopsis uninucleata* and the commensal dimorphic fungus, *Candida albicans* from the incomplete β-oxidation of exogenous arachidonic acid into 3-HETE (78, 79). Oxygenation of 3-HETE by purified COX-2 enzymes leads to the production of a milieu of 3-HETE-derived compounds, one of which (3-hydroxy-PGE_2, Figure 1A) induces elevated expression of IL-6 mRNA in A549 cells when compared to PGE_2.) (Figure 2). Co-incubation of *C. albicans* (which lacks a canonical COX-2 enzyme to produce 3-

hydroxy-PGE_2) with HeLa cells led to the production of 3-hydroxy-PGE_2. Thus fungal derived oxylipin products can be modified by host cells into compounds that modify host cellular responses (Figure 2) (79). Oxylipin transcellular biosynthesis is well documented in different cell types of mammals, particularly for leukotrienes (80–83).

ppoC has been extensively studied in the context of pathogenicity for *A. fumigatus.* In addition to the reduction in asexual spores upon *ppoC* deletion*,* disruption alters conidial shape, germination rate, hydrogen peroxide susceptibility, and spore neutralization by alveolar macrophages (32). Interestingly, even though Dagenais *et al* observed an increase in hydrogen peroxide resistance in the Δ*ppoC* strain, spores were *more* susceptible to killing by alveolar macrophages, which carry out their killing via the production of superoxide anion. Thus, while catalase activity may be greater than or equal to that of WT spores, the activity of superoxide dismutase is diminished when PpoC is absent.

1.5 Thesis Overview

This thesis begins with work describing a novel clearance mechanism by which the mammalian host clears spores involving fucosylated mucins and immune cells. Spore recognition and uptake mechanisms are reviewed in the introduction of Chapter 2. However, the predominant focus of this work investigates the effects of disruption and overexpression of lipoxygenase (*loxB)* and cyclooxygenase (*ppoA)* homologs on *A. fumigatus* development. The overarching hypotheses driving this work are the following:

1.) Oxylipins are intimately linked to basic fungal development as demonstrated by increases in asexual development, germination rates, mycotoxin (e.g. secondary metabolite) synthesis, and hyphal branching phenotypes.
2.) Fungal oxygenase activity can exacerbate host immune responses.

Efforts to investigate the first hypothesis resulted in two studies: the first examining germination phenotypes of *loxB* disruption and overexpression mutants (Chapter 3) and the second quantifying defects in spore production, mycotoxin production, and hyphal branching with *ppoA* disruption and overexpression mutants (Chapter 4). To investigate the second hypothesis, a murine asthma model was used to assess *loxB* mutant fungal extracts for their ability to induce allergenic responses (Chapter 3). A concluding remarks section summarizes the findings of this work and potential areas for future study.

1.6 FIGURES AND LEGENDS

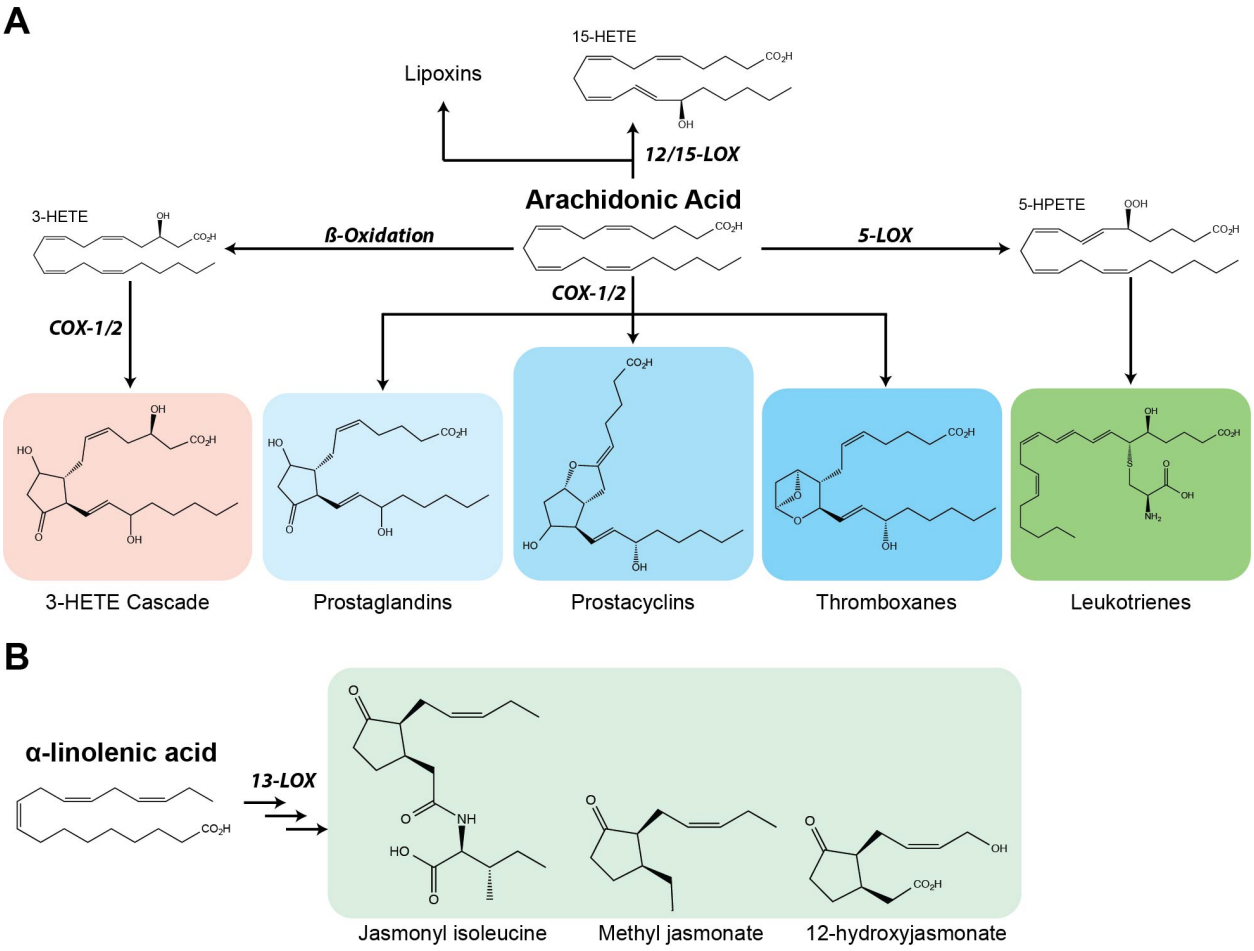

Figure 1. Partial eicosanoid and jasmonic acid pathways and oxylipin products with biological activities.

(A) Arachidonic acid (AA) can be modified by lipoxygenases (LOXs) or cyclooxygenases (COX-1/2) to yield different eicosanoids (prostanoids: blue boxes, leukotrienes: green box). A prostaglandin intermediate can be modified into thromboxanes or prostacyclins. Incomplete β-oxidation of AA by several fungi in co-culture with mammalian cells produces 3-HETE, that upon further modification by host COX enzymes yields a potent prostaglandin derivative, 3-OH-PGE2 (red box) (79). 5-LOX is the first committed step to

leukotriene production, yielding the unstable intermediate, 5-hydroperoxyeicosatetraenoic acid (5-HPETE), from AA. 12- and 15-LOXs produce other immune-modulating compounds including lipoxins, which resolve inflammation, and 15-hydroxyeicosatetraenoic acid (15-HETE), a MAP kinase and PPAR-γ pathway activator (84). **(B)** α-linoleic acid is modified by a 13-lipoxygenase enzyme yielding 13(S)-HPOTE (13(S)-hydroperoxyoctadecatrienoic acid) that after additional modification yields jasmonic acid (JA). JA is further modified into several compounds including jasmonyl isoleucine (JA-Ile), methyl jasmonate (MeJA), and 12-hydroxyjasmonate (12-OH-JA) all of which are implicated in host-pathogen interactions.

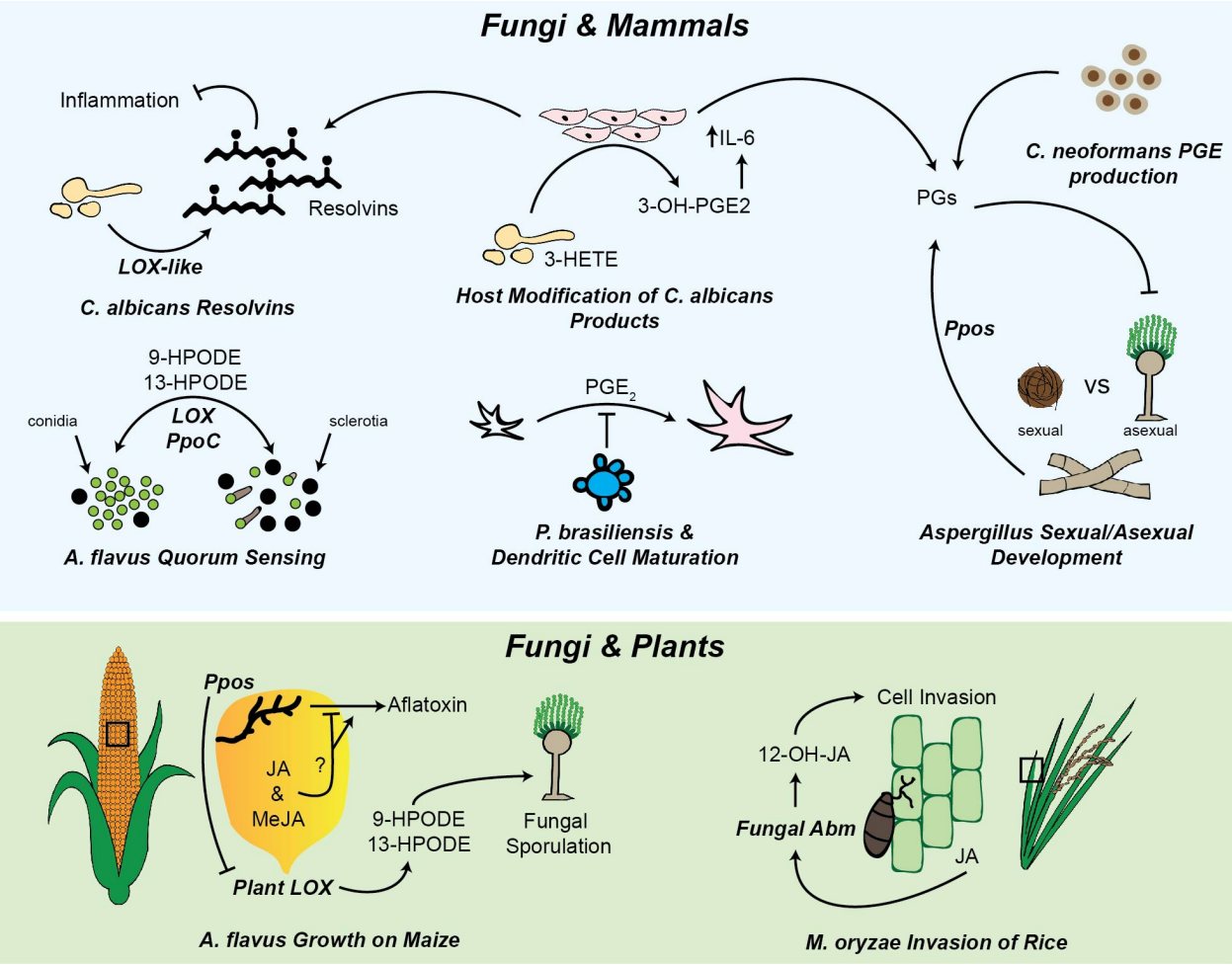

Figure 2. Cross-species oxylipin signaling between plants, animals, and fungi.

Oxylipins produced by fungi are documented in mammals and mediate important immunological responses and promote cell maturation. *Candida albicans* and *P. brasiliensis* both produce compounds that can impact host immunological responses, such as resolution of inflammation or immune cell maturation, respectively. Prostaglandins are central to many mammalian immune responses, but are also produced by many fungi and have been shown to impact sporulation. Fungal LOX activity is implicated in sporulation, but has been investigated more extensively in the plant context. Both fungal Ppos and LOXs can impact plant LOX expression through oxylipin

production, inducing fungal sporulation in the plant host. A secreted *M. oryzae* monooxygenases modifies endogenous and plant jasmonic acid (JA) into 12-OH-JA greatly, increasing the efficiency at which the fungus infiltrates the plant cell.

1.7 TABLES

Table 1. Polyunsaturated fatty acids and their cognate oxylipins.

Fatty Acid	Lipid Name	Structure	Oxylipins
α-linolenic acid	18:3 (n-3)	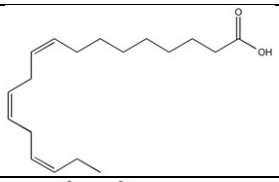	Hydroperoxyoctadecatrienoic acid (HPOTEs), Hydroxyoctadecatrienoic acid (HOTEs), di-hydroxyoctadecatrienoic acid (diHOTES).
Eicosapentaenoic acid	20:5 (n-3)	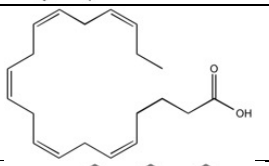	Resolvin E1
Linoleic acid	18:2 (n-6)	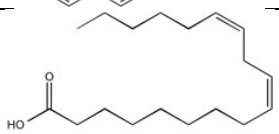	Hydroperoxyoctadecadienoic acid (HPODES), Hydroxyoctadecadienoic acid (HODES), di-hydroxyoctadecadienoic acid (diHODES)
δ-linolenic acid	18:3 (n-6)	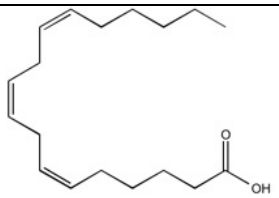	Hydroperoxyoctadecatrienoic acid (HPOTEs), Hydroxyoctadecatrienoic acid (HOTEs), di-hydroxyoctadecatrienoic acid (diHOTES).
Arachidonic acid	20:4 (n-6)	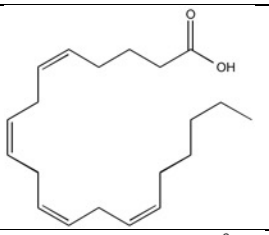	Hydroperoxyeicosatetraenoic acid (HPETE), Hydroxyeicosatetraenoic acid (HETEs), di-hydroxyeicosatetraenoic acid (diHETEs), Leukotrienes (LTs), Prostaglandins (PGs), Lipoxins, Thromboxanes
Oleic acid	18:1 (n-9)	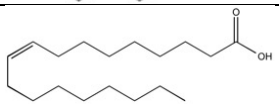	Hydroperoxyoctanoic acid (HPOMES), Hydroxyoctanoic acid (HOMEs), di-hydroxyoctanoic acid (diHOMEs)

Table 2. Oxylipins with cross-kingdom roles in mammals, plants, and fungi.

Oxylipin	Full Name	PUFA	Enzyme	Mammals	Plants	Fungi
9-HODE (9-HPODE)	9S-Hydroxyoctadecadienoic acid	Linoleic Acid	LOX	Induce Ca^{2+} mobilization via G2A GPCR receptor (50).	Induce programmed cell death in tomato protoplasts (85).	Altered *A. nidulans* sporulation (31). Promote cAMP production via fungal GPCR signaling (52).
13-HODE (13-HPODE)	13S-Hydroxyoctadecadienoic acid	Linoleic Acid	LOX	Airway hyperresponsiveness (86, 87) and disruption of Ca^{2+} homeostasis in airway epithelial cells and bronchial cell injury (Ng, Huang, Reddy, Falck, Lin, & Kroetz, 2007; Spears, *et al.*, 2009).	Produced as product of lipid body mobilization during cucumber germination (90). Proposed to be "labeled form" of lipid stores for β-oxidation during germination (91, 92).	Suppress mycotoxin production (51) and promote asexual spore production (31). Promote cAMP production via fungal GPCR signaling (52).
5-HETE (5-HPETE)	5-Hydroxyeicosatetraenoic acid	Arachidonic Acid	LOX	Precursor to leukotriene biosynthesis. Potent survival factor that inhibits apoptosis of human prostate cancer cells (93).	Induce programmed cell death in tomato protoplasts (85).	--
15-HETE (15-HPETE)	15-Hydroxyeicosatetraenoic acid	Arachidonic Acid	LOX	Precursor to lipoxin biosynthesis. Induces constriction of pulmonary arteries in response to hypoxia (94). Modulate vascular smooth muscle and endothelial cell function (95) and cell proliferation (96).	Induce programmed cell death in tomato protoplasts (85).	--
JA	Jasmonic Acid	α-Linolenic Acid	LOX/Allene Oxide Synthase	Suppresses proliferation and induces apoptosis in human lymphoblastic leukemia cells (97).	Global plant stress, defense, and developmental processes (54).	JA and numerous analogs produced by *F. oxysporum* (98) and *A. niger* (99).
MeJA	Methyl Jasmonate	α-Linolenic Acid	LOX/Allene Oxide Synthase/Others	Membrane depolarization and cytochrome C release of human leukemic cancer lines (100). Suppress proliferation and induces apoptosis in human lymphoblastic leukemia cells (97).	Global plant stress, defense, and developmental processes (45, 54).	Secondary metabolite induction (101).
12-OH-JA	12-hydroxy-jasmonic acid	α-Linolenic Acid	Monooxygenase	--	Promotes flower and tuber development, suppresses plant defense responses (45).	Produced during host penetration and suppresses methyl jasmonate formation (45).

8-HODE	8-hydroxyoctadecadienoic acid	Linoleic Acid	COX-like	--	--	*Aspergillus* fungal sporulation factor (18, 102). Secreted by *Laetisaria arualis* and is antifungal to plant pathogenic strains of *Pythium ultimum* (103).
5,8-diHODE	5,8-dihydroxyoxctadecadienoic acid	Linoleic Acid/ 8-HODE	COX-like	--	--	Inducer of sexual development in *A. nidulans* and regulates ratio of asexual to sexual spores (Champe & El-Zayat, 1989; Horowitz Brown, Zarnowski, Sharpee, & Keller, 2008; Mazur, Meyers, Nakanishi, Elzayat, & Champe, 1990; Mazur, Nakanishi, Elzayat, & Champe, 1991; Tsitsigiannis & Keller, 2007).
PGs	Prostaglandins (PGD_2, PGE_2, $PGF_{2,}$)	Arachidonic Acid	COX/COX-like	Central role in initiation of inflammatory responses. For review, see (105). PGE_2 enhances Th17 host defenses of mucosa (106).	--	Produced by COX-like enzymes Ppos in *A. fumigatus* (Tsitsigiannis, Bok, Andes, Nielsen, Frisvad, & Keller, 2005) and produced by *C. neoformans* and *C. albicans* (12). Production of PGE_2 by *C. neoformans* suppresses IL-17-dependent antimicrobial responses (106).
LTs	Leukotrienes (LTB_4, LTC_4, LTD_4, LTE_4)	Arachidonic Acid	LOX	Induce bronchial smooth muscle contraction (107), promote mucus secretion in airway (72), and promote recruitment of leukocytes (73). For review, see (74).	--	Produced by pathogenic fungi (11). No documented response on fungi.
3-HETE	3-Hydroxyeicosatetraenoic acid	Arachidonic Acid	Unclear/ Monooxygenase	Affects signal transduction in human neutrophils and tumor cells (108, 109).	--	Regulatory role of sexual cycle in *D. uninucleata*(110). Associated with proper aggregation of ascospores in *D. uninucleata* (111).

1.8 REFERENCES

1. **Stahl PD**, **Klug MJ**. 1996. Characterization and differentiation of filamentous fungi based on fatty acid composition. Appl Env Microbiol **62**:4136–46.

2. **Li X**, **Lin Y**, **Chang M**, **Jin Q**, **Wang X**. 2015. Efficient production of arachidonic acid by *Mortierella alpina* through integrating fed-batch culture with a two-stage pH control strategy. Bioresour Technol **181**:275–282.

3. **Samadlouie HR**, **Hamidi-Esfahani Z**, **Alavi SM**, **Varastegani B**. 2014. Expression analysis for genes involved in arachidonic acid biosynthesis in *Mortierella alpina* CBS 754.68. Braz J Microbiol **45**:439–445.

4. **Ells R**, **Kemp G**, **Albertyn J**, **Kock JLF**, **Pohl CH**. 2013. Phenothiazine is a potent inhibitor of prostaglandin E2 production by *Candida albicans* biofilms. FEMS Yeast Res **13**:849–55.

5. **Goulah CC**, **Zhu G**, **Koszelak-Rosenblum M**, **Malkowski MG**. 2013. The crystal structure of α-dioxygenase provides insight into diversity in the cyclooxygenase-peroxidase superfamily. Biochemistry **52**:1364–72.

6. **Noverr M**, **Erb-Downward JR**, **Huffnagle GB**. 2003. Production of eicosanoids and other oxylipins by pathogenic eukaryotic microbes. Society **16**:517–533.

7. **Funk CD**. 2001. Prostaglandins and leukotrienes: advances in eicosanoid biology. Science **294**:1871–1875.

8. **Marks F**. 1999. Arachidonic acid and companions: an abundant source of biological signals, p. 1–46. *In* Marks, F, Fürstenberger, G (eds.), Prostaglandins, Leukotrienes, and Other Eicosanoids: From Biogenesis to Clinical Application. Wiley-VCH.

9. **Griffiths G**. 2015. Biosynthesis and analysis of plant oxylipins. Free Radic Res **49**:565–582.

10. **Brodhun F**, **Feussner I**. 2011. Oxylipins in fungi. FEBS J **278**:1047–1063.

11. **Noverr M**, **Toews GB**, **Huffnagle GB**. 2002. Production of prostaglandins and leukotrienes by pathogenic fungi. Infect Immun **70**:400–402.

12. **Noverr M**, **Phare SM**, **Toews GB**, **Coffey MJ**, **Huffnagle GB**. 2001. Pathogenic yeasts *Cryptococcus neoformans* and *Candida albicans* produce immunomodulatory prostaglandins. Infect Immun **69**:2957–2963.

13. **Kock J**, **Coetzee M**, **van Dyk M**, **Truscott P**, **Cloete V**, **van Wyk V**, **Augustyn O**. 1991. Evidence for pharmacologically active prostaglandins in yeasts. S Afr J Sci **80**:73–76.

14. **Biondo GA**, **Dias-Melicio LA**, **Bordon-Graciani AP**, **Acorci-Valério MJ**, **Soares AMVC**. 2010. *Paracoccidioides brasiliensis* uses endogenous and exogenous arachidonic acid for PGEx production. Mycopathologia **170**:123–130.

15. **Bordon AP**, **Dias-Melicio LA**, **Acorci MJ**, **Biondo GA**, **Fecchio D**, **Peraçoli MTS**, **de Soares AMVC**. 2007. Prostaglandin E(2) production by high and low virulent strains of *Paracoccidioides brasiliensis*. Mycopathologia **163**:129–35.

16. **Tsitsigiannis D**, **Bok J**, **Andes D**, **Nielsen K**, **Frisvad J**, **Keller N**. 2005. *Aspergillus* cyclooxygenase-like enzymes are associated with prostaglandin production and virulence. Infect Immun **73**:4548–4559.

17. **Champe SP**, **Rao P**, **Chang A**. 1987. An endogenous inducer of sexual development in *Aspergillus nidulans*. J Gen Microbiol **133**:1383–1387.

18. **Champe SP**, **El-Zayat AA**. 1989. Isolation of a sexual sporulation hormone from *Aspergillus nidulans*. J Bacteriol **171**:3982–3988.

19. **Tsitsigiannis DI**, **Kowieski TM**, **Zarnowski R**, **Keller NP**. 2004. Endogenous lipogenic regulators of spore balance in *Aspergillus nidulans*. Eukaryot Cell **3**:1398–1411.

20. **Tsitsigiannis D**, **Kowieski T**, **Zarnowski R**, **Keller N**. 2005. Three putative oxylipin biosynthetic genes integrate sexual and asexual development in *Aspergillus nidulans*. Microbiology **151**:1809–1821.

21. **Horowitz Brown S**, **Zarnowski R**, **Sharpee WC**, **Keller NP**. 2008. Morphological transitions governed by density dependence and lipoxygenase activity in *Aspergillus flavus*. Appl Env Microbiol **74**:5674–85.

22. **Brown SH**, **Scott JB**, **Bhaheetharan J**, **Sharpee WC**, **Milde L**, **Wilson RA**, **Keller NP**. 2009. Oxygenase coordination is required for morphological transition and the host-fungus interaction of *Aspergillus flavus*. Mol Plant Microbe Interact **22**:882–894.

23. **Wadman M**, **de Vries R**, **Kalkhove S**, **Veldink G**, **Vliegenthart J**. 2009. Characterization of oxylipins and dioxygenase genes in the asexual fungus *Aspergillus niger*. BMC Microbiol **9**:59.

24. **Jernerén F**, **Garscha U**, **Hoffmann I**, **Hamberg M**, **Oliw E**. 2010. Reaction mechanism of 5,8-linoleate diol synthase, 10R-dioxygenase, and 8,11-hydroperoxide isomerase of *Aspergillus clavatus*. Biochim Biophys Acta **1801**:503–507.

25. **Calvo A**, **Gardner H**, **Keller N**. 2001. Genetic connection between fatty acid metabolism and sporulation in *Aspergillus nidulans*. J Biol Chem **276**:25766–25774.

26. **Mazur P**, **Nakanishi K**, **Elzayat AAE**, **Champe SP**. 1991. Structure and synthesis of sporogenic psi factors from *Aspergillus nidulans*. Chem Soc Chem Commun 1486–1487.

27. **Brodhun F**, **Gobel C**, **Hornung E**, **Feussner I**. 2009. Identification of PpoA from *Aspergillus nidulans* as a fusion protein of a fatty acid heme dioxygenase/peroxidase and a cytochrome P450. J Biol Chem **284**:11792–11805.

28. **Garscha U**, **Jerneren F**, **Chung D**, **Keller NP**, **Hamberg M**, **Oliw EH**. 2007. Identification of dioxygenases required for *Aspergillus* development. Studies of products,

stereochemistry, and the reaction mechanism. J Biol Chem **282**:34707–34718.

29. **Fielding AJ**, **Brodhun F**, **Koch C**, **Pievo R**, **Denysenkov V**, **Feussner I**, **Bennati M**. 2011. Multifrequency electron paramagnetic resonance characterization of PpoA, a CYP450 fusion protein that catalyzes fatty acid dioxygenation. J Am Chem Soc **133**:9052–9062.

30. **Tsitsigiannis DI**, **Zarnowski R**, **Keller NP**. 2004. The lipid body protein, PpoA, coordinates sexual and asexual sporulation in *Aspergillus nidulans*. J Biol Chem **279**:11344–11353.

31. **Calvo A**, **Hinze L**, **Gardner H**, **Keller N**. 1999. Sporogenic effect of polyunsaturated fatty acids on development of *Aspergillus* spp . Appl Env Microbiol **65**:3668–3673.

32. **Dagenais TR**, **Chung D**, **Giles SS**, **Hull CM**, **Andes D**, **Keller NP**. 2008. Defects in conidiophore development and conidium-macrophage interactions in a dioxygenase mutant of *Aspergillus fumigatus*. Infect Immun **76**:3214–3220.

33. **Jerneren F**, **Sesma A**, **Francheschetti M**, **Hamberg M**, **Oliw EH**. 2010. Gene deletion of 7,8-linoleate diol synthase of the rice blast fungus: studies on pathogenicity, stereochemistry, and oxygenation mechanisms. J Biol Chem **285**:5308–5316.

34. **Cristea M**, **Osbourn AE**, **Oliw EH**. 2003. Linoleate diol synthase of the rice blast fungus *Magnaporthe grisea*. Lipids **38**:1275–80.

35. **Shim WB**, **Dunkle LD**. 2002. Identification of genes expressed during cercosporin biosynthesis in *Cercospora zeae-maydis*. Physiol Mol Plant Pathol **61**:237–248.

36. **Huber S**, **Lottspeich F**, **Kämper J**. 2002. A gene that encodes a product with similarity to dioxygenases is highly expressed in teliospores of *Ustilago maydis*. Mole Genet Genomics **267**:757–71.

37. **Scala V**, **Giorni P**, **Cirlini M**, **Ludovici M**, **Visentin I**, **Cardinale F**, **Fabbri AA**, **Fanelli C**, **Reverberi M**, **Battilani P**, **Galaverna G**, **Dall'Asta C**. 2014. LDS1-produced oxylipins are negative regulators of growth, conidiation and fumonisin synthesis in the fungal maize pathogen *Fusarium verticillioides*. Front Microbiol **5**:1–14.

38. **Erb-Downward JR**, **Huffnagle GB**. 2007. *Cryptococcus neoformans* produces authentic prostaglandin E2 without a cyclooxygenase. Eukaryot cell **6**:346–50.

39. **Erb-Downward JR**, **Noggle RM**, **Williamson PR**, **Huffnagle GB**. 2008. The role of laccase in prostaglandin production by *Cryptococcus neoformans*. Mol Microbiol **68**:1428–37.

40. **Satoh T**, **Matsuda Y**, **Takashio M**, **Satoh K**, **Arima K**. 1975. Isolation of lipoxygenase-like enzyme from *Fusarium oxysporum*. Agr Biol Chem **40**:953–961.

41. **Nazzaro-Porro M**, **Passi S**, **Picardo M**, **Mercantini R**, **Breathnach AS**. 1986. Lipoxygenase activity of *Pityrosporum in vitro* and *in vivo*. Invest Dermatol **87**:108–112.

42. **De Luca C**, **Picardo M**, **Breathnach A**, **Passi S**. 1996. Lipoperoxidase activity of *Pityrosporum*: Characterization of by-products and possible role in pityriasis versicolor. Exp Dermatol **5**:49–56.

43. **Su C**, **Oliw EH**. 1996. Purification and characterization of linoleate 8-dioxygenase from the fungus *Gaeumannomyces graminis* as a novel hemoprotein. J Biol Chem **271**:14112–14116.

44. **Heshof R**, **Jylha S**, **Haarmann T**, **Jorgensen AL**, **Dalsgaard TK**, **de Graaff LH**, **Jylhä S**, **Haarmann T**, **Jørgensen ALW**, **Dalsgaard TK**, **de Graaff LH**. 2014. A novel class of fungal lipoxygenases. Appl Microbiol Biotechnol **98**:1261–1270.

45. **Patkar R**, **Benke P**, **Qu Z**, **Chen Y**, **Yang F**, **Swarup S**, **Naqvi N**. 2015. A fungal monooxygenase-derived jasmonate attenuates host innate immunity. Nat Chem Biol **11**:733–740.

46. **Arita M**, **Bianchini F**, **Aliberti J**, **Sher A**, **Chiang N**, **Hong S**, **Yang R**, **Petasis NA**, **Serhan CN**. 2005. Stereochemical assignment, antiinflammatory properties, and receptor for the omega-3 lipid mediator resolvin E1. J Exp Med **201**:713–22.

47. **Tjonahen E**, **Oh SF**, **Siegelman J**, **Elangovan S**, **Percarpio KB**, **Hong S**, **Arita M**, **Serhan CN**. 2006. Resolvin E2 identification and anti-inflammatory actions: pivotal role of human 5-lipoxygenase in resolvin E series biosynthesis. Chem Biol **13**:1193–1202.

48. **Haas-Stapleton EJ**, **Lu Y**, **Hong S**, **Arita M**, **Favoreto S**, **Nigam S**, **Serhan CN**, **Agabian N**. 2007. *Candida albicans* modulates host defense by biosynthesizing the pro-resolving mediator resolvin E1. PLoS One **2**:e1316.

49. **Bhattacharya M**, **Peri KG**, **Almazan G**, **Ribeiro-da-Silva A**, **Shichi H**, **Durocher Y**, **Abramovitz M**, **Hou X**, **Varma DR**, **Chemtob S**. 1998. Nuclear localization of prostaglandin E2 receptors. Proc Natl Acad Sci U S A **95**:15792–15797.

50. **Obinata H**, **Hattori T**, **Nakane S**, **Tatei K**, **Izumi T**. 2005. Identification of 9-hydroxyoctadecadienoic acid and other oxidized free fatty acids as ligands of the G protein-coupled receptor G2A. J Biol Chem **280**:40676–40683.

51. **Burow G**, **Nesbitt T**. 1997. Seed lipoxygenase products modulate *Aspergillus* mycotoxin biosynthesis. Mol Plant Microbe Interact **10**:380–387.

52. **Affeldt K**, **Brodhagen M**, **Keller NP**. 2012. *Aspergillus* oxylipin signaling and quorum sensing pathways depend on G protein-coupled receptors. Toxins **4**:695–717.

53. **Affeldt K**, **Carrig J**, **Amare M**, **Keller NP**. 2014. Global survey of canonical *Aspergillus flavus* G protein-coupled receptors. MBio **5**:1501–14.

54. **Wasternack C**. 2014. Action of jasmonates in plant stress responses and development - Applied aspects. Biotechnol Adv **32**:31–39.

55. **Wang L**, **Halitschke R**, **Kang JH**, **Berg A**, **Harnisch F**, **Baldwin IT**. 2007. Independently silencing two JAR family members impairs levels of trypsin proteinase inhibitors but not nicotine. Planta **226**:159–167.

56. **Kang J**, **Wang L**, **Giri A**, **Baldwin IT**. 2006. Silencing threonine deaminase and JAR4 in *Nicotiana attenuata* impairs jasmonic acid-isoleucine-mediated defenses against *Manduca sexta*. Plant Cell **18**:3303–3320.

57. **Goodrich-Tanrikulu M**, **Mahoney NE**, **Rodriguez SB**. 1995. The plant growth regulator methyl jasmonate inhibits aflatoxin production by *Aspergillus flavus*. Microbiology **141**:2831–2837.

58. **Vergopoulou S**, **Galanopoulou D**, **Markaki P**. 2001. Methyl jasmonate stimulates aflatoxin B-1 biosynthesis by *Aspergillus parasiticus*. J Agric Food Chem **49**:3494–3498.

59. **Thatcher LF**, **Manners JM**, **Kazan K**. 2009. *Fusarium oxysporum* hijacks COI1-mediated jasmonate signaling to promote disease development in *Arabidopsis*. Plant J **58**:927–939.

60. **Riemann M**, **Haga K**, **Shimizu T**, **Okada K**, **Ando S**, **Mochizuki S**, **Nishizawa Y**, **Yamanouchi U**, **Nick P**, **Yano M**, **Minami E**, **Takano M**, **Yamane H**, **Iino M**. 2013. Identification of rice allene oxide cyclase mutants and the function of jasmonate for defence against *Magnaporthe oryzae*. Plant J **74**:226–238.

61. **Scarpari M**, **Punelli M**, **Scala V**, **Zaccaria M**, **Nobili C**, **Ludovici M**, **Camera E**, **Fabbri AA**, **Reverberi M**, **Fanelli C**. 2014. Lipids in *Aspergillus flavus*-maize interaction. Front Microbiol **5**:1–9.

62. **Gardner HW**. 1995. Biological roles and biochemistry of the lipoxygenase pathway. HortScience **30**:197–205.

63. **Ludovici M**, **Ialongo C**, **Reverberi M**, **Beccaccioli M**, **Scarpari M**, **Scala V**. 2014. Quantitative profiling of oxylipins through comprehensive LC-MS/MS analysis of *Fusarium verticillioides* and maize kernels. Food Addit Contam Part A Chem Anal Control Expo Risk Assess **31**:2026–2033.

64. **Wilson R a**, **Gardner HW**, **Keller NP**. 2001. Cultivar-dependent expression of a maize lipoxygenase responsive to seed infesting fungi. Mol Plant Microbe Interact **14**:980–987.

65. **Burow G**, **Gardner H**, **Keller N**. 2000. A peanut seed lipoxygenase responsive to *Aspergillus* colonization. Plant Mol Biol **42**:689–701.

66. **Tsitsigiannis DI**, **Kunze S**, **Willis DK**, **Feussner L**, **Keller NP**. 2005. *Aspergillus* infection inhibits the expression of peanut 13S-HPODE-forming seed lipoxygenases. Mol Plant Microbe Interact **18**:1081–1089.

67. **Brodhagen M**, **Tsitsigiannis DI**, **Hornung E**, **Goebel C**, **Feussner I**, **Keller NP**. 2008. Reciprocal oxylipin-mediated cross-talk in the *Aspergillus*-seed pathosystem. Mol Microbiol **67**:378–391.

68. **Gao X**, **Kolomiets M V.** 2009. Host-derived lipids and oxylipins are crucial signals in modulating mycotoxin production by fungi. Toxin Rev **28**:79–88.

69. **Wang N**, **Xiao B**, **Xiong L**. 2011. Identification of a cluster of PR4-like genes involved in stress responses in rice. J Plant Physiol **168**:2212–2224.

70. **van Loon LC**, **Rep M**, **Pieterse CMJ**. 2006. Significance of inducible defense-related proteins in infected plants. Annu Rev Phytopathol **44**:135–162.

71. **Gao X**, **Brodhagen M**, **Isakeit T**, **Brown SH**, **Göbel C**, **Betran J**, **Feussner I**, **Keller NP**, **Kolomiets M V**. 2009. Inactivation of the lipoxygenase ZmLOX3 increases susceptibility of maize to *Aspergillus* spp. Mol Plant Microbe Interact **22**:222–231.

72. **Henderson WR**. 1994. The role of leukotrienes in inflammation. Ann Intern Med **121**:684–697.

73. **Ford-Hutchinson AW**. 1985. Leukotrienes: their formation and role as inflammatory mediators. Fed Proc **44**:25–29.

74. **Singh RK**, **Tandon R**, **Dastidar SG**, **Ray A**. 2013. A review on leukotrienes and their receptors with reference to asthma. J Asthma **50**:922–931.

75. **Simmons DL**, **Botting RM**, **Hla T**. 2004. Cyclooxygenase isozymes: the biology of prostaglandin synthesis and inhibition. Pharmacol Rev **56**:387–437.

76. **Park J**, **Pillinger M**, **Abramson S**. 2006. Prostaglandin E2 synthesis and secretion: The role of PGE2 synthases. Clin Immunol **119**:229–240.

77. **Fernandes RK**, **Bachiega TF**, **Rodrigues DR**, **Golim MD a**, **Dias-Melicio L a**, **Balderramas HD a**, **Kaneno R**, **Soares ÂMVC**. 2015. *Paracoccidioides brasiliensis*

interferes on dendritic cells maturation by inhibiting PGE2 production. PLoS One **10**:e0120948.

78. **van Dyk M**, **Kock J**, **Coetzee D**, **Augustyn O**, **Nigam S**. 1991. Isolation of a novel arachidonic acid metabolite 3-hydroxy-5,8,11,14-eicosatetraenoic acid (3-HETE) from the yeast *Dipodascopsis uninucleata* UOFs-Y128. FEBS Lett **283**:195—198.

79. **Ciccoli R**, **Sahi S**, **Singh S**, **Prakash H**, **Zafiriou M-P**, **Ishdorj G**, **Kock JLF**, **Nigam S**. 2005. Oxygenation by COX-2 (cyclo-oxygenase-2) of 3-HETE (3-hydroxyeicosatetraenoic acid), a fungal mimetic of arachidonic acid, produces a cascade of novel bioactive 3-hydroxyeicosanoids. Biochem J **390**:737–747.

80. **Fabre JE**, **Goulet JL**, **Riche E**, **Nguyen MT**, **Coggins K**, **Offenbacher S**, **Koller BH**. 2002. Transcellular biosynthesis contributes to the production of leukotrienes during inflammatory responses *in vivo*. J Clin Invest **109**:1373–1380.

81. **Folco G**, **Murphy RC**. 2006. Eicosanoid transcellular biosynthesis: from cell-cell interactions to *in vivo* tissue responses. Pharmacol Rev **58**:375–388.

82. **Gijon MA**, **Zarini S**, **Murphy RC**. 2007. Biosynthesis of eicosanoids and transcellular metabolism of leukotrienes in murine bone marrow cells. J Lipid Res **48**:716–725.

83. **Zarini S**, **Gijon MA**, **Ransome AE**, **Murphy RC**, **Sala A**. 2009. Transcellular biosynthesis of cysteinyl leukotrienes *in vivo* during mouse peritoneal inflammation. Proc Natl Acad Sci U S A **106**:8296–8301.

84. **Yang J**, **Schmelzer K**, **Georgi K**, **Hammock BD**. 2009. Quantitative profiling method for oxylipin metabolome by liquid chromatography electrospray ionization tandem mass spectrometry. Anal Chem **81**:8085–8093.

85. **Knight VI**, **Wang H**, **Lincoln JE**, **Lulai EC**, **Gilchrist DG**, **Bostock RM**. 2001. Hydroperoxides of fatty acids induce programmed cell death in tomato protoplasts. Physiol Mol Plant Pathol **59**:277–286.

86. **Cooper PR**, **Mesaros AC**, **Zhang J**, **Christmas P**, **Stark CM**, **Douaidy K**, **Mittelman MA**, **Soberman RJ**, **Blair IA**, **Panettieri RA**. 2010. 20-HETE mediates ozone-induced, neutrophil-independent airway hyper-responsiveness in mice. PLoS One **5**:e10235.

87. **Henricks P**, **Engels F**, **Vanderlinde H**, **Garssen J**, **Nijkamp F**. 1995. 13-hydroxy-linoleic acid induces airway hyperresponsiveness to histamine and methacholine in guinea pigs *in vivo*. J Allergy Clin Immunol **96**:36–43.

88. **Ng VY**, **Huang Y**, **Reddy LM**, **Falck JR**, **Lin ET**, **Kroetz DL**. 2007. Cytochrome P450 eicosanoids are activators of peroxisome proliferator-activated receptor alpha. Drug Metab Dispos **35**:1126–1134.

89. **Spears M**, **Donnelly I**, **Jolly L**, **Brannigan M**, **Ito K**, **McSharry C**, **Lafferty J**, **Chaudhuri R**, **Braganza G**, **Bareille P**, **Sweeney L**, **Adcock IM**, **Barnes PJ**, **Wood S**, **Thomson NC**. 2009. Bronchodilatory effect of the PPAR-γ agonist rosiglitazone in smokers with asthma. Clin Pharmacol Ther **86**:49–53.

90. **Feussner I**, **Wasternack C**, **Kindl H**, **Kühn H**. 1995. Lipoxygenase-catalyzed oxygenation of storage lipids is implicated in lipid mobilization during germination. Proc Natl Acad Sci U S A **92**:11849–11853.

91. **Feussner I**, **Kühn H**, **Wasternack C**. 1997. Do specific linoleate 13-lipoxygenases initiate β-oxidation? FEBS Lett **406**:1–5.

92. **Feussner I**, **Kühn H**, **Wasternack C**. 2001. Lipoxygenase-dependent degradation of storage lipids. Trends Plant Sci **6**:268–273.

93. **Ghosh J**, **Myers CE**. 1998. Inhibition of arachidonate 5-lipoxygenase triggers massive apoptosis in human prostate cancer cells. Proc Natl Acad Sci U S A **95**:13182–13187.

94. **Zhu D**. 2003. Chronic hypoxia activates lung 15-lipoxygenase, which catalyzes production of 15-HETE and enhances constriction in neonatal rabbit pulmonary arteries. Circ Res **92**:992–1000.

95. **Campbell WB**, **Gauthier KM**. 2013. Inducible endothelium-derived hyperpolarizing factor: role of the 15-lipoxygenase-EDHF pathway. J Cardiovasc Pharmacol **61**:176–87.

96. **Schneider C**, **Pozzi A**. 2011. Cyclooxygenases and lipoxygenases in cancer. Cancer Metastasis Rev **30**:277–294.

97. **Fingrut O**, **Flescher E**. 2002. Plant stress hormones suppress the proliferation and induce apoptosis in human cancer cells. Leukemia **16**:608–616.

98. **Miersch O**, **Bohlmann H**, **Wasternack C**. 1999. Jasmonates and related compounds from *Fusarium oxysporum*. Phytochemistry **50**:517–523.

99. **Miersch O**, **Porzel A**, **Wasternack C**. 1999. Microbial conversion of jasmonates-hydroxylations by *Aspergillus niger*. Phytochemistry **50**:1147–1152.

100. **Rotem R**, **Heyfets A**, **Fingrut O**, **Blickstein D**, **Shaklai M**, **Flescher E**. 2005. Jasmonates: Novel anticancer agents acting directly and selectively on human cancer cell mitochondria. Cancer Res **65**:1984–1993.

101. **Ren A**, **Qin L**, **Shi L**, **Dong X**, **Mu DS**, **Li YX**, **Zhao MW**. 2010. Methyl jasmonate induces ganoderic acid biosynthesis in the basidiomycetous fungus *Ganoderma lucidum*. Bioresour Technol **101**:6785–6790.

102. **Mazur P**, **Meyers H**, **Nakanishi K**, **Elzayat A**, **Champe S**. 1990. Structural elucidation of sporogenic fatty-acid metabolies from *Aspergillus nidulans*. Tetrahedron Lett **31**:3837–3840.

103. **Bowers WS**, **Hoch HC**, **Evans PH**, **Katayama M**. 1986. Thallophytic allelopathy: isolation and identification of laetisaric acid. Science **232**:105–106.

104. **Tsitsigiannis DI**, **Keller NP**. 2007. Oxylipins as developmental and host-fungal communication signals. Trends Microbiol **15**:109–118.

105. **Ricciotti E**, **Fitzgerald GA**. 2011. Prostaglandins and inflammation. Arter Thromb Vasc Biol **31**:986–1000.

106. **Valdez PA**, **Vithayathil PJ**, **Janelsins BM**, **Shaffer AL**, **Williamson PR**, **Datta SK**. 2012. Prostaglandin E2 suppresses antifungal immunity by inhibiting interferon regulatory factor 4 function and interleukin-17 expression in T cells. Immunity **36**:668–679.

107. **Barnes NC**, **Piper PJ**, **Costello JF**. 1984. Comparative effects of inhaled leukotriene C4, leukotriene D4, and histamine in normal human subjects. Thorax **39**:500–4.

108. **Nigam S**, **Schewe T**, **Kock JL**. 1999. (3R)-hydroxy-oxylipins--a novel family of oxygenated polyenoic fatty acids of fungal origin. Adv Exp Med Biol **469**:663–668.

109. **Kock J**, **Strauss C**, **Pohl C**, **Nigam S**. 2003. The distribution of 3-hydroxy oxylipins in fungi. Prostaglandins Other Lipid Mediat **71**:85–96.

110. **Kock J**, **Venter P**, **Linke D**, **Schewe T**, **Nigam S**. 1998. Biological dynamics and distribution of 3-hydroxy fatty acids in the yeast *Dipodascopsis uninucleata* as investigated by immunofluorescence microscopy. Evidence for a putative regulatory role in the sexual reproductive cycle. FEBS Lett **427**:345–8.

111. **Kock J**, **van Wyk P**, **Venter P**, **Coetzee D**, **Smith D**, **Viljoen B**. 1999. An acetylsalicylic acid-sensitive aggregation phenomenon in *Dipodascopsis uninucleata*. Antonie Van Leeuwenhoek **75**:261–266.

112. **Kühn H**, **O'Donnell VB**, **Kuhn H**, **O'Donnell VB**. 2006. Inflammation and immune regulation by 12/15-lipoxygenases. Prog Lipid Res **45**:334–356.

CHAPTER 2: FleA expression in *Aspergillus fumigatus* is recognized by fucosylated structures on mucins and macrophages to prevent lung infection

This work has been published as:
Kerr, S.‡, **Fischer, G**‡., Sinha, M., McCabe, O., Palmer, J., Choera, T., Lim, F., Wimmerova, M., Carrington, S., Yuan, S., Lowell, C., Oscarson, S., Keller, N., & Fahy, J. (2016) FleA expression in *Aspergillus fumigatus* is recognized by fucosylated structures in mucins and macrophages to prevent lung infection. *PLoS Path* 12(4):e1005555.

‡ These authors contributed equally to this work.

My contribution was the development and growth of all *A. fumigatus fleA* strains for mucin binding and infection studies, timelapse and fluorescent microscopy of FleA localization during fungal growth, and growth of fungal strains at developmental timepoints for FleA western blotting.

2.1. ABSTRACT

The immune mechanisms that recognize inhaled *Aspergillus fumigatus* conidia to promote their elimination from the lungs are incompletely understood. FleA is a lectin expressed by *Aspergillus fumigatus* that has twelve binding sites for fucosylated structures that are abundant in the glycan coats of multiple plant and animal proteins. The role of FleA is unknown: it could bind fucose in decomposed plant matter to allow *Aspergillus fumigatus* to thrive in soil, or it may be a virulence factor that binds fucose in lung glycoproteins to cause *Aspergillus fumigatus* pneumonia. Our studies show that FleA protein and *Aspergillus fumigatus* conidia bind avidly to purified lung mucin glycoproteins in a fucose-dependent manner. In addition, FleA binds strongly to macrophage cell surface proteins, and macrophages bind and phagocytose *fleA*-deficient *(*Δ*fleA*) conidia much less efficiently than wild type (WT) conidia. Furthermore, a potent fucopyranoside glycomimetic inhibitor of FleA inhibits binding and phagocytosis of WT conidia by macrophages, confirming the specific role of fucose binding in macrophage recognition of WT conidia. Finally, mice infected with *ΔfleA* conidia had more severe pneumonia and invasive aspergillosis than mice infected with WT conidia. These findings demonstrate that FleA is not a virulence factor for *Aspergillus fumigatus.* Instead, host recognition of FleA is a critical step in mechanisms of mucin binding, mucociliary clearance, and macrophage killing that prevent *Aspergillus fumigatus* pneumonia.

2.2. INTRODUCTION

Aspergillus fumigatus (*A. fumigatus*) is an ubiquitous opportunistic pathogen that causes invasive and often fatal lung infection, particularly in immunocompromised patients (1).

Aspergillus fumigatus produces small hydrophobic conidia that are easily inhaled into the lungs and require robust host defense mechanisms to prevent infection. The mechanisms of clearance of conidia from the lung are incompletely understood but phagocytosis by macrophages is known to be important (2–5). Macrophages express Dectin-1, a C-type lectin that recognizes β-1-3 glucan on the surface of *A. fumigatus* conidia. Although the amount of surface accessible β-1-3 glucan is low on resting conidia, it is much higher in swollen conidia that appear early during germination and infection (6). Binding of β-glucan by Dectin-1 promotes macrophage killing of *A. fumigatus* conidia, and other macrophage receptors, such as the mannose receptor and toll-like receptors (TLR) -2 and -4, cooperate in this killing effect (7, 8). Notably, however, the phagocytosis of *A. fumigatus* conidia by macrophages is incompletely blocked by inhibitors of Dectin-1, mannose receptor, and TLR-2/4 (9), which means that macrophages must employ additional mechanisms to phagocytose and kill *A. fumigatus*.

Many microorganisms use lectins as adhesins to interact with host glycoproteins. For example, *Pseudomonas, Burkholderia, Ralstonia*, and *Chromobacterium* bacteria all express adhesins that include galactophilic and fucophilic lectins that initiate bacterial adherence to glycan receptors on host cells and tissues (10–14). In addition, fungi such as *Aleuria aurantia*, *A. oryzae,* and *A. fumigatus* all express fucophilic lectins (15–18) with multiple fucose binding sites (11, 19). For example, *A. fumigatus* lectin (AFL, also known as FleA) exists as a dimer with 12 fucose-binding sites available for strong multivalent interactions with fucosylated structures (18). As a result, FleA has unusually high binding affinity for fucosylated structures (18, 20), but its role in fungal biology is unknown.

Fucosylated glycans are abundant in plants and animals, and FleA expression by fungi may help them bind plant or animal tissues, as has been found for fucose binding lectins in bacteria (11, 21). *Aspergillus fumigatus* conidia enter the human host via inhalation, and fucosylated proteins in the lung that could bind conidial FleA include mucins in the airway mucus gel and multiple glycoproteins in the glycocalyx of macrophages (22–24). Fucose in different linkages is a common carbohydrate structure in gel-forming mucins (22) such as MUC5AC and MUC5B (23), and recent studies in transgenic mice have revealed the essential role of gel-forming mucins in host defense against lung infection (25). In addition, membrane-tethered mucins (such as MUC1 and MUC4) function as receptors in epithelial cells (26) and macrophages (24) and it is possible that they may function as adhesins for *A*. *fumigatus*. To determine the role of FleA in the pathogenesis of *A. fumigatus* pneumonia, we studied the behavior of recombinant FleA and *fleA*-deficient conidia in multiple complimentary functional assays, including mucin binding assays, macrophage binding assays, and a mouse model of *A. fumigatus* pneumonia.

2.3. MATERIALS AND METHODS

Subjects and clinical samples. Induced sputum was collected from 5 healthy nonsmoking, non-allergic subjects aged between 24-55 years (4 male) as described (27). Bronchoalveolar lavage (BAL) was collected from 3 healthy non-smoking, non-allergic subjects aged 30 - 45 years (2 male, 1 female) by instilling 4 aliquots of 50mLs of warmed (37ºC) normal saline into a segmental bronchus in the right middle lobe or lingula. After the first two 50mL aliquots were instilled and aspirated from one segmental bronchus, the

bronchoscope was moved to an adjacent bronchus in the same segment for collection of two additional 50 mL aliquots.

Purification of high molecular weight mucin from sputum. 8M guanidine hydrochloride was added in 1:1 volume to sputum samples and the samples rotated at 4^{o}C until homogenized. Mucins were then purified from the sputum as described previously (28, 29) with additional details in S1 text.

FleA binding to mucin. Recombinant FleA (prepared as described previously (18) was biotinylated with EZ-link sulfo NHS biotin (Pierce, Thermo Fisher, Rockford, IL). Purified human mucin was coated on a Nunc maxisorp plate at 20 µg/ml in carbonate bicarbonate buffer pH 9.6 overnight at 4ºC, washed and blocked with TBS + 0.05% Tween-20, 10mM $CaCl_2$, 3% BSA. Biotinylated recombinant FleA was incubated at 5 µg/ml in TBS + 0.05% Tween-20, 10 mM $CaCl_2$, 1% BSA (binding buffer) in the presence or absence of 100mM L-fucose or 100mM L-galactose. For inhibition assays, recombinant FleA was incubated with a dilution series of synthesized carbohydrate compounds starting at 5mM. Plates were washed with binding buffer, incubated with ExtrAvidin-alkaline phosphatase (Sigma-Aldrich, St Louis, MO) and detected using phosphatase substrate (Sigma-Aldrich, St Louis, MO) in carbonate bicarbonate buffer pH 9.6 + 1 mM $MgCl_2$ and read at 405nm (Biotek Synergy plate reader, Winooski, VT).

Synthesis of carbohydrates. The disaccharides were synthesized by glycosylating appropriately protected glucose acceptors with a fucosyl bromide donor, 2,3,4-tri-O-

benzyl-L-fucopyranosyl bromide, using Lemieux's halide assisted conditions (30), followed by deprotection of the α-linked disaccharides using catalytic hydrogenolysis to give the target structures. Detailed synthesis methods are in S1 text.

***Aspergillus* strains and culture**. Unless noted, all *A. fumigatus* strains were propagated on solid glucose minimal media (GMM) at 37 °C (31). *A. fumigatus* asexual spore suspensions were fixed, where appropriate, in 4% formaldehyde in PBS. All strains used in this study are listed in Table 2.

Generation of FleA mutant conidia. *A. fumigatus* strains expressing GFP were constructed using pJMP51 to transform AF293.1 and AF293.6 which yielded TJMP131.5 (*GFP::H2A*) and TGJF5.3 (*GFP::H2A, argB1*), respectively. A *fleA* gene disruption cassette (Fig 2A) was used to transform TGJF5.3 to create TGJF6.7, 6.8 and 6.13 (*GFP::H2A, ΔfleA*). The strain was confirmed by Southern and northern analysis (Figure 2B,C). TGJF5.3 was also transformed with a FleA RFP (*fleA:RFP*) tagged cassette yielding the prototrophic *fleA:RFP* strain, TGJF7.11. FleA tagging was confirmed microscopically and by Southern and northern analysis Figure 2D,E). *A. flavus ΔfleA* deletion mutants were created by transforming the deletion construct into parental strain CA14Δ*ku70*Δ*pyrG* (32) to create strains TFYL62.1-62.3. Single integration of the deletion cassette was verified via Southern analysis (Figure 2). More detailed methods are available in S1 text.

Immunofluorescence of *Aspergillus* conidia. *A. fumigatus* strains were cultured on GMM at 37°C for 3 days, spores were harvested, placed on a pre-cleaned glass slide and coverslipped. Images were taken of GFP and RFP fluorescence using a Nikon Ti inverted microscope equipped with a Nikon Plan Apo VC 60x/1.40 Oil DIC/∞/0.17 WD. Time-course microscopy was carried out over 27 hours at 37°C. The average fluorescent intensity at each developmental state (resting conidia, swollen conidia, and hyphae) of untagged FleA (TJMP131.5 or wild type) was subtracted from the mean fluorescent intensity value of two different transformants (TGJF7.11 and TGJF7.15) expressing RFP-tagged versions of FleA. The adjusted mean fluorescence was then standardized to area.

Western blot of *A. fumigatus* extracts and supernatant. Resting and swollen *A. fumigatus* conidia and hyphae were isolated from WT and *ΔfleA* cultures as described in S1 text and extracted in 50mM Tris/HCl pH 7.4, 50 mM EDTA, 2% SDS, and 40 mM β-Mercaptoethanol. Protein concentrations were determined by BCA assay and 15 µg of protein was loaded into each well of a 4-12% BOLT SDS PAGE gel (Life Technologies, Grand Island, NY) and electrophoresed. Gel was then blotted onto nitrocellulose, blocked with non fat milk and stained with an anti-FleA rabbit polyclonal antibody (18) and donkey anti-rabbit HRP (Jackson immunoresearch, West Grove, PA) prior to chemiluminescent detection. Culture supernatants were filtered through a 0.2 µM filter and concentrated 10x in a 0.5 ml Amicon Ultra (EMD Millipore, Billirica, MA) before being run as described above.

Mucin conidia binding assay. 8 well glass chamber slides (Labtek, Scotts Valley,CA) were coated with 20 μg/ml purified human mucin in dH_2O overnight at 37ºC and then blocked in PBS + 1% BSA for 1 hour. Fixed *A. fumigatus* conidia suspensions were centrifuged at 6000 x g for 5 minutes to pellet and resuspended in PBS + 1% BSA in the presence or absence of 10mM (2E)-hexenyl α-L-fucopyranoside (2EHex) or 100mM fucose. $2x10^7$ conidia were added per well and incubated for 4 hours at room temperature. Unbound conidia were removed by washing in PBS+ BSA, the slides were mounted in Prolong Gold anti-fade reagent (Life Technologies, Grand Island, NY) and allowed to cure for 24 hours prior to sealing. Images were acquired using an FV10i confocal microscope (Olympus, Center Valley, PA) using the multipoint Z-stack mode to acquire 9 fields per well with 3 wells imaged per condition per experiment. Each Z-stack image was compressed into a single plane of focus and conidia were counted using NIH Image J with the ITCN plugin. Each experiment was repeated at least 3 times. *A. flavus*-mucin interactions were investigated as described above with one exception. These conidia lack GFP so were stained with Calcofluor white for 5 minutes to allow imaging prior to adding to mucin-coated slides.

Cell culture. RAW 264.7 cells (UCSF cell culture facility) were maintained in DMEM + 10% fetal bovine serum + 1% penicillin/streptomycin until seeded and grown on 8 well chamber slides (Labtek, Scotts Valley, CA) overnight. Human alveolar macrophages from BAL were centrifuged at 450 x g for 10 minutes and washed with PBS prior to plating on poly-L-lysine coated 8 well chamber slides in RPMI 1640+ 10% fetal bovine serum + 1%

penicillin/streptomycin + 0.5µg/ ml amphotericin B. Cells were washed after 2 hours of adherence and cultured overnight prior to experiments.

FleA binding to macrophages by flow cytometry. RAW264.7 or primary human lung macrophages were incubated with Alexa-488 tagged recombinant FleA in the presence or absence of 100mM fucose prior to analysis on a Becton Dickenson FACScalibur and Flow Jo software (Treestar, Ashland, OR).

Phagocytosis assay. RAW 264.7 cells were plated at $5x10^4$/well on 8 well chamber slides (Labtek, Scotts Valley, CA) and allowed to grow overnight in culture media. $5x10^6$ conidia from either the PFA-fixed WT or *Δ fleA* strain were added per well in the presence or absence of 10mM 2EHex or 500mM fucose and incubated at 37°C for 1 hour. Wells were washed and incubated for a further 2 hours at 37ºC for complete uptake. Cells were stained with 7.5µg/ml CellMask Deep Red plasma membrane stain (Life Technologies, Grand Island, NY) and calcofluor white (Sigma, St Louis, MO), washed with PBS and mounted with Fluoromount-G (Southern Biotech, Birmingham, AL). Z-stack images were acquired using an FV10i confocal microscope (Olympus, Center Valley, PA). Each Z-stack image was compressed into a single plane of focus and both internalized conidia and cell number were counted using NIH Image J with the cell counter plugin. Phagocytic index was calculated as the number of conidia internalized per cell. Internalized conidia were counted as conidia within the boundary of the cell that were not stained with calcofluor white. Calcofluor white stained conidia were excluded from the count as they were not internalized. For human macrophages, cells were plated at $5x10^5$ per well and

grown overnight. $1.5x10^6$ conidia from the PFA fixed WT or *ΔfleA* strains were added per well in the presence or absence of 10mM 2EHEX, incubated at 37ºC for 30 minutes then washed, stained and mounted.

Flow cytometry analysis of *A. fumigatus* conidia. Recombinant Dectin-1 was purchased from R&D Systems (Minneapolis, MN) and biotinylated using the EZ-link sulfo NHS biotin kit (Thermo Fisher Waltham, MA) according to manufacturers recommendations. $1x10^7$ WT or *ΔfleA* conidia were labeled with biotinylated Dectin-1 and Streptavidin-PE (Biolegend, San Diego, CA) and fixed in 4% paraformaldehyde prior to analysis on a Becton Dickenson FACSCalibur and FlowJo software (TreeStar, Ashland, OR).

Phagocytosis of FleA-coated particles. Yellow-green 1μM sulfate treated FluoSpheres (Life Technologies, Grand Island, NY) were coated with recombinant FleA, added to RAW264.7 cells in the presence or absence of 500mM fucose and incubated with agitation for 2 hours at 37°C prior to extensive washing with DMEM to remove unattached FluoSpheres from the cell surface. Cells were fixed in 4% paraformaldehyde prior to analysis on a Becton Dickenson FACSCalibur and FlowJo software (TreeStar, Ashland, OR).

Mice. Male C57BL/6 mice from Charles River Laboratories (Wilmington, Massachusetts, MA) were housed in a pathogen free facility at UCSF. Animal experiments followed protocols approved by the UCSF Institutional Animal Care and Use Committee.

Mouse model of *Aspergillus* infection. Eight to ten week old C57BL/6 mice were infected intranasally with $5x10^7$ of WT or *ΔfleA* conidia. Mice were sacrificed 3 days post infection. Measures of lung inflammation, infection and lung injury were evaluated using methods described in S1 text.

Statistical methods. Data analyses were performed GraphPad Prism version 6 (GraphPad, San Diego, CA). ANOVA was used for three-group comparisons followed by pairwise analyses with the Tukey multiple comparisons test when appropriate. Two group comparisons were analyzed using the Students t-test or for non-parametric analyses, a ranked Mann-Whitney test.

Ethics Statement. Human samples were obtained from the UCSF Airway Tissue Bank (ATB). All participants signed two informed consent forms - one for the original study protocol and the other for the ATB protocol. All study and ATB procedures were reviewed and approved by the UCSF Committee on Human Research, protocol number 11-05176. All animal studies were carried out in strict accordance with the recommendations in the Guide for the Care and Use of Laboratory Animals of the National Institute of Health. All protocols involving animals were approved by the animal care and use committee at UCSF and are in compliance with Public Health Service Policy (PHS), (IACUC protocol number AN090458-03).

2.4 RESULTS

2.4.1. Phylogenetic analysis of FleA.

We generated a phylogenetic tree to illustrate the fungal genera and species that contain a putative FleA ortholog. The tree shows that FleA is not widespread in the Kingdom Fungi and is found in several pathogenic species of fungi. FleA is present in the genomes of only a few *Aspergillus* species, including *A. fumigatus*, *A. flavus, A. oryzae and A. calidoustus* (Supplemental Figure 1). FleA is also present in other human pathogens including dermatophytes (*Trichophyton, Microsporum* and *Arthroderma)*, entomopathogenic fungi (*Metarhizium, Ophiocordyceps),* a nematode pathogen (*Arthrobotrys oligospora*), several plant pathogens (*Penicillium expansum, Marssonina, Magnaporthiopsis, Ceratocystis, Gaumannomyces, Rhizoctonia*) and *Trichoderma* spp. (pathogenic on other fungi).

2.4.2. FleA mediates binding of *A. fumigatus* conidia to airway mucin in a fucose dependent manner.

To determine if *A. fumigatus* conidia can bind to mucin glycans in a FleA-dependent manner, we coated microtiter plates with mucins that we purified from the induced sputum of healthy subjects, and we used labeled recombinant FleA to quantify FleA-mucin binding. We found that FleA binds strongly to airway mucin and that this binding is inhibited by fucose (Figure 1A). No inhibition was observed with galactose (Figure 1A). To examine the specificity of FleA for the different linkage forms of fucose found naturally on mucins, we synthesized disaccharides with fucose linked to glucose in α1,2, α1,3,

α1,4, or α1,6 positions. These fucose-glucose compounds all strongly inhibited FleA binding to mucin in a dose dependent manner (Figure 1B).

2.4.3. Generation of *ΔfleA A. fumigatus* and *A. flavus* conidia.

To further characterize *fleA* in *A. fumigatus* and examine the functional role of FleA binding to mucin, we created reagents to allow us to make quantitative measurements of *A. fumigatus* binding to mucin and to dissect the specific binding role of FleA. To facilitate visualization of the conidia, we created strains of *A. fumigatus* expressing nuclear GFP by transformation of AF293.1 and AF293.6 strains with the plasmid pJMP51 resulting in histone 2A fused GFP prototrophic (TJMP131.5) and auxotrophic (TGJF5.3) strains, respectively. TGJF5.3 was further modified and transformed to prototrophy using a disruption cassette targeting disruption of the *fleA* locus (Figure 2A) and multiple *ΔfleA* deletion transformants were identified. Confirmation of *fleA* deletion was demonstrated by Southern and northern blotting (Figure 2B,C). Despite repeated attempts to complement the *ΔfleA* deletion strains, we encountered problems such as phenotypic abnormalities in spore size and shape, which precluded generation of reliable complement reagents. Hence the mucin binding studies described below were repeated with several *ΔfleA* deletions to confirm the role of FleA as an *A. fumigatus* fucose binding protein. The mucin binding studies were also repeated using a novel synthetic glycomimetic inhibitor of FleA as an alternative experimental approach. To assess localization of FleA in conidia, we made a C-terminal RFP tagged *fleA* mutant in *A. fumigatus* by modifying the native *fleA* locus using a disruption cassette similar to that

used to delete the *fleA ORF* (Figure 2D,E). Multiple *ΔfleA* deletion *A. flavus* strains were generated using the same methods described for *A*. *fumigatus* above and as illustrated in Supplemental Figure 2.

2.4.4. FleA is present on resting and swollen *A. fumigatus* conidia.

Protein levels of FleA on *A. fumigatus* conidia and hyphae have not been characterized. We found that RFP-tagged FleA is present on *A. fumigatus* conidia when *fleA-rfp* is expressed under its endogenous promoter (Figure 3A), and we used two different strains of FleA-RFP tagged conidia to quantify FleA levels over time by fluorescence microscopy (Figure 3B). FleA fluorescence was high on resting conidia (with some variation among conidia), low in swollen conidia, and largely absent in hyphae (Figure 3B,C). Time-lapse microscope images of germinating conidia show that FleA begins to decrease by 21 hours and is almost entirely absent by 27 hours (Figure 3C). These results were confirmed in extracts from resting and swollen conidia and from hyphae that were analyzed for FleA protein by western blot (Figure 3D). We also investigated the possibility that FleA was secreted by conidia, even though FleA lacks a canonical secretion signal peptide according to the Signal P 4.0 server (33). Analysis of proteins in concentrated culture supernatant of *A. fumigatus* at various developmental timepoints revealed that resting conidia shed significant amounts of FleA, whereas conditioned media from swollen conidia and hyphal culture supernatant did not have detectable FleA (Figure 3D).

2.4.5. Binding of *A. fumigatus* conidia to airway mucins and phagocytosis by macrophages is FleA dependent.

To examine if binding of *A. fumigatus* conidia to airway mucins is FleA dependent, we first developed a binding assay to determine the specific binding role of FleA. For the conidia-binding assay, we coated mucins onto chamber slides and used confocal microscopy to image binding of conidia. As shown in Figures 4A and 4B, the binding of three independent *ΔfleA* deletion mutant strains (TGJF 6.7, 6.8 and 6.13) to mucin is much weaker than the binding of WT conidia. These data demonstrate that *A. fumigatus* conidia bind to mucin in a FleA-dependent manner. After confirming that all 3 *ΔfleA* mutant strains showed identical patterns in mucin binding assays, we chose the *A. fumigatus* strain TGJF6.7 for all further functional studies.

2.4.6. Binding of *A. flavus* conidia to airway mucins is FleA dependent.

To determine if FleA is also required for binding of *A. flavus* conidia to mucin, we examined the binding of WT and *ΔfleA A. flavus* conidia in our chamber slide assay. As shown in Figure 4C, the binding of three independent *ΔfleA* deletion mutant strains of *A. flavus* (TFYL 62.1, 62.2 and 62.3) to mucin is much weaker than the binding of WT conidia.

Fucosylated glycoproteins are not restricted to mucin glycoproteins. Macrophages also express multiple fucosylated proteins on their cell surface, including membrane-tethered mucins (24). We therefore explored whether *fleA* expression by *A. fumigatus* might

mediate binding or phagocytosis by macrophages. We first explored binding of recombinant FleA to macrophages by flow cytometry and showed that FleA binds very strongly to the surface of RAW264.7 mouse macrophages and primary human alveolar macrophages in a fucose-dependent manner (Figure 5A,B). Next, we investigated phagocytosis of *A. fumigatus* conidia to RAW264.7 mouse macrophages. Using confocal microscopy, we found that *A. fumigatus* WT conidia bound to RAW264.7 cells and that many are internalized/phagocytosed (Figure 5C). Notably, the internalization of *ΔfleA* conidia was 50% less than that of WT (Figure 5C,D). We repeated these experiments in alveolar macrophages isolated from bronchoalveolar lavage from healthy human subjects. Similar to data from the RAW264.7 cells, we found that *A. fumigatus* conidia are internalized and phagocytosed by human macrophages and that *ΔfleA* conidia show a reduction in phagocytosis of 40% compared to WT (Figure 5E,F). Thus, fucosylated structures on lung macrophages act as receptors for *A. fumigatus* FleA, resulting in enhanced phagocytosis of conidia.

To rule out the possibility that deletion of FleA causes changes to β-glucan in the fungal cell wall that could be affecting binding and phagocytosis, we used FACS to examine the binding of a β–glucan ligand (Dectin-1) to *ΔfleA* and WT conidia. We found no significant differences in the affinity of recombinant biotinylated Dectin-1 for *ΔfleA* and WT conidia in these experiments (Figure 5G*)*. We also coated fluorescent microspheres with FleA to create a simplified model of conidia and found that FleA causes a significant and fucose-dependent increase in binding and phagocytosis of microspheres by RAW264.7 cells (Figure 5H).

2.4.7. (2E)-hexenyl α-L-fucopyranoside is a potent functional inhibitor of FleA.

To provide additional evidence that binding of *A. fumig*atus conidia to mucins and alveolar macrophages is FleA-dependent, we synthesized a library of modified fucopyranoside structures using methods we previously described for inhibitors of the FimH lectin in *E. coli* (34) (Figure 6). To screen for the relative potency of different fucopyranosides, we used the FleA-mucin binding assay. In this way, we found that (2E)-hexenyl α-L-fucopyranoside (2EHex) (Figure 6A) inhibits FleA with marked (nanomolar) potency (Figure 6B). In contrast to its potent inhibition of FleA binding to mucin, 2EHex does not show potent inhibition of PA-IIL (a fucose-binding lectin from *Pseudomonas aeruginosa*) binding to mucin (Figure 6C). We next tested the effects of 2EHex and fucose on interactions between *A. fumigatus* conidia and mucins and macrophages. We found that both 2EHex and fucose decreased the mucin binding of WT *A. fumigatus* conidia to the levels observed with *ΔfleA* conidia (Figure 6D). 2EHex also decreased the phagocytosis of WT *A. fumig*atus conidia by RAW264.7 cells and primary human macrophages to the levels observed with the *ΔfleA* conidia (Figure 6E, F). These inhibition studies confirm that binding of *A. fumigatus* conidia to mucins and macrophages requires the fucose binding activity of FleA.

2.4.8. FleA loss increases lung infection and lung injury by *A. fumigatus*.

Based on our data that FleA is required for binding and phagocytosis of conidia by macrophages, we hypothesized that *ΔfleA* conidia might evade phagocyte killing leading

to increased lung infection compared to WT. To test this hypothesis, we infected immunocompetent C57BL/6 mice intranasally with WT conidia or *ΔfleA* conidia. H&E staining of infected lung tissue showed that mice infected with WT conidia had well-contained pneumonia (Figure 7A) whereas *ΔfleA* conidia treated animals had a poorly contained pneumonia (Figure 7B). GMS staining showed limited numbers of conidia with little evidence of germination in sections from WT treated animals (Figure 7C, E). In contrast, a large number of conidia from *ΔfleA* treated animals showed hyphae generation (germlings) evident on the GMS stain, typical of invasive aspergillosis (Figure 7D,F). Both the total number and percentage of germinating conidia are significantly higher in mice infected with *ΔfleA* conidia than WT conidia (Figure 7G-H). Lung injury is more severe in *ΔfleA*-infected mice, as evidenced by a higher concentration of hemoglobin in bronchoalveolar lavage (BAL) (Figure 7I). *Aspergillus* 18S gene expression in lung homogenates from *ΔfleA*-infected mice is higher than in lung homogenates from WT infected mice, indicative of higher fungal burden (Figure 7J).

BAL cells from mice infected with WT and *ΔfleA* conidia were analyzed by flow cytometry to quantify multiple immune cells and by multiplex immunoassay to quantify multiple cytokines, chemokines and growth factors. Mouse BAL cells were labeled with a panel of antibodies including CD11c, F4/80, CD11b, MHCII, Ly6G, Ly6C, NK1.1, TCRβ, B220, CD4 and CD8. Compared to mice infected with WT conidia, we found that several cell types were decreased in BAL from mice infected with *ΔfleA* conidia, including alveolar macrophages, neutrophils, NK and NKT cells and CD4 and γΔ T cells (Figure 8). No significant differences were observed for eosinophils, dendritic cells, B cells, monocytes

and inflammatory monocytes and CD8 T cells. Compared to mice infected with WT conidia, we found that the concentrations of multiple cytokines, chemokines and growth factors were similar in BAL from mice infected with *ΔfleA* conidia, including IL-6, IFNγ, KC and VEGF in BAL fluid (Supplmental Table 1).

2.5. DISCUSSION

We have discovered that FleA produced by *A. fumigatus* conidia allows airway mucins to bind conidia and macrophages to effectively phagocytose them. Notably, when we engineer conidia that lack FleA, the resultant *ΔfleA* conidia show increased virulence in a mouse model of *A. fumigatus* pneumonia. Together these data uncover a novel mechanism of host defense against *A. fumigatus* infection in which fucosylated receptors in the airway mucus gel and on the surface of macrophages bind FleA to hasten the elimination of *A. fumigatus* conidia.

To date, research on binding of *A. fumigatus* conidia to lung proteins has focused on binding to basement membrane proteins in the airway epithelium (35–38). But mucins provide the first line of defense against inhaled pathogens in the bronchi and bronchioles (25), and studies of binding of *A. fumigatus* conidia to human airway mucins are highly relevant to mechanisms of infection and invasion. Mucin glycans include multiple fucosylated structures (22), and we report avid binding of FleA to human airway mucins that is inhibited by a wide range of fucose structures, including fucose in α1,2, α1,3, α1,4, or α1,6 linkages. We also report that deletion of FleA in *Aspergillus fumigatus* conidia markedly decreases mucin binding and that this role for FleA is conserved in the

pathogenic *A. flavus*. We conclude that a range of sterically available fucosylated glycans in mucins can act as FleA ligands and the airway mucus gel is a powerful “sticky” barrier that can capture and remove conidia to guard against invasive infection.

Phagocytosis of inhaled conidia by alveolar macrophages represents an important innate immune defense against *A*. *fumigatus* infection, especially in the alveolar lung compartment where mucocilliary clearance does not operate. We explored the role of FleA in phagocytosis of *A*. *fumigatus* conidia by murine and human macrophages using two approaches. First, we compared the phagocytosis of wild type (WT) conidia and *fleA*-deficient *(*Δ*fleA*) conidia and showed that macrophage phagocytosis of the Δ*fleA* conidia is decreased by 40-50%. Second, we screened a library of fucopyranosides to reveal that (2E)-hexenyl α-L-fucopyranoside (2EHex) inhibits FleA with nanomolar efficacy and also inhibits the binding and phagocytosis of WT *A*. *fumigatus* conidia by lung macrophages. Together, these two lines of evidence leads us to conclude that *A. fumigatus* conidia interact with macrophages in a mechanism that requires the fucose binding activity of FleA. Multiple glycoproteins on the surface of macrophages could act as the receptors for FleA, including membrane-tethered mucins (24). Neutrophils are also important in cellular immunity against *Aspergillus* (39, 40), but we did not study whether neutrophils have defective uptake of *fleA*-deficient conidia, and it remains unknown whether fucosylated receptors on neutrophils have a role in host defense against *Aspergillus*. The identity of all of the cell types participating in FleA-dependent host defense in the lung has not been elucidated in this study. While we have described an alveolar macrophage dependent

mechanism, it is also likely that other non-alveolar macrophage dependent cellular mechanisms, including neutrophils or monocytes, can contribute to FleA mediated host defense.

The FleA-dependent binding of *A. fumigatus* conidia to mucin and the poor uptake of *ΔfleA* conidia by lung macrophages indicate that FleA is not a virulence factor. Instead, we propose it is a fungal protein recognized by the host to promote defense against invasive aspergillosis. We provide evidence for this in our experiments in which we infected immunocompetent mice with *A. fumigatus* WT or *ΔfleA* conidia. The mice infected with the *ΔfleA* conidia developed invasive aspergillosis whereas those infected with WT conidia did not. Notably, the *ΔfleA* infected mice showed blunted recruitment of immune cells integral to the fungal immune response. Specifically, FACS analysis of BAL cells showed a significant decrease in the number of alveolar macrophages, neutrophils, NK and NKT cells and CD4 and γΔ T cells. Thus, it appears that *ΔfleA* conidia fail to elicit the same inflammatory response as WT conidia resulting in reduced recruitment of key effector cells in the fungal immune response in the lung. We conclude that the absence of FleA in *A*. *fumigatus* conidia results in a hypo-inflammatory response and promotes invasive infection.

Our experiments prove that FleA is a pathogen-associated molecular pattern that can be recognized by lung mucins and macrophages to protect the host from infection. The fact that we show that *A. flavus* also uses FleA to bind lung mucin and that phylogenetic

analysis reveals FleA present in several pathogenic species may suggest a conserved role for FleA in fucose-mediated host pathogen interactions. It is unclear why *A. fumigatus* and other pathogenic fungi have evolved to express *fleA*. Since fungi commonly grow on carbon-rich carbohydrate substrates, it is possible that FleA is involved in helping these organisms to establish a niche on the surface of carbohydrate-rich substrates.

Our finding for a role for FleA-fucose mediated mechanism of host defense against *A. fumigatus* does not cast any doubt on the validity of the well established role for β-glucan/Dectin-1 interactions (41). β-glucan is abundant on swollen conidia and hyphae, and Dectin-1 binds β-glucan on swollen conidia to trigger a robust host defense response (42). But Dectin-1 does not bind to resting conidia, because these conidia have masked exposure of β-glucans due to the action of hydrophobin proteins (43, 44) and the mechanism of clearance of resting conidia from the lung is not completely understood. We propose a model whereby fucosylated receptors on mucins and macrophages interact with FleA on resting conidia to facilitate clearance of resting conidia via the mucociliary escalator and/or macrophage ingestion. Conidia that escape this initial response and mature (swell and germinate), possibly through the shedding of FleA, would be cleared by Dectin-1 mediated phagocytosis (9). Our data thus reveal contrasting roles for distinct protein carbohydrate interactions in host immune responses to *A. fumigatus*. On one hand, a macrophage expressed lectin - Dectin-1 - recognizes and binds a β-glucan on *A. fumigatus* conidia to promote phagocytosis and killing. On the other hand, we reveal here that fucosylated carbohydrates on macrophages engage a *conidial* lectin (FleA) to promote phagocytosis and killing. We conclude that protein- and carbohydrate-based

defenses on macrophages provide complimentary mechanisms to prevent potentially fatal *Aspergillus* lung infections.

2.6. AKNOWLEDGMENTS

We wish to thank Dr Prescott Woodruff for his assistance in quantifying the number of germlings in mouse lung tissue. We would also like to thank Dr. Philipp Wiemann for his assistance in development of the phylogenetic tree.

2.7. FIGURES AND LEGENDS

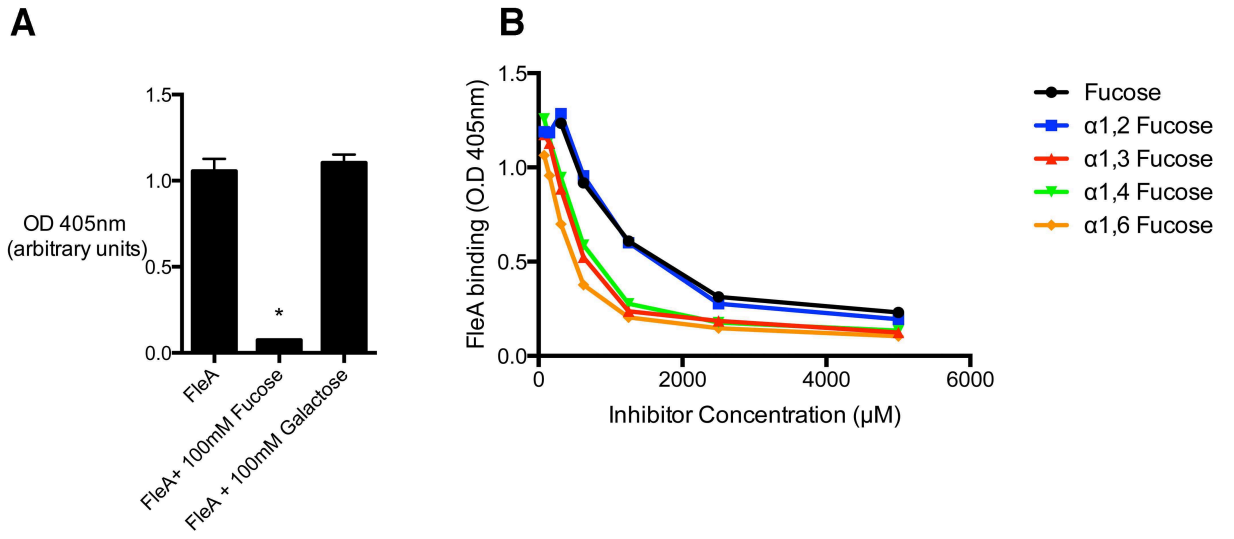

Figure 1. FleA binding to airway mucin is inhibited by fucose.

(A) Biotinylated FleA binding to mucin is inhibited by fucose, but not by galactose. The substrate is mucin purified separately from induced sputum collected from 5 donors and then pooled. Data shown is a representative experiment +/- S.D of 3 replicates, representative of at least 3 experiments. *Denotes significantly different from control, p=<0.0001. **(B)** α1,2, α1,3, α1,4 and α1,6 linked fucose all inhibit FleA binding to mucin in a dose dependent manner.

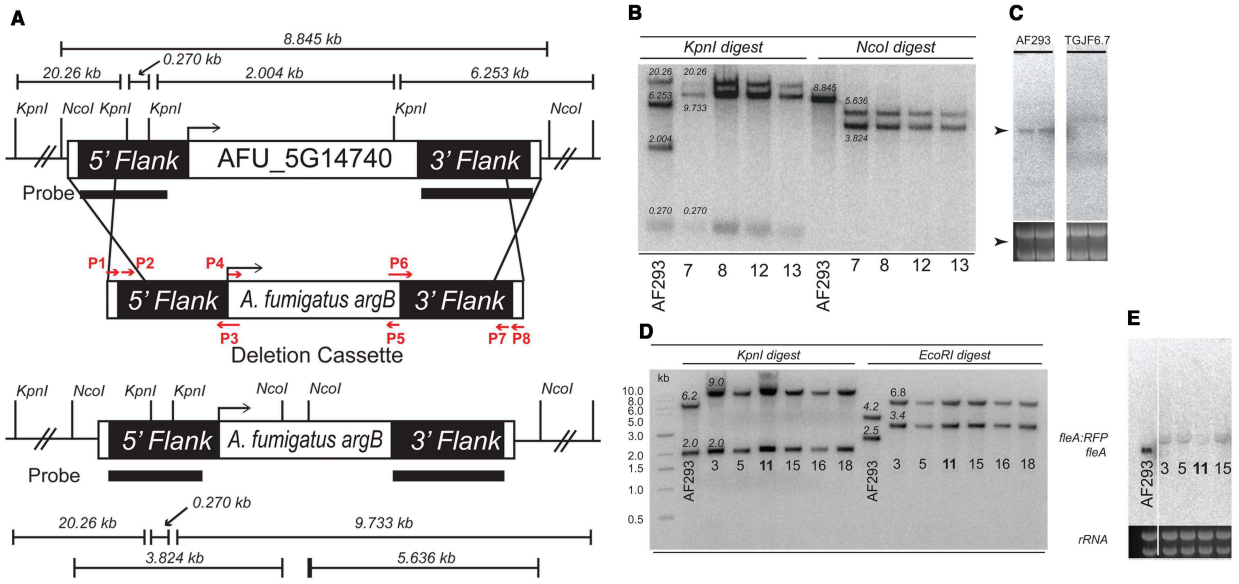

Figure 2. Generation of *ΔfleA* conidia in *A. fumigatus*.

(A) Diagram showing the gene disruption cassette used to generate *ΔfleA* conidia. **(B)** Southern blot depicting successful deletion of *fleA*. The restriction digest pattern corresponding to deletion of *fleA* was used to identify those strains where *fleA* was deleted. **(C)** Confirmation of *fleA* deletion was provided by northern blotting; *fleA* transcript is visible in the WT strain AF293 whereas *fleA* deletion was confirmed by the absence of this *fleA* transcript in TGJF6.7, 6.8, and 6.12. **(D)** Confirmation of successful RFP tagging of *fleA* as shown by Southern blotting and northern blotting **(E)**.

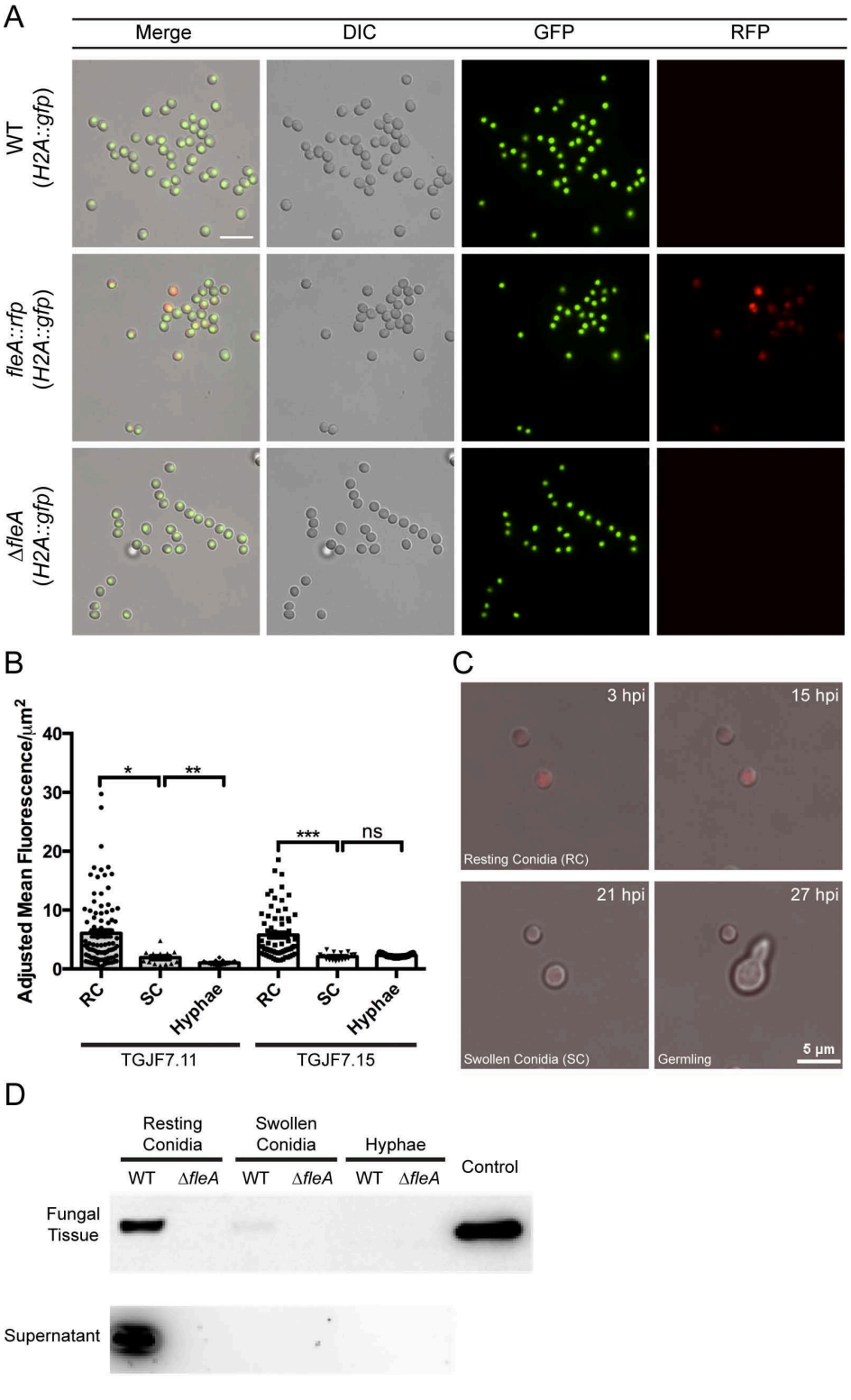
A
Merge
DIC
GFP
RFP
WT (H2A::gfp)
fleA::rfp (H2A::gfp)
ΔfleA (H2A::gfp)
B
Adjusted Mean Fluorescence/μm²
40
30
20
10
0
*
**
***
ns
RC
SC
Hyphae
RC
SC
Hyphae
TGJF7.11
TGJF7.15
C
3 hpi
15 hpi
Resting Conidia (RC)
21 hpi
27 hpi
Swollen Conidia (SC)
Germling
5 μm
D
Resting Conidia
Swollen Conidia
Hyphae
Control
WT
ΔfleA
WT
ΔfleA
WT
ΔfleA
Fungal Tissue
Supernatant

Figure 3. FleA is expressed in *A. fumigatus* conidia.

(A) RFP-tagged FleA is present in *A. fumigatus* conidia when *fleA-rfp* is expressed under its endogenous promoter. No FleA signal is visible in the *ΔfleA* deletion conidia or the non-RFP-tagged WT conidia. Data is representative of at least 3 experiments. Scale bar is 10μM. **(B)** RFP-tagged FleA was quantified by fluorescence microscopy in 2 different strains (TGJF7.11, TGJF7.15) showing higher levels of FleA in resting conidia compared to swollen conidia and hyphae. **(C)** Still images showing RFP fluorescence during germination, at time points representative of resting and swollen conidia and hyphae. **(D)** Western blot image showing strong expression of FleA in resting WT conidia with weak expression in swollen conidia. Control lane shows recombinant FleA running at the expected molecular weight of 34kD. No protein was detected in hyphal extract or extracts from *ΔfleA* conidia (TGJF6.7). Secreted FleA was detected in 10x concentrated culture supernatants from resting conidia of WT only.

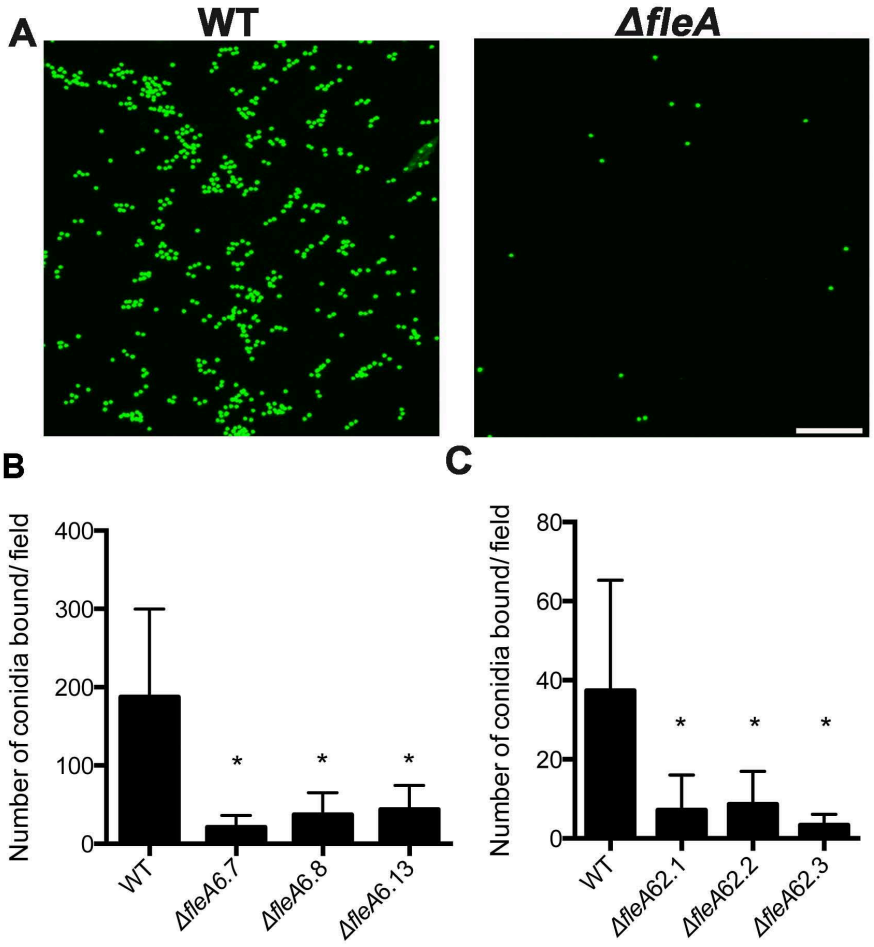

Figure 4. Binding of *Aspergillus* conidia to airway mucins is FleA dependent.

(A) Z-stack confocal images showing binding of WT *A. fumigatus* conidia (TJMP131.5) to mucin and that *ΔfleA* conidia have very limited binding. **(B)** Quantitative binding of WT *A. fumigatus* conidia to mucin or *ΔfleA* deletion mutants. **(C)** Quantitative binding of WT *A. flavus* conidia to mucin or *ΔfleA* deletion mutants. Note that *A. fumigatus*-mucin interactions were investigated using GFP labeled conidia whereas the *A. flavus*-mucin interactions were investigated using Calcofluor white-stained conidia (since the *A. flavus* conidia lack GFP). The data shown in panels B and C (27 replicates) reflects the mean ± SD of three independent experiments.

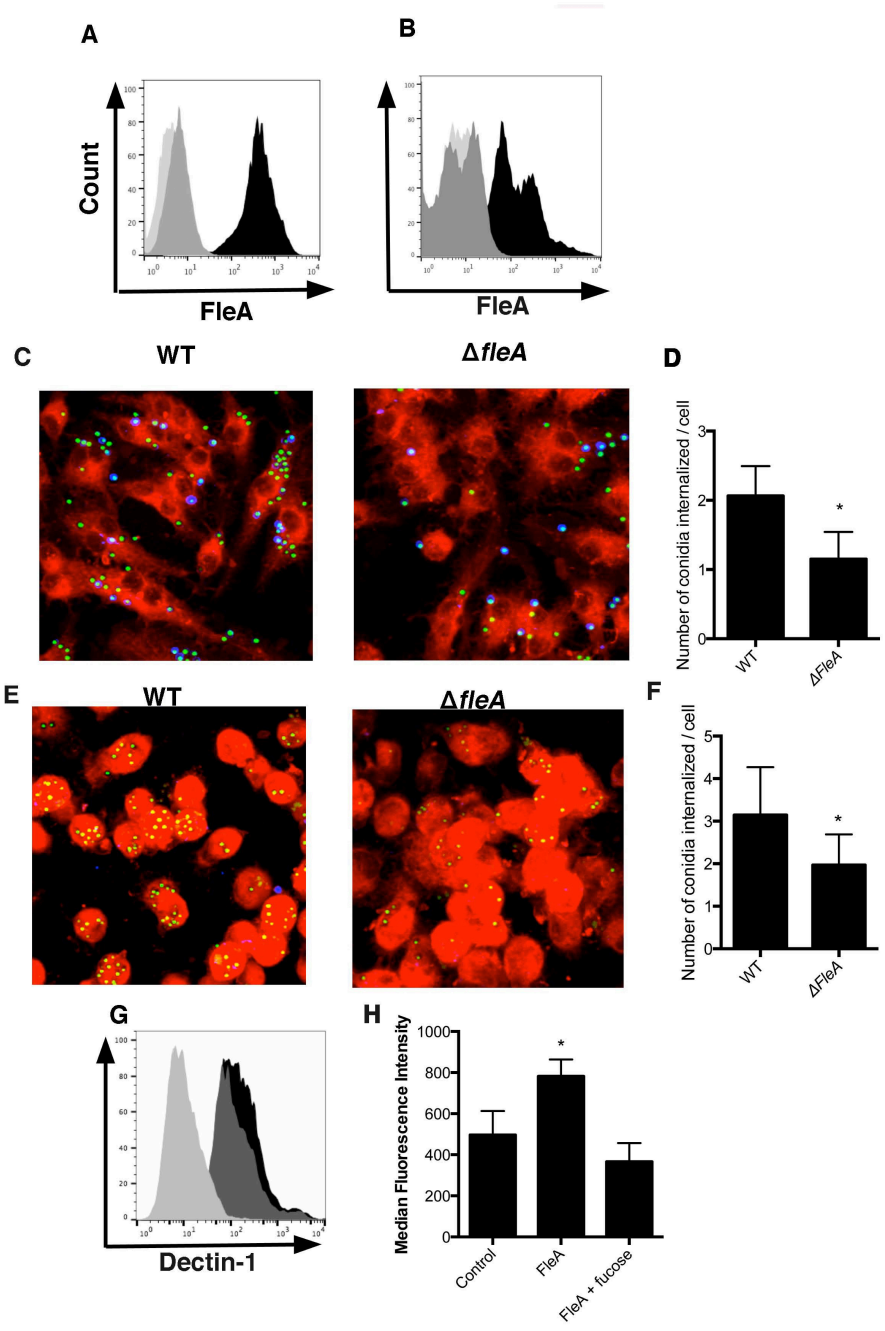

Figure 5. Binding of *A. fumigatus* conidia to alveolar macrophages is FleA-dependent.

FACS data showing binding of FleA (black) to **(A)** RAW264.7 or **(B)** primary human alveolar macrophages. 100mM fucose (dark grey) inhibits binding almost down to the

background level (light grey). Z-stack confocal images show binding and phagocytosis of GFP expressing WT conidia by **(C)** RAW264.7 cells, **(E)** primary human alveolar macrophages and that *ΔfleA* conidia are not bound well or phagocytosed effectively. Cells were dyed with CellMask Deep red (red); internalized conidia express GFP (green); calcofluor white (non-internalized conidia) stain blue. Quantitative data (expressed as an index of total number of conidia internalized/total cell number) demonstrate how loss of FleA significantly inhibits binding and phagocytosis of *A. fumigatus* conidia by **(D)** RAW264.7 cells or **(F)** primary human alveolar macrophages. Calcofluor white stained conidia were excluded from these counts to reflect only internalized conidia. The data shown in D (6 replicates) reflects the mean ± SD of three independent experiments whereas the data in panel F (6 replicates) reflects the mean ± SD of three independent donors. **(G)** FACS plots showing that binding of Dectin-1 is not significantly different between WT (dark grey) and *ΔfleA* (black) conidia compared to control (light grey). **(H)** Binding and internalization of FleA coated microspheres by RAW264.7 cells is significantly higher than control and inhibited by 500mM fucose. *Denotes significantly different from control, $p=<0.05$. Scale bar is 10μM.

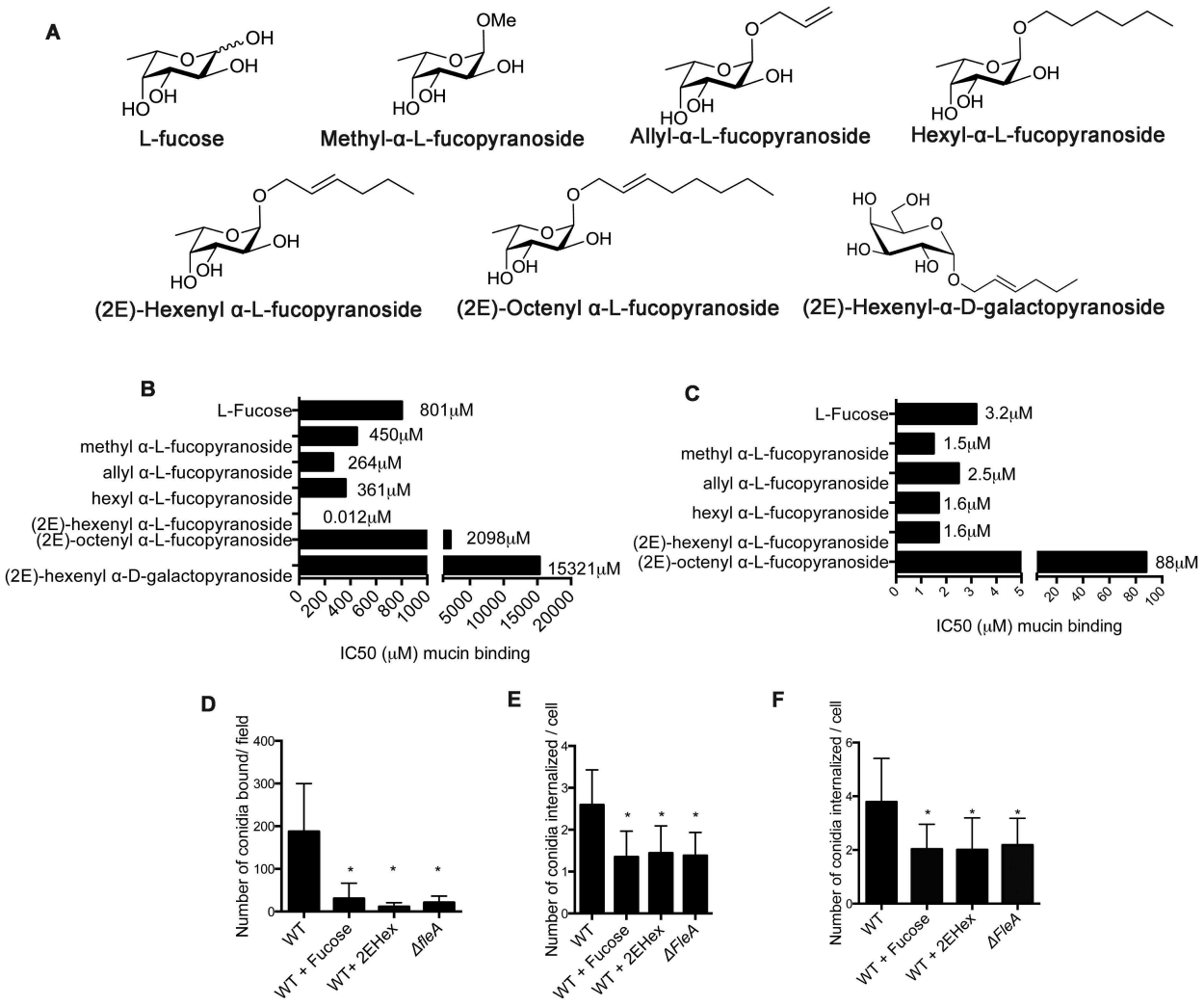

Figure 6. Inhibition of FleA by 2EHex or fucose results in a loss of mucin binding and greatly reduced phagocytosis by macrophages.

(A) Structures of fucopyranoside compounds. **(B)** Amount of compound required to inhibit binding of labeled FleA to mucin by 50% (IC50 [μM]). Addition of a methyl or allyl group to the anomeric position of fucose (methyl α-L-fucopyranoside, allyl α-L-fucopyranoside) improves inhibition by 2-4 fold but inclusion of a longer (6-carbon) unsaturated chain improves inhibition by 3 orders of magnitude. Removing the double bond or extending the

carbon chain beyond 6 carbons (hexyl α-L-fucopyranoside, (2E)-octenyl α-L-fucopyranoside) markedly decreases inhibition. (2E)-hexenyl α-D-galactopyranoside has no effect on FleA binding to mucin. **(C**) Amount of compound required to inhibit PAIIL binding to mucin by 50% (IC50 [μM]). 2EHex does not have a strong inhibitory effect on PAIIL-mucin interactions. **(D)** Inhibiting WT conidia with 10mM 2EHex or 100mM fucose significantly reduced binding of conidia to mucin. WT conidia were poorly phagocytosed in the presence of 2EHex or fucose by RAW264.7 cells **(E)** or primary human macrophages **(F)**. The data shown in D and E (6 replicates) reflects the mean ± SD of three independent experiments whereas the data in panel F (6 replicates) reflects the mean ± SD of three independent donors. *Denotes significantly different from control, p=<0.05.

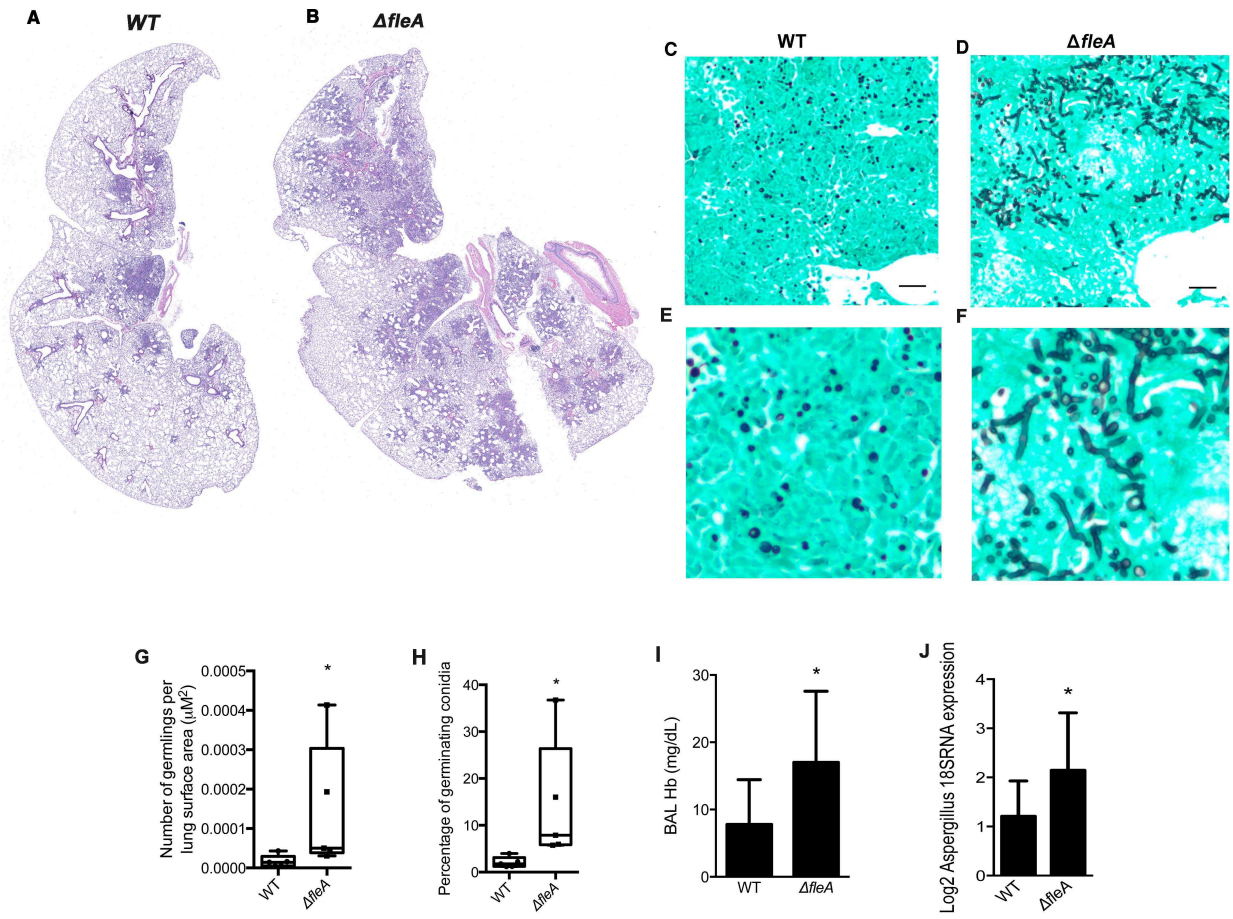

Figure 7. Mice infected with FleA-deficient *A. fumigatus* conidia have more severe *Aspergillus* lung infection.

(A) Section of whole mouse lung after infection with WT conidia. **(B)** Section of whole mouse lung after infection with *ΔfleA* conidia. **(C)(D)** GMS stained sections (20x image) of mouse lung after intranasal infection with WT conidia or *ΔfleA* conidia. **(E)(F)** GMS stained sections (zoom image) of mouse lung after intranasal infection with WT conidia or *ΔfleA* conidia. **(G)** Germination of *A. fumigatus* conidia in the lungs of mice infected with WT or *ΔfleA* conidia. The tissue is stained with GMS and the number of germinating conidia are quantified in at least 20 high power fields per mouse using lung surface area

(μM^2) as a reference (n = 5 mice per group). **(H)** The percentage of germinating *A. fumigatus* conidia in the lungs of mice infected with WT or *ΔfleA* conidia. Germinating conidia are significantly more prevalent in the lungs of mice infected with *ΔfleA* conidia (n = 5 mice per group). **(I)** Hemoglobin concentration is significantly higher in lung lavage from mice infected with *ΔfleA* conidia than WT conidia (n=10 mice per group) **(J)**. Gene expression for *Aspergillus* 18S is significantly higher in lung homogenates from mice infected with *ΔfleA* conidia than from mice infected with WT conidia (n=10 per group). All mouse samples were harvested 3 days after infection. Scale bar is 10μM. Data are mean +/- SD. *Denotes significantly different from control, p=<0.05.

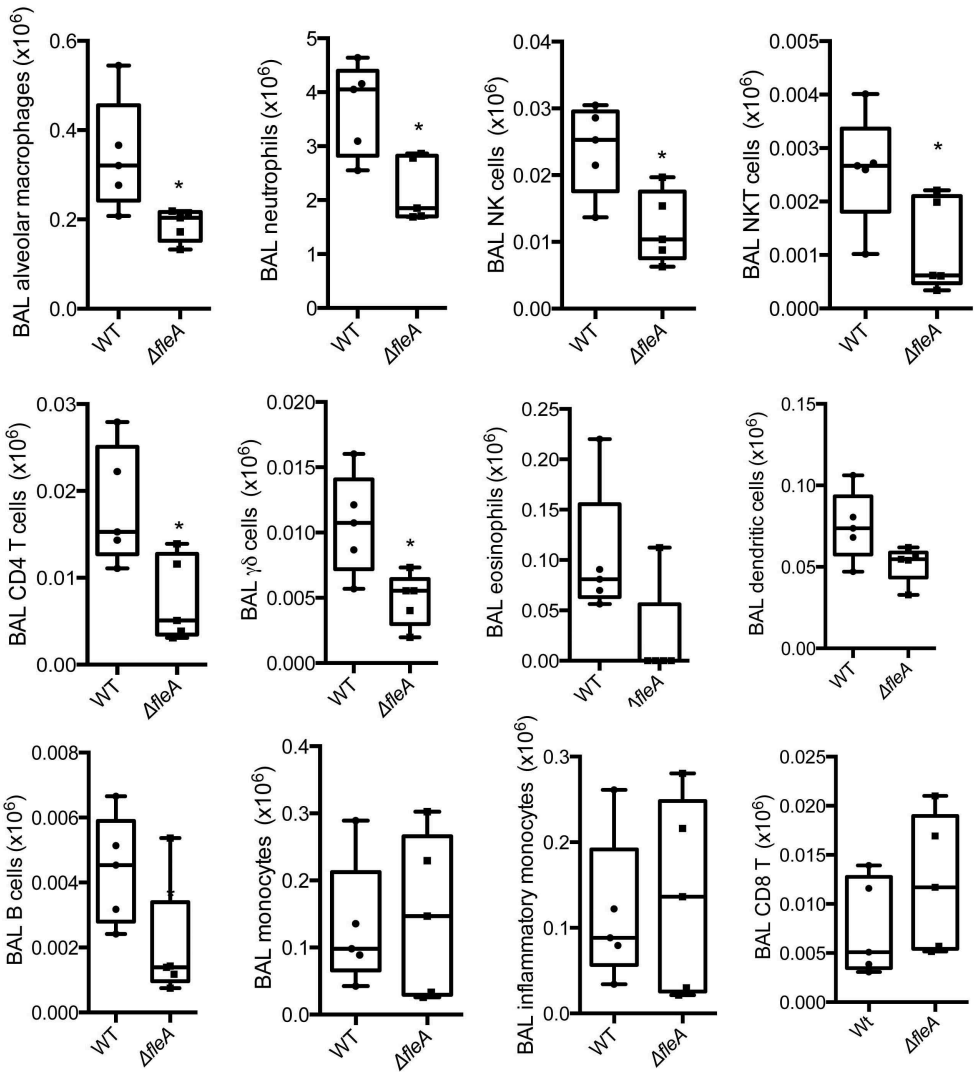

Figure 8. *ΔfleA* conidia treated animals have more severe lung injury and reduced recruitment of some immune cell types.

FACS-based identification and quantification of immune cells in bronchoalveolar lavage of mice infected with WT conidia or *ΔfleA* conidia (n=5 per group). All mouse samples were harvested 3 days after infection.

2.8. TABLES

Table 1. Luminex assay in BALF from WT and Δ*fleA* treated mice.

	WT Concentration	*ΔfleA* Concentration (pg/ml)	p value
Cytokines			
GM-CSF	27.6 ± 13.6	38.7 ± 16.1	0.27
IFN-γ	187.2 ± 91.6	118.1 ± 24.0	0.14
IL-1α	53.8 ± 13.24	66.7 ± 39.0	0.50
IL-1β	184.0 ± 27.9	181.6 ± 26.9	0.89
IL-2	93.5 ± 36.9	79.1 ± 8.4	0.42
IL-4	17.4 ± 2.6	20.1 ± 4.8	0.30
IL-5	93.5 ± 31.0	125.3 ± 95.0	0.50
IL-6	1444.86 ± 337.3	2571.2 ± 1242.4	0.09
IL-10	Below Range	Below Range	
IL-12	3330.1 ± 1338.4	2211.9 ± 839.2	0.15
IL-13	Below Range	Below Range	
IL-17	747.6 ± 541.7	495.8 ± 338.2	0.40
TNF-α	Above Range	Above Range	
Chemokines			
MIP-1α	4453.4 ±1354.3	9797.4 ± 8686.9	0.12
MCP-1	2581.7 ± 1065.8	7834.7 ± 4540.6	0.22
IP-10	15344.8 ± 21573.5	4375 .2 ± 4333.2	0.31
MIG	13497.9 ± 6266.1	6795.7 ± 5143.0	0.10
KC	Below Range	Below Range	0.14
Growth Factors			
FGF Basic	16.7 ± 5.2	19.8 ± 5.9	0.41
VEGF	2821.7 ± 552.5	3709.2 ± 38.9	0.09

Table 2. Strains used or developed in this study.

Fungal Strain	Genotype	Source or Reference
Aspergillus fumigatus		
AF293	Wild type	(45)
AF293.1	*pyrG1*	(46)
AF293.6	*pyrG1, argB1*	(45)
TJMP131.5	*pyrG1; AfpyrG::gpdA*(p):GFP:H2A	This study
TGJF5.3	*pyrG1, argB1; AfpyrG::gpdA*(p)::GFP::H2A	This study
TGJF6.7	*pyrG1, argB1; AfpyrG::gpdA*(p)::GFP::H2A, ∆*fleA::A. fumigatus argB*	This study
TGJF6.8	*pyrG1, argB1; AfpyrG::gpdA*(p)::GFP::H2A, ∆*fleA::A. fumigatus argB*	This study
TGJF6.13	*pyrG1, argB1; AfpyrG::gpdA*(p)::GFP::H2A, ∆*fleA::A. fumigatus argB*	This study
TGJF7.11	*pyrG1, argB1, gpda*(p):*gfp*:H2A in pJMP51, *pyrG* from *A. fumi, fleA:rfp:argB* from *A. fumi*	This study
TGJF7.15	*pyrG1, argB1, gpda*(p):*gfp*:H2A in pJMP51, *pyrG* from *A. fumi, fleA:rfp:argB* from *A. fumi*	This study
Aspergillus flavus		
CA14	Wild type	(47)
∆ku70∆pyrG	*ΔpyrG::cypA; ΔnkuA*	(32)
TKJA13.1	*ΔpyrG::cypA; ΔnkuA::fumi pyrG*	(48)
TFYL62.1	*ΔfleA::fumi pyrG; ΔpyrG::cypA. ΔnkuA*	This study
TFYL62.2	*ΔfleA::fumi pyrG; ΔpyrG::cypA. ΔnkuA*	This study
TFYL62.3	*ΔfleA::fumi pyrG; ΔpyrG::cypA. ΔnkuA*	This study

Table 3. Primers and plasmids used in this study.

Primer/Plasmid	Sequence	Purpose
GF FleA del F (P1)	**5'-**CATTAGGTGCATATGACGTG**-3'**	5' Flank
GF FleA del F (P2)	**5'-**GGCCTTAGAAGAGTCAGTC**-3'**	Cassette
GF FleA del R (P3)	**5'-** GAAAATTTGTCTTGGATGCAGACCGCG	5' Flank
GF A. fumi argB F (P4)	**5'-**GAACGCGGTCTGCATCCAAG**-3'**	argB
GF A. fumi argB R (P5)	**5'-**GAAGGAGAGACCCATACATCC**-3'**	argB
GF FleA del F (P6)	**5'-** GATCAAATGGATGTATGGGTCTCTCCT	3' Flank
GF FleA del R (P7)	**5'-**GGGAACATGTACGTGCTAG**-3'**	Cassette
GF FleA del R (P8)	**5'-**GGATGAGATCCTCCTTGTAG**-3'**	3' Flank, 3' *fleA* RFP
GF argB QC F (pGJF7)	**5'-** CGTTAAAAGTTCCGTGGAGTTACCAG TG	pGJF7.2 Plasmid
GF argB QC R (pGJF6-7)	**5'-** GCCCTCTGTCTGAGAGGAGGCACTGAT	pGJF7.2 Plasmid
GF FleA Native Tag P1	**5'-**GGAACAACCGTCTAGCTACATGC**-**	5' *fleA* RFP
GF FleA Native Tag P3 R	**5'-** GGCACCGGCTCCAGCGCCTGCACCAG	5' *fleA* RFP Flank
GF FleA Native Tag P6 F	**5'-** TCCTTCGCATCAGTGCCTCCTCTCAGA	3' *fleA* RFP Flank
GF/JP GFP/RFP F	5'- GGAGCTGGTGCAGGCGCTG	RFP/*argB* cassette
GF/JP GFP/RFP R	5'- CTGTCTGAGAGGAGGCACTG**-3'**	RFP/*argB* cassette

GF FleA Native Tag P2F	5’-GGCCTCAATGGCCTCTATGC-**3’**	RFP cassette fusion
JP AfpyrG ClaI For	**5’-**GAGAATATCGATCCTCAAACAATGCT	AfpyrG
JP AfpyrG ClaI Rev	**5’-**	AfpyrG
pGJF7.2	Plasmid	RFP*:argB* tag
pJMP51	Plasmid	Histone GFP
FY AFLA FleA 5’ FOR	**5’-**GGTGGAGACTCGATACAGCTC**-3’**	5’ flank
FY AFLA FleA 5’ REV	**5’-**GAAGAGGGTGAAGAGCATTGTTTGAGG	5’ flank
FY AFLA FleA 3’ FOR	**5’-**GACGACAATACCTCCCGACGATACCTG	3’ flank
FY AFLA FleA 3’ REV	**5’-**CGCCATTAACCCTCATCGCTG**-3’**	3’ flank
FY AFLA FleA Nest FOR	**5’-**GGCCAAGGTGCTCTAGCC**-3’**	Whole deletion
FY AFLA FleA Nest REV	**5’-**CGGACACGATGGAGGGTCG**-3’**	Whole deletion
KS Afu pyrG FOR	**5’-**TGCCTCAAACAATGCTCTTC**-3’**	A. fumigatus
KS Afu pyrG REV	**5’-**CCAGGTATCGTCGGGAGGT**-3’**	A. fumigatus
18S RNA forward	**5’-**ACGAGACCTCGGCCCTTA**-3’**	5’ flank
18S RNA reverse	**5’-**AGGGCATCACAGACCTGTT**-3’**	3’ flank
18S RNA probe	**5’-**CTATCGGCTCAAGCCGATGGAAG**-**	qPCR
HPRT forward	**5’-**AGGTTGCAAGCTTGCTGGT**-3’**	5’ flank
HRPT reverse	**5’-**	3’ flank
HPRT probe	**5’-**TGTTGGATACAGGCCAGACTTTGT**-**	qPCR

2.9. SUPPLEMENTARY FIGURES AND LEGENDS

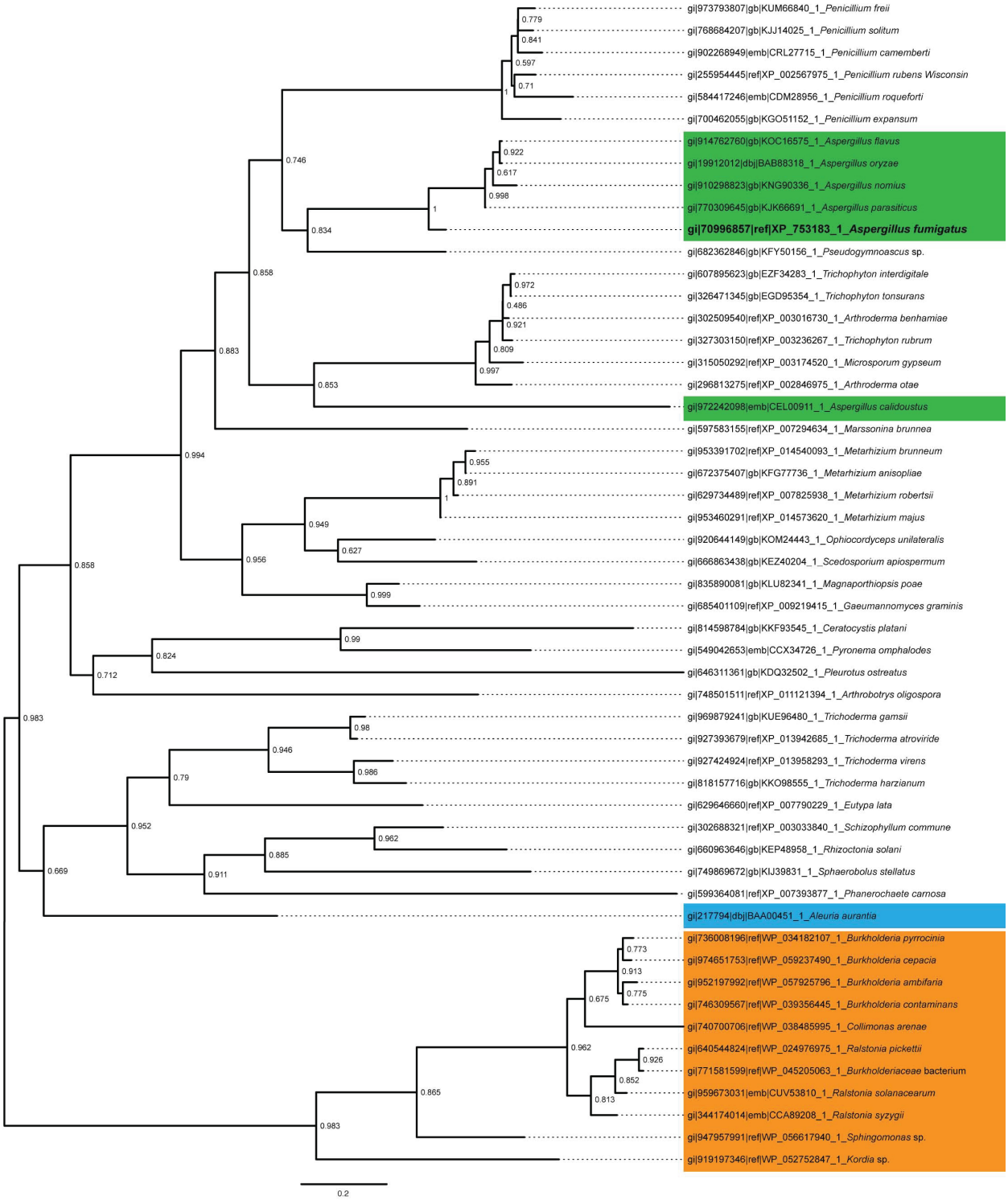

Supplemental Figure 1. Phylogenetic analysis of fucose-binding lectins using FastTree Neighbor-Joining method.

Aspergillus and bacterial fucose-binding lectins are highlighted in green and orange boxes, respectively. *Aleuria aurantia* lectin (AAL) was used to BLAST fungal and bacterial fucose-binding lectin protein sequences deposited in NCBI (blue box). A multiple sequence alignment of the selected sequences was used to identify the conserved region among bacterial and fungal sequences, which was extracted and subsequently used for phylogenetic analysis. Bootstrap values are presented at nodes.

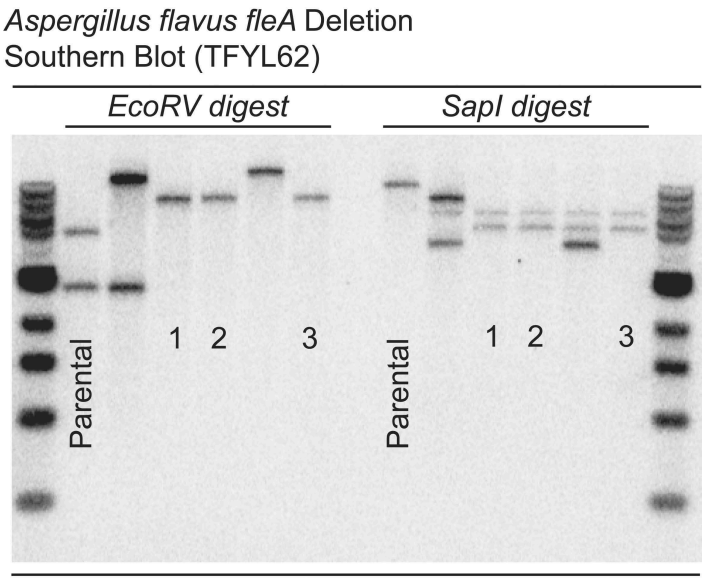

Supplemental Figure 2. Generation of Δ*fleA* condia in *A. flavus*.

Southern blot depicting successful deletion of *fleA* in *A. flavus*. This work was completed by FangYun Lim.

Supplemental Text 1. Detailed Material and Methods.

Phylogenetic analysis of fucose-binding lectins using FastTree Neighbor-Joining method

Phylogenetic analysis of fucose-specific lectins was carried out based on previous homology searches to *Aleuria aurantia* lectin (AAL; protein sequence BAA00451 (11, 18)). The AAL protein sequence was used to identify fungal and bacterial sequences from the National Center for the Biotechnology Information (NCBI) database by performing a protein BLAST search. A sole bacterial fucose-binding lectin was identified in *Ralstonia solanacearum* (RSL; protein sequence CUV53810.1), which was used to subsequently BLAST bacterial sequences. Bacterial and fungal sequences with an e-value less than or equal to $1x10^{-10}$ were included in subsequent steps. An initial multiple sequence alignment of complete sequences was performed using MAFFT (http://mafft.cbrc.jp/alignment/software/) (49). Using the AliView multiple sequence alignment editor (50), the conserved region among bacterial and fungal sequences was extracted and run through FastTree (http://www.microbesonline.org/fasttree/) (51) to compute a phylogenetic tree based on the Neighbor-Joining method. Results were visualized using FigTree (http://tree.bio.ed.ac.uk/soft- ware/figtree/) and midpoint rooted.

Sputum Induction

Sputum inductions were performed according to standard protocols (27). Briefly, subjects inhaled a nebulized solution of 3% saline through a mouthpiece for 20 minutes, pausing every 2 minutes to spit saliva into a saliva cup and sputum into a sputum cup. A 1ml aliquot of sputum was processed for total and differential cell counts by the addition of 10% Sputolysin (EMD Millipore, Billerica, MA) at a 1:1 g/ml (sputum weight: Sputolysin)

ratio, mixing with a pipette and incubating at 37^{o}C with agitation. Samples were removed for additional physical mixing every 5 minutes for a total of 15 minutes and used for measurement of cell differentials. Samples containing less than 50% squamous cells were approved for mucin purification. An equal volume of 8M guanidine hydrochloride was added to the remainder of the sputum and rotated at 4^{o}C until homogenized.

Purification of high molecular weight mucin from sputum

High molecular weight mucin was purified from induced sputum from healthy subjects, as described previously (29). Briefly, sputum samples mixed with 8M GuHCl in a 1:1 ratio were subjected to a cesium chloride gradient with a density of 1.4 g/mL to separate the mucins from proteins, glycoproteins and nucleic acids. Carbohydrate-rich fractions as confirmed by slot blotting with PAS detection pertaining to 1.3-1.47 g/mL were then subjected to gel filtration on a Sepharose CL4B column in 50 mM Tris, 100mM KCl pH 7.5. Undegraded mucins identified by PAS staining on a slot blot were present in the Vo fraction of this column. This material was then desalted on Sephadex G25 prior to freeze drying and quantified by dried weight.

Mucin plate- binding assay

Recombinant FleA (prepared as (18)) was incubated with 100 mM fucose in PBS for 1 hour then biotinylated with EZ-link sulfo NHS biotin (Pierce, Thermo Fisher, Rockford, IL) according to manufacturers instructions. Labeled protein was dialysed against TBS to remove fucose. Purified human mucin was coated on a Nunc maxisorp plate at 20 µg/ml in carbonate bicarbonate buffer pH 9.6 overnight at 4^{o}C. After washing with TBS + 0.05%

Tween-20, 10 mM $CaCl_2$, 3% BSA, plates were blocked with the same buffer. Biotinylated recombinant FleA was incubated at 5 μg/ml in TBS + 0.05% Tween-20, 10 mM $CaCl_2$, 1% BSA (binding buffer) in the presence or absence of 100 mM fucose or 100 mM galactose. For inhibition assays, recombinant FleA was incubated with a dilution series of synthesized carbohydrate compounds starting at 5 mM. Plates were washed three times with binding buffer and incubated with ExtrAvidin-alkaline phosphatase (Sigma-Aldrich, St Louis, MO) at 1:10000 in binding buffer. After three washes with binding buffer, the plates were detected using Phosphatase substrate (Sigma-Aldrich, St Louis, MO) in carbonate bicarbonate buffer pH 9.6 + 1 mM $MgCl_2$ and read at 405nm in a Biotek Synergy plate reader (Biotek, Winooski, VT).

General Methods

Unless noted, chemical reagents and solvents were used without further purification from commercial sources. Full description of the general methods for carbohydrate synthesis can be found online at: http://journals.plos.org/plospathogens/article/asset?unique&id=info:doi/10.1371/journal.ppat.1005555.s007.

Aspergillus *strains and culture*

All strains utilized or developed are listed in Table 2. Unless noted, all *A. fumigatus* strains were propagated on solid glucose minimal media (GMM) at 37°C (31). *A. fumigatus* asexual spores were collected in water supplemented with 0.01% Tween 80, counted using a hemocytometer, and maintained at -80°C in 50% glycerol. Fixed spore

suspensions were prepared as follows: 1 x 10^9 spores were added to a 4% formaldehyde solution prepared in 1x PBS and allowed to incubate for 30 minutes at room temperature. Aldehydes were quenched by adding glycine to a final concentration of 100 mM and incubated at room temperature for an additional 10 minutes. Conidia were washed via centrifugation in Tween water three times and resuspended to a final concentration of 1 X 10^8 spores/mL using Tween water. Killing of spores was confirmed by lack of growth on GMM media after three days.

Generation of FleA mutant conidia

Construction, isolation, and maintenance of fusion PCR products was carried out according to standard methods (52). Primers used are listed in Table 3. Genomic DNA was isolated from lyophilized hyphal tissue as previously described (53). The ORF of *A. fumigatus fleA* (Afu5g14740) was identified via the AspGD database (http://www.aspergillusgenome.org).

Nuclear-tagged GFP *A. fumigatus* strains were created by transforming *A. fumigatus* with a plasmid termed pJMP51 containing histone H2A N-terminally fused to GFP driven by the constitutive *gpdA* promoter (*gpdA(p)*::GFP::H2A) and harboring the *A. fumigatus pyrG* gene for selection. Briefly, pJMP51 was created from pSK505 (54) which already contained the *gpdA(p)*::GFP::H2A cassette by enzymatic digestion with *ClaI*. A *ClaI-ClaI* fragment of *Aspergillus fumigatus pyrG* was then amplified with the primer pair "JP AfpyrG ClaI For/Rev" and sub-cloned into the *ClaI* site to create pJMP51. pJMP51 was used to transform AF293.1 and AF293.6 to construct TJMP131.5 (*GFP::H2A*) and TGJF5.3

(*GFP::H2A, argB1*) respectively. Integration was confirmed by Southern blot (data not shown) and nuclear GFP signal confirmed via microscopy. We then generated a gene disruption cassette for *fleA* using published protocols [13] and transformed the cassette into TGJF5.3 to create TGJF6.7 (*GFP::H2A,* Δ*fleA*). The *fleA* disruption cassette was constructed by fusion of a 2kb region upstream and downstream of the *fleA* open reading frame amplified using "GF FleA del F (P1)" with "GF FleA del R (P3)" and "GF FleA del F (P6)" with "GF FleA del P8 R", respectively. The *A. fumigatus argB* gene was amplified via genomic DNA using "GF A. fumi argB F (P4)" with "GF A. fumi argB R (P5)" and fused to the flanking *fleA* PCR fragments using "GF FleA del F (P2)" and "GF FleA del P7 R" primers via fusion PCR (55). Deletion of *fleA* was confirmed by Southern and northern blot (Figure 2B,C).

To identify FleA localization, the native *fleA* locus was tagged with RFP through double homologous recombination using the *A. fumigatus argB* gene as a marker. For RFP tagging, the auxotrophic marker, *pyrG,* was replaced with *A. fumigatus argB* within pXDRFP4 (56) via QuickChange site-directed mutagenesis (57) using the primer pair "GF argB QC F (pGJF7)" and "GF argB QC R (pGJF6-7)", yielding the plasmid, pGJF7.2. A gene disruption cassette was developed as described for deletion of *fleA.* Briefly, a 2kb region upstream and downstream of the *fleA* stop codon was amplified using "GF FleA Native Tag P1" with "GF FleA Native Tag P3" and "GF FleA Native Tag P6" with "GF FleA del P8 R", respectively. An *rfp/argB* cassette was amplified from pGJF7.2 using "GF/JP GFP/RFP F" with "GF/JP GFP/RFP R" and fused to the flanking *fleA* PCR fragments using "GF FleA Native Tag P2" and "GF FleA del P7" primers via fusion PCR [13].

TGJF5.3 was then transformed using the cassette yielding the prototrophic *fleA:RFP* strain, TGJF7.11. FleA tagging was confirmed microscopically and using Southern and northern blots (Figure 2 D,E).

The *fleA* deletion mutants in *A. flavus* were made by targeted integration of a deletion cassette via transformation. To construct the *fleA* deletion cassette in *A. flavus*, a 1.0 - 1.5 kb region flanking the *fleA* open reading frame was amplified from gDNA (5' Flank: "FY AFLA FleA 5' FOR" with "FY AFLA FleA 5' REV", 3' Flank: "FY AFLA FleA 3' FOR" with "FY AFLA FleA 3' REV"). The flanking fragments were fused to the selectable auxotrophic marker (*A. fumigatus pyrG,* amplified with primer pair "KS Afu pyrG FOR" and "KS Afu pyrG REV") using a double-joint fusion PCR approach ("FY AFLA FleA Nest FOR" with "FY AFLA FleA Nest REV") as described above. The deletion construct was transformed into parental strain CA14Δ*ku70*Δ*pyrG* (32) to create strains TFYL62.1-62.3. Single integration of the deletion cassette was verified via Southern analysis using two distinct restriction digests (Supplemental Figure 2).

Immunofluorescence of Aspergillus *conidia*

For imaging of spores, *A. fumigatus* strains were cultured on GMM at 37°C for 3 days, and spores harvested in 0.1% Tween 20. 2µl of spore suspension was plated on a pre-cleaned glass slide with 15 µL of H_2O spotted in the center of the slide, a coverslip was added, and sealed with nail polish. Images were taken using a Nikon T*i* inverted microscope equipped with a Nikon Plan Apo VC 60x/1.40 Oil DIC/∞/0.17 WD objective and a Nikon Intensilight C-HGFIE light source using the Nikon NIS-Elements Advanced

Research V3.22 software package. Microscope settings were kept identical for all images. Time-course microscopy was carried out over 27 hours at 37°C to monitor FleA production on hyphae, resting conidia, and swollen conidia using the Nikon NIS Elements-AR software package (v.4.3). The average fluorescent intensity at each developmental state (resting conidia, swollen conidia, and hyphae) of untagged FleA (TJMP131.5 or wild type) was subtracted from the mean fluorescent intensity value of two different transformants (TGJF7.11 and TGJF7.15) expressing RFP-tagged versions of FleA. The adjusted mean fluorescence was then standardized to area. The adjusted fluorescence/area of the different developmental states were then compared using the Student's T-test ($n \geq 13$).

Western blot of A. fumigatus *extracts and supernatant*

Resting and swollen *A. fumigatus* conidia and hyphae were isolated from WT and *ΔfleA* cultures. Resting conidia grown on solid GMM were immediately collected in liquid GMM, enumerated, and diluted to a final concentration of $8.3x10^6$ spores/mL. Six milliliters of spore suspension ($5x10^7$ spores) was separated from supernatant via centrifugation at 13,000 RPM for 5 minutes and resting conidia supernatant immediately frozen. For swollen conidia, $5X10^7$ spores were inoculated in 50 mL liquid GMM ($1X10^6$ spores/mL) and grown 6 hours at 37°C, after which swollen spore tissue was separated from supernatant as described above. Hyphal tissue and supernatant was collected from identical growth conditions after 24 hours at 37°C. Hyphal tissue was lyophilized and ground to a fine powder. Tissue from resting and swollen conidia and 100 µL of ground hyphal powder were resuspended in 1 mL 50mM Tris/HCl pH 7.4, 50 mM EDTA, 2% SDS,

and 40 mM β-Mercaptoethanol and homogenized using sterile 0.5 mm beads and beat for 5 minutes. After, extracts were boiled for 1 hour and centrifuged to remove insoluble material. Protein concentrations were determined by BCA assay and 15 µg of protein was loaded into each well of a 4-12% BOLT SDS PAGE gel (Life Technologies, Grand Island, NY) and electrophoresed under reducing conditions. The gel was then blotted onto nitrocellulose, blocked with 5% non fat milk for 2 hours and stained with an anti-FleA rabbit polyclonal antibody at 1µg/ml [1] and donkey anti-rabbit HRP (Jackson Immunoresearch, West Grove, PA) prior to chemiluminescent detection. Culture supernatants were filtered through a 0.2 µM filter and concentrated 10x in a 0.5 ml 3 kDa, MWCO Amicon Ultra (EMD Millipore, Billirica, MA) before being run as described above.

Mucin conidia binding assay

8 well glass chamber slides (Labtek, Scotts Valley, CA) were coated with 20 µg/ml purified human mucin in MilliQ dH_2O overnight at 37^{o}C until material was dried onto surface. The slide was then blocked in PBS + 1% BSA for 1 hour at room temperature. Fixed conidia suspensions were centrifuged at 6000 x g for 5 minutes to pellet and resuspended in PBS + 1% BSA in the presence or absence of 10 mM (2E)-hexenyl α-L-fucopyranoside (2EHex) or 100 mM fucose. $2x10^7$ conidia were added per well and incubated for 4 hours at room temperature. Unbound conidia were removed by washing in PBS+ BSA, the slides were mounted in Prolong Gold anti-fade reagent (Life Technologies, Grand Island, NY) and allowed to cure for 24 hours prior to sealing. Images were acquired using an FV10i confocal microscope (Olympus, Center Valley, PA) using the multipoint Z-stack

mode to acquire 9 fields per well with 3 wells imaged per condition per experiment. Each Z-stack image was compressed into a single plane of focus and conidia were counted using NIH Image J with the ITCN plugin. Each experiment was repeated at least 3 times. *A. flavus*-mucin interactions were investigated as described above with one exception. These conidia lack GFP so were stained with Calcofluor white for 5 minutes to allow imaging prior to adding to mucin-coated slides.

Cell culture

RAW 264.7 cells were obtained from the UCSF cell culture facility and maintained in DMEM + 10% fetal bovine serum + 1% penicillin/streptomycin. Cells were seeded and grown on 8 well chamber slides (Labtek, Scotts Valley, CA) overnight prior to use in assays. Primary alveolar macrophages were obtained from bronchoalveolar lavage (BAL) taken during research bronchoscopy. BAL was centrifuged at 450 x g for 10 minutes and cells were washed with PBS prior to plating on poly-L-lysine coated 8 well chamber slides in RPMI 1640+ 10% fetal bovine serum + 1% penicillin/streptomycin + 0.5 μg/ ml amphotericin B. Cells were washed after 2 hours of adherence and cultured overnight prior to use in experiments. All cell culture reagents were purchased from Life Technologies, Grand Island, NY.

Flow cytometry analysis of macrophages

Recombinant FleA was tagged with Alexa-488 using the microscale labeling kit according to manufacturers instructions (Life Technologies, Grand Island NY). RAW264.7 macrophages were harvested by scraping or primary human lung macrophages were

freshly isolated from bronchoalveolar lavage from research bronchoscopy. $5x10^5$ cells per sample were washed with PBS and incubated with 20 μg/ml recombinant FleA-488 in PBS + 0.25% BSA + 0.02% sodium azide (PBA) on ice, in the dark for 1 hour. Controls included unstained cells and FleA in the presence of 100 mM fucose. Cells were washed three times in PBA and fixed in 4% paraformaldehyde for 20 minutes at room temperature. Cells were analyzed using a FACScalibur (Beckton Dickenson, San Jose, CA) and Flow Jo software (Treestar, Ashland, OR).

Confocal phagocytosis assay

RAW 264.7 cells were plated at $5x10^4$ per well of an 8 well chamber slide (Labtek, Scotts Valley, CA) and allowed to grow overnight in culture media. $5x10^6$ conidia from either the PFA fixed WT or *ΔfleA* strain were added per well in a 1:10 dilution of growth media in the presence or absence of 10 mM (2E)-hexenyl α-L-fucopyranoside or 500 mM fucose and incubated at 37°C for 1 hour. Wells were washed gently with warm media and incubated for a further 2 hours at 37°C for complete uptake. Cells were then incubated with a 7.5 μg/ml solution of CellMask Deep Red plasma membrane stain (Life Technologies, Grand Island, NY) for 5 minutes at 37°C, prior to staining with calcofluor white for 1 minute at room temperature (Sigma, St Louis, MO), washing with PBS and mounting with Fluoromount-G (Southern Biotech, Birmingham, AL). Z-stack images were acquired using an FV10i confocal microscope (Olympus, Center Valley, PA). Each Z-stack image was compressed into a single plane of focus and conidia were manually counted using NIH Image J with the cell counter plugin. Internalized conidia were counted as conidia within the boundary of the cell that were not stained with Calcofluor white.

Calcofluor white stained cells were excluded from the count. For primary human alveolar macrophages, cells were plated at $5x10^5$ per well on a poly-L-lysine coated 8 well chamber slide (Labtek, Scotts Valley, CA) and allowed to grow overnight in culture media. $1.5x10^6$ conidia from either the PFA fixed WT or *ΔfleA* strains were added per well in a 1:10 dilution of growth media in the presence or absence of 10 mM (2E)-hexenyl α-L-fucopyranoside or 500 mM fucose, incubated at 37°C for 30 minutes then washed, stained and mounted as described above.

Flow cytometry analysis of A. fumigatus *conidia*

Recombinant Dectin-1 was purchased from R&D Systems (Minneapolis, MN) and biotinylated using the EZ-link sulfo NHS biotin kit (Thermo Fisher Waltham, MA) according to manufacturers recommendations. $1x10^7$ WT or *ΔfleA* conidia were centrifuged and resuspended in a solution of 20 μg/ml biotinylated Dectin-1 in PBS for 1 hour at 4°C. Conidia were washed in PBS and the Dectin-1 detected using Streptavidin-PE (Biolegend, San Diego, CA) in PBS at 20 μg/ml for a further 1 hour at 4°C. Conidia were washed in PBS then fixed in 4% paraformaldehyde prior to analysis on a Becton Dickenson FACSCalibur and FlowJo software (TreeStar, Ashland, OR).

Phagocytosis of FleA-coated particles

Yellow-green 1μM sulfate treated FluoSpheres (Life Technologies, Grand Island, NY) were coated with 50μg/ml recombinant FleA in H_2O and incubated for 2 hours at room temperature. Beads were washed 3 times to remove unattached protein and resuspended in 1:10 dilution of RAW264.7 growth media in the presence or absence of 500 mM fucose

and incubated for 30 minutes with agitation. FluoSpheres were added to RAW264.7 cells at a ratio of 10:1 and incubated with agitation for 2 hours at 37^{o}C prior to extensive washing with DMEM to remove unattached FluoSpheres from the cell surface. Cells were fixed in 4% paraformaldehyde prior to analysis on a Becton Dickenson FACSCalibur and FlowJo software (TreeStar, Ashland, OR).

Mice

Male C57BL/6 mice were purchased from Charles River Laboratories (Wilmington, Massachusetts, MA) and housed in a specific pathogen free facility at the University of California, San Francisco (UCSF). Animal experiments followed protocols approved by the UCSF Institutional Animal Care and Use Committee.

Mouse model of Aspergillus *infection*

Eight to ten week old C57BL/6 mice (Charles River Laboratories, Hollister, CA), were anaesthetized with isoflurane and infected intranasally with 5x10^{7} of either WT or *ΔfleA* conidia. Mice were sacrificed 3 days post infection. For the first experiment, 5 mice were treated per group and analyzed by flow cytometry for lung inflammation with histology, qPCR and hemoglobin measurements made for assessment of fungal burden and invasive disease. For the second experiment 10 mice were treated per group and analysis focused on fungal burden, hemoglobin measurements and histological outcomes. The left lung lobe was snap frozen in liquid nitrogen for RNA analysis. The remaining lung lobes were either fixed for histology analysis or used for flow cytometry analysis. For histology, lung lobes were fixed in 4% PFA and subsequently embedded into paraffin,

sectioned and stained for H&E or Grocott's Methanamine Silver (GMS) stain by the UCSF Pathology core. Snap frozen lung was homogenized in 1.2 ml of RLT (Qiagen, Valencia, CA) containing 0.14 M β-ME using Tissumizer (Tekmar, Cincinnati, Ohio). From that lysate, 600 µl was spun at 20,000 x g for 3 minutes. RNA was purified from the clarified lysate using the RNeasy mini kit with on-column DNase digestion (Qiagen, Valencia, CA) according to manufacturer's protocol. 1 µg of RNA was used to make cDNA with the iScript cDNA kit (Biorad, Hercules, CA) following manufacturer's protocols. Real-time qPCR was performed using 2 µl of cDNA in a 25 µl reaction to measure the relative levels of *Aspergillus* 18S RNA. The HPRT gene was used as a loading control to normalize the amount of cDNA input in the PCR reaction. All primer sequences used are shown in the Supplemental Table 3.

Bronchoalveolar lavage (BAL) was performed with 1 ml of ice cold PBS + 2% FBS. BAL was centrifuged at 1500 rpm for 5 minutes at 4^{o}C. The supernatant was removed and 10 µL was used to measure the hemoglobin (Hb) concentration using a Plasma / Low Hb Photometer (HemoCue AB, Angelholm, Sweden). Two million BAL cells were transferred into V-bottomed 96 well plates for flow cytometric staining and analysis. Cells were spun down and resuspended in 25 µl/well FACS buffer (PBS with 2% FBS, 1mM EDTA and 0.1% sodium azide) containing Fc receptor (CD16/32) blocking antibody (clone 2.4G2). After 15 min incubation on ice, fluorescent-conjugated antibodies diluted in 25 µl/well FACS buffer were added to the cells for 45 mins on ice. The cells were washed twice with 200 µl/well FACS buffer and resuspended in 100 µl/well FACS buffer containing propidium iodide (0.5 µg/ml) for live/dead discrimination. Samples were acquired on an LSRFortessa cell analyzer (BD Biosciences) in the DERC Flow Cytometry and Cell

Sorting Core Facility at UCSF. Data analysis was done using FlowJo software (TreeStar, Ashland, OR). Antibodies used for flow cytometric staining were: CD11c (clone HL3), F4/80 (clone CI:A3-1), CD11b (clone M1/70), MHCII (clone M5/114.15.2), Ly6G (clone 1A8), Ly6C (HK1.4), NK1.1 (PK136), TCRβ (H57-597), B220, CD4 and CD8. Antibodies were purchased from BD Biosciences, eBiosciences or Biolegend.

Quantification of conidia germination

GM*S* stained slides of mouse lung infected with WT or *ΔfleA* conidia (n=5 per group) were examined at 20X using an integrated microscope (Olympus, Albertslund, Denmark), video camera (JVC Digital Color; JVC, Tatstrup, Denmark), automated microscope stage, and computer (Dell Optiplex GS270 PC running Computer-Assisted Stereology Toolbox (CAST) software; Olympus, Albertslund, Denmark) (58). For each slide, the software systematically selected at least 20 fields, and the number of conidia and the number of germlings were counted in each field.

Number of conidia: The number of germlings was expressed as the number per lung surface area (μM^2). The surface area of lung tissue was quantified using the point-counting and line-segment grid tools available in the CAST software.

Percentage of germinating conidia: The percentage of germinating conidia was calculated as the number of germinating conidia divided by the sum of non-germinating and germinating conidia (x100).

Statistical methods

Data analyses were performed GraphPad Prism version 6 (GraphPad, San Diego, CA). ANOVA was used for three-group comparisons followed by pairwise analyses with the Tukey multiple comparisons test when appropriate. Two group comparisons were made using Students t-test or for non parametric analyses, a ranked Mann-Whitney test.

Accession numbers

FleA, A. fumigatus, NC_007198.1, XP_753183.1

FleA, A. flavus, NW_002477244.1, XP_002380155.1

PAIIL, NC_002516.2 NP_252051.1

Dectin-1, NM_022570.4, NP_072092.2

MUC5AC, NM_001304359.1, NP_001291288.1

MUC5B, NM_002458.2, NP_002449.2

2.10. REFERENCES

1. **Dagenais TRT**, **Keller NP**. 2009. Pathogenesis of *Aspergillus fumigatus* in invasive aspergillosis. Clin Microbiol Rev **22**:447–465.

2. **Bhatia S**, **Fei M**, **Yarlagadda M**, **Qi Z**, **Akira S**, **Saijo S**, **Iwakura Y**, **van Rooijen N**, **Gibson GA**, **St. Croix CM**, **Ray A**, **Ray P**. 2011. Rapid host defense against *Aspergillus fumigatus* involves alveolar macrophages with a predominance of alternatively activated phenotype. PLoS One **6**.

3. **Dubourdeau M**, **Athman R**, **Balloy V**, **Huerre M**, **Chignard M**, **Philpott DJ**, **Latge J-P**, **Ibrahim-Granet O**. 2006. *Aspergillus fumigatus* induces innate immune responses in alveolar macrophages through the MAPK pathway independently of TLR2 and TLR4. J Immunol **177**:3994–4001.

4. **Philippe B**, **Ibrahim-Granet O**, **Prevost MC**, **Gougerot-Pocidalo MA**, **Sanchez Perez M**, **Van der Meeren A**, **Latge JP**. 2003. Killing of *Aspergillus fumigatus* by alveolar macrophages is mediated by reactive oxidant intermediates. Infect Immun **71**:3034–3042.

5. **Saijo S**, **Iwakura Y**. 2011. Dectin-1 and Dectin-2 in innate immunity against fungi. Int Immunol **23**:467–472.

6. **Luther K**, **Torosantucci A**, **Brakhage AA**, **Heesemann J**, **Ebel F**. 2007. Phagocytosis of *Aspergillus fumigatus* conidia by murine macrophages involves recognition by the dectin-1 beta-glucan receptor and Toll-like receptor 2. Cell Microbiol **9**:368–381.

7. **Underhill DM**. 2004. Toll-like receptors and microbes take aim at each other. Curr Opin Immunol **16**:483–487.

8. **Willment JA**, **Brown GD**. 2008. C-type lectin receptors in antifungal immunity. Trends Microbiol **16**:27–32.

9. **Slesiona S**, **Gressler M**, **Mihlan M**, **Zaehle C**, **Schaller M**, **Barz D**, **Hube B**, **Jacobsen ID**, **Brock M**. 2012. Persistence versus escape: *Aspergillus terreus* and *Aspergillus fumigatus* employ different strategies during interactions with macrophages. PLoS One **7**:e31223.

10. **Gilboa-Garber N**. 1982. *Pseudomonas aeruginosa* lectins. Methods Enzymol **83**:378–385.

11. **Kostlanova N**, **Mitchell EP**, **Lortat-Jacob H**, **Oscarson S**, **Lahmann M**, **Gilboa-Garber N**, **Chambat G**, **Wimmerova M**, **Imberty A**. 2005. The fucose-binding lectin from *Ralstonia solanacearum*. A new type of beta-propeller architecture formed by oligomerization and interacting with fucoside, fucosyllactose, and plant xyloglucan. J Biol Chem **280**:27839–27849.

12. **Ramphal R**, **Arora SK**. 2001. Recognition of mucin components by *Pseudomonas aeruginosa*. Glycoconj J **18**:709–713.

13. **Zinger-Yosovich K**, **Sudakevitz D**, **Imberty A**, **Garber NC**, **Gilboa-Garber N**. 2006. Production and properties of the native *Chromobacterium violaceum* fucose-binding lectin (CV-IIL) compared to homologous lectins of *Pseudomonas aeruginosa* (PA-IIL) and *Ralstonia solanacearum* (RS-IIL). Microbiology **152**:457–463.

14. **Sulak O**, **Cioci G**, **Delia M**, **Lahmann M**, **Varrot A**, **Imberty A**, **Wimmerova M**. 2010. A TNF-like trimeric lectin domain from *Burkholderia cenocepacia* with specificity for fucosylated human histo-blood group antigens. Structure **18**:59–72.

15. **Fukumori F**, **Takeuchi N**, **Hagiwara T**, **Ohbayashi H**, **Endo T**, **Kochibe N**, **Nagata Y**, **Kobata a**. 1990. Primary structure of a fucose-specific lectin obtained from a mushroom, *Aleuria aurantia*. J Biochem **107**:190–196.

16. **Ishida H, Moritani T, Hata Y, Kawato A, Suginami K, Abe Y, Imayasu S**. 2002. Molecular Cloning and Overexpression of *fleA* Gene Encoding a Fucose-specific Lectin of *Aspergillus oryzae*. Biosci Biotechnol Biochem **66**:1002–1008.

17. **Matsumura K**, **Higashida K**, **Hata Y**, **Kominami J**, **Nakamura-Tsuruta S**, **Hirabayashi J**. 2009. Comparative analysis of oligosaccharide specificities of fucose-specific lectins from *Aspergillus oryzae* and *Aleuria aurantia* using frontal affinity chromatography. Anal Biochem **386**:217–221.

18. **Houser J**, **Komarek J**, **Kostlanova N**, **Cioci G**, **Varrot A**, **Kerr SC**, **Lahmann M**, **Balloy V**, **Fahy J V.**, **Chignard M**, **Imberty A**, **Wimmerova M**. 2013. A soluble fucose-specific lectin from *Aspergillus fumigatus* conidia - Structure, specificity and possible role in fungal pathogenicity. PLoS One **8**:1–15.

19. **Wimmerova M**, **Mitchell E**, **Sanchez JF**, **Gautier C**, **Imberty A**. 2003. Crystal structure of fungal lectin. Six-bladed ß-propeller fold and novel fucose recognition mode for Aleuria aurantia lectin. J Biol Chem **278**:27059–27067.

20. **Houser J**, **Komarek J**, **Cioci G**, **Varrot A**, **Imberty A**, **Wimmerova M**. 2015. Structural insights into *Aspergillus fumigatus* lectin specificity: AFL binding sites are functionally non-equivalent. Acta Crystallogr D Biol Crystallogr **71**:442–453.

21. **Audfray A**, **Claudinon J**, **Abounit S**, **Ruvoen-Clouet N**, **Larson G**, **Smith DF**, **Wimmerova M**, **Le Pendu J**, **Romer W**, **Varrot A**, **Imberty A**. 2012. Fucose-binding lectin from opportunistic pathogen *Burkholderia ambifaria* binds to both plant and

human oligosaccharidic epitopes. J Biol Chem **287**:4335–4347.

22. **Rose MC**. 1992. Mucins: structure, function, and role in pulmonary diseases. Am J Physiol **263**:L413–29.

23. **Thornton DJ**, **Rousseau K**, **McGuckin MA**. 2008. Structure and function of the polymeric mucins in airways mucus. Annu Rev Physiol **70**:459–486.

24. **Xu X**, **Padilla MT**, **Li B**, **Wells A**, **Kato K**, **Tellez C**, **Belinsky SA**, **Kim KC**, **Lin Y**. 2014. MUC1 in macrophage: contributions to cigarette smoke-induced lung cancer. Cancer Res **74**:460–470.

25. **Roy MG, Livraghi-Butrico A, Fletcher AA, McElwee MM, Evans SE, Boerner RM, Alexander SN, Bellinghausen LK, Song AS, Petrova YM, Tuvim MJ, Adachi R, Romo I, Bordt AS, Bowden MG, Sisson JH, Woodruff PG, Thornton DJ, Rousseau K, De la Garza MM, Moghaddam SJ, Karmouty-Quintana H, Blackburn MR, Drouin SM, Davis CW, Terrell KA, Grubb BR, O'Neal WK, Flores SC, Cota-Gomez A, Lozupone CA, Donnelly JM, Watson AM, Hennessy CE, Keith RC, Yang I V, Barthel L, Henson PM, Janssen WJ, Schwartz DA, Boucher RC, Dickey BF, Evans CM**. 2014. Muc5b is required for airway defence. Nature 505:412–416.

26. **Kim KC**. 2012. Role of epithelial mucins during airway infection. Pulm Pharmacol Ther **25**:415–419.

27. **Peters MC**, **Mekonnen ZK**, **Yuan S**, **Bhakta NR**, **Woodruff PG**, **Fahy J V**. 2014. Measures of gene expression in sputum cells can identify TH2-high and TH2-low subtypes of asthma. J Allergy Clin Immunol **133**:388–394.

28. **Kerr SC**, **Carrington SD**, **Oscarson S**, **Gallagher ME**, **Solon M**, **Yuan S**, **Ahn JN**, **Dougherty RH**, **Finkbeiner WE**, **Peters MC**, **Fahy J V**. 2014. Intelectin-1 is a

prominent protein constituent of pathologic mucus associated with eosinophilic airway inflammation in asthma. Am J Respir Crit Care Med. **189**(8):1005-1007.

29. **Royle L**, **Matthews E**, **Corfield A**, **Berry M**, **Rudd PM**, **Dwek RA**, **Carrington SD**. 2008. Glycan structures of ocular surface mucins in man, rabbit and dog display species differences. Glycoconj J **25**:763–773.

30. **Lemieux RU**, **Hendriks KB**, **Stick R V**, **James K**. 1975. Halide ion catalyzed glycosidation reactions. Syntheses of alpha-linked disaccharides. J Am Chem Soc **97**:4056–4062.

31. **Shimizu K**, **Keller NP**. 2001. Genetic involvement of a cAMP-dependent protein kinase in a G protein signaling pathway regulating morphological and chemical transitions in *Aspergillus nidulans*. Genetics **157**:591–600.

32. **Chang P-K**, **Scharfenstein LL**, **Wei Q**, **Bhatnagar D**. 2010. Development and refinement of a high-efficiency gene-targeting system for *Aspergillus flavus*. J Microbiol Methods **81**:240–246.

33. **Petersen TN**, **Brunak S**, **von Heijne G**, **Nielsen H**. 2011. SignalP 4.0: discriminating signal peptides from transmembrane regions. Nat Methods **8**:785–786.

34. **Bouckaert J, Berglund J, Schembri M, De Genst E, Cools L, Wuhrer M, Hung C-S, Pinkner J, Slattegard R, Zavialov A, Choudhury D, Langermann S, Hultgren SJ, Wyns L, Klemm P, Oscarson S, Knight SD, De Greve H**. 2005. Receptor binding studies disclose a novel class of high-affinity inhibitors of the *Escherichia coli* FimH adhesin. Mol Microbiol **55**:441–455.

35. **Bouchara JP**, **Sanchez M**, **Chevailler A**, **Marot-Leblond A**, **Lissitzky JC**, **Tronchin G**, **Chabasse D**. 1997. Sialic acid-dependent recognition of laminin and

fibrinogen by *Aspergillus fumigatus* conidia. Infect Immun **65**:2717–2724.

36. **Bromley IM**, **Donaldson K**. 1996. Binding of *Aspergillus fumigatus* spores to lung epithelial cells and basement membrane proteins: relevance to the asthmatic lung. Thorax **51**:1203–1209.

37. **Tronchin G**, **Bouchara JP**, **Larcher G**, **Lissitzky JC**, **Chabasse D**. 1993. Interaction between *Aspergillus fumigatus* and basement membrane laminin: binding and substrate degradation. Biol Cell **77**:201–208.

38. **Wasylnka JA**, **Moore MM**. 2000. Adhesion of *Aspergillus* species to extracellular matrix proteins: evidence for involvement of negatively charged carbohydrates on the conidial surface. Infect Immun **68**:3377–3384.

39. **Bonnett CR**, **Cornish EJ**, **Harmsen AG**, **Burritt JB**. 2006. Early neutrophil recruitment and aggregation in the murine lung inhibit germination of *Aspergillus fumigatus* conidia. Infect Immun **74**:6528–6539.

40. **Cunha C**, **Kurzai O**, **Loffler J**, **Aversa F**, **Romani L**, **Carvalho A**. 2014. Neutrophil responses to aspergillosis: new roles for old players. Mycopathologia **178**:387–393.

41. **Taylor PR**, **Tsoni S V**, **Willment JA**, **Dennehy KM**, **Rosas M**, **Findon H**, **Haynes K**, **Steele C**, **Botto M**, **Gordon S**, **Brown GD**. 2007. Dectin-1 is required for beta-glucan recognition and control of fungal infection. Nat Immunol **8**:31–38.

42. **Hohl TM**, **Van Epps HL**, **Rivera A**, **Morgan LA**, **Chen PL**, **Feldmesser M**, **Pamer EG**. 2005. *Aspergillus fumigatus* triggers inflammatory responses by stage-specific ß-glucan display. PLoS Pathog **1**:0232–0240.

43. **Carrion S de J**, **Leal SMJ**, **Ghannoum MA**, **Aimanianda V**, **Latge J-P**, **Pearlman E**. 2013. The RodA hydrophobin on *Aspergillus fumigatus* spores masks dectin-1- and dectin-2-dependent responses and enhances fungal survival in vivo. J Immunol **191**:2581–2588.

44. **Gersuk GM**, **Underhill DM**, **Zhu L**, **Marr KA**. 2006. Dectin-1 and TLRs permit macrophages to distinguish between different *Aspergillus fumigatus* cellular states. J Immunol **176**:3717–3724.

45. **Xue T**, **Nguyen CK**, **Romans A**, **Kontoyiannis DP**, **May GS**. 2004. Isogenic auxotrophic mutant strains in the *Aspergillus fumigatus* genome reference strain AF293. Arch Microbiol **182**:346–353.

46. **Osherov N**, **Kontoyiannis DP**, **Romans A**, **May GS**. 2001. Resistance to itraconazole in *Aspergillus nidulans* and *Aspergillus fumigatus* is conferred by extra copies of the *A. nidulans* P-450 14alpha-demethylase gene, *pdmA*. J Antimicrob Chemother **48**:75–81.

47. **Hua S-ST**, **Tarun AS**, **Pandey SN**, **Chang L**, **Chang P-K**. 2007. Characterization of AFLAV, a Tf1/Sushi retrotransposon from *Aspergillus flavus*. Mycopathologia **163**:97–104.

48. **Affeldt K**, **Carrig J**, **Amare M**, **Keller NP**. 2014. Global survey of canonical *Aspergillus flavus* G protein-coupled receptors. MBio **5**:1501–14.

49. **Katoh K**, **Misawa K**, **Kuma K**, **Miyata T**. 2002. MAFFT: a novel method for rapid multiple sequence alignment based on fast Fourier transform. Nucleic Acids Res **30**:3059–3066.

50. **Larsson A**. 2014. AliView: a fast and lightweight alignment viewer and editor for large datasets. Bioinformatics **30**:3276–3278.

51. **Price MN**, **Dehal PS**, **Arkin AP**. 2009. FastTree: computing large minimum evolution trees with profiles instead of a distance matrix. Mol Biol Evol **26**:1641–1650.

52. **Sambrook J**, **Russell DW**. 2001. Molecular Cloning: A Laboratory Manual. Cold Spring Harbor Laboratory Press, New York.

53. **Innis MA**, **Gelfand DH**, **Sninsky JJ**, **White TJ**. 2012. PCR protocols: a guide to methods and applications. Academic press.

54. **Szewczyk E**, **Krappmann S**. 2010. Conserved regulators of mating are essential for *Aspergillus fumigatus* cleistothecium formation. Eukaryot Cell **9**:774–783.

55. **Szewczyk E**, **Nayak T**, **Oakley CE**, **Edgerton H**, **Xiong Y**, **Taheri-Talesh N**, **Osmani S a**, **Oakley BR**. 2006. Fusion PCR and gene targeting in *Aspergillus nidulans*. Nat Protoc, **1**:3111–3120.

56. **Yang L**, **Ukil L**, **Osmani A**, **Nahm F**, **Davies J**, **De Souza CP**, **Dou X**, **Perez-Balaguer A**, **Osmani SA**. 2004. Rapid production of gene replacement constructs and generation of a green fluorescent protein-tagged centromeric marker in *Aspergillus nidulans*. Eukaryot Cell, **3**:1359–1362.

57. **Bok JW**, **Keller NP**. 2012. Fast and easy method for construction of plasmid vectors using modified quick-change mutagenesis. Methods Mol Biol **944**:163–174.

58. **Woodruff PG**, **Boushey HA**, **Dolganov GM**, **Barker CS**, **Yang YH**, **Donnelly S**, **Ellwanger A**, **Sidhu SS**, **Dao-Pick TP**, **Pantoja C**, **Erle DJ**, **Yamamoto KR**, **Fahy J V**.

2007. Genome-wide profiling identifies epithelial cell genes associated with asthma and with treatment response to corticosteroids. Proc Natl Acad Sci **104**:15858–15863.

CHAPTER 3: Programmed spore germination and allergenic responses in a murine model of asthma are mediated by lipoxygenase activity in *Aspergillus fumigatus.*

This work is being resubmitted as:

Fischer, G., Yang, J., Bacon, W., Palmer, J., Dagenais, T., Huang, X., Hammock, B., & Keller, N., (2016) Programmed spore germination and allergenic responses in a murine model of asthma are mediated by lipoxygenase activity in *Aspergillus fumigatus*. *Environ. Micro. (Resubmission).*

Strain development (besides the *loxB* disruption mutant, which was completed by J.P. and T.G.) was carried out by G.F. Experiments were conceived by G.F. and N.P.K. and all data collected by G.F. with assistance from W.B. X.H. performed all murine allergenic assessments. The manuscript was written by G.F. with assistance from N.P.K.

3.1 ABSTRACT

The opportunistic human pathogen *Aspergillus fumigatus* initiates invasive growth through a programmed germination process that progresses from dormant spore (DS) to swollen spore (SS) to germling (GL) to invasive hyphal growth. We find a lipoxygenase, LoxB, impacts the transition of these programmed stages of germination. Deletion of *loxB* (Δ*loxB*) or its signal peptide delays progression to the SS stage in the presence of the LoxB substrate arachidonic acid (AA); this delay is remediated by the LoxB AA product 5-hydroxyeicosatetraenoic acid (5-HETE). In contrast, overexpression of *loxB* (*OE::loxB*) increases germination with rapid advance to the GL stage regardless of substrate. LoxB shows considerable identity (24.3%) to the human lipoxygenases 5-Lox and 15-Lox, both of which are important in asthma development. Extracts of the *OE::loxB* strain lead to hallmark traits of asthma including increases in airway hyperresponsiveness, macrophage and eosinophil recruitment, and IgE levels in a murine asthma model. We propose that *A. fumigatus* acquisition of LoxB (found in few fungi) enhances germination rates in environments such as the lung containing elevated polyunsaturated fatty acids, and its activity may contribute to the exacerbation of allergic and asthmatic responses in sensitive patients.

3.2 INTRODUCTION

Pathogenic and saprophytic fungi begin interactions with their environment through contact of airborne conidia with a host or substrate. In response to the right signals, this can lead to spore germination followed by extensive hyphal (vegetative) growth. The genus *Aspergillus,* composed of *ca.* 300 species, contains both pathogenic and

saprophytic species which break spore dormancy through three distinct stages of spore maturation, collectively known as the germination process. The dormant spore (DS), or resting spore/conidium, when activated by specific cues undergoes isotrophic growth and swells to almost double its initial size into what is termed the swollen spore (SS). Additional cues signal polarized germ tube emergence from the swollen spore to form a germling (GL) which may or may not lead to extensive hyphal growth (also called mycelium, Figure 1).

Genetic approaches to identify phase-specific germination mutants have identified only a handful of candidates. A genetic screen for temperature-sensitive germination mutants of *A. nidulans* identified genes directly involved in translation and protein folding, a putative malonyl-CoA synthatase, and a *ras* homolog (1). Overexpression of dominant negative forms of *rasA* in *A. nidulans* delays germination, whereas overexpression of dominant active forms yields large multinucleate spores where early germ tube formation is inhibited (2). Spermidine levels are also important for progression from GL to hyphal growth, and deletion of the spermidine synthase gene *spdA* results in enlarged multinucleate spores that can germinate but not proceed to hyphal growth (3). Additionally, many studies have described delays in the general germination process in *Aspergillus* spp., either associated with genetic mutations or treatment with chemicals, but provide little detail on the effects on specific aspects of the germination program (4, 5 and reviewed in 6).

The environmental triggers which initiate germination of dormant spores are thought to include sugars, amino acids, and inorganic salts (7). Studies with *Neurospora crassa* found a carbon source and salt are sufficient to initiate germination, but a carbon source alone is sufficient to induce germination in *A. nidulans* (1, 8). Sensing of host-specific substances such as surface hydrophobicity and hardness regulate spore germination in *Magnaporthe grisea* (9). Host compounds such as the isoflavanoid pisatin induce germination of *Fusarium solani* (10). Alternatively, compounds produced by fungi themselves can inhibit germination. The auto-inhibitors cis-ferulic acid methyl ester and 3,4-dimethoxycinnamic acid methyl ester inhibit germination of certain rust fungi (11). Another auto-inhibitor, 1-octene-3-ol, is an oxylipin volatile derived from the oxygenation and breakdown of linoleic acid. Density-dependent germination effects have been attributed to 1-octene-3-ol in *Penicillium paneum* (12) and *A. nidulans* (13, 14), although conflicting results have been observed in *Aspergillus flavus* (15).

The transition from DS to SS and eventual GLs is a critical fungal process for host recognition and establishment of infection by *Aspergillus fumigatus.* This opportunistic human pathogen causes diseases ranging from invasive aspergillosis (IA) in hypo-immune states or allergic bronchopulmonary aspergillosis (ABPA) in hyper-immune states. Host recognition of *A. fumigatus* spores is initially delayed upon inhalation because the hydrophobic rodlet layer covering the spore evades immune recognition (16). As the spore swells, the proteinaceous rodlet layer is shed, exposing numerous cell wall components that function as pathogen-associated molecular patterns (PAMPs) (for review, see 17). In ABPA, numerous PAMPs on SS can elicit hypersensitivity responses

and as extensive hyphal growth is not associated with this disease, it is presumed fungal development is largely limited to SS and/or GL stages. In contrast, in IA, the host is unable to destroy SS or GLs and the fungus transitions to invasive hyphal growth.

A coordinated immune response is necessary for the proper response and clearance of spores. Oxylipins, potent signaling molecules that influence biological responses in fungi, plants, and mammals (for review, see 18), play a critical role in the coordination of these immune responses. Oxylipins are derived from the incorporation of molecular oxygen into a diverse set of polyunsaturated fatty acids (PUFAs). As mentioned above, oxylipins derived from C18 linoleic acid (LA) have been associated with some germination defects. Oxylipins derived from C20 arachidonic acid (AA) are called eicosanoids and are indispensable for proper mammalian immune responses. Different eicosanoids have been implicated in inflammatory conditions including arthritis, cancer, allergy, and extensively in asthma (reviewed in 19) and several fungal diseases (20–22) including *A. fumigatus* (23).

A key eicosanoid generating enzyme is lipoxygenase. Humans have several lipoxygenases, but one of the most characterized is 5-lipoxygenase (5-Lox). 5-Lox is associated with inflammatory pathway(s) leading to prolonged, severe asthma and is the first committed step in cysteinyl leukotriene production (Supplemental Figure 1) through the production of 5-HPETE (5-Hydroperoxyeicosatetraenoic acid, the unstable oxylipin precursor of 5-Hydroxyeicosatetraenoic acid or 5-HETE). Cysteinyl leukotrienes (CysLTs, including LTC_4, LTD_4, LTE_4) exacerbate airway inflammation by affecting vascular

permeability, mucus production, smooth muscle constriction, and airway remodeling (24). A second Lox product derived from a 15-Lox acting on linoleic acid, 13-HODE, is a mediator of anti-inflammatory responses and exacerbates airway constriction (25, 26).

Some fungi also contain lipoxygenases which fall in two groups based on their C terminal sequence: either a conserved WRYAK motif with a C-terminal isoleucine or a WL-L/F-AK motif with a C-terminal valine (27). C-terminal valine Lox also contain signal peptides implicating them as secreted Loxs. Only a few *Aspergillus* spp. contain any *lox* genes in their genomes. *Aspergillus flavus* encodes one lipoxygenase, *Aflox*, (a valine-type Lox) with a role in quorum sensing and developmental switching from asexual to sexual growth (28). Interestingly, the *A. fumigatus* genome contains two lipoxygenases, one Val-Lox (Afu4g02770, here on referred to as *loxB*) homologous to the sole *A. flavus* Lox, and one Ile-Lox (Afu7g00860, *loxA*). Purification and *in vitro* reaction found LoxB predominantly synthesizes 13-hydroperoxyoctadecadienoic acid, the unstable precursor to 13-hydroxyoctadecadienoic acid (13-HODE), the same metabolite produced by human 15-Lox (Supplemental Figure 1) (27).

Considering the reports linking oxylipins to fungal development, the role of eicosanoids in immune responses to infection, and the shared chemistry of LoxB and human Lox substrates and products, we investigated possible fungal/host interactions mediated by *A. fumigatus* LoxB. As reported here, we find LoxB an important mediator in transition stages of programmed germination and its activity a potential trigger of allergic asthma. Overexpression of *loxB* significantly increases the ability of *A. fumigatus* to progress to

GL stage whereas deletion of *loxB* or its signal peptide region delays progression to the SS stage in the presence of AA. This delay is remediated by the LoxB AA product 5-HETE. Extracts from an overexpression *loxB* strain elicits acute respiratory distress and elevated serum IgE in a murine model of asthma. We propose that the acquisition of LoxB may represent a mechanism by which *A. fumigatus* enhances germination rates in environments such as the lung containing elevated polyunsaturated fatty acids, and its activity may contribute to the exacerbation of allergic and asthmatic responses in sensitive patients.

3.3 MATERIALS AND METHODS

Fungal strains and culture conditions. All strains utilized or developed are listed in Table 1. Strains were propagated on solid glucose minimal media (GMM), amended as necessary with supplements for auxotrophs, at 37°C (29). *A. fumigatus* asexual spores were collected in water supplemented with 0.01% Tween 80, enumerated using a hemocytometer and maintained as glycerol stocks. Spore suspensions of the various mutants were used to inoculate liquid GMM and RPMI 1640 media (Sigma, St. Louis, MO) for oxylipin profiling.

Creation of lipoxygenase mutants. Construction, isolation, and maintenance of recombinant plasmids was performed according to standard methods (30). Primers used are listed in Table 2. The ORF of *A. fumigatus loxB* (Afu4g02770) was identified via the AspGD database (http://www.aspergillusgenome.org).

Deletion of *loxB* was achieved by creating a double-joint PCR fragment consisting of approximately 1 kb flanking regions of *loxB* and utilization of the *argB* gene of *A. fumigatus*. Briefly, the regions upstream and downstream of *loxB* were amplified using TDLoxB P1 F with TD LoxB P3 R and TDLoxB P4 F with TDLoxB P6 R, respectively. The *A. fumigatus argB* gene was amplified using JP Afumi argB F and JP Afumi argB R. The corresponding *loxB*-disruption fragment was amplified using the three PCR fragments described above with the primer pair TDLoxB P2 F and TDLoxB P5 R and used to transform AF293.6 to arginine prototrophy according to previously published methods (31). The strain TTRD51 was isolated and confirmed to be a single integration disruption mutant by Southern blot (Supplemental Figure 2A). TTRD51 was then transformed to prototrophy with *A. parasiticus pyrG* via the plasmid pJW24 (32). Single copy integration of *A. parasiticus pyrG* was confirmed by Southern blot (data not shown), which resulted in the prototrophic Δ*loxB* strain, TJMP39.6 (Supplemental Figure 2A).

An overexpression *loxB* plasmid construct, pGJF1.1, carrying *A. parasiticus pyrG* as a marker gene was developed as described. *GF gpdA/loxB-loxB(t) F* and *GF loxB(t) XbaI Site R* were used to amplify the *loxB* ORF and a 0.581 kb 3' flanking region. These primers introduced 30 base pairs of the 3' end of the *A. nidulans* glyceraldehyde-3-phosphate dehydrogenase (*gpdA)* promoter to the 5' end of the PCR product and an *XbaI* restriction site to the 3' end of the PCR product. The *A. nidulans gpdA* promoter was amplified from pJMP8 (33) using *GF gpdA F* and *GF gpdA/loxB R* which introduced a *SpeI* restriction site to the 5' end of the product and 30 bp of the 5' region of the *loxB* PCR product to the 3' end of the *gpdA* amplicon. In order to fuse the *loxB* PCR product downstream of the

gpdA promoter amplicon, fusion PCR was performed as previously described (31). The *gpdA*:*loxB* fusion product was digested with *XbaI* and *SpeI* and ligated into pJMP7 (33), an *A. parasiticus pyrG*-containing plasmid. pGJF1.1 was used to transform AF293.1 to yield TGJF1.5 and TGJF1.7 and TTRD51 transformed to produce TGJF34.9 and TGJF34.10 (Table 1) (31). Verification of ectopic plasmid integration was confirmed by PCR and Southern blot (Supplemental Figure 2A). Complementation of *loxB* was achieved by amplifying the flanking intergenic region of *loxB* using the primer pair "GF loxB Complement F" and "GF loxB Complement R", which introduced *NotI* and *SpeI* sites at the end of the *loxB* intergenic DNA fragment. The *loxB* cassette was digested with *NotI* and *SpeI* and ligated into pJMP7, yielding the plasmid pGJF22.1. This plasmid was then transformed into TTRD51, yielding the prototrophic ectopic *loxB* complement strain, TGJF33.6. Integration was confirmed via Southern blot (Supplemental Figure 2A).

For deletion of the signal peptide of *loxB*, pGJF1.1 was subjected to quick-change mutagenesis using a modified approach as previously described (34). For *loxB* lacking the signal peptide region, "GF d1-20:loxB F" was used to amplify a modified version of pGJF1.1 lacking residues 1-20 (ΔSP1) yielding pGJF10.1, while "GF d1-26:loxB" was used to amplify a modified version yielding pGJF11.2 which lacked N-terminal residues 1-26 (ΔSP2).

Tagging of LoxB with *gfp* was achieved via modifications to pGJF1.1, pGJF10.1, and pGJF11.2 using quick-change mutagenesis. The primer pair "GF loxB-Nterm GFP F" and "GF loxB-Nterm GFP R" were used to amplify a *gfp*-GA linker amplicon from a

synthesized G-Block fragment (IDT) with 30 bp of homology to sequence directly upstream and downstream of LoxB residues 30 and 31. This nested location was selected since it was downstream of the putative signal peptide regions but upstream of the predicted lipoxygenase domain. The G-block was synthesized using the sequence of *gfp* from pFNO3 (35) with the addition of a C-terminal 5x glycine/alanine linker codon optimized for *A. niger*. The purified *gfp* cassette was used to amplify gfp-tagged versions of full-length *loxB* (pGJF26.3), ΔSP1 *loxB* (pGJF27.2), and ΔSP2 *loxB* (pGJF28.5).

Together, pGJF10.1, pGJF11.2, pGJF26.3, pGJF27.2, and pGJF28.5 were all independently transformed into the fungal strain TTRD51, yielding TGJF35.4 & 35.5, TGJF36.1 & 36.3, TGJF43.8, TGJF44.14, and TGJF45.15, respectively. Integration of the corresponding plasmids was verified via Southern blot (Supplemental Figure 2A) based on genome structure outlined in (Supplemental Figure 2C).

Disruption and overexpression of *loxB* was confirmed using a combination of northern blots and semi-qPCR. For northern blotting, total RNA was extracted with TRIzol reagent from lyophilized mycleia. Probes for northern analysis are indicated in Supplemental Figure 4B and labeled with dCTP-αP^{32}. Because transcript levels for *loxB* were not detectable in wild type nor the complementation strain (Supplemental Figure 2D), semi-qPCR was used to further verify wild type *loxB* expression, disruption, and complementation (Supplemental Figure 2E). Semi-qPCR was carried out as follows: 5 μg of RNA from lyophilized mycelium was treated with DNAseI for 1 hour at 37°C. 500 ng of DNAse-treated RNA was converted to cDNA using the Bio-Rad (Hercules, CA) iScript

cDNA synthesis kit according to manufacturer's protocol. 25 ng of cDNA was used as template for cDNA-specific amplicon production. For *loxB* cDNA, the primer pair "GF loxB qPCR F" and "GF loxB qPCR R" was used to amplify a 225 bp amplicon lacking *loxB* intron 2. For *loxA,* a cDNA amplicon was produced via PCR using the primer pair "GF loxA seq 1F" and "GF loxA Probe R". Actin cDNA served as a loading control and an amplicon was produced via PCR using the primer pair "FY act1 RT FOR" and "FY act1 RT REV".

Fatty acid germination assay and loxB qRT-PCR. Germination assays were carried out on spores derived from the various *loxB* mutant strains. Two milliliters of 1 X 10^5 spores/mL in GMM supplemented with 0.5% tergitol (Sigma, St. Louis, MO) in the presence or absence of arachidonic or linoleic acids (Sigma, St. Louis, MO) were used to inoculate each well of a Costar® 12-well dish (Corning, Corning, NY). For germination studies in lung homogenate, one lung was harvested from wild type mice after sacrifice and homogenized in 1 mL water/lung. The homogenate was then filter sterilized using a 0.2 μm syringe filter. Microscopic images were captured using a Nikon Eclipse T*i* inverted microscope equipped with a OKO-Lab microscopic enclosure to maintain the temperature at 37°C for *A. fumigatus and A. nidulans,* and 30°C for *A. flavus* (OKO Lab, Burlingame, CA). Germinated spores were observed using a Nikon Plan Fluor 20xPh1 DLL objective and phase-contrast images captured every 1-2 hours using the Nikon NIS Elements AR software package (v. 4.13). Germinated spores were counted with slight modifications as previously described (36). Briefly, a dormant spore was considered swollen if the diameter was double in size to dormant spores or a GL if an emerging germ tube was clearly

present. One hundred spores were observed for each strain (n=3) and growth condition. Values in figures represent the average percentage of spores germinated ± SEM. The Student t test was carried out to determine statistical significance using the Graphpad Prism software (La Jolla, CA).

Mycelial growth in the presence of AA was monitored using an OD_{600} reading in a 96-well plate format. To establish a mycelial network, 10^5 spore were inoculated in GMM +0.5% tergitol and grown overnight at 37ºC. Initial absorbance values were collected using a BioTek EPOCH 2 microplate reader with Gen5 acquisition software. Arachidonic acid was added to wells at a final concentration of 1.0, 0.5, and 0.25 μg/μL to challenge mycelial growth. Twenty-two hours after AA treatment, another absorbance reading was collected and the net growth calculated.

Fluorescent microscopy of GFP localization was carried out on the same platform but using a 60x Nikon Plan Apo VC Oil DIC objective. Briefly 10^4 spores were used to inoculate glass coverslips immersed in GMM + 0.5% tergitol overnight at 30°C (to reduce sample autofluorescence), after which the slides were imaged. Spores were inoculated directly on a coverslip and imaged similarly.

For quantification of *loxB* expression in the presence of arachidonic and linoleic acid, quantitative RT-PCR was carried out as follows: RNA for cDNA synthesis was isolated as previously described for semi-qPCR from total fungal tissue after 48 hours of growth (increase tissue yield) in the presence of 0.5 μg/μL LA and AAs. Samples were analyzed

in a volume of 20 μL using iQ SYBRGreen Supermix (Bio-Rad Laboratories, Inc.). Reactions were performed in triplicate using cDNA template for *loxB* and actin. A mastermix of SYBRGreen and primers was prepared for each primer pair (*loxB*: "GF loxB qPCR F with "GF loxB qPCR R", actin: "FY act1 RT FOR" with "FY act1 RT REV"). Each reaction contained 25 ng of cDNA and a final primer concentration of 300 nM. Reactions were performed with the MyiQ Real-Time PCR detection system (Bio-Rad Laboratories, Inc.) using the "2-step amplification plus melting curve" protocol: 95ºC for 3 min followed by 40 cycles of 95ºC for 1 min. (denaturation) and 55ºC for 45 s (annealing and elongation). The determination of the threshold values (Ct) was generated automatically by the MyiQ software. The identities of the amplicons and the specificity of the reactions (absence of primer-dimers) were confirmed by the melt curve profile of the amplified products. The amount of *loxB* cDNA was standardized to the amount of the actin internal standard cDNA for each sample and normalized to *loxB* expression with no fatty acid treatment (vehicle).

Development of antigenic extract/oxylipin solutions from *Aspergillus fumigatus* for asthma studies. The wild type and *loxB* mutant strains from *A. fumigatus* were grown in RPMI media within CoStar 12-well cell culture plates (Corning, Corning NY) containing 3 mL of RPMI media inoculated with the respective strain to a final concentration of 1 X 10^6 spores/mL. Plates were covered with AeraSeal Breathable Sealing Film (Excel Scientific, Victorville, CA) and incubated for 3 days at 37˚C and 185 rpms. On the third day, arachidonic acid (Sigma, St. Louis, MO) suspended in 100% ethanol was added to a final concentration of 10 μm and allowed to incubate 2 hours. Eighteen 3 mL cultures for each

strain were pooled together and fungal tissue was separated from culture supernatant using Miracloth (EMD Millapore). Fungal tissue was lyophilized overnight and weighed. Fungal antigenic extract solution was prepared from a modified protocol (37). Briefly, an extraction solution comprised of 0.25% sodium chloride, 0.125% sodium bicarbonate, 50% glycerol, and 0.4% phenol was added to the ground, lyophilized tissue in a 1:10 ratio (w/v). The solution was incubated overnight at 4°C and then run through a 0.45 μm cellulose acetate filter to remove insoluble material (Thermo Scientific). A Bradford assay was used to determine protein concentration within the filtered solution and adjusted to 0.667 μg/μL using extraction solution lacking glycerol. Culture supernatant was filter sterilized using a 0.45 μm cellulose acetate syringe filter (Thermo Scientific) and added to the protein antigenic solution in a 1:1 ratio for a final protein concentration of 0.333 μg/μL.

Murine analysis of airway hyperresponsiveness, immune cell recruitment, and IgE antibody production. A mouse model of allergic lung disease was established using methods described previously with minor modifications (38) under a protocol approved by the UCSF IACUC. Thirty microliters of fungal antigenic extract solution (see prep above) was delivered into female C57BL/6 mice 3 times per week for 3 weeks. Control mice were given saline or 10 μg of *A. fumigatus* commercial extract (Hollister-Stier Laboratories, Spokane, WA). To measure airway reactivity, mice were anesthetized 48 h after the last antigen delivery with ketamine (100 mg/kg of body weight), xylazine (10 mg/kg), and acepromazine (3 mg/kg) and the trachea cannulated with a 20 gauge tubing adaptor. Mice were attached to a ventilator and pulmonary mechanics analyzer

(FlexiVent) and ventilated at 9 ml/kg tidal volume, 150 breaths/minute frequency, and 2 cmH_2O positive end-expiratory pressure. Mice were paralyzed with pancuronium (0.1 mg/kg i.p.) and airway mechanics were measured continuously using the linear single compartment model while challenged with escalating doses of acetylcholine (0.03, 0.1, 0.3, 1 and 3 µg/g i.v.). BAL was performed via the tracheal cannula. Lungs were washed 3 times with 1 ml PBS, erythrocytes were lysed, and total BAL cells were counted with a hemocytometer. Percentages of cell types were determined using cytospin preparations stained with HEMA 3 (Fisher) by evaluating >300 cells/slide by light microscopy. Lavaged lungs were inflated with 10% buffered formalin to 25 cm H_2O of pressure and fixed for 1 day. Multiple paraffin-embedded 5-µm sections of the entire mouse lung were prepared and stained with Hemotaxylin & Eosin (H&E) to evaluate the morphology and with Periodic acid-Schiff (PAS) to evaluate mucus production. Total serum IgE level was evaluated by enzyme-linked immunosorbent assay using microplates coated with anti-mouse IgE (BD Biosciences — Pharmingen). Diluted serum samples were added to each well, and the bound IgE was detected with biotinylated anti-mouse IgE (BD Biosciences — Pharmingen). Color development was achieved using streptavidin-conjugated HRP (BD Biosciences — Pharmingen) followed by the addition of HRP substrate (TMB; BD Biosciences — Pharmingen).

3.4 RESULTS

3.4.1 Identification of 5-Lox and 15-Lox homologs within *Aspergillus fumigatus.*

The human 5-Lox protein sequence was used to identify homologs within the *A. fumigatus* genome. Genome-wide BLAST analysis identified two lipoxygenases with considerable homology to human 5-Lox, *Afu7g00860 (*LoxA*,* 24.2% identity) and *Afu4g02770 (*LoxB*,* 24.3% identity), both of which were also identified by Heshof *et al*. Both proteins show similar identities to 15-Lox (LoxA, 25% identity and LoxB, 23% identity). Within human 5-Lox*,* Leu-368, 373, 414, 607, and Ile-406 are necessary for proper alignment of the AA pentadiene for catalysis (39). Conservative substitutions for Ile406 are present in both *loxA* (I406L) and *loxB* (I406V) (Supplemental Figure 3). Amino acid residues important for positional specificity in 15-Lox are partially conserved in LoxB, but not LoxA (Supplemental Figure 3) (40). Moreover, a distinguishing characteristic of LoxB is the presence of a predicted signal peptide for LoxB, which is absent from LoxA. An examination of published microarray data and mRNA expression studies identified *loxB* but not *loxA* as an expressed gene (41). We confirmed these findings by probing for *loxB* and *loxA* expression when *A. fumigatus* was inoculated in different media (GMM or RPMI) and at varying spore concentrations (10^5-10^6 spores/mL). We observed expression of *loxB* in all conditions tested, but never expression of *loxA* (Figure 2A). Thus, due to lack of expression of *loxA*, and the possibility of secretion of LoxB, we focused on this latter gene and created both deletion and overexpression mutants of *loxB* (Supplemental Figure 2).

3.4.2 *Aspergillus fumigatus loxB* affects programmed germination.

A previous study had shown changes in development of *A. fumigatus* exposed to disks soaked in AA (42), thus we investigated this response microscopically to determine if *loxB* was important for this alteration in development. Both AA and LA were tested at 2.0, 1.0, and 0.5 μg/μL in GMM + 0.5% tergitol (to aid in PUFA solubility) with ethanol used as a vehicle. The degree of germination was quantified by assessing the percentage of DS that had progressed to the SS or GL stage at a particular timepoint.

Tergitol was verified to have no effect on SS or GL formation compared to GMM media (Supplemental Figure 4A). At 2.0 and 1.0 μg/μL of AA or LA, all spores remained arrested at the DS stage: even after 24 hours at 37°C, no SS were observed (data not shown). At 0.5 μg/μL AA, after 15 hours at 37°C, the percentage of wild type spores progressing to SS and GL was 30% less than spores grown in the mock condition (Figure 2B). However at 0.5 μg/μL LA no significant difference in the total number of SS and GL was recorded in wild type (Figure 2C). We were curious whether the presence of these PUFAs had an effect on *loxB* expression, so quantitative RT-PCR was done from the wild type strain grown in the presence of vehicle (ethanol) and 0.5 μg/μL AA and LA. We found that AA increased *loxB* expression two-fold, whereas LA increased *loxB* expression, but not significantly from the vehicle treatment (Figure 2D).

Based on the differences in growth observed at 0.5 μg/μL AA and that *loxB* expression was induced 2-fold in the presence of AA, we quantified the differences in SS and GL levels upon *loxB* deletion (Δ*loxB*) or overexpression (*OE:: loxB*). Timecourse microscopy

was used to monitor SS and GL formation for the wild type and *loxB* mutants over a period of 36 hours under mock and 0.5 μg/μL AA treatments. In the control treatment, the *OE::loxB* strain consistently had more spores germinate through 15 hpi whereas the Δ*loxB* and Δ*loxB* complemented (*loxB(c)*) strains had equivalent numbers of SS and GL as wild type through 15 hpi (Figure 2E). Although all strains were delayed in germination processes under AA treatment, the *OE::loxB* strain again transitioned to SS and GL stages faster than the other three strains. Notably, the proportion of Δ*loxB* dormant spores (DS) that became SS or GL was less than wild type and at all time points tested (Figure 2E). Due to the fact that differences in all treatments could be observed at the 15 hpi, all further experimentation were quantified at this time point unless otherwise specified.

Next we asked if the delay in germination of Δ*loxB* was a function of PUFA treatment and compared germination of all four strains on 0.5 μg/μL LA to the 15 hpi of control and the AA treatment of Figure 2E. As shown in Figure 2F, whereas the *OE::loxB* strain again showed accelerated germination processes, the Δ*loxB* presented the same phenotype as the wild type and complemented strains. Thus the Δ*loxB* delay in SS and GL formation was a function of AA.

To confirm that *OE::loxB* increased the transition of DS to SS and GL stages, additional *OE::loxB* strains were examined including strains containing both an *OE::loxB* and wild type *loxB* allele (TGJF 1.5 and TGJF1.7) or just *OE::loxB* allele (TGJF34.9 and

TGJF34.10). All strains had a higher percentage of SS and GL than wild type on GMM + 0.5% tergitol (Supplemental Figure 5A). Even on lung homogenate media that contains endogenous AA, overexpression of *loxB* led to increased levels of SS and GLs (only TGJF1.5 tested, Supplemental Figure 5B).

Finally, we asked if AA had any differential impact on the *loxB* mutants and wild type in post-germination growth. In contrast to the *loxB*-dependent regulation of germination by AA, there was no difference in mycelial growth by the three strains on AA amended medium (Supplemental Figure 5CD).

3.4.3 LoxB loss delays entry into swollen spore stage and overexpression of *loxB* accelerates both swollen spore and germling transitions.

To clarify if *loxB* overexpression or loss impacted specific germination stage transitions on AA, SS and GL were individually assessed. Differences in the number of SS were observed at several time points. Particularly at 15 and 19 hpi, the Δ*loxB* strain consistently had less SS than wild type or the *loxB(c)* strains. The *OE::loxB* strain maintained a higher number of SS that peaked approximately 19 hpi (Figure 3A) as a reflection of transition to GL stage which was higher at all time points in this mutant (Figure 3B). No difference in the number of GLs was observed between the wild type, Δ*loxB*, and *loxB(c)* strains until 29 hpi at which the number of Δ*loxB* GLs was significantly less than the wild type or *loxB(c)* strains (Figure 3B).

3.4.4 Disruption of the LoxB signal peptide impairs germination in presence of AA and affects protein localization.

Heshof *et al* 2014 commented that fungal lipoxygenases with a C-terminal valine also contain an N-terminal signal sequence, suggestive of a protein trafficked through the canonical ER-Golgi apparatus for secretion. LoxB has two putative cleavage sites demarcating the signal peptide region: one between residues 20 and 21 and another between residues 26 and 27 according to predictions by the Signal P 4.0 server (Figure 4A) (43).

To visually investigate LoxB localization, signal peptide deficient and full-length versions of LoxB were tagged with GFP and transformed into *A. fumigatus* (See Material and Methods and Supplemental Figures 2AD). Full-length GFP:LoxB localized to punctate spots within hyphae but also the cell wall and septa (Figure 4B, white arrow). In spores, full-length GFP:LoxB localized on the periphery of DS (Figure 4B, white arrow) as well as in puncta within the spore. When the first 20 N-terminal residues were absent, GFP:LoxB protein was found uniformly throughout the cytoplasm of hyphae with no localization to the cell wall or septa, and at undetectable levels in DS. The same cytoplasmic localization was observed when the first 26 N-terminal residues were deleted, and barely detectable fluorescent signal in DS. The strain overexpressing untagged full-length LoxB was used as a negative fluorescence control for both hyphae and spores (Figure 4B).

To determine if the LoxB signal peptide was important for germination, we created two overexpression constructs of *loxB* lacking the signal peptides. Strains overexpressing

versions of *loxB* lacking the first 20 N-terminal residues (*OE::ΔSP1-loxB)* or the first 26 N-terminal residues (*OE::ΔSP2-loxB*) were created in a Δ*loxB* background (Supplemental Figures 2AD). In control GMM +0.5% tergitol media (mock), *OE::ΔSP1-loxB* and *OE::ΔSP2-loxB* strains germinated the same as wild type in contrast to the two *OE::loxB* strains (Figure 4C). Interestingly, the number of functional *loxB* alleles impacted germination as the strain with both a wild type and *OE::loxB* allele showed accelerated germination over the strain with only an *OE::loxB* allele (Figure 4C). Upon addition of 0.5 μg/μL AA, strains overexpressing versions of *loxB* lacking signal peptides had significantly less SS and GLs than strains overexpressing full-length *loxB*. However, with the exception of one *OE::ΔSP1-loxB* mutant, all of these strains maintained increased SS and GLs compared to the wild type (Figure 4D), suggestive of partial activity in contrast to the delayed germination phenotype of Δ*loxB* on AA (Figure 2E and 3A).

3.4.5 Synthetic lipoxygenase expression promotes germination in *Aspergillus nidulans.*

From the results obtained with *A. fumigatus*, we were curious whether lipoxygenase expression impacted germination process in other Aspergilli. *Aspergillus nidulans* does not contain a native Lox but a synthetically expressed and enzymatically active *Zea mays* 9-lipoxygenase (*Zmlox3)* strain of *A. nidulans* was available from a previous study (44). Therefore, germination of two *A. nidulans* transformants overexpressing *zmlox3* compared to wild type was investigated.

Germination of *A. nidulans* spores occurs significantly faster than *A. fumigatus,* with SS and GLs observed as early as 5 hpi at 37ºC. Like *A. fumigatus*, 0.5 μg/μL AA decreased the proportion of SS and GLs in wild type (Figure 5A). Germination was monitored in the presence and absence of AA for the three strains for 17 hours (Figure 5B). The proportion of SS and GLs in the mock treatment for the *OE::zmlox3* strains (RDIT99.2 and RDIT98.5) was 20% higher than wild type (Figure 5C). However after 17 hpi the wild type strain had equivalent spore germination to the *OE::zmlox3* strains (Figure 5B). When 0.5 μg/μL AA was present, the reduction in SS and GLs from wild type was further exacerbated: 7 hpi *OE::zmlox3* SS and GL levels were almost 1-fold greater than the wild type (Figure 5D). Tergitol was found to have no effect on any of the *A. nidulans* strains (Supplemental Figure 4B).

Aspergillus flavus encodes an endogenous Lox (Aflox1 or Lox), important in asexual to sexual shifts in this species, with high identity (82%) to *A. fumigatus* LoxB (28). The *A. flavus* wild type was sensitive to AA, with levels of SS and GLs reduced by 77% compared to the mock treatment at 9 hpi (Figure 5E). Using *A. flavus lox* disruption and complementation mutants previously characterized (28), we examined the germination profile over 16 hours at 30ºC in the presence and absence of AA (Figure 5F). While germination of all strains was delayed at 9 hpi in the presence of AA compared to the mock treatment, unlike in *A. fumigatus* or *A. nidulans* there was no statistical difference in SS or GLs levels in the Δ*lox* mutant in the presence or absence of AA (Figure 5G and 5H). Tergitol did not impact spore germination (Supplemental Figure 4C).

3.4.6 The human 5-Lox oxylipin metabolite 5-HETE promotes swollen spore and germling formation.

The differences in germination stage progression of both *OE::loxB* and *ΔloxB* strains treated with AA (Figures 2, 3 and 4) suggested a possible role for a LoxB generated oxylipin in *A. fumigatus* germination. Given the similarity of LoxB to human Lox sequences (5-,12-,15-Loxs, Supplemental Figure 3), we hypothesized *loxB* produced various AA products including the commercially available 5-HETE (Figure 6A), the stable surrogate for 5-Hydroperoxyeicosatetraenoic acid (5-HPETE) of the 5-Lox pathway in mammals (Supplemental Figure 1).

Specifically we wanted to test whether the delay of DS transition to SS and/or GLs in the *ΔloxB* strain in AA medium was due to either AA toxicity or lack of an induction cue, possibly 5-HETE. To ascertain this, all four strains (both *loxB* mutants, wild type and complemented *ΔloxB*) were grown on mock, 0.5 μg/μL AA alone, 0.5 μg/μL 5-HETE alone, or both metabolites at 0.5 μg/μL. Germination profiles were repeated as before on mock and AA medium (Figure 6B and 6C) with *ΔloxB* delayed on AA (Figure 6C). Treatment with 5-HETE resulted in a profile similar to that of control medium where ΔloxB had equivalent levels of SS and GLs as the wild type and complement while *OE::loxB* showed accelerated germination (Figure 6D). This restoration of germination levels of *ΔloxB* to wild type levels by the AA product 5-HETE still did not distinguish between inhibition by AA or induction by 5-HETE. Thus, we assessed germination on both

compounds. Germination rates increased for all four strains, with *OE::loxB* still germinating faster than the other three strains (Figure 6E).

Because the *ΔloxB* strain showed similar germination rates as the wild type and complement control, it appeared that 5-HETE could act as a germination cue. To further tease apart the effects of the AA/5-HETE co-treatment and to understand the increases in germination for all strains, we counted just SS (Figure 6F) or GLs (Figure 6G). Progression to SS was greatly increased in wild type, ΔloxB and complement (Figure 6F), whereas *OE::loxB* had largely exited out of this stage and was primarily in the GL stage (Figure 6G).

3.4.7 LoxB induction of asthmatic symptoms in a murine asthma model.

Considering oxylipins associated with human allergenic diseases seemed to act as a germination cue in a LoxB-dependent manner, we were curious whether elevated levels of these compounds through *loxB* overexpression could exacerbate asthmatic-like responses. A cocktail composed of fungal antigens and oxylipins (see Materials and Methods) was prepared from wild type, *ΔloxB*, and *OE::loxB* and subjected to mice using a previously established murine model of asthma (38). The murine response to the fungal preparations was compared to positive (commercial antigenic preparation of *A. fumigatus*) and negative (saline) controls (37). The *OE::loxB* conditioned mice displayed the highest airway hyperresponsiveness among all treatments, statistically more

significant than either wild type or *ΔloxB* with increasing application of acetylcholine, a signaling molecule that induces airway constriction (Figure 7AB).

We next assessed any impact of these treatments on pulmonary inflammatory cell recruitment in bronchoalveolar lavage fluid (BALF). The levels of macrophages, eosinophils, lymphocytes, and neutrophils were compared among treatments. The total cell count for all of these cells was significantly increased in mice treated with the overexpression *loxB* cocktail (Figure 7C). Specifically, significantly more macrophages and eosinophils were detected than in mice treated with the wild type or Δ*loxB* (macrophages only) cocktails (Figure 7DE). However, no difference in lymphocyte or neutrophil levels was observed among wild type, Δ*loxB,* or *OE::loxB*-treated mice (Figure 7FG). Finally, serum IgE levels were assessed due to a canonical increase of this antibody in asthmatic patients (45). Total serum IgE levels were almost three times higher in mice treated with the *OE::loxB* antigenic cocktail than mice treated with wild type or *ΔloxB* cocktail (Figure 7H).

3.5 DISCUSSION

Programmed spore germination is a critical process for survival and entry into vegetative growth for all fungi. The spore should remain dormant in unfavorable environments and respond to cues in favorable settings for entry into vegetative growth. Despite the importance of germination, surprisingly little is know about this process, particularly for human pathogenic fungi. Here we present unexpected insight into this programmed event in *A. fumigatus* where we find an important role for a lipoxygenase in accelerating

the transitions of DS to SS and GL stages of germination. We find both substrate and product of LoxB, AA and potentially its oxylipin product 5-HETE, are key molecules in these transitions, where 5-HETE appears to act as a germination accelerator for this species. Coupling these data with the finding that extracts from *A. fumigatus OE::loxB* induce hallmark allergenic response in a murine model of asthma, we speculate that the lung environment is a favorable milieu for *Aspergillus* germination which, in the case of susceptible hosts, can contribute to worsening of allergenic diseases such as allergic bronchopulmonary aspergillosis (ABPA).

Whereas our work, to our knowledge, is the first to identify molecules directly affecting the germination program in *A. fumigatus*, deletion of the G protein RasA or spermidine synthase SpdA have been shown to impact the SS to GL stage in *A. nidulans* (2, 3). Inactivation of the RasA homolog in *A. fumigatus* also delays germination, although detailed assessment was not analyzed in this mutant (46). However, loss of function RasA or SpdA mutations have pleiotropic effects on fungal growth resulting in significantly aberrant morphologies beyond delays in spore germination. In contrast, both deletion and over-expression of *loxB* appear to only affect transition of germination stages with the former mutant (Δ*loxB*) only showing a phenotype when AA is incorporated into the media.

Several PUFAS have been shown to be important in the germination process of multiple fungi, often as an inhibitor (47). However, AA has not been investigated except as a potential germination inducer in *Mortierella alpine* (48). This fungus, which produces high

levels of endogenous AA, displays a similar germination program as *A. fumigatus* with rapid AA depletion during the SS stage for this species. The authors speculated that this was related to fatty acid desaturase activity but no mechanism was described. Here we suggest a process in *A. fumigatus* where *loxB* is induced by AA, the enzyme secreted and exogenous AA converted to 5-HETE (and other subsequent oxylipins) (Figure 8). Both AA and 5-HETE altered the dynamics of the germination program in a *loxB*-dependent fashion. Whereas AA treatment delays germination in all strains, overexpression of *loxB* overcomes AA suppression at the DS to SS stage. In contrast, Δ*loxB* is delayed at this same transition; this delay may be associated not with AA inhibition per se but with the lack of 5-HETE, as Δ*loxB* presents an identical phenotype as wild type in both 5-HETE and 5-HETE/AA treatments (Figure 6DE). This phenomenon appears specific to AA, as LA did not affect germination in either a *loxB*-dependent or independent manner. We suggest that possession of an AA metabolizing lipoxygenase presents an advantage to *A. fumigatus* in PUFA rich environments through acceleration of the germination program. Supporting this statement was our observation that *A. nidulans,* a species that does not contain a lipoxygenase, showed accelerated germination in synthetic strains containing a plant lipoxygenase (Figure 5BCD). However, we did not see a statistical difference in germination of the *A. flavus* Δ*lox* strain treated with AA so it remains to be determined if lipoxygenases in general play roles in germination of fungi.

As hypothesized in an earlier study (27), LoxB is a secreted protein and its proper localization is required for full function in germination dynamics (Figure 4C and 4D). GFP-

tagged versions of full-length LoxB revealed the protein localized to the cell wall and septa of the mycelium as well as the cell wall of DS when overexpressed (Figure 4B), which is the expected localization pattern for secreted fungal proteins such as the fumiquinozoline C oxidoreductase, *fmqD* in *A. fumigatus* (49) and a glucoamylase-GFP fusion protein in *A. niger* (50). Truncated GFP-LoxB no longer localized to the cell wall or septa but appeared diffused throughout the cytoplasm of the cell, similar to localization of truncated versions of FmqD-GFP lacking the signal peptide sequence carried out by (49). Secretion of LoxB would aid in rapid conversion of environmental AA (germination inhibitor) to 5-HETE (germination stimulator).

We found 5-HETE increased the proportion of SS in a *loxB*-independent manner. The proportion of GLs was significantly greater in all strains when compared to AA treatment, suggesting that 5-HETE promotes the formation of SS *and* GLs (Figure 8). Although we only assessed the impact of 5-HETE on germination (due to cost of these metabolites), it is possible that other LoxB oxylipins may affect germination. Oxylipins thus far have been described as inhibitors of germination. In some studies, the volatile 1-octene-3-ol was found to inhibit germination in a density dependent manner (12–14), although not in *A. flavus* (15). Also, several plant-derived oxylipins have inhibitory properties against spore germination of the oomycetes *Phytophthora infestans* and *P. parasitica,* and the ascomycete *Botrytis cinerea* (51). To the best of our knowledge this is the first example of an oxylipin inducer of fungal spore germination.

Aspergillus fumigatus is one of the most common fungi associated with allergenic diseases and the primary pathogen causing ABPA. This work supports a potential role of LoxB in potentiating these associations at two levels, one by altering host recognition of the spore and one where LoxB metabolites – identical to several immunomodulatory oxylipins produced by the host itself - could contribute to harmful inflammatory processes. Considering the first point, it is known that germination kinetics have a profound impact on host recognition and clearance of fungal spores. The speed at which host immune cells can clear fungal spores is dependent on the size and shape of the spore and interactions with spore surface receptors (PAMPs) (52). PAMPs are masked by a layer of rodlet proteins on dormant spores of *A. fumigatus*, which are shed during isotrophic growth to the SS stage. Many studies have identified *A. fumigatus* PAMPs that influence macrophage clearance of *A. fumigatus* spores, such as ß-1,3-glucan (53, 54), mannans (55), and lectins (56). Once phagocytosed, reactive oxygen killing through macrophage NADPH oxidase (57) and acidification of the phagolysosome (58) are thought to be the predominant ways macrophages neutralize spores. The *A. fumigatus* spore pigment DHN melanin suppresses acidification (59) and is thought to allow for rapid germination and escape from the macrophage, but also renders *A. fumigatus* more vulnerable to antifungal agents, since hyphae are generally more susceptible than spores (60, 61). In changing germination kinetics, LoxB activity – or lack of it – could have influence on all of these fungal developmental factors and subsequent host/microbe interactions.

With regard to LoxB products, 5-HETE and many of the other oxylipins differentially produced by *loxB* overexpression may play a role in immune function. IgE, the hallmark

indicator of asthmatic responses, was elevated in the *OE::loxB* treated mice, as was airway hyperresponsiveness and macrophage/eosinophil infiltration of lung tissue. 20-HETE and 13-HODE (previously shown to be produced by *A. fumigatus* LoxB, 27) are both implicated in airway hyperresponsiveness (25, 62), while 13-HODE has also been implicated in disruption of airway epithelial cells calcium homoeostasis and mitochondrial structure, resulting in bronchial cell injury (63). This injury leads to severe airway remodeling, increased airway neutrophilia, and an increase in stress-related pro-inflammatory cytokine release. DiHETrEs are able to activate PPARα and PPARγ, transcription factors which regulate the inflammatory state of many airway diseases (64, 65). Whether DiHOMES and TriHOMES play a role in inflammation is unclear, however these compounds are elevated in asthmatics compared to healthy individuals (66). Thus, while the actual contribution of fungal oxylipins in an environmental setting to asthma is unclear, we suggest future studies should attempt to delineate whether particular oxylipins (produced directly or indirectly through *loxB* perturbation) are sufficient to induce elevated asthmatic responses in mammalian hosts.

In conclusion, we have characterized a previously described *A. fumigatus* lipoxygenase, LoxB, the substrate (AA) and various oxylipins products (e.g. 5-HETE) of which could provide *A. fumigatus* a competitive edge in colony establishment in varied environments. The mammalian host is one such environment where kinetics of spore germination are intimately linked with immune recognition and clearance. Considering that germination is the first developmental program of fungal growth where antimicrobial intervention could reduce the incidence of infection, our findings also provide insights into *A. fumigatus*

germination processes which may be useful for development of future therapeutics. Several Lox inhibitors have been developed for treatment of asthma and other inflammatory diseases (67, 68), and it would be interesting if measures along these lines could impact diseases caused by *A. fumigatus.*

3.6 ACKNOWLEDGEMENTS

B.D.H. is a George and Judy Marcus senior fellow of the American Asthma Society. Partial support was provided by American Asthma Foundation (09-0269), NIEHS R01-ES002710 and Superfund P42-ES004699 and NIH West Coast Metabolomics U24-DK097154. This work was funded by a Predoctoral Training Program in Genetics award for G.J.F. (5T32GM07133) and awards to N.P.K. from the American Asthma Foundation (11-0137) and the NIH (R01-AI065728). All authors declare no conflict of interest.

3.7 FIGURES AND LEGENDS

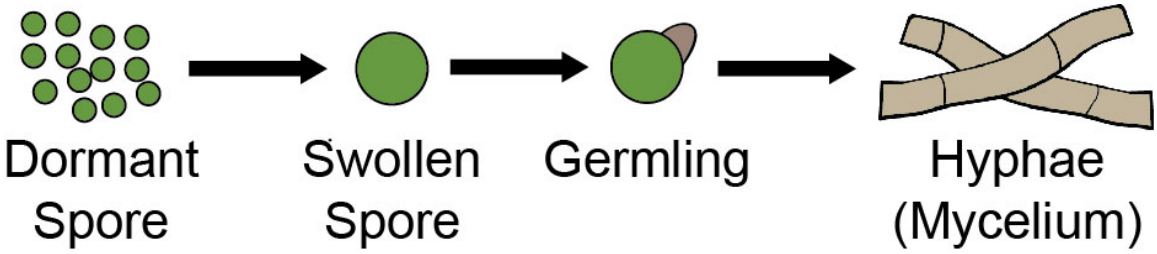

Figure 1. Germination of *A. fumigatus.*

Development of *A. fumigatus* begins with the isotrophic growth of dormant spores into swollen spores. Emergence of hyphae demarks germling formation which leads to a hyphal network or mycelium.

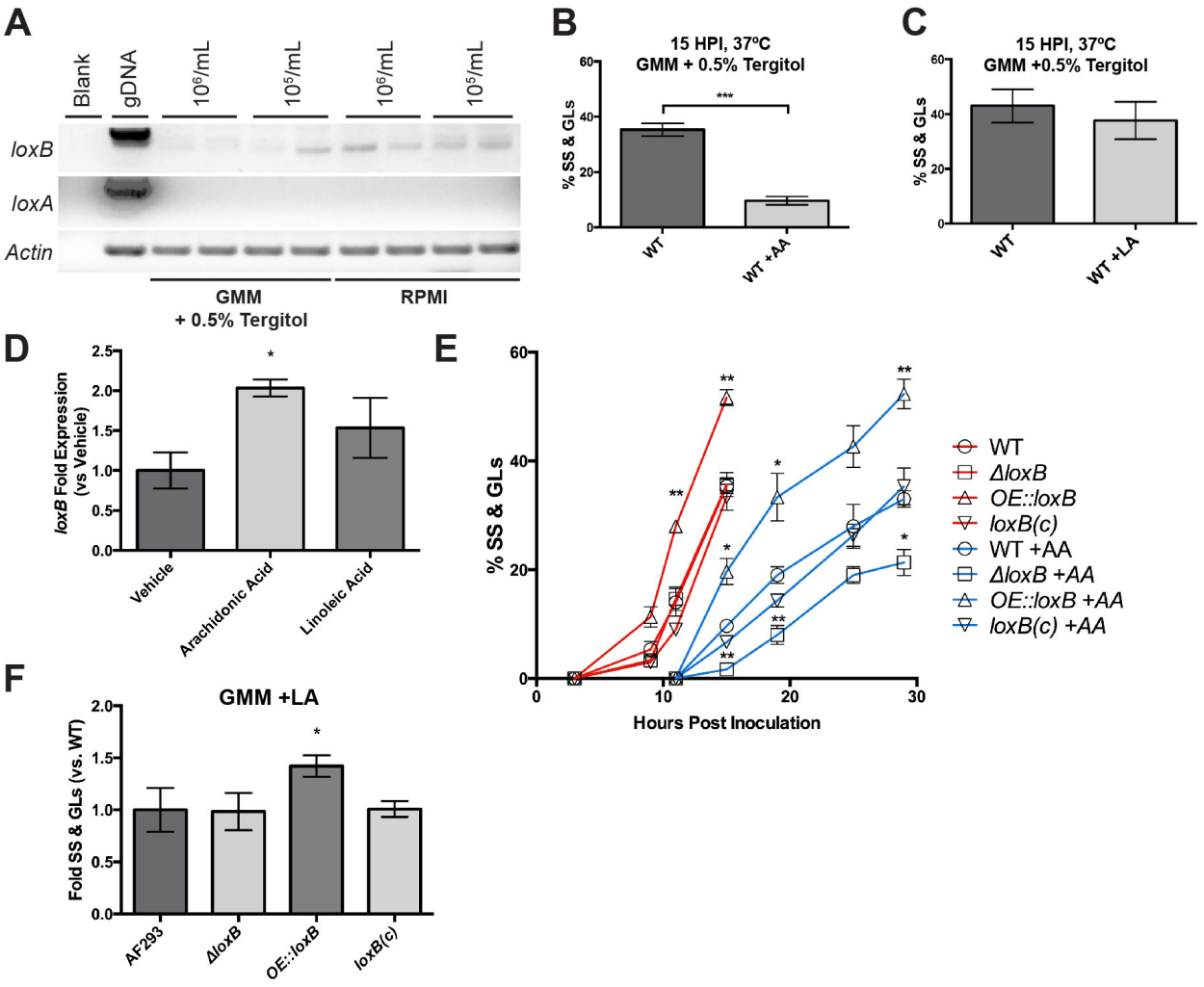

Figure 2. LoxB is up-regulated upon arachidonic acid exposure and promotes germination.

(A) *loxB* but not *loxA* is expressed in glucose minimal media (GMM) +0.5% tergitol and RPMI. Different spore concentrations of 1 X 10^6 and 1 X 10^5 spores were tested to look at density-dependent effects on lipoxygenase expression. *loxB* was up-regulated at 1 X 10^6 spores/mL in RPMI media compared to GMM. Actin served as a loading control for semi-qPCR analysis. **(B)** Addition of 0.5 μg/μL arachidonic acid (AA) reduces the number

of wild type swollen spores (SS) and germlings (GLs) compared to mock treatment, however the same concentration of linoleic acid (LA) does not **(C)**. **(D)** *loxB* is up-regulated in the presence of AA. Values are average (n=3) fold expression ± SEM after standardization to wild type tissue from mock treatment (vehicle). **(E)** Germination assay for *loxB* strains grown in GMM + 0.5% tergitol in the presence and absence of AA. Addition of AA significantly delays SS and GL formation of all strains compared to the mock treatment. **(F)** Upon exposure to 0.5 μg/μL linoleic acid, no difference in growth is observed after 15 hpi between wild type, *ΔloxB*, and *loxB(c)* complement strains, however the increase in SS and GLs when *loxB* is overexpressed is maintained as in **(E)**. Values represent average of n=3 trials ± SEM and Student's t-test was used to identify statistical differences, *p<0.05, **p<0.01, ***p<0.001.

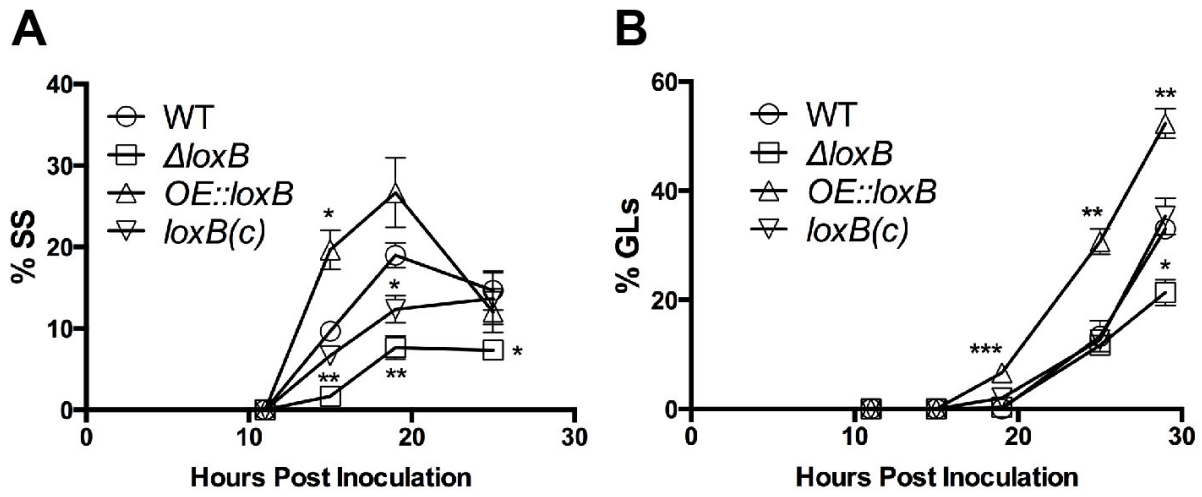

Figure 3. LoxB affects swollen spore and germling formation.

Breakdown of the total number of germinating spores by swollen spore (SS) **(A)** or germlings (GLs) **(B)** in the presence of AA. Overexpression of *loxB* yields a higher number of GLs through 29 hpi. Difference in the number of SS were more significant at multiple timepoints, with the greatest difference among the strains observed 15 hpi. Values represent average of n=3 trials ± SEM and Student's t-test was used to identify statistical differences, *p<0.05, **p<0.01, ***p<0.001.

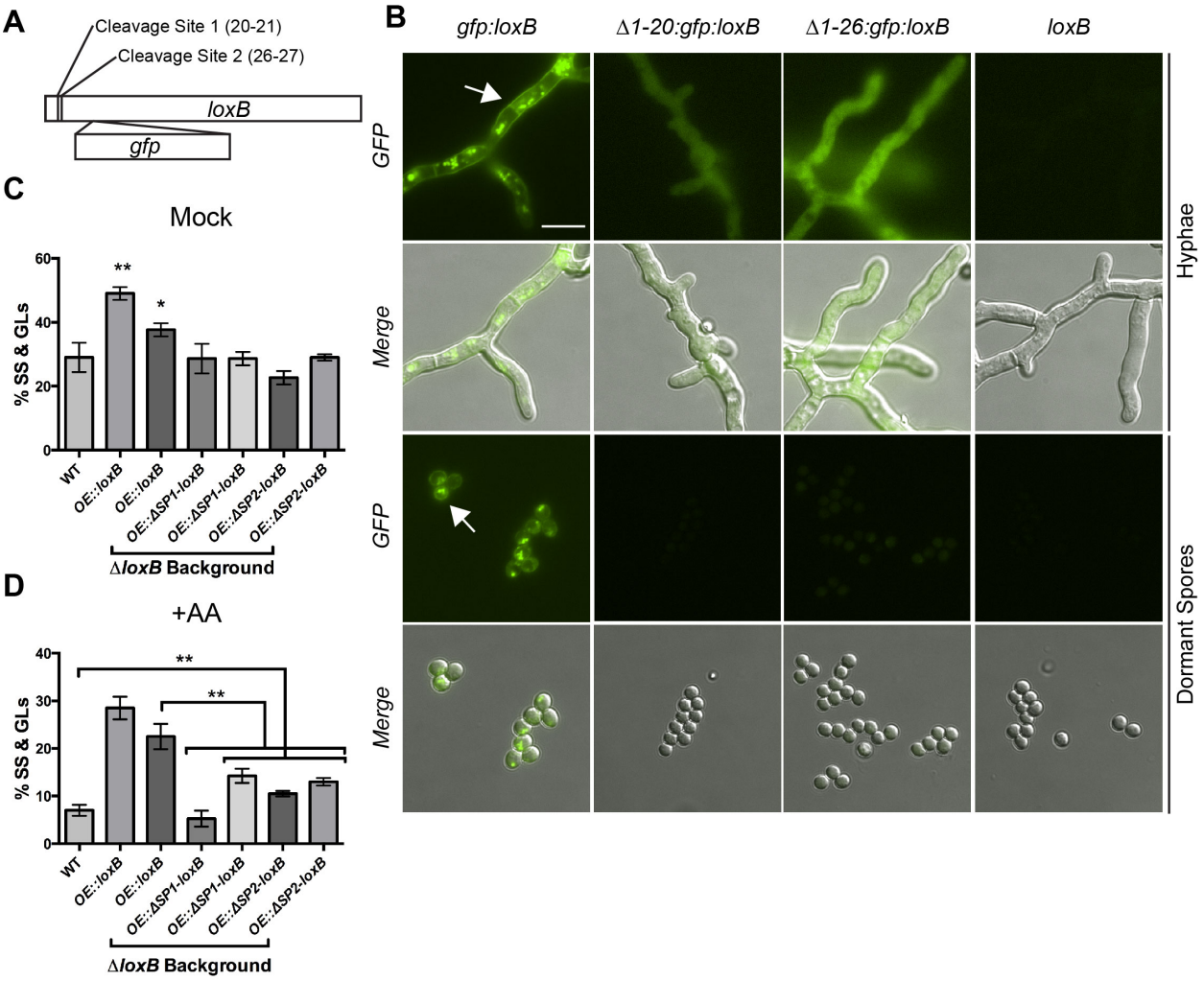

Figure 4. Disruption of signal peptide affects LoxB localization and dormant spore maturation.

(A) Location of the putative signal peptide cleavage sites predicted by Signal P 4.0 server (43). Cleavage site are predicted between resides 20 and 21 or residues 26 and 27. **(B)** Localization of various permutations of GFP-LoxB fusion proteins. Full-length GFP-LoxB protein localizes to the cell wall, septa, and puncta within hyphae and cell wall and puncta within dormant spores. GFP-LoxB protein lacking the first 20 or 26 amino acids localizes throughout the cytoplasm of the hyphae only and is undetectable in dormant spores. A

strain overexpressing untagged full-length *loxB* was used as a fluorescence negative control. **(C)** Spores derived from strains overexpressing truncated versions of *loxB* (*Δ1-20: OE:ΔSP1-loxB*, *Δ1-26*: *OE:ΔSP2-loxB*) germinate to the same degree as wild type spores, whereas spores derived from strains expressing full-length *loxB* in wild type and *ΔloxB* backgrounds maintain a higher degree of swollen spores (SS) and germlings (GLs) than wild type. **(D)** Upon incubation with 0.5 μg/μL AA, dormant spores derived from strains overexpressing truncated versions of *loxB* produce significantly more SS and GLs than wild type, with the exception of one *Δ1-20: OE:ΔSP1-loxB* strain. However, the percentage of dormant spores that proceed to SS or GLs is still significantly less than those expressing full-length versions of *loxB*. Values represent average of n=3 ± SEM and Student's t-test was used to identify statistical differences, *p<0.05, **P<0.01, ***p<0.001.

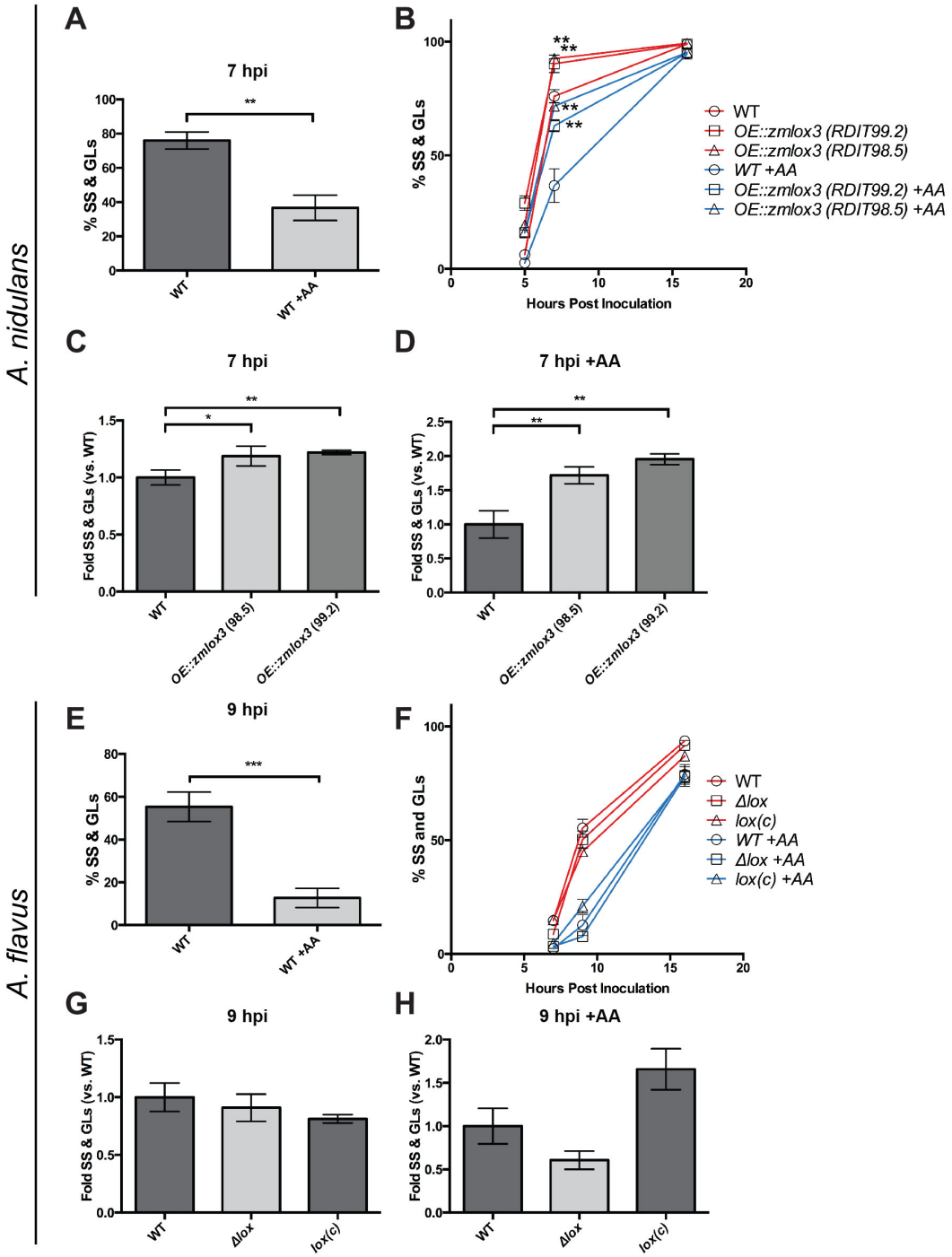

Figure 5. Synthetic lipoxygenase expression promotes germination in *Aspergillus nidulans*.

(A) Addition of 0.5 μg/μL AA reduced the number of swollen spores (SS) and germlings (GL) compared to mock treatment in the wild type. **(B)** *Aspergillus nidulans* mutants overexpressing a synthetic *Zea mays* lipoxygenase (*zmlox3)* have a higher degree of SS and GLs than wild type in both the mock and AA treatment through 16 hpi, at which equivalent profiles to the mock treatment are observed. Differences were quantified and compared at 7 hpi in both the mock treatment **(C)** and AA treatment **(D)**. **(E)** Addition of 0.5 μg/μL AA inhibited germination of *A. flavus* wild type, particularly 9 hpi. However, by 16 hpi, equivalent numbers of SS and GLs were observed when treated with AA compared to the mock. Disruption and complementation of the bonefide *lox* had no differential effect on SS and GL formation compared to wild type **(F)**. Comparisons were made 9 hpi and no differences observed in both the mock **(G)** or AA treatment **(H)**. Values represent average of n=3 trials ± SEM and Student's t-test was used to identify statistical differences, *$p<0.05$, **$p<0.01$, ***$p<0.001$.

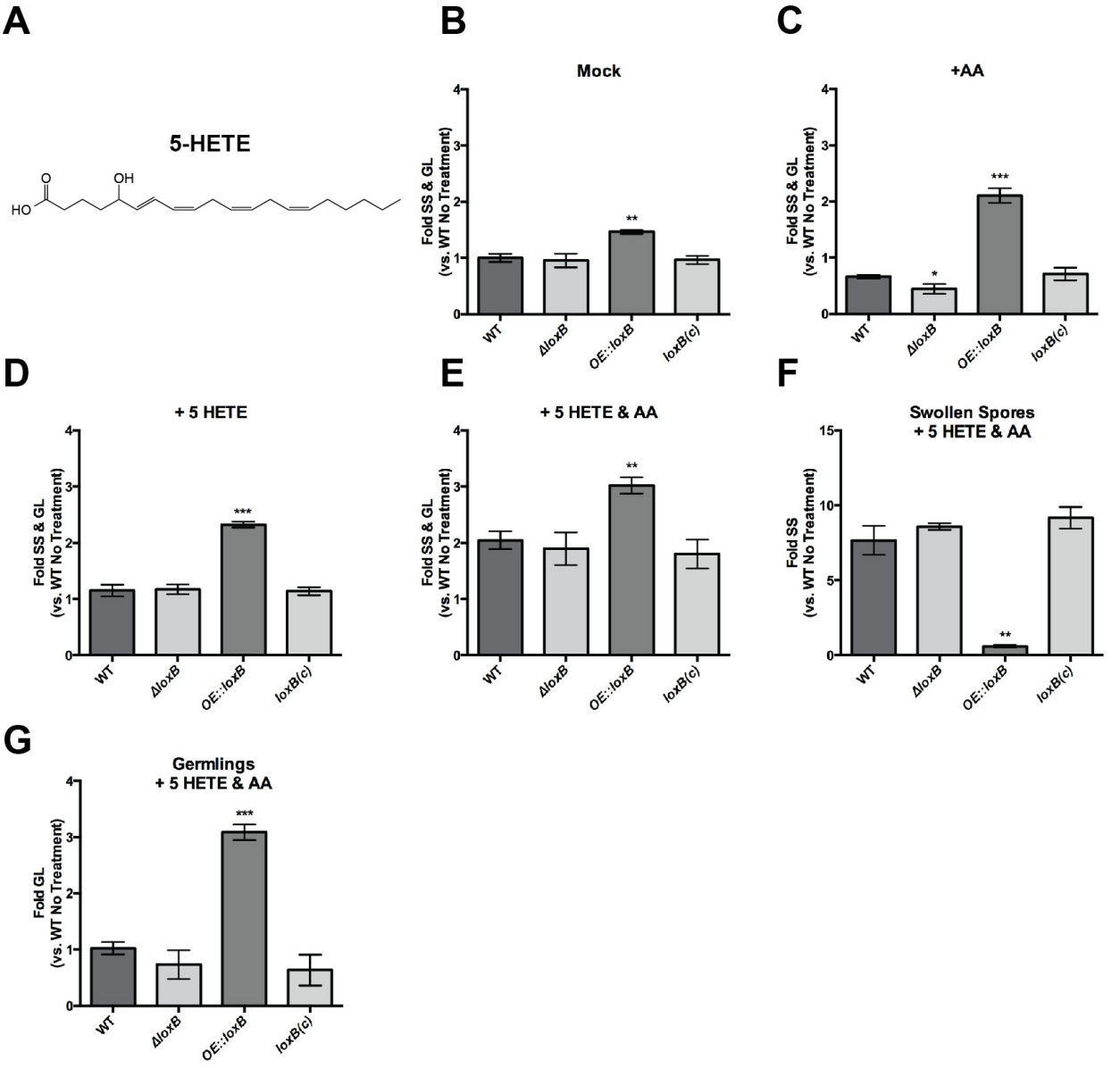

Figure 6. 5-HETE promotes swollen spore and germling formation

(A) The human 5-Lox metabolite, 5-HETE. Quantification of swollen spores (SS) and germlings (GL) for *loxB* strains grown in GMM +0.5% tergitol (mock) **(B)**, 0.5 μg/μL AA **(C)** or 5-HETE **(D)** or both **(E)**. While exposure to AA reduces the number of SS and GLs

compared to wild type in the Δ*loxB* strain, exposure to 0.5 μg/μL 5-HETE, or AA and 5-HETE maintains or increases the proportion of SS and GLs compared to the mock treatment, respectively. **(F)** SS are significantly increased compared to the mock treatment in the presence of AA and 5-HETE. Few SS were observed in the *OE::loxB* strain since all dormant spores had already progressed to the GL stage **(G)**. Values represent average of n=3 ± SEM and Student's t-test was used to identify statistical differences, *p<0.05, **p<0.01, ***p<0.001.

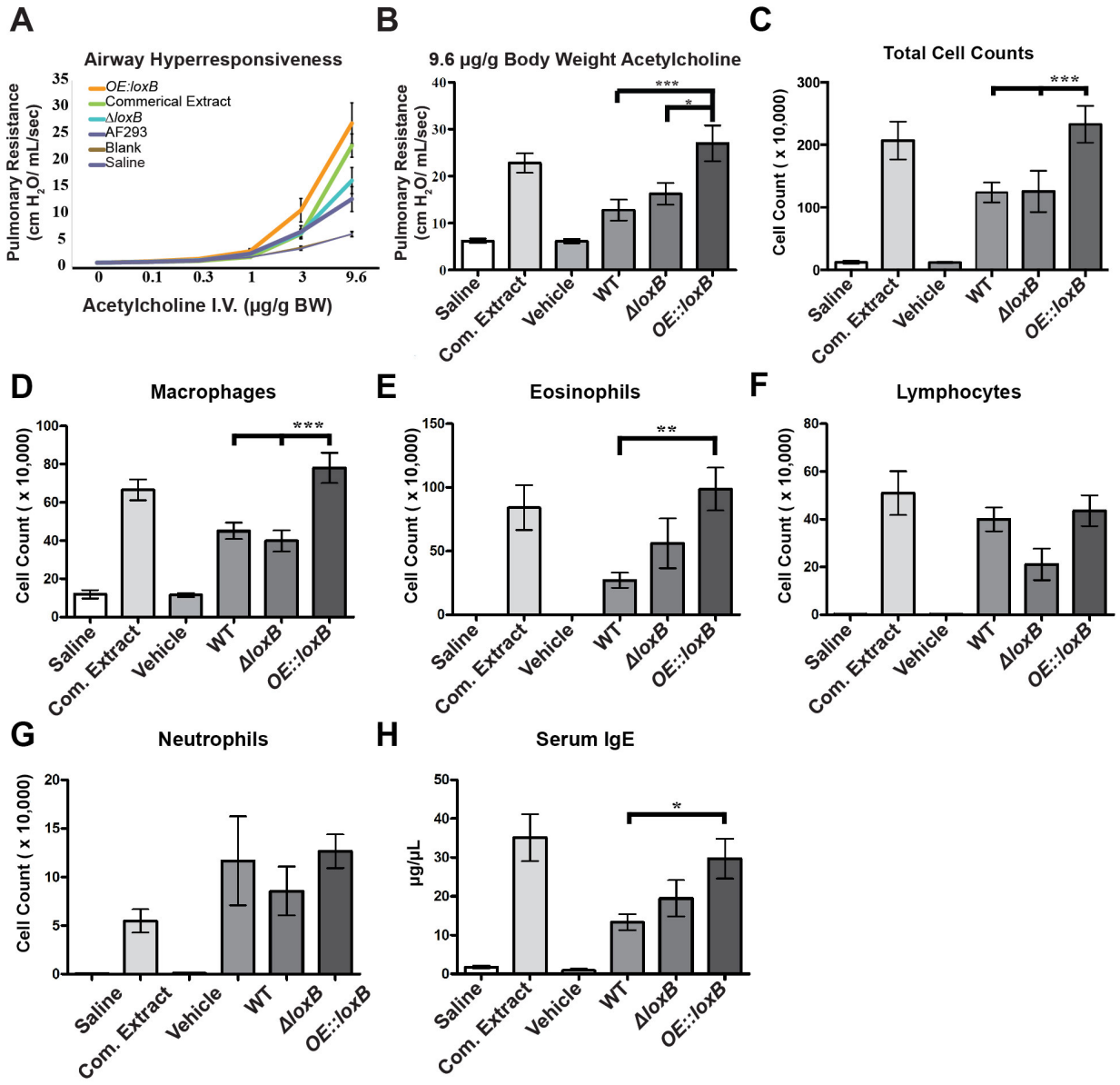

Figure 7. LoxB fungal extract and culture supernatant induce airway hyperresponsiveness, promote macrophage/eosinophil recruitment and elevated *IgE* levels in a murine asthma model.

(A) Fungal extract and culture supernatant from the *OE::loxB* strain resulted in mice with an airway much more responsive to acetylcholine challenge than mice treated with wild

type or Δ*loxB* fungal extract and culture supernatant. **(B)** Differences in airway hyperresponsiveness was greatest at 9.6 μg/g body weight, the highest concentration of acetylcholine administered. In mice treated with overexpression *loxB* fungal extract and culture supernatant, significantly more total immune cells **(C)** were observed in bronchoalveolar lavage fluid of treated mice. Specifically, macrophages **(D)** and eosinophils **(E)** were increased compared to mice treated with wild type or Δ*loxB* fungal extract and culture supernatant. No difference in lymphocytes **(F)** or neutrophils **(G)** was observed among the *loxB* strains. (H) Serum IgE levels were almost three times higher in mice treated with *OE::loxB* fungal extract and culture supernatant than mice treated with wild type or Δ*loxB* extract and supernatant. Values are mean of nine replicates ± SEM. *p<0.05, **p<0.01, ***p<0.001.

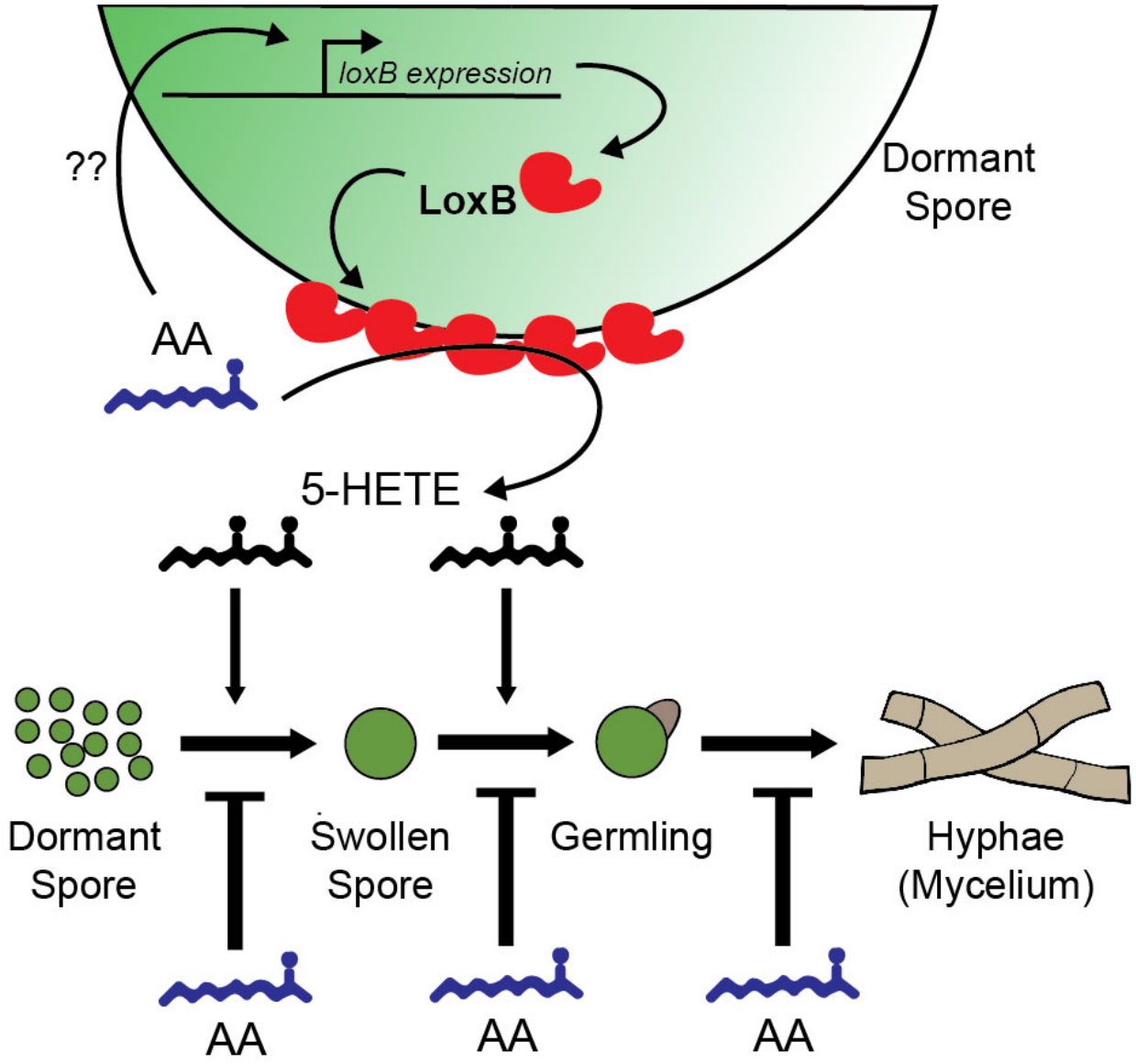

Figure 8. Hypothetical model for the effects of AA, LoxB, and oxylipins on the germination of spores in *A. fumigatus.*

Arachidonic acid (AA) has inhibitory effects on each stage of *A. fumigatus* development from dormant spores to mycelial network. The inhibitory effects of AA can be suppressed in a *loxB*-dependent fashion through the AA-dependent up-regulation of *loxB* via unknown

mechanisms. Upon proper localization, LoxB is poised to convert the germination program inhibitor AA to stimulatory 5-HETE.

3.8 TABLES

Table 1. *Aspergillus fumigatus* strains used in this study.

Fungal strain	Genotype	Source or reference
AF293	Wild type	(69)
AF293.1	*pyrG1*	(70)
AF293.6	*pyrG1 argB1*	(69)
TGJF1.5	*pyrG1;gpdA*(p):*loxB A. parasiticus pyrG*	This study
TGJF1.7	*pyrG1; gpdA*(p):*loxB A. parasiticus pyrG*	This study
TTRD51	*pyrG1, argB1, ΔloxB::A. fumigatus argB*	This study
TJMP39.6	*pyrG1 argB1; ΔloxB::A. fumigatus argB, A. parasiticus pyrG*	This study
TGJF33.6	*pyrG1 argB1, ; ΔloxB::A. fumigatus argB, loxB(p):loxB A. parasiticus pyrG*	This study
TGJF34.9	*pyrG1, argB1, ΔloxB::A. fumigatus argB gpdA*(p)*:loxB A. parasiticus pyrG*	This study
TGJF34.10	*pyrG1, argB1, ΔloxB::A. fumigatus argB gpdA*(p):*loxB A. parasiticus pyrG*	This study
TGJF35.4	*pyrG1, argB1, ΔloxB::A. fumigatus argB gpdA*(p)*:Δ1-20:loxB A. parasiticus pyrG*	This study
TGJF35.5	*pyrG1, argB1, ΔloxB::A. fumigatus argB*	This study

	gpdA(p):Δ1-20:loxB A. parasiticus pyrG	
TGJF36.1	*pyrG1, argB1, ΔloxB::A. fumigatus argB gpdA(p):Δ1-26:loxB A. parasiticus pyrG*	This study
TGJF36.3	*pyrG1, argB1, ΔloxB::A. fumigatus argB gpdA(p):Δ1-26:loxB A. parasiticus pyrG*	This study
TGJF43.8	*pyrG1, argB1, ΔloxB::A. fumigatus argB gpdA(p):gfp:loxB A. parasiticus pyrG*	This study
TGJF44.14	*pyrG1, argB1, ΔloxB::A. fumigatus argB gpdA(p):Δ1-20:gfp:loxB A. parasiticus pyrG*	This study
TGJF45.15	*pyrG1, argB1, ΔloxB::A. fumigatus argB gpdA(p):Δ1-26:gfp:loxB A. parasiticus pyrG*	This study
RDIT9.32	Wild type	(71)
RDIT99.2	*gpdA(p)::ZmLOX3::pyroA veA*	(44)
RDIT98.5	*gpdA(p)::ZmLOX3::pyroA veA*	(44)
NRRL3357	Wild type	(72)
TSHB2.39	*ΔpyrG, ΔAflox::pyrG*	(28)

TSHB3.1c	∆*pyrG, ∆Aflox::pyrG; Aflox::phleomycin*	(28)

Table 2. Primers used in this study.

Primer	Sequence	Purpose
GF gpdA/loxB-loxB(t) F	5'-AGCTACCCCGCTTGAGCAGACATCACCATGATGGTCTTCAGTGATTGCCT-3'	Overexpress *loxB*
GF loxB(t) XbaI Site R	5'-GGCGGCCGCTCTAGAAGCAGAC-3'	Overexpress *loxB*
GF gpdA F	5'-CTCTCTACTAGTATCCGGATGTCGAAGGCTTGGGGCACCTGC-3'	gpdA(promoter)
GF gpdA/loxB R	5'-CGAGAAAATCAGGCAATCACTGAAGACCATCATGGTGATGTCTGCTCAAG-3'	gpdA(promoter)
JP Afumi argB F	5'- GAACGCGGTCTGCATCCAAG-3'	argB
JP Afumi argB R	5'- GAAGGAGAGACCCATACATCC-3'	argB
TDLoxB P1 F	5'-GAAAGACATCCCAGACAA-3'	5' Flank
TDLoxB P2 F	5'-GCATGTAAGCACCCTTGTC-3'	Nested For
TD LoxB P3 R	5'-CTTGGATGCAGACCGCGTTCGCCAAAGTGTTTCTCATCGTC-3'	*loxB* 5' Flank cassette

TDLoxB P4 F	5'-GGATGTATGGGTCTCTCCTTCCGTTTGCTGACGCTGGAAGTA-3'	*loxB* 3' Flank cassette
TDLoxB P5 R	5'-GTCAGGAAATGGCCTCTGA-3'	Nested Rev
TDLoxB P6 R	5'-ATACCCTGGGCTCGATTAG-3'	3' Flank
GF d1-20:loxB F	5'-CCCCGCTTGAGCAGACATCACCATGCTGCCAGTGGTTCCCGGCCAAACAG-3'	*loxB* Signal Peptide Deletion (1-20)
GF d1-26:loxB R	5'-CCCCGCTTGAGCAGACATCACCATGCAAACAGTGATGGAACCTTCCGCAGC-3'	*loxB* Signal Peptide Deletion (1-26)
GF loxB Complement F	5'-CTCTCTACTAGTTTGGAGACGAGAAATGTGATCCAAAGG-3'	*loxB* Complement
GF loxB Complement R	5'-GCTCAGGCGGCCGCTTGGTTTGCAGCATCGTATCAGG-3'	*loxB* Complement
GF loxB-Nterm GFP F	5'-CTGCCAGTGGTTCCCGGCCAAACAGTGATGAGTAAAGGAGAAGAACTTTTCACTGG-3'	loxB gfp

GF loxB-Nterm GFP R	5'-CCCGTCATCAGGAAGGGCTGCGGAAGGTTCGGCACCGGCTCCAGCGCCTGCACCAGC-3'	loxB gfp
GF loxB qPCR F	5'-CCATGAGCGCTCGTCATCC-3'	loxB qPCR
GF loxB qPCR R	5'-CGCGGTCAAACAGGTCTTGG-3'	loxB qPCR
GF loxA seq 1F	5'-CGAGCCTTTGGTTCCATCG-3'	loxA qPCR
GF loxA Probe R	5'-GCATCGCTGTACCAATCTGG-3'	loxA qPCR
FY act1 RT FOR	5'-CGGCCGTGATCTGACGGAC-3'	Actin qPCR
FY act1 RT REV	5'-AGCTCTGGGAGGCAGTCTG-3'	*Actin* qPCR

.

3.9 SUPPLEMENTAL FIGURES AND LEGENDS

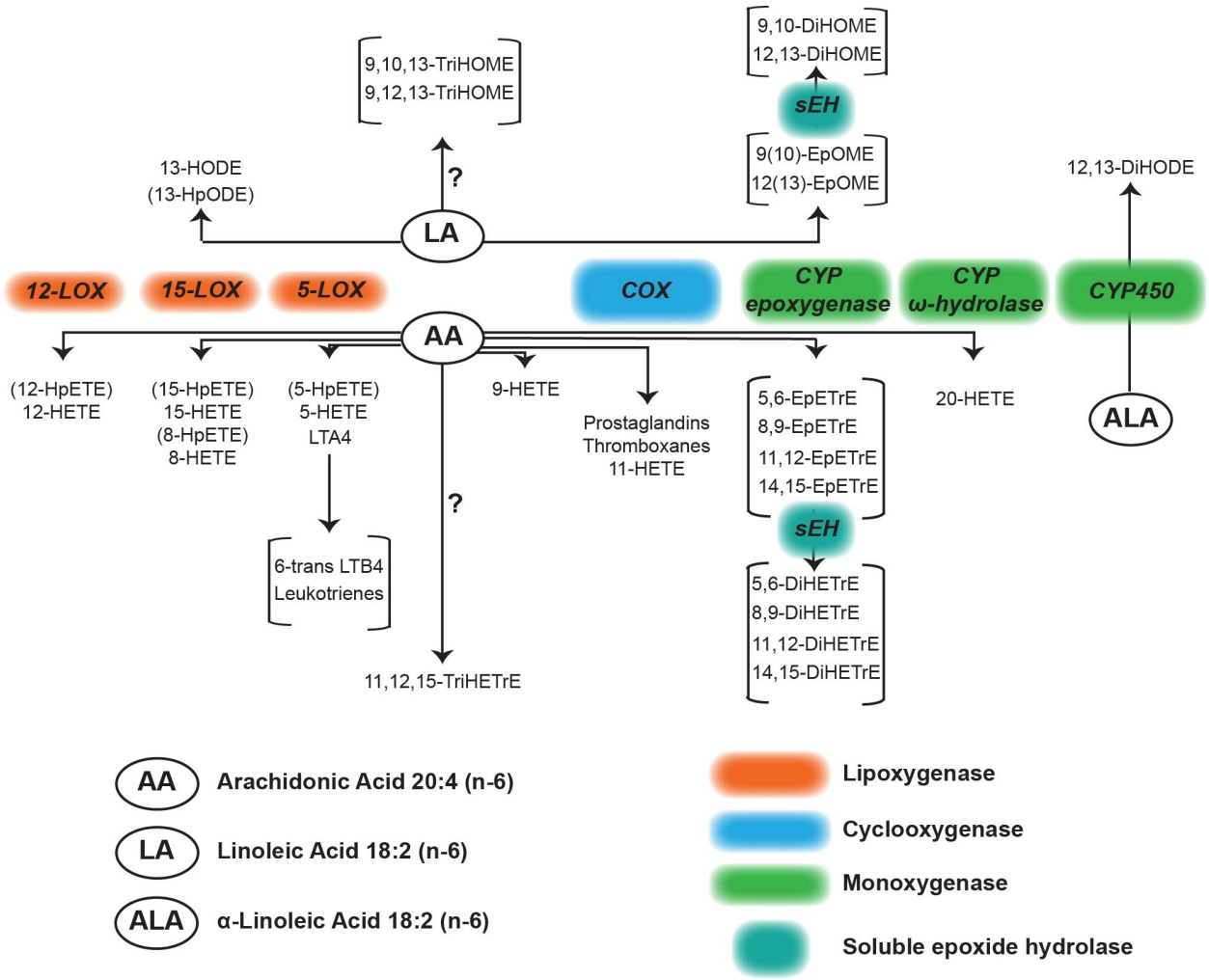

Supplemental Figure 1. Oxylipin biosynthetic pathway and corresponding fatty acid precursors.

The major classes of enzymes that act upon polyunsaturated fatty acids include lipoxygenases (Lox), cyclooxygenases (Cox), cytochrome (Cyp) P450 epoxygenases, cytochrome (Cyp) P450 ω-hydrolases, and soluble epoxide hydrolases (sEH). Cox

enzymes are responsible for the synthesis of 11-HETE, prostaglandins, and thromboxanes. Epoxygenases act upon either linoleic or arachidonic acid to produce epoxyoctadecanoic acids (EpOMEs) and epoxyeicosatrenoic acids (EpETrEs), respectively. sEHs further convert these epoxides into dihydroxyoctadecanoic acids (DiHOMEs) and dihydroxyeicosatrenoic acid (DiHETrEs). The exact mechanism of trihydroxyeicosatrenoic (TriHETrE) and trihydroxyoctadecanoic (TriHOME) is not completely elucidated. Linolenic acid can be acted upon by cytochrome P450 enzymes to produce di-hydroxyoctadecadienoic acids (DiHODES), such as 12,13-DiHODE. Lipoxygenases, including 12-Lox*,* 15-Lox*, and* 5-Lox, oxygenate arachidonic acid to produce hydroperoxyeicosatrenoic acids (HpETEs) that are further reduced to hydroxyeicosatrenoic acids (HETEs). 5-HPETE, produced by human 5-Lox, is the first committed step in leukotriene synthesis. Conversely, lipoxygenase activity yields hydroxyoctadecadienoic acids (HODEs) from linoleic acid.

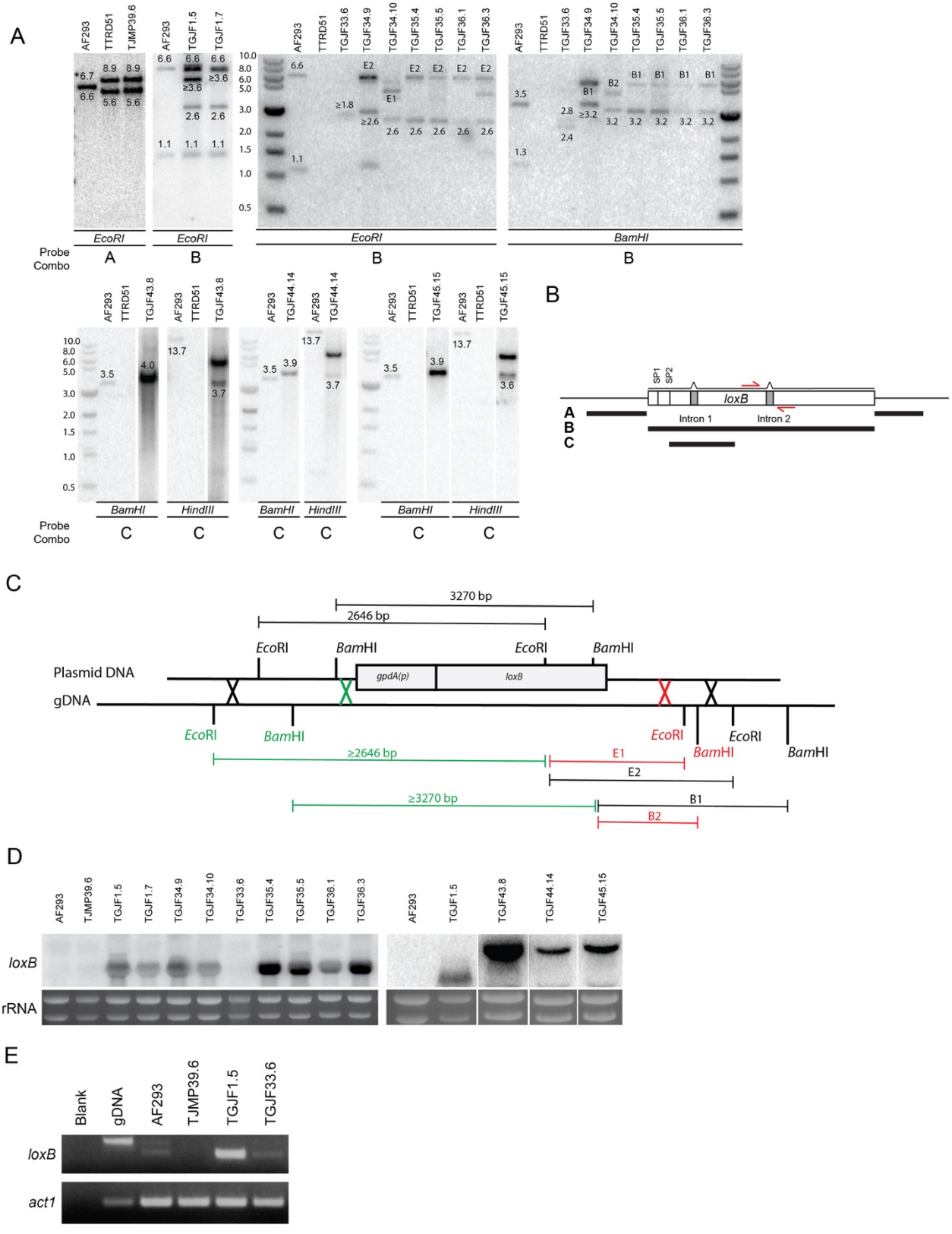
A
AF293
TTRD51
TJMP39.6
TGJF1.5
TGJF1.7
TGJF33.6
TGJF34.9
TGJF34.10
TGJF35.4
TGJF35.5
TGJF36.1
TGJF36.3
EcoRI
BamHI
HindIII
Probe Combo
A
B
C
B
SP1
SP2
loxB
Intron 1
Intron 2
C
3270 bp
2646 bp
EcoRI
BamHI
Plasmid DNA
gDNA
gpdA(p)
loxB
≥2646 bp
E1
E2
≥3270 bp
B1
B2
D
loxB
rRNA
E
Blank
gDNA
AF293
TJMP39.6
TGJF1.5
TGJF33.6
loxB
act1

Supplemental Figure 2. Development and verification of *A. fumigatus loxB* mutant strains.

(A) Auxotrophic strains in the AF293 background were utilized to make various *loxB* mutants. As described in Experimental Procedures, various disruption cassettes and plasmid constructs were used to transform AF293.6 or AF293.1 auxotrophic strains to prototrophy. Verification of the appropriate strain was carried out via Southern blot using the specified restriction enzyme and radiolabeled DNA probe as diagramed in **(B).** TTRD51 (Δ*loxB* auxotroph), TJMP39.6 (Δ*loxB* prototroph, used in this study), TGJF1.5 & TGJF1.7 (*OE::loxB*, used in this study), TGJF33.6 (*loxB* complement in Δ*loxB* background, used in this study), TGJF34.9 & TGJF34.10 (*OE::loxB* in Δ*loxB* background, used in this study), TGJF35.4 & TGJF35.5 (*OE::[ΔSP1]:loxB* in Δ*loxB* background, used in this study), and TGJF36.1 & TGJF36.3 (*OE::[ΔSP2]:loxB* in Δ*loxB* background, used in this study), TGJF43.8 (*OE::gfp:loxB* in Δ*loxB* background, used in this study), TGJF44.14 (*OE::[ΔSP1]:gfp:loxB* in Δ*loxB* background, used in this study), and TGJF45.15 (*OE::[ΔSP2]:gfp:loxB* in Δ*loxB* background, used in this study) were all compared to the AF293 (WT) strain and confirmed. SP1 and SP2 refer to the two putative N-terminal signal peptide regions as diagramed in **(B). (B).** Gene structure for *loxB* and regions used for radiolabeled probes in Southern and northern blots. **(C)** Restriction digest pattern used to confirm ectopic integration of *loxB* constructs. Depending on the location of the recombination event, different size products are identified via Southern blot. **(D)** Northern analysis of total RNA isolated from mycelial tissue. The entire ORF of *loxB* was used to

probe for transcript. Ribosomal RNA was used as a loading control. Note the shift in the band size for the gfp-*loxB* fusion construct (TGJF43.8, TGJF44.14, and TGF45.15). **(E**) To further verify deletion and complementation of *loxB,* semi RT-PCR was carried out of cDNA produced from total RNA (see Experimental Procedures). Amplicons corresponding to cDNA from spliced *loxB* mRNA (vs. genomic DNA or gDNA) were identified in the wild type (AF293), *loxB* complement (TGJF33.6), and *loxB* overexpression (TGJF1.5) strains. No amplicon was detected in the deletion strain (TJMP39.6). *act1* was used as a cDNA loading control.

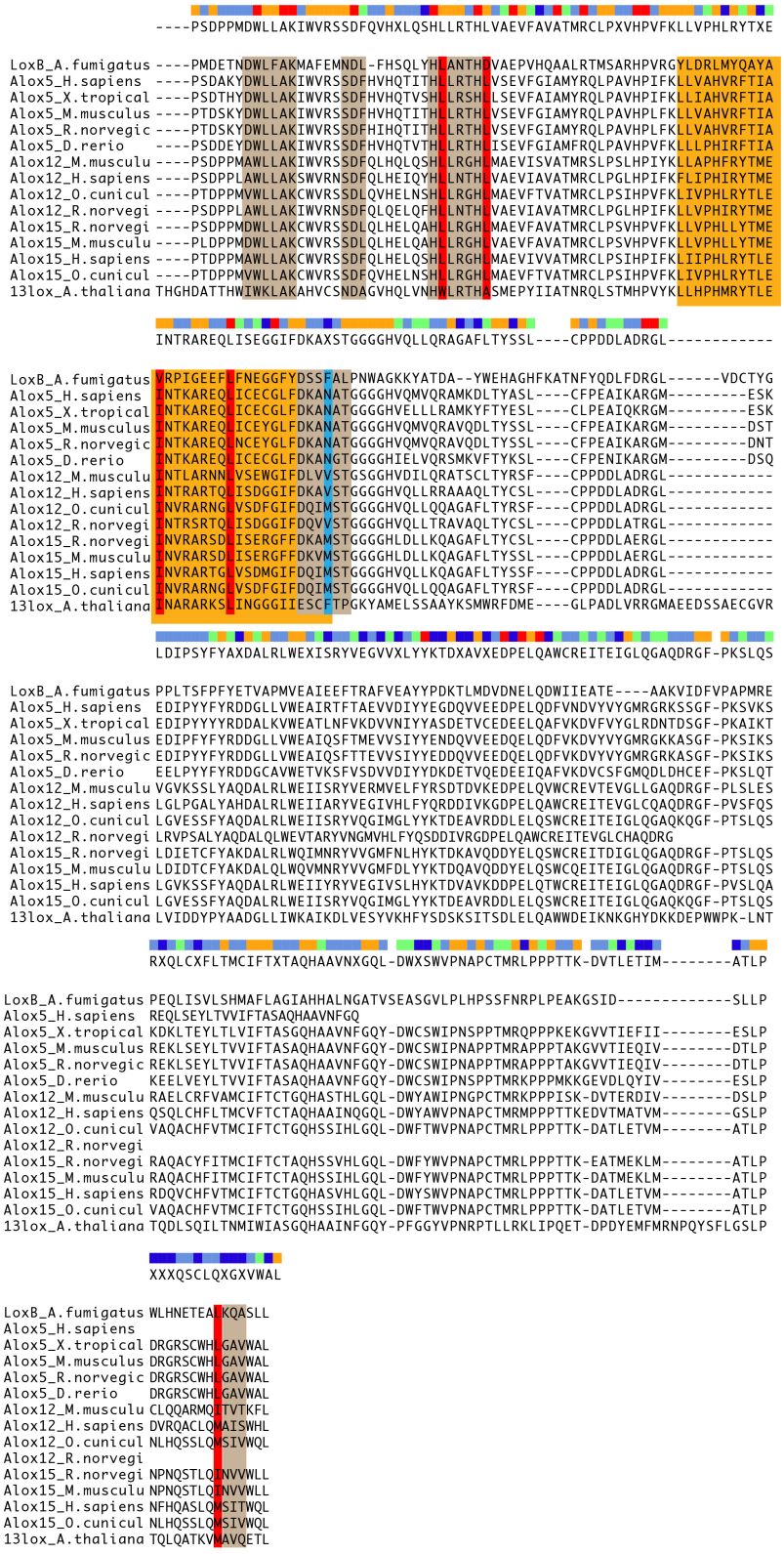

Supplemental Figure 3. Multiple sequence alignment of *A. fumigatus* LoxB with mammalian 5-,12-,and 15-Lox sequences as well as a 13-Lox sequence from *Arabidopsis thaliana*.

Numerous studies have investigated domains of mammalian Loxs to predict oxylipin product formation. For example, 5-Lox residues important for proper alignment of the arachidonic acid pentadiene motif within the active site are highlighted in red (39) while a 15-Lox splice variant lacking the region highlighted in orange yields a 15-Lox that produces predominantly 5- and 15-HETE from arachidonic acid (73). Residues implicated in catalytic activity, metal ion coordination, and sequence determinants for positional specificty of oxygenation are depicted in tan (40). Other residues implicated in positional specificty include those shaded in blue (12- vs. 15-Lox) (74). While most human Loxs contain a iron coordination doman, Heshof et al reports that *A. fumigatus* LoxB is a manganese-containing lipoxygenase (27).

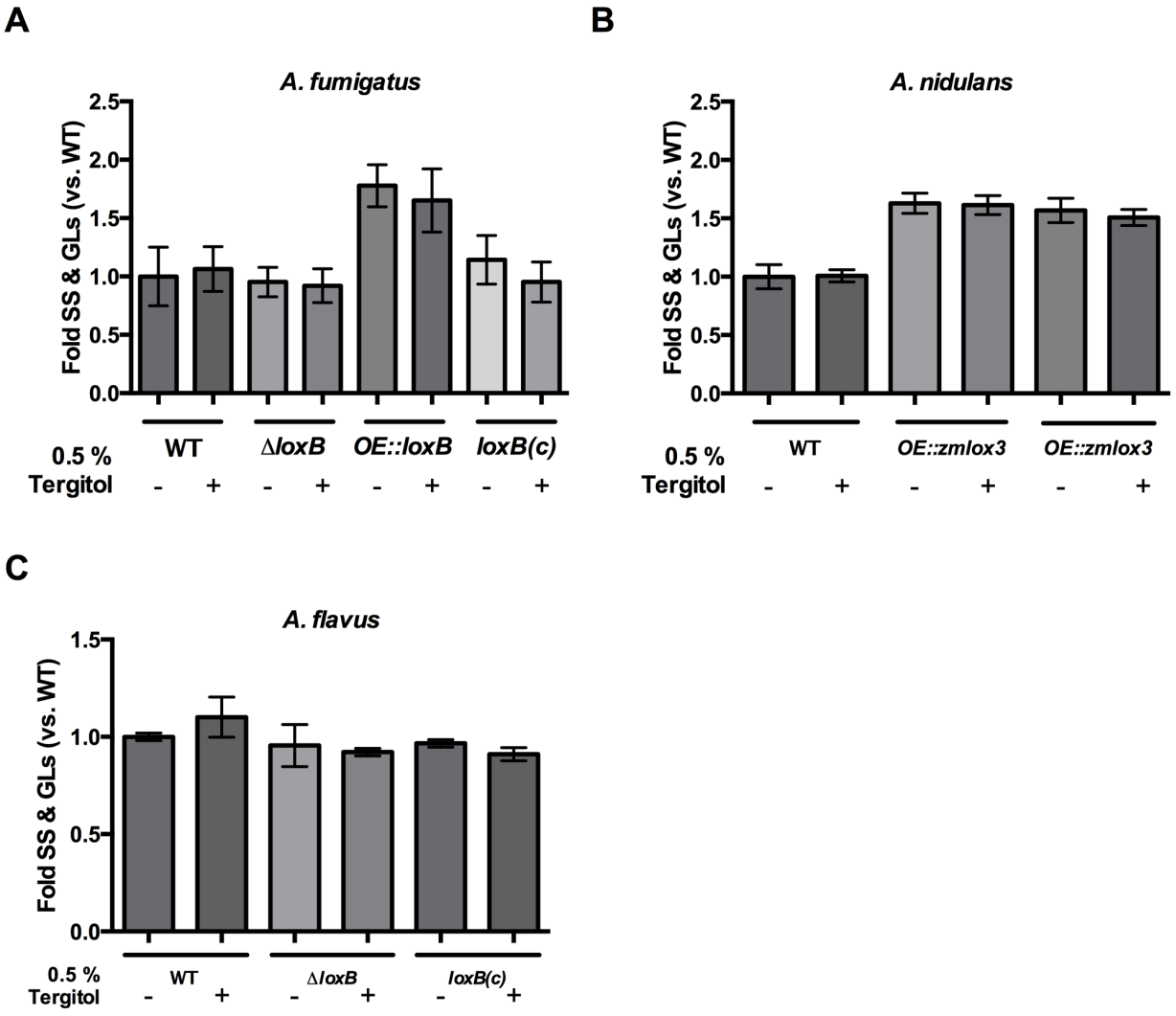

Supplemental Figure 4. Effects of 0.5% tergitol on various lipoxygenase mutants.

Aspergillus fumigatus **(A)**, *A. nidulans* **(B)**, and *A. flavus* **(C)** were all tested.

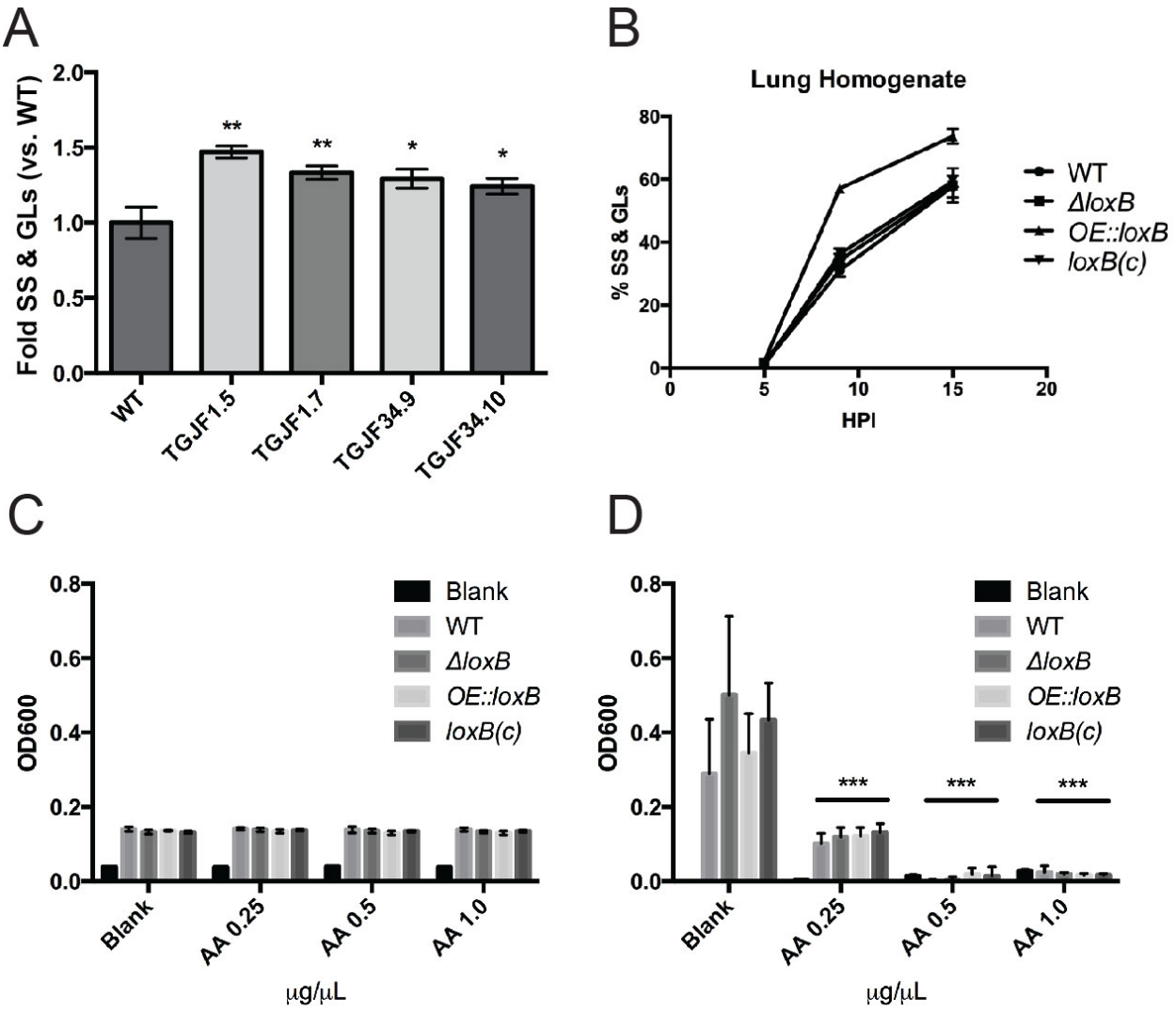

Supplemental Figure 5. Germination and *loxB* expression in various *A. fumigatus* *loxB* mutants.

(A) The proportion of swollen spores (SS) and germlings (GL) in *A. fumigatus* mutants overexpressing *loxB* in wild type (TGJF1.5 and TGJF1.7) or Δ*loxB* (TGJF34.9 and TGJF34.10) backgrounds is elevated compared to wild type. **(B)** Percent SS and GLs

over 15 hours in lung homogenate media. All strains had similar levels of SS and GLs, with the exception of the *OE::loxB* strain, which had significantly more SS and GLs at all timepoints tested. **(C)** Mycelial growth of wild type and *loxB* mutant strains. 1 X 10^5 spores were inoculated in 100 µL of GMM +0.5% tergitol and grown in a 96 well plate overnight, after which and OD_{600} reading revealed no difference in mycelial growth. Arachidonic acid was added to the mycelium at a final concentration of 0.25, 0.5, and 1.0 µg/µL and an additional OD_{600} reading collected 22 hours later **(D)**. Arachidonic acid inhibited mycelial growth in a dose-dependent fashion, but *loxB* disruption or overexpression had no differential effect on growth.

3.10 REFERENCES

1. **Osherov N**, **May G**. 2000. Conidial germination in *Aspergillus nidulans* requires RAS signaling and protein synthesis. Genetics **155**:647–656.

2. **Som T**, **Kolaparthi VS**. 1994. Developmental decisions in *Aspergillus nidulans* are modulated by Ras activity. Mol Cell Biol **14**:5333–5348.

3. **Jin Y**, **Bok JW**, **Guzman-De-Peña D**, **Keller NP**, **Guzman-de-Pena D**, **Keller NP**. 2002. Requirement of spermidine for developmental transitions in *Aspergillus nidulans*. Mol Microbiol **46**:801–812.

4. **Liebmann B**, **Muller M**, **Braun A**, **Brakhage AA**. 2004. The cyclic AMP-dependent protein kinase a network regulates development and virulence in *Aspergillus fumigatus*. Infect Immun **72**:5193–5203.

5. **Kwon NJ**, **Garzia A**, **Espeso EA**, **Ugalde U**, **Yu JH**. 2010. FlbC is a putative nuclear C2H2 transcription factor regulating development in *Aspergillus nidulans*. Mol Microbiol **77**:1203–1219.

6. **Osherov N**, **May GS**. 2001. The molecular mechanisms of conidial germination. FEMS Microbiol Lett **199**:153–160.

7. **Carlile MJ**, **Watkinson SC**. 1994. The Fungi. Academic Press, London, 1994., London.

8. **Schmit JC**, **Brody S**. 1976. Biochemical genetics of *Neurospora crassa* conidial germination. Bacteriol Rev **40**:1–41.

9. **Talbot NJ**. 1995. Having a blast: exploring the pathogenicity of *Magnaporthe grisea*. Trends Microbiol **3**:9–16.

10. **Ruan Y**. 1995. Flavonoids stimulate spore germination in *Fusarium solani pathogenic* on legumes in a manner sensitive to inhibitors of cAMP-dependent protein kinase. Mol Plant-Microbe Interact. **8:**929.

11. **Macko V**, **Staples RC**, **Renwick JAA**. 1971. Germination self-inhibitor of sunflower and snapdragon rust uredospores. Phytopathology **61**:902.

12. **Chitarra GS, Abee T, Rombouts FM, Posthumus M a, Dijksterhuis J**. 2004. Germination of *Penicillium paneum* conidia is regulated by 1-Octen-3-ol, a volatile self-inhibitor. Appl. Environ. Micro. **70**:2823–2829.

13. **Fischer G**, **Schwalbe R**, **Möller M**, **Ostrowski R**, **Dott W**. 1999. Species-specific production of microbial volatile organic compounds (MVOC) by airborne fungi from a compost facility. Chemosphere **39**:795–810.

14. **Herrero-Garcia E**, **Garzia A**, **Cordobs S**, **Espeso EA**, **Ugalde U**. 2011. 8-Carbon oxylipins inhibit germination and growth, and stimulate aerial conidiation in *Aspergillus nidulans*. Fungal Biol **115**:393–400.

15. **Miyamoto K**, **Murakami T**, **Kakumyan P**, **Keller NP**, **Matsui K**. 2014. Formation of 1-octen-3-ol from *Aspergillus flavus* conidia is accelerated after disruption of cells independently of Ppo oxygenases, and is not a main cause of inhibition of germination. PeerJ **2**:e395.

16. **Aimanianda V**, **Bayry J**, **Bozza S**, **Kniemeyer O**, **Perruccio K**, **Elluru SR**, **Clavaud C**, **Paris S**, **Brakhage AA**, **Kaveri S V.**, **Romani L**, **Latgé J-P**. 2009. Surface hydrophobin prevents immune recognition of airborne fungal spores. Nature **460**:1117–1121.

17. **van de Veerdonk FL**, **Kullberg BJ**, **van der Meer JW**, **Gow NA**, **Netea MG**. 2008. Host-microbe interactions: innate pattern recognition of fungal pathogens. Curr Opin Microbiol **11**:305–312.

18. **Fischer GJ**, **Keller NP**. 2016. Production of cross-kingdom oxylipins by pathogenic fungi: An update on their role in development and pathogenicity. J Microbiol **54**:254–264.

19. **Buczynski MW**, **Dumlao DS**, **Dennis EA**. 2009. Thematic Review Series: Proteomics. An integrated omics analysis of eicosanoid biology. J Lipid Res **50**:1015–38.

20. **Santos PC, Santos DA, Ribeiro LS, Fagundes CT, de Paula TP, Avila TV, Baltazar L de M, Madeira MM, Cruz R de C, Dias ACF, Machado FS, Teixeira MM, Cisalpino PS, Souza DG**. 2013. The pivotal role of 5-Lipoxygenase-derived LTB4 in controlling pulmonary *Paracoccidioidomycosi*s. PLoS Negl Trop Dis 7.

21. **Secatto A**, **Soares EM**, **Locachevic GA**, **Assis PA**, **Paula-Silva FWG**, **Serezani CH**, **de Medeiros AI**, **Faccioli LH**. 2014. The leukotriene B_4/BLT_1 axis is a key determinant in susceptibility and resistance to histoplasmosis. PLoS One **9**:e85083.

22. **Colby JK**, **Gott KM**, **Wilder JA**, **Levy BD**. 2016. Lipoxin Signaling in Murine Lung Host Responses to *Cryptococcus neoformans* Infection. Am J Respir Cell Mol Biol **54**:25–33.

23. **Liu H**, **Zheng M**, **Qiao J**, **Dang Y**, **Zhang P**, **Jin X**. 2014. Role of prostaglandin D2 /CRTH2 pathway on asthma exacerbation induced by *Aspergillus fumigatus*. Immunology **142**:78–88.

24. **Hallstrand TS**, **Henderson Jr. WR**. 2010. An update on the role of leukotrienes in asthma. Curr Opin Allergy Clin Immunol2009/11/17. **10**:60–66.

25. **Henricks P**, **Engels F**, **Vanderlinde H**, **Garssen J**, **Nijkamp F**. 1995. 13-hydroxy-linoleic acid induces airway hyperresponsiveness to histamine and methacholine in guinea pigs *in vivo*. J Allergy Clin Immunol **96**:36–43.

26. **Kühn H**, **O'Donnell VB**, **Kuhn H**, **O'Donnell VB**. 2006. Inflammation and immune regulation by 12/15-lipoxygenases. Prog Lipid Res **45**:334–356.

27. **Heshof R**, **Jylha S**, **Haarmann T**, **Jorgensen AL**, **Dalsgaard TK**, **de Graaff LH**, **Jylhä S**, **Haarmann T**, **Jørgensen ALW**, **Dalsgaard TK**, **de Graaff LH**. 2014. A novel class of fungal lipoxygenases. Appl Microbiol Biotechnol **98**:1261–1270.

28. **Horowitz Brown S**, **Zarnowski R**, **Sharpee WC**, **Keller NP**. 2008. Morphological transitions governed by density dependence and lipoxygenase activity in *Aspergillus flavus*. Appl Env Microbiol **74**:5674–85.

29. **Shimizu K**, **Keller NP**. 2001. Genetic involvement of a cAMP-dependent protein kinase in a G protein signaling pathway regulating morphological and chemical transitions in *Aspergillus nidulans*. Genetics **157**:591–600.

30. **Sambrook J**, **Russell DW**. 2001. Molecular Cloning: A Laboratory Manual. Book, Cold Spring Harbor Laboratory Press, New York.

31. **Szewczyk E**, **Nayak T**, **Oakley CE**, **Edgerton H**, **Xiong Y**, **Taheri-Talesh N**, **Osmani S a**, **Oakley BR**. 2006. Fusion PCR and gene targeting in *Aspergillus nidulans*. Nat Protoc. **1**:3111–3120.

32. **Calvo A**, **Bok J**, **Brooks W**, **Keller N**. 2004. veA is required for toxin and sclerotial production in *Aspergillus parasiticus*. Appl Env Microbiol **70**:4733–4739.

33. **Sekonyela R**, **Palmer JM**, **Bok J-W**, **Jain S**, **Berthier E**, **Forseth R**, **Schroeder F**, **Keller NP**. 2013. RsmA regulates *Aspergillus fumigatus* gliotoxin cluster metabolites including cyclo(L-Phe-L-Ser), a potential new diagnostic marker for invasive aspergillosis. PLoS One **8**:doi: 10.1371/journal.pone.0062591.

34. **Bok JW**, **Keller NP**. 2012. Fast and easy method for construction of plasmid vectors using modified quick-change mutagenesis. Methods Mol Biol **944**:163–174.

35. **Yang L**, **Ukil L**, **Osmani A**, **Nahm F**, **Davies J**, **De Souza CP**, **Dou X**, **Perez-Balaguer A**, **Osmani SA**. 2004. Rapid production of gene replacement constructs and generation of a green fluorescent protein-tagged centromeric marker in *Aspergillus nidulans*. Eukaryot Cell2004/10/08. **3**:1359–1362.

36. **Dagenais TR**, **Chung D**, **Giles SS**, **Hull CM**, **Andes D**, **Keller NP**. 2008. Defects in conidiophore development and conidium-macrophage interactions in a dioxygenase mutant of *Aspergillus fumigatus*. Infect Immun2008/04/30. **76**:3214–3220.

37. **Little SA**, **Longbottom JL**, **Warner JO**. 1993. Optimized preparation of *Aspergillus fumigatus* extracts for allergy diagnosis. Clin Exp Allergy **23**:835–842.

38. **Gordon ED**, **Sidhu SS**, **Wang ZE**, **Woodruff PG**, **Yuan S**, **Solon MC**, **Conway SJ**, **Huang X**, **Locksley RM**, **Fahy J V**. 2012. A protective role for periostin and TGF-β in IgE-mediated allergy and airway hyperresponsiveness. Clin Exp Allergy **42**:144–155.

39. **Gilbert NC**, **Bartlett SG**, **Waight MT**, **Neau DB**, **Boeglin WE**, **Brash AR**, **Newcomer ME**. 2011. The structure of human 5-lipoxygenase. Science **331**:217–9.

40. **Schwarz K**, **Walther M**, **Anton M**, **Gerth C**, **Feussner I**, **Kuhn H**. 2001. Structural basis for lipoxygenase specificity - Conversion of the human leukocyte 5-lipoxygenase to

a 15-lipoxygenating enzyme species by site-directed mutagenesis. J Biol Chem **276**:773–779.

41. **Muller S**, **Baldin C**, **Groth M**, **Guthke R**, **Kniemeyer O**, **Brakhage AA**, **Valiante V**. 2012. Comparison of transcriptome technologies in the pathogenic fungus *Aspergillus fumigatus* reveals novel insights into the genome and MpkA dependent gene expression. BMC Genomics **13**:519.

42. **Tsitsigiannis D**, **Bok J**, **Andes D**, **Nielsen K**, **Frisvad J**, **Keller N**. 2005. *Aspergillus* cyclooxygenase-like enzymes are associated with prostaglandin production and virulence. Infect Immun **73**:4548–4559.

43. **Petersen TN**, **Brunak S**, **von Heijne G**, **Nielsen H**. 2011. SignalP 4.0: discriminating signal peptides from transmembrane regions. Nat Methods **8**:785–786.

44. **Brodhagen M**, **Tsitsigiannis DI**, **Hornung E**, **Goebel C**, **Feussner I**, **Keller NP**. 2008. Reciprocal oxylipin-mediated cross-talk in the *Aspergillus*-seed pathosystem. Mol Microbiol **67**:378–391.

45. **Kurup VP**, **Banerjee B**, **Hemmann S**, **Greenberger PA**, **Blaser K**, **Crameri R**. 2000. Selected recombinant *Aspergillus fumigatus* allergens bind specifically to IgE in ABPA. Clin Exp Allergy **30**:988–993.

46. **Fortwendel JR**, **Fuller KK**, **Stephens TJ**, **Bacon WC**, **Askew DS**, **Rhodes JC**. 2008. *Aspergillus fumigatus* RasA regulates asexual development and cell wall integrity. Eukaryot Cell **7**:1530–1539.

47. **Liu S**, **Ruan W**, **Li J**, **Xu H**, **Wang J**, **Gao Y**, **Wang J**. 2008. Biological control of phytopathogenic fungi by fatty acids. Mycopathologia **166**:93–102.

48. **Lounds C**, **Eagles J**, **Carter AT**, **MacKenzie DA**, **Archer DB**. 2007. Spore germination in *Mortierella alpina* is associated with a transient depletion of arachidonic acid and induction of fatty acid desaturase gene expression. Arch Microbiol **188**:299–305.

49. **Lim FY**, **Ames B**, **Walsh CT**, **Keller NP**. 2014. Co-ordination between BrlA regulation and secretion of the oxidoreductase FmqD directs selective accumulation of fumiquinazoline C to conidial tissues in *Aspergillus fumigatus*. Cell Microbiol2014/03/13. **16**:1267–83.

50. **Khalaj V**, **Brookman JL**, **Robson GD**. 2001. A study of the protein secretory pathway of *Aspergillus niger* using a glucoamylase-GFP fusion protein. Fungal Genet Biol2001/03/30. **32**:55–65.

51. **Kift N, Prost I, Dhondt S, Rothe G, Vicente J, Jose M, Rosahl S, Carbonne F, Griffiths G, Rodriguez MJ, Kift N, Carbonne F, Griffiths G, Esquerre-Tugaye M-T, Rosahl S, Castresana C, Hamberg M, Fournier J.** 2005. Evaluation of the antimicrobial activities of plant oxylipins supports their involvement in defense against pathogens. Plant Physiol 139:1902–1913.

52. **Hoffmann E**, **Marion S**, **Mishra BB**, **John M**, **Kratzke R**, **Ahmad SF**, **Holzer D**, **Anand PK**, **Weiss DG**, **Griffiths G**, **Kuznetsov SA**. 2010. Initial receptor-ligand interactions modulate gene expression and phagosomal properties during both early and late stages of phagocytosis. Eur J Cell Biol **89**:693–704.

53. **Hohl TM**, **Van Epps HL**, **Rivera A**, **Morgan LA**, **Chen PL**, **Feldmesser M**, **Pamer EG**. 2005. *Aspergillus fumigatus* triggers inflammatory responses by stage-specific ß-glucan display. PLoS Pathog **1**:0232–0240.

54. **Luther K**, **Torosantucci A**, **Brakhage AA**, **Heesemann J**, **Ebel F**. 2007. Phagocytosis of *Aspergillus fumigatus* conidia by murine macrophages involves

recognition by the dectin-1 beta-glucan receptor and Toll-like receptor 2. Cell Microbiol **9**:368–381.

55. **Willment JA**, **Brown GD**. 2008. C-type lectin receptors in antifungal immunity. Trends Microbiol **16**:27–32.

56. **Kerr SC**, **Fischer GJ**, **Sinha M**, **McCabe O**, **Palmer JM**, **Choera T**, **Yun Lim F**, **Wimmerova M**, **Carrington SD**, **Yuan S**, **Lowell CA**, **Oscarson S**, **Keller NP**, **Fahy J V**. 2016. FleA expression in *Aspergillus fumigatus* is recognized by fucosylated structures on mucins and macrophages to prevent lung infection. PLoS Pathog **12**:e1005555.

57. **Philippe B**, **Ibrahim-Granet O**, **Prevost MC**, **Gougerot-Pocidalo MA**, **Sanchez Perez M**, **Van der Meeren A**, **Latge JP**. 2003. Killing of *Aspergillus fumigatus* by alveolar macrophages is mediated by reactive oxidant intermediates. Infect Immun **71**:3034–3042.

58. **Ibrahim-Granet O**, **Philippe B**, **Boleti H**, **Boisvieux-Ulrich E**, **Grenet D**, **Stern M**, **Latge JP**. 2003. Phagocytosis and intracellular fate of *Aspergillus fumigatus* conidia in alveolar macrophages. Infect Immun **71**:891–903.

59. **Jahn B**, **Langfelder K**, **Schneider U**, **Schindel C**, **Brakhage AA**. 2002. PKSP-dependent reduction of phagolysosome fusion and intracellular kill of *Aspergillus fumigatus* conidia by human monocyte-derived macrophages. Cell Microbiol **4**:793–803.

60. **Diamond RD**. 1988. Fungal surfaces : Effects of interactions with phagocytic cells. Rev Infect Dis **10**:S428–S431.

61. **Slesiona S**, **Gressler M**, **Mihlan M**, **Zaehle C**, **Schaller M**, **Barz D**, **Hube B**, **Jacobsen ID**, **Brock M**. 2012. Persistence versus escape: *Aspergillus terreus* and

Aspergillus fumigatus employ different strategies during interactions with macrophages. PLoS One **7**:e31223.

62. **Cooper PR**, **Mesaros AC**, **Zhang J**, **Christmas P**, **Stark CM**, **Douaidy K**, **Mittelman MA**, **Soberman RJ**, **Blair IA**, **Panettieri RA**. 2010. 20-HETE mediates ozone-induced, neutrophil-independent airway hyper-responsiveness in mice. PLoS One **5**:e10235.

63. **Mabalirajan U**, **Rehman R**, **Ahmad T**, **Kumar S**, **Singh S**, **Leishangthem GD**, **Aich J**, **Kumar M**, **Khanna K**, **Singh VP**, **Dinda AK**, **Biswal S**, **Agrawal A**, **Ghosh B**. 2013. Linoleic acid metabolite drives severe asthma by causing airway epithelial injury. Sci Rep **3**:1349.

64. **Ng VY**, **Huang Y**, **Reddy LM**, **Falck JR**, **Lin ET**, **Kroetz DL**. 2007. Cytochrome P450 eicosanoids are activators of peroxisome proliferator-activated receptor alpha. Drug Metab Dispos **35**:1126–1134.

65. **Spears M, Donnelly I, Jolly L, Brannigan M, Ito K, McSharry C, Lafferty J, Chaudhuri R, Braganza G, Bareille P, Sweeney L, Adcock IM, Barnes PJ, Wood S, Thomson NC.** 2009. Bronchodilatory effect of the PPAR-γ agonist rosiglitazone in smokers with asthma. Clin Pharmacol Ther 86:49–53.

66. **Larsson N**, **Lundstrom SL**, **Pinto R**, **Rankin G**, **Karimpour M**, **Blomberg A**, **Sandstrom T**, **Pourazar J**, **Trygg J**, **Behndig AF**, **Wheelock CE**, **Nording ML**. 2014. Lipid mediator profiles differ between lung compartments in asthmatic and healthy humans. Eur Respir J **43**:453–463.

67. **Eleftheriadis N**, **Neochoritis CG**, **Leus NGJ**, **Van Der Wouden PE**, **Demling A**, **Dekker FJ**. 2015. Rational development of a potent 15-Lipoxygenase-1 inhibitor with *in vitro* and *ex vivo* anti-inflammatory properties. J Med Chem **58**:7850–7862.

68. **Suh JH**, **Yum K**, **Cho YS**. 2015. Synthesis and biological evaluation of N-Aryl-5-aryloxazol-2-amine derivatives as 5-Lipoxygenase inhibitors. Chem Pharm Bull (Tokyo) **63**:573–578.

69. **Xue T**, **Nguyen CK**, **Romans A**, **Kontoyiannis DP**, **May GS**. 2004. Isogenic auxotrophic mutant strains in the *Aspergillus fumigatus* genome reference strain AF293. Arch Microbiol **182**:346–353.

70. **Osherov N**, **Kontoyiannis DP**, **Romans A**, **May GS**. 2001. Resistance to itraconazole in *Aspergillus nidulans* and *Aspergillus fumigatus* is conferred by extra copies of the *A. nidulans* P-450 14alpha-demethylase gene, *pdmA*. J Antimicrob Chemother **48**:75–81.

71. **Tsitsigiannis DI**, **Kowieski TM**, **Zarnowski R**, **Keller NP**. 2004. Endogenous lipogenic regulators of spore balance in *Aspergillus nidulans*. Eukaryot Cell **3**:1398–1411.

72. **He Z-M**, **Price MS**, **Obrian GR**, **Georgianna DR**, **Payne G a**. 2007. Improved protocols for functional analysis in the pathogenic fungus *Aspergillus flavus*. BMC Microbiol **7**:104.

73. **Kilty L**, **Logan A**, **Vickers PJ**. 1999. Differential characteristics of human 15-Lipoxygenase isozymes and a novel splice variant of 15s-Lipoxygenase. Eur J Biochem **266**:83–93.

74. **Sloane DL**, **Sigal E**. 1994. On the positional specificity of 15-lipoxygenase. Ann N Y Acad Sci **744**:99–106.

CHAPTER 4: *Aspergillus fumigatus* PpoA-derived 5,8-diHODE induces hyperbranching while disruption influences asexual development and endocrocin production

Fischer, G., Palmer, J., Henke, M., Lim, F.Y., Berthier, E., Kelleher, N., Oliw, E.H., & Keller, N., (2016) *Aspergillus fumigatus* PpoA-derived 5,8-diHODE induces hyperbranching while disruption influences asexual development and endocrocin production. *(In Preparation).*

Strain development was carried out by J.P, F.Y.L., & G.F. E.B. designed microfluidic mold device. M.H. & N.K. carried out oxylipin quantification and E.O. provided purified oxylipin compounds. All experiments were conceived by G.F. and N.P.K. and all data collected by G.F. The manuscript was written by G.F. with assistance from N.P.K.

4.1 ABSTRACT

The fungal opportunistic pathogen *Aspergillus fumigatus* contains three cyclooxygenase (COX)-like enzymes termed PpoA, PpoB and PpoC. Ppos produce bioactive oxygenated lipid signaling molecules (oxylipins) important for fungal development and prostaglandins implicated in human immunological responses. Previous work showed that PpoA disruption promotes asexual development and reduces secondary metabolite production in the model fungus, *Aspergillus nidulans. Aspergillus fumigatus* developmental studies of PpoA loss and overexpression also revealed changes in asexual spore production and secondary metabolite production, particularly those classified as conidial metabolites such as the neutrophil chemotaxis inhibitor, endocrocin. Furthermore, the oxylipin product of PpoA (5,8-dihydroxyoctadecadienoic acid) induces mycelial hyperbranching in a dose-dependent manner while the other PpoA product, 8-hydroxyoctadecadienoic acid inhibits this phenomenon. This study reaffirms that oxylipins (both endogenous and external) serve an important role in coordination of developmental cues for asexual development, secondary metabolite production, and can drastically change mycelial morphology when manipulated.

4.2 INTRODUCTION

The *Aspergillus* life cycle begins with spore germination and culminates in either sexual or asexual sporulation, a developmental program that is carefully coordinated and influenced by the production and detection of signaling molecules known as oxylipins (1). Oxylipins are derived from oxygenation of polyunsaturated fatty acids and mediate many critical processes in plants, animals, and fungi. These processes include the regulation

of inflammatory responses in humans (eicosanoid pathway), regulation of defense genes in plants, and signaling molecules for committed developmental programs and pathogenicity (reviewed in Fischer and Keller, 2016). *Aspergillus* oxylipins were initially characterized in the context of the asexual/sexual spore development program (1, 3–6) and later, in mediating fungal/plant interactions (7). In the course of these later studies, it was found that both *Aspergillus* and plants could produce similar or even identical oxylipins and respond to each other's oxylipins in a manner that affected disease development (7–9). Concurrently, *Aspergillus* spp. were also found to produce and developmentally respond to specific mammalian oxylipins known as prostaglandins (10). The *Aspergillus* proteins responsible for prostaglandin synthesis (Ppo proteins) share considerable homology to cyclooxygenase enzymes responsible for mammalian prostaglandin production (10, 11).

Both *A. fumigatus* and *A. nidulans* contain three Ppo proteins (PpoA, PpoB, and PpoC) (5). Although chemical characterization has been assessed primarily with linoleic acid as a substrate, additional work suggests that Ppo proteins also oxidize oleic, linolenic, and arachidonic acids (3, 10, 12, 13). PpoA in *A. nidulans* is the most characterized enzyme and contains two heme domains each of which catalyze specific reactions (14). The N-terminal heme peroxidase domain oxidized linoleic acid to 8R-hydroperoxyoctadecadienoic acid (8R-HPODE) which can spontaneously reduce to 8R-hydroxyoctadecadienoic acid (8R-HODE), or further isomerized by the C-terminal P450 heme thiolate domain to 5,8-dihydroxyoctadecadienoic acid (5,8-diHODE) (14–16). Similar products have been described for the *ppoA* homolog in *A. clavatus* (17) and other

oxylipin diols (7,8-dihydroxyoctadecadienoic acid or 7,8-diHODE) from Ppo homologs such as 7,8-LDS (linoleate diol synthase) in the take-all fungus, *Magnaporthe oryzae* (18).

Ppo genes and their products have a profound effect on development and secondary metabolite production in *Aspergillus* species (19). Overeexpression or deletion of *ppo* genes, or exogenous application of the oxylipins and their respective substrate produced by these (and host) enzymes, affects sporulation in *Aspergillus* spp. (5, 9). Detailed work with *A. nidulans* showed deletion of either *ppoA* or *ppoB* results in increased production of asexual spores with a corresponding decrease in sexual spore production, whereas loss of *ppoC* yields the opposite phenotype (4–6). Regulation of asexual sporulation in these mutants was positively correlated with expression data for *brlA*, a zinc finger transcription factor necessary for asexual conidiophore development in *Aspergillus* species (20). That is *brlA* expression was increased in Δ*ppoA* strains but decreased in Δ*ppoC* mutants. An association of either or both genes with sporulation processes has since been noted in several developmental studies in *A. nidulans* (21, 22), however not investigated in *A. fumigatus.*

As noted above, *ppo* expression is linked with secondary metabolite production, potentially directly as a result of their influence on spore development. Both asexual and sexual spore development is associated with specific secondary metabolites – some playing important roles in virulence of pathogenic strains such as *A. flavus* and *A. fumigatus.* For example, endocrocin, fumigaclavines, trypacidin, and fumiquinozoline C are present in the asexual spores of *A. fumigatus* (23–26). Because *A. fumigatus* is

associated with hyper-immune (allergic bronchopulmonary aspergillosis, allergy, and asthma) and hypo-immune (invasive aspergillosis) conditions, oxylipin-dependent perturbations of metabolite production are of particular interest for opportunistic pathogens such as *A. fumigatus.*

Hyphal branching and the signals that influence mycelial growth are of particular interest for fungi that cause invasive growth, which can lead to further tissue damage in the lung. However little data has been recorded on the mechanisms that may influence this phenomenon in fungi such as *A. fumigatus.* Branching begins with the recruitment of the morphogenetic machinery necessary for vesicle trafficking leading to cell wall expansion and deposition. Polarization occurs when this morphogenetic machinery (Spitzenkörper complex, or apical organizing body) establishes a polarity axis leading to established polarized growth at a maximal extension rate (27). The regulatory mechanisms of branch formation have been investigated in *A. nidulans* where GTPases such as and Cdc42 (ModA) and Rac1 (RacA) play and important role in polarity establishment by marking specific sites for growth (28). ROS and the activation of plasma membrane calcium channels have also been implicated in the establishment of new axes of hyphal growth (29, 30). External cues that influence hyphal morphogenesis in arbuscular mycorrhizal fungi such as *Gigaspora* and *Glomus* and the rice blast fungus, *Magnaporthe oryzae* have been recorded (31, 32) (for review, see 29). Plant pathogenic species such as *Magnaporthe oryzae* precisely regulate their hyphal branching during infection. Hyphae do not branch prior to appresorium formation until inside the plant host, after which hyphae branch extensively presumably due to host signals within the cell (32). However

to our knowledge, no external factor has been implicated in the induction of branching in *Aspergillus*.

Considering the existing evidence that *ppoA* is a critical regulator of the developmental decision to proceed with either asexual or sexual development and its ability to produce bioactive oxylipins such as prostaglandins, we investigated the physiological roles of *ppoA* in the opportunistic pathogen, *A. fumigatus*. We find disruption of *ppoA* significantly up-regulates the master regulator of sporulation, *brlA,* and numerous secondary metabolites, particularly the known inhibitor of neutrophil chemotaxis, endocrocin. This up-regulation is remediated when Δ*ppoA* tissue is transferred to conditioned media derived from either the wild type or an overexpression *ppoA* strain, both of which contain the known oxylipin products of PpoA, 8R-HODE and 5,8-diHODE. Interestingly, purified 5,8-diHODE and a subset of diol-oxylipins induce mycelial hyperbranching in a dose-dependent manner, while 8R-HODE can inhibit this phenomenon. We propose that the products of PpoA are used to carefully regulate the coordinated development of *A. fumigatus,* ranging from asexual sporulation, secondary metabolite production, and even mycelial branching. The fact that specific oxylipins can regulate such critical processes of *A. fumigatus* development may provide insight into the recognition and control of invasive growth within the human host.

4.3 MATERIALS AND METHODS

Fungal strains and culture conditions. All strains utilized or developed are listed in Table 1. Strains were propagated on solid glucose minimal media (GMM), supplemented

as necessary for auxotrophies at 37°C (33). *A. fumigatus* asexual spores were collected in water supplemented with 0.01% Tween 80, enumerated using a hemocytometer, and maintained as glycerol stocks at -80°C. Fresh spore suspensions of the various mutants were used to inoculate liquid GMM media for developmental and hyperbranching studies.

Deletion and overexpression of *ppoA*. Construction, maintenance, and purification of recombinant DNA fragments was performed according to established methods (34). Primers used are listed in Table 2. The ORF of *A. fumigatus ppoA* (Afu4g10770) was identified via the AspGD database (http://www.aspergillusgenome.org).

Overexpression of *ppoA* was achieved by development of a double joint PCR fragment (35) targeting replacement of the native *ppoA* promoter with an overexpression promoter via homologous recombination. A 1.5 kb region upstream and downstream of the *ppoA* start codon was amplified (upstream: JP OE Af ppoA 5' F For with JP OE Af ppoA 5' F Rev, downstream: JP OE Af ppoA 3' F For with JP OE Af ppoA 3' R For) from AF293 genomic DNA template and fused to a 3.6 kb DNA fragment consisting of the *Aspergillus parasiticus pyrG* gene and the *A. nidulans gpdA* promoter amplified (primers: JP modified T7 promoter For with JP gpdA(p) Fusion Rev) from the plasmid pJMP9.1 (36). The promoter replacement construct was amplified via fusion of the three PCR fragments described above with a nested primer pair (JP OE Af ppoA Nest For with JP OE Af ppoA Nest Rev) and used to transform AF293.1 to uridine/uracil prototrophy according to previously published methods (37).

Development and confirmation of the Δ*ppoA* deletion mutant (TDWC1.13) was described previously (38). For development of the Δ*ppoA* Δ*akuA* mutant, the previously described TFYL45.1 (39) was transformed with pJMP4 (containing *A. fumigatus argB*) to create TFYL80.1, an Δ*akuA* uridine/uracil auxotrophic strain. To generate the Δ*ppoA* Δ*encA* Δ*tpcC* Δ*akuA* strain, a *pyrG* auxotrophic strain (TFYL110.1), was developed by removal of *A. parasiticus pyrG* from the *encA* locus through transformation of the previously characterized strain TFYL72.1 (39) with a single-joint PCR product containing 0.5–1 kb genomic DNA fragments flanking the *pyrG* sequence. Transformants were plated onto sorbitol minimal media supplemented with the above-mentioned concentrations of uridine, uracil and sub-inhibitory concentration (0.75 mg ml^{-1}) of 5-fluoroorotic acid (5-FOA) as previously described (39).

Together TFYL80.1 and TFYL110.1 were transformed with a Δ*ppoA* deletion cassette amplified from pDWC4.2 (GF ppoA del Cassette F with GF ppoA del Cassette R) (38) generating the prototrophic Δ*ppoA,* Δ*akuA* strain TGJF40.9 and the prototrophic Δ*ppoA* Δ*encA* Δ*tpcC* Δ*akuA* strain TGJF41.1. Deletion was verified via Southern blot (Supplemental Figure 1).

Verification of 8R-HODE and 5,8-diHODE absence and overproduction in the Δ*ppoA* and *OE::ppoA* strains, respectively, was carried out using LC-MS analysis. Strains were grown according to conditions previously described for 8R-HODE and 5,8-diHODE detection (40). Briefly, 250 mL of GMM was inoculated each respective strain to a final concentration of 10^6 spores/mL and grown at 37˚C for 96 hours at 250 rpms. Total

oxylipins were extracted from tissue and supernatant using 8:1:1 ethyl acetate:methanol:dichloromethane overnight. The organic phase was separated and evaporated to dryness using a Buchi Rotovap R-210 and standardized to dry mycelial mass. Extracts were resuspended in methanol to a final concentration of 2 mg/mL.

Fifty micrograms of sample was loaded onto a Phenomenex Luna C18 column (150 mm × 2 mm, 3 µm). Analysis was performed using an Agilent 1150 system at a flow rate of 0.2 mL min−1. A 30 minute gradient was employed using water/0.1% formic acid (solvent A) and acetonitrile/0.1% formic acid (solvent B). The LC was placed in-line with a Q-Exactive mass spectrometer for MS analysis. Full MS spectra were acquired at 70,000 resolution for the mass range m/z 150−1500 for all samples. Following each full MS scan, the top three most intense ions were selected for a dependent MS2 scan. MS2 was conducted using HCD with a normalized collisional energy of 25. Following each duty cycle (an MS1 scan followed by 3 MS2 scans) instrument polarity was switched. Each strain analyzed was prepared in biological triplicate.

Culture conditions for expression studies. For liquid shake expression studies, wild type, Δ*ppoA, and OE::ppoA* spore suspensions were used to inoculate 50 mL liquid GMM media to a final concentration of 10^7 spores/mL and grown at 25°C, 250 rpms for 72, 96, and 120 hours. For 37°C, spores were inoculated into 50 mL of liquid GMM to a final concentration of 10^6 spores/mL and grown for 72 hours at 250 rpms. At the appropriate timepoint, fungal tissue was separated from culture supernatant via Miracloth (Calbiochem) and both culture supernatant and tissue lyophilized. Total RNA from

lyophilized tissue was extracted with TRIzol reagent (Invitrogen) following manufacturer's protocol. Probes for northern analysis were constructed within the gene using primers listed in Table 2 and labeled with dCTP αP^{32}.

For tissue transfer studies, conditioned media were generated by inoculating 500 mL of liquid GMM to a final concentration of 10^6 spores/mL with wild type, Δ*ppoA*, and *OE::ppoA* spores and grown for 96 hours at 37˚C as previously described for 8R-HODE and 5,8-diHODE production (40). Supernatants were filtered through miracloth to remove mycelial mass followed by centrifugation at 7,000 rpms for 15 minutes. The supernatant was removed from pelleted material and subsequently filter sterilized. Simultaneously, 50 mL cultures of GMM were inoculated to a final concentration of 10^6 spores/mL and grown at 37˚C for 72 hours at 250 rpms. The Δ*ppoA* tissue was collected and separated from supernatant by centrifugation at 4,000 rpms for 10 minutes and rinsed and centrifuged twice with double distilled water. Fifty milliliters of conditioned media from either the wild type, Δ*ppoA,* or *OE::ppoA* strains was used to resuspend the tissue and incubated at 37˚C 250 rpms for either 0, 1, or 3 hours after which a portion of tissue was collected and freeze-dried. Total RNA was extracted from lyophilized tissue as described above. Probes for northern analysis were constructed within the gene using primers listed in Table 2 and labeled with dCTP αP^{32}.

HPLC Analysis of Secondary Metabolites. Culture supernatants from each respective growth conditions were prepared as follows: 50 mL of supernatant was lyophilized and resuspended in 10 mL double distilled (dd) H_2O with 1% (v/v) formic acid. After

centrifugation at 4,000 rpms for 10 minutes, 5 mL of aqueous solution was removed and added to 10 mL of ethyl acetate in a glass vial. After vigoruous vortexing, 8 mL of the organic layer was removed and dried down using a Thermo Scientific Savant SC250EXP SpeedVac Concentrator. The extracts were then resuspended in 200 µL 20% Acetonitrile (ACN) + 1% (v/v) formic acid and 50 µL examined by HPLC photo diode array (PDA) analysis. The samples were separated as previously described (41). Briefly, samples were separated using a ZORBAX Eclipse XDB-C18 column (Agilent, 4.6 mm by 150 mm with a 5 µm particle size) with a binary gradient of 1% formic acid (Solvent A) and 1% formic acid in ACN (Solvent B) using a Flexar Binary Liquid Chromatography Pump (PerkinElmer). Starting conditions were 80% A for 2 min followed by linear gradient to 40% A in 10 min and an additional linear gradient to 100% B in 30 sec. The column was rinsed for 5 minutes between each sample using 100% B and equilibrated for the next run at 80% A for 4 minutes. The flow rate for all steps was 1.5 mL/min. Purified endocrocin was used as metabolite standard (Dr. Clay Wang, personal communication).

Microfluidic Analysis of Hyperbranching. A microfluidic O-Channel template was designed according to previously established methods (24). The device was designed to allow microscopic observation of 5 µL stationary cultures of spore suspensions. The Illustrator template file is available upon request. The microfluidic arrays were developed using the O-channel mold using a silicone-polymer, PDMS (Sylgaard 184, Dow Corning, USA) in a ratio of 10:1 polymer to curing agent and placed in vacuum for 30 minutes to de-gas. The molding process was completed by placing items in order on a hotplate: a transparency sheet, O-channel mold, de-gassed PDMS with curing agent, a second

transparency sheet, a 1 mm thick layer of silicon foam (McMaster, USA), a rectangle of plexiglass, and 5 kg weight (24). The hotplate was heated to 65˚C for 6 hours and cooled completely before removal of the PDMS layer from the mold, which was then bonded non-covalently inside a polystyrene Omnitray dish (NUNC, USA). The Omnitray and bonded PDMS device was plasma treated for 2 minutes using a Unitronics device (Plasma Etch, Carson City NV) to develop a hydrophilic surface for inoculation.

Five microliters of liquid GMM cultures inoculated with spores to a final concentration of 5 X 10^4 spores/mL with or without the various treatments was inoculated into the O-channel device and allowed to incubate overnight (16 hours) in a heated microscope enclosure at 37˚C (OKO Labs, Burlingame, CA) developed for a Nikon Eclipse T*i* inverted microscope. Germinating spores were identified 16 hours later and monitored using a Nikon Plan Fluor 20x Ph1 DLL objective and phase-contrast images captured every 15 minutes using the Nikon NIS Elements AR software package (v. 4.13) for 5 hours. At least 6 germinating spores were monitored and the number of branches/ 100 µm leading hyphae quantified with slight adjustments to previously described methods (42) (see Results section for quantification description).

For calcofluor white staining of the fungal cell wall and septa after oxylipin treatment, the PDMS-devices were bonded to sterilized 1.5 mm coverslips instead of Omintrays (interferes optically with fluorescent microscopy) and plasma treated as described above. The devices were inoculated and grown under the same conditions as with the Omnitrays, except after 21 hours, the PDMS portion removed and discarded. The coverslip

containing established fungal colonies was treated with CFW (1 μg/μL) for 10 minutes and rinsed with GMM. DAPI fluorescent images were captured using the same objective and microscope platform described above.

4.4 RESULTS

4.4.1 PpoA deletion accelerates while overexpression delays asexual sporulation.

To further understand how *A. fumigatus* PpoA could impact asexual development and fungal physiology, we utilized an existing Δ*ppoA* strain (38) and developed an overexpression *ppoA* strain (*OE::ppoA*). Deletion and overexpression was verified by northern blot (Supplemental Figure 1) as well as mass spectrometry of culture supernatants for loss and up-regulation of 8R-HODE and 5,8-diHODE, the known oxylipin products of PpoA (16). Neither 8R-HODE or 5,8-diHODE were detected in Δ*ppoA* strain culture supernatants and only 8R-HODE was detected in the wild type. In *OE::ppoA* strain supernatant, both 8R-HODE and 5,8-diHODE were detected at 3 orders of magnitude higher levels than 8R-HODE in the wild type (Figure 1A).

We began our assessment of the PpoA mutants by investigating any difference in asexual sporulation and secondary metabolite production under previously described growth conditions at 25˚C (see Material and Methods) (43). After 120 hours at 25˚C, the Δ*ppoA* strain had a clear accelerated asexual developmental phenotype: fungal tissue had a pronounced green pigmentation, while the wild type strain had no green coloration, but only slight yellow pigmentation. The *OE::ppoA* strain had no pigmentation: fungal tissue

was bright white in color (Figure 1B). Conidiophores were present in Δ*ppoA* cultures, however few were observed in wild type or *OE::ppoA* tissue (Figure 1C). Quantification of conidia production after 120 hours at 25˚C also revealed a significant increase in spores in the Δ*ppoA* strain: asexual conidia were present at concentrations almost 3 times greater than those observed in the wild type or *OE::ppoA* strains (Figure 1D). To induce synchronized asexual development of the *ppoA* strains on solid media, vegetative tissue grown in liquid media was transferred to solid media as previously described (44) and asexual conidia quantified 0, 24, and 48 hours post transfer (hpt) at 25˚C. At 24 hpt, significantly more conidia were produced compared to the wild type and *OE::ppoA* strains. However by 48 hpt, all strains had equivalent numbers of conidia (Figure 1E).

Since more conidia and their respective conidiophores were observed at 25˚C, we were curious whether the expression of the master conidiation regulator *brlA* was altered. *brlA* expression was significantly up-regulated compared to wild type or the *OE::ppoA* strain at both 72 and 120 hour timepoints (Figure 1F). Numerous studies have focused on the conidiation suite of genes both up and downstream of *brlA.* We decided to test whether those genes directly downstream of *brlA* (*abaA, wetA*) were also differentially regulated. We found that *abaA* and *wetA* were slightly up-regulated at both timepoints in the Δ*ppoA* strain, but not to the same degree as *brlA* (Figure 1F).

4.4.2 *ppoA* deletion disrupts the regulation of secondary metabolite clusters.

Since *ppoA* disruption affects *brlA* expression, we hypothesized that secondary metabolites associated with *brlA* activity may also be dysregulated. (particularly those spore-associated) and would be up-regulated in the *ΔppoA* strain. Therefore, we examined the production of various secondary metabolites in culture supernatants grown at both 25˚C and 37˚C: conditions documented to yield very different metabolite profiles. For example, the spore-specific metabolite endocrocin (described in 44) is not observed at 37˚C, but only at lower temperatures such as 25˚C (24).

We observed numerous metabolites that were differentially produced in the Δ*ppoA* strain at 25˚C, 120 hours after inoculation (Supplemental Figure 2). Significant levels of the spore-specific metabolite endocrocin were observed at 25˚C, with undetectable levels in the wild type or *OE::ppoA* strains (likely due to the fact that the wild type and *OE::ppoA* strains had not yet undergone conidiation at this timepoint) (Figure 2A). To further verify our HPLC results, we probed both the endocrocin polyketide synthase (PKS) (*encA)* and oxidoreductase (*encD)* necessary for endocrocin production (45) and found both to be up-regulated in the Δ*ppoA* strain. *encA* nor *encD* transcripts were detected in the wild type or *OE::ppoA* strains grown in similar conditions (Figure 2B).

Since previous reports found higher temperatures (such as 37˚C) to be nonconductive to endocrocin production (even within spores) (24), we grew the *ppoA* strains at 37˚C for 72 hours to determine whether this temperature-specific regulation was maintained in the Δ*ppoA* strain. We were surprised to find that endocrocin production was maintained in the Δ*ppoA* strain, with even higher levels of the metabolite being produced than at 25˚C (Figure 2C). Again we probed both the endocrocin PKS and oxidoreductase and found

both to be significantly up-regulated in the vegetative tissue of the Δ*ppoA* strain. *brlA* expression was also significantly up-regulated: while none of these transcripts were detected in the wild type strain and only basal expression of *brlA* detected in the *OE::ppoA* strain (Figure 2D).

While HPLC analysis with purified endocrocin indicated the novel peak was indeed endocrocin, and expression studies revealed up-regulation of this biosynthetic gene cluster, to conclusively show this was indeed endocrocin we developed disruption mutants of both *encA* and *tpcC* (a polyketide synthase primarily responsible for the production of the secondary metabolite trypacidin, but also capable of producing endocrocin intermediates; 45) in a Δ*ppoA,* Δ*akuA* background. The double Δ*ppoA,* Δ*akuA* mutant produced an endocrocin-associated peak much like the Δ*ppoA* strain in the wild type background. However, the Δ*ppoA*, Δ*encA*, Δ*tpcC,* Δ*akuA* mutant no longer produced an endocrocin-associated peak at 37˚C, providing strong evidence that this peak was indeed endocrocin (Figure 2E).

4.4.3 Growth of Δ*ppoA* tissue in wild type or *OE::ppoA*-conditioned medium suppresses *brlA* expression.

Since *ppoA* disruption significantly up-regulates *brlA* and endocrocin under non-permissive conditions, we wanted to confirm whether the lack of the PpoA-specific oxylipins (8R-HODE and 5,8-diHODE) was directly responsible for *brlA* up-regulation.

Because 8R-HODE and 5,8-diHODE are not commercially available and purified in small quantities, we utilized previous data confirming production of both 8R-HODE and 5,8-diHODE in the culture supernatants of the wild type and *OE::ppoA* strains.

The *OE::ppoA,* wild type, and Δ*ppoA* strain were grown in identical conditions to that used for oxylipins analysis (Figure 1A) and tissue separated from conditioned media via centrifugation (see Material and Methods). Tissue from the Δ*ppoA* strain was then collected, rinsed, and transferred to either wild type, Δ*ppoA,* or *OE::ppoA*-conditioned media and tissue samples collected 0, 1, 3 hours post transfer. We found that Δ*ppoA* tissue moved to either wild type or *OE::ppoA* conditioned media saw a decrease in *brlA* expression as soon as one hour post transfer (Figure 3). However, in tissue transferred to Δ*ppoA*-conditioned media, while the initial *brlA* expression seemed to be lower in both biological replicates (series C and D) compared to wild type or *OE::ppoA* treatments (series A,B or E,F, respectively), only a slight decrease was observed after 3 hours post transfer in one of the samples (series D, Figure 3).

4.4.4. Purified 5,8-diHODE but not 8-HODE induce hyperbranching.

We attempted RNA extraction from tissue grown in a microfluidic device (4 µL culture volumes, see Material and Methods) to investigate *brlA* expression with purified 8R-HODE and 5,8-diHODE but were unsuccessful. During this attempt growth was observed microscopically which revealed a pronounced hyperbranching phenotype in hyphae treated with 50 ng/µL 5,8-diHODE but not 8R-HODE (Figure 4A). The ability of this compound to induce this distinct phenomenon has not been described previously.

Therefore, we continued our examination of the *ppoA* mutants and explored the ability of the PpoA oxylipin product 5,8-diHODE to induce mycelial hyperbranching.

To quantify the degree of hyperbranching, we developed a modified method based on that previously described (42). The distances between primary branches emanating from the leading hypha, or hypha directly derived from the germinated spore, were quantified for a given mycelial colony and used to calculate the number of branches over a 100 μm segment of the leading hyphae (Figure 4B). Using this quantification scheme, we found that addition of 50 ng/μL 5,8-diHODE increased the number of branches/ 100 μm by 2-fold in the wild type strain (Figure 2A). This phenomenon was also dose-dependent: with a significant increase in branching observed when 5,8-diHODE was added at a concentration of 0.5 ng/μL (Figure 4CD). The ppoA disruption strain had a higher degree of branching than that of the wild type at 5 ng/μL (Figure 4E). We next compared branching of the *OE::ppoA* strain (confirmed to produce more 8R-HODE and 5,8-diHODE) in the absence and presence of exogenous 5,8-diHODE, hypothesizing that overexpression would *increase* the basal level of mycelial branching compared to wild type. However, we observed no difference in the degree of branching of the *OE::ppoA* strain in the absence or presence of 5 ng/μL 5,8-diHODE (Figure 4F).

PpoA does not make a single oxylipin product, but rather a mixture of 8R-HODE and 5,8-diHODE (16 and Figure 1A). Therefore, 8R-HODE could be acting to suppress the hyperbranching activity of 5,8-diHODE. We added 5 ng/μL of either 8R-HODE, 5,8-diHODE, or both simultaneously to wild type spores. As previously observed, hyperbranching only occurred in tissue treated with 5,8-diHODE, not 8R-HODE.

However, when both oxylipins were added simultaneously in equal concentrations, hyperbranching was significantly reduced compared to the sole 5,8-diHODE treatment, but still significantly increased compared to the mock treatment (ethanol treatment), suggesting 8R-HODE could block the hyperbranching activity of 5,8-diHODE (Figure 4G).

4.4.5 5,8-diHODE induces hyperbranching of *A. fumigatus* and *A. flavus* hyphae, but not *A. nidulans* and is one of several diol-oxylipins that induce hyperbranching.

PpoA homologs are prevalent in many genera of fungi including *Blastomyces, Magnaporthe,* as well as other aspergilli. We extended our investigation to the hyperbranching ability of 5,8-diHODE on other *Aspergillus* species. We found 5 ng/µL 5,8-diHODE was capable of inducing hyperbranching in *A. flavus* but not *A. nidulans* (Figure 5A). As observed in *A. fumigatus,* 5,8-diHODE increased the number of branches / 100 µm leading hyphae by two-fold in *A. flavus* compared to the mock treatment, but no significant increase in branching was observed with *A. nidulans* treated hyphae (Figure 5B).

5,8-diHODE is just one of several diol-oxylipins (containing two hydroxyl groups) that have been characterized or are commercially available. Oxygenase enzymes such as PpoA are promiscuous in their substrate utilization, producing related but different compounds depending on the substrate fatty acid used, for example prostaglandins when fed exogenous arachidonic acid (10), or 5,8-dihydroxyoctadecaenoic acid (5,8-diHOME) by PpoA when oleic acid is present (47). Furthermore, a *ppoA* homolog in *Magnaporthe*

*grisea (*now *M. oryzae)* (7,8-linoleate diol synthase or 7,8-LDS) produces 8R-HODE and 7,8-dihydroxyoctadecadienoic acid (7,8-diHODE) from linoleic acid (46). To determine whether 5,8-diHODE solely induced hyperbranching in *A. fumigatus*, a collection of commercially available diol-oxylipin compounds were tested. Interestingly, only 5,8-diHOME and 7-8-diHODE were able to induce hyperbranching similar to 5,8-diHODE. 5,8-diHODE and 5,8-diHOME increased the number of branches/ 100 μm by almost 3 fold, whereas 7,8-diHODE increased branching by almost 2 fold (Figure 6).

4.4.6 Induction of hyperbranching by 5,8-diHODE can be suppressed by addition of exogenous calcium.

Hyperbranching is a common phenotype for many mutants in *A. fumigatus* that can be induced by altered production or localization of ROS species (48, 49), hypoxic stress (50), disrupted cell wall synthesis (51, 52), and calcium signaling through disruption of the calcineurin pathway (53, 54). Mutants where either the regulatory or catalytic subunits of calcineurin have been disrupted show pronounced defects in growth: characterized by a significant degree of hyperbranching and reduced distance between septa (55).

Because of the similarities in the hyperbranching morphology of the 5,8-diHODE treated tissue with calcineurin mutants, we were curious whether the septal network and spacing were similar to calcineurin mutants when wild type tissue was treated with 5,8-diHODE. Calcofluor white was used to stain mock and 5,8-diHODE-treated wild type hyphae. In the mock treatment, septal differences were variable, with values as high and low as 70

μm and 5 μm, with an average septal distance of 30 μm. In wild type hyphae treated with 5,8-diHODE, septal distances were reduced and much more consistent: the average distance decreased from approximately 30 μm to 18 μm (Figure 7AB).

Because calcineurin disruption is intimately linked with cytosolic calcium homoeostasis, we hypothesized that 5,8-diHODE may be inducing hyperbranching through a similar mechanism. Therefore, we monitored branching in the presence or absence of 5,8-diHODE with addition of exogenous $CaCl_2$, $MgCl_2$, NaCl, or KCl. Addition of 4.5 mM calcium, magnesium, sodium, or potassium chloride had no impact on hyphal branching compared to the mock treatment, although a slight (but not statistically significant) increase was observed with the addition of $MgCl_2$. The addition of 5,8-diHODE induced hyperbranching to the same degree in the presence of these ions as when the ions were absent, with the sole exception being $CaCl_2$, which suppressed the hyperbranching morphology in the presence of 5,8-diHODE (Figure 7CD), suggesting 5,8-diHODE disrupted calcium homeostasis and led to hyperbranching.

4.5 DISCUSSION

Since the discovery of Psi factor oxylipins in the 1980s, 8R-HODE (also known as PsiBα) and 5,8-diHODE (also known as PsiCα) and other Ppo-derived compounds have been known almost exclusively for their ability to promote either sexual/asexual development in *A. nidulans*. Later work revealed *A. fumigatus* Ppo enzymes were capable of producing prostaglandins similar in structure to the human equivalents (10). This work ascribes two novel functions to the already characterized psi-factor producing oxygenase PpoA:

disruption accelerates asexual development through the up-regulation of *brlA*, subsequently changing the secondary metabolite profile of *A. fumigatus*. Secondly, we find that both oxylipin products have antagonistic roles in hyphal branching: 8R-HODE is capable of blocking the hyperbranching activity of 5,8-diHODE which likely acts through calcium-dependent mechanisms.

Physiological characterization of *ppoA* mutants have been well described in *A. nidulans.* Champe and colleagues isolated a fungal compound that could influence the ratio between asexual (conidia) to sexual (ascospores) development (1, 3), which later was identified to be a collection of oxylipin compounds, known as psi factors, for their ability to induce precocious sexual development (**p**recocious **s**exual **i**nducer). Two of these compounds were 8R-HODE and 5,8-diHODE (56), which were later associated with the enzymatic activity of *A. fumigatus* and *A. nidulans* PpoA through biochemical characterization (16). Deletion of *ppoA* led to *A. nidulans* strains with increased conidia compared to ascospores while overexpression led to the opposite phenotype. This phenomenon was attributed to the presence or absence of 8R-HODE in each respective PpoA mutant (6), however since 5,8-diHODE has subsequently been linked to PpoA activity in both *A. fumigatus* and *A. nidulans* (16), it cannot be ruled out that either or both PpoA oxylipin products are responsible for the change in the asexual/sexual spore ratio.

Continued developmental observations of both *ppoA* and *ppoC* disruption mutants revealed feedback regulation among *ppoA* and *ppoC* expression: while the Δ*ppoA* strains had increased numbers of asexual spores, the *ppoC* disruption mutants had *increased*

numbers of ascospores (4). These observations correlated with expression of the transcriptional regulators for both asexual (*brlA*) and sexual (*nsdA*) development: the Δ*ppoA* strain had increased expression of *brlA* while the Δ*ppoC* strain had increased expression of *nsdA* (4). Interestingly *ppoC* expression was down-regulated in Δ*brlA,* Δ*nsdA,* and *OE::nsdA* strains and *ppoA* unaffected in Δ*brlA,* induced in the Δ*nsdA,* and suppressed in the *OE::nsdA* backgrounds (4). *Aspergillus fumigatus* reproduces almost exclusively through asexual sporulation, although the sexual cycle has been described (57). Thus our study focused on the asexual sporulation phenotypes in the *A. fumigatus ppoA* mutants. Our observations that *ppoA* disruption in *A. fumigatus* induces *brlA* expression and increases asexual sporulation mirror documented phenotypes in *A. nidulans.*

Aspergillus fumigatus is the causative agent of invasive aspergillosis (IA) among the immunocompromised. While many of its secondary metabolites have ecological roles related to antimicrobial activity and environmental protection, many compounds have immunomodulatory and cytotoxic characteristics (e.g. endocrocin). Cases describing oxylipin-dependent regulation of secondary metabolite production are limited. In *A. nidulans* Δ*ppoA* Δ*ppoC* and Δ*ppoA* Δ*ppoB* Δ*ppoC* mutants did not produce sterigmatocystin in axenic culture or on a plant host and led to increased production of penicillin (19). Disruption of *ppo* homologs in *Fusarium sporotrichioides* compromises T2 toxin synthesis (58) and cercosporin production is correlated with up-regulation of a *ppo* homolog in *Cercospora zeae-maydis* (59). The regulation of secondary metabolism in

fungi, particularly with respect to spatial and temporal control has been the focus of numerous recent studies (reviewed in 58). Spore associated compounds, which include endocrocin (24, 45), DHN melanin (61–63), fumigaclavines (25), and fumiquinozoline C (23) are of particular interest since their localization within spores may contribute to the invasive growth and pathogenicity of *A. fumigatus.*

Endocrocin has been shown to inhibit neutrophil recruitment dose-dependently using an *in vitro* microfluidics platform and an *in vivo* zebrafish model. Furthermore endocrocin production is temperature dependent, with temperatures higher than 32˚C found to be inhibitory to detection in spores (24). Our work shows that the absence of PpoA disrupts this regulation and metabolite localization, with significant levels of endocrocin being produced in vegetative tissue grown at 37˚C. This may be a direct effect from the up-regulation of *brlA*. Further investigation through development of a Δ*brlA* Δ*ppoA* double mutant could elucidate whether endocrocin production is mediated through BrlA activity. Endocrocin has also been shown to be produced through the trypacidin biosynthetic pathway, with endocrocin being an intermediate in trypacidin production (39), however induction of the trypacidin PKS *(tpcC,* 39) in the Δ*ppoA* strain was not observed (Supplemental Figure 3).

While immune modulation via secondary metabolite production may allow niche establishment for *A. fumigatus* in the lung, invasive growth of hyphae into lung tissue is the most damaging effect to the host. The mechanisms that induce invasive growth (i.e. hyphal branching) are somewhat understood but to date no external factor influencing

this behavior has been described for *A. fumigatus.* We find that the PpoA product 5,8-diHODE and the *M. oryzae* 7,8-LDS product 7,8-diHODE can drastically increase the branching behavior of *A. fumigatus* hyphae. Strigolactones and synthetic analogues (GR24) induce hyphal branching of the arbuscular mycorrhizal (AM) fungus *Gigaspora margarita* (31). Interestingly, hydroxy fatty acids from carrot root exudates are the only documented case of oxylipin compounds inducing hyphal branching, specifically for the AM fungus *Gigaspora gigantea.* Length of the hydroxyl fatty acid was critical for hyperbranching activity, as 2-hydroxytetradecanoic acid (14C) and 2-hydroxydodecanoic acid (12C) induce branching while 2-hydroxydecanoic (10C) and 2-hydroxyhexadecanoic acids (17C) do not. Positioning of the hydroxyl group is critical for the hyperbranching activity as well: 3-hydroxytetradecanoic acid has no effect on hyphal branching (64). We observed similar phenomenon with the diol oxylipin tested in Figure 6. Our observations implicated only C18 oxylipins where both hydroxylations were near the carboxylic acid functional group and after the last unsaturated ω carbon (ω-10). Future work with synthetic derivatives of these compounds could help elucidate the structural characteristics of these oxylipins necessary to induce hyperbranching.

Our observations of 5,8-diHODE-induced hyperbranching lead to and increase in lateral branches only. Hyphae for the most part exhibit apical dominance, targeting exocytic vesicles containing cell wall components to the hyphal tip instead of potential novel branching sites. Only when sufficient distance is achieved between the growing hyphal tip and a potential branch site is the new branch initiated (27). Observations in *Neurospora crassa* reveal that lateral branching initiates from *de novo* formation of a

vesicular organizing center collectively known as the Spitzenkörper, compared to apical branching which is initiated from a transient loss of Spitzenkörper activity at the hyphal tip (65). Studies in *A. nidulans* have implicated GTPases (FadA and Cdc42) in the regulation of lateral branching as disruption of these genes yields hyphae devoid of lateral branches (66), with similar observations in *Cochliobolus heterostrophus, Fusarium oxysporum, Alternaria alternata* (67–69). A specific class of GTPases known as Ras proteins transduce environmental signals into the cell. Disruption of a particular Ras protein (RasA) results in hyperbranched hyphae and appears to act through a CDC42 (ModA)/MAPK pathway in *A. fumigatus* (70). 5,8-diHODE likely acts as an endogenous signal, which can be blocked through the presence of 8R-HODE, that yields a hyperbranching phenotype from aberrant intracellular signaling. Besides the MAPK cascade, the central elements of these conserved pathways in *A. fumigatus* include calcium signaling (calcineurin/calmodulin) and cAMP protein kinase A (71–73). Since exogenous calcium suppresses the hyperbranching phenotype, we hypothesize 5,8-diHODE likely targets a component of calcium regulation.

Calcium homeostasis has been linked with aberrant branching behavior in *Neurospora crassa* through calcium gradient establishment at existing hyphal tips and emerging branchpoints (74). In *N. crassa*, the hyphal growth rate correlates with the difference in calcium at the hyphal tip compared to sub-apical zones in older segments of the hyphae where activation of cell wall enzymes appears to be calcium-dependent (74). *Neurospora crassa* calcium/calmodulin activity has been shown to activate chitin synthases (75), cAMP phosphodiesterases (76), and associations with microtubule proteins (77) all of

which are necessary for polarity establishment and growth. Interestingly, spontaneous calcium gradients are sufficient to initiate lateral branches as microinjection of Ca^{2+} induces hyphal branching (78).

In *A. fumigatus,* disruption of calcium homeostasis through the calcineurin/calmodulin pathway yields hyperbranching phenotypes. Calcium homeostasis is maintained through the expression of various calcium efflux and influx pumps (vacuolar, stretch-activated, voltage-gated, and high-affinity Ca^{2+}/Mn^{2+} P-type ATPases) which are modulated by the activity of the transcription factor, CrzA. CrzA translocation to the nucleus is dependent on its dephosphorylation by the heterodimeric calcineurin complex (79), composed of the calcineurin catalytic subunit CnaB, the regulatory subunit CnaA, which when bound and associated with calmodulin (CmdA) in the presences of calcium yields an active phosphatase (80–82). Calcineurin is critical to the proper activation of Protein Kinase C (PKC), which is also associated with cell wall integrity (83). Mutants where various calcium channels or pathway components are disrupted are attenuated in virulence and display hyperbranching phenotypes. Disruption of the catalytic subunit of calcineurin (*cnaA)* yields irregularly septated hyphae that are blunt and hyperbranched (similar to the septation pattern observed with 5,8-diHODE treatment—Figure 7B), which is exacerbated when both *cnaA* and *cnaB* are disrupted (53–55). Furthermore, disruption of two high-affinity calcium influx sensors (voltage-gated and stretch-activated calcium channels *cchA* and *midA*, respectively) results in hyperbranched hyphae in the presence of EGTA, a calcium chelater (84). Whether 5,8-diHODE is able to disrupt the calcium

uptake system(s) of *A. fumigatus* which yields a hyperbranching phenotype remains an interesting area for further research.

4.6 ACKNOWLEDGEMENTS

We are grateful to Dr. Ernst Oliw for the generous gift of purified 8R-HODE and 5,8-diHODE. To Layla Barkel for the production of microfluidic molds from templates and Dr. Philipp Wiemann for HPLC assistance. This work was funded by a Pre-Doctoral Training Program in Genetics award for G.J.F. (5T32GM07133) and award to N.P.K. from the American Asthma Foundation (11-0137) and the NIH (R01-AI065728).

4.7 FIGURES AND LEGENDS

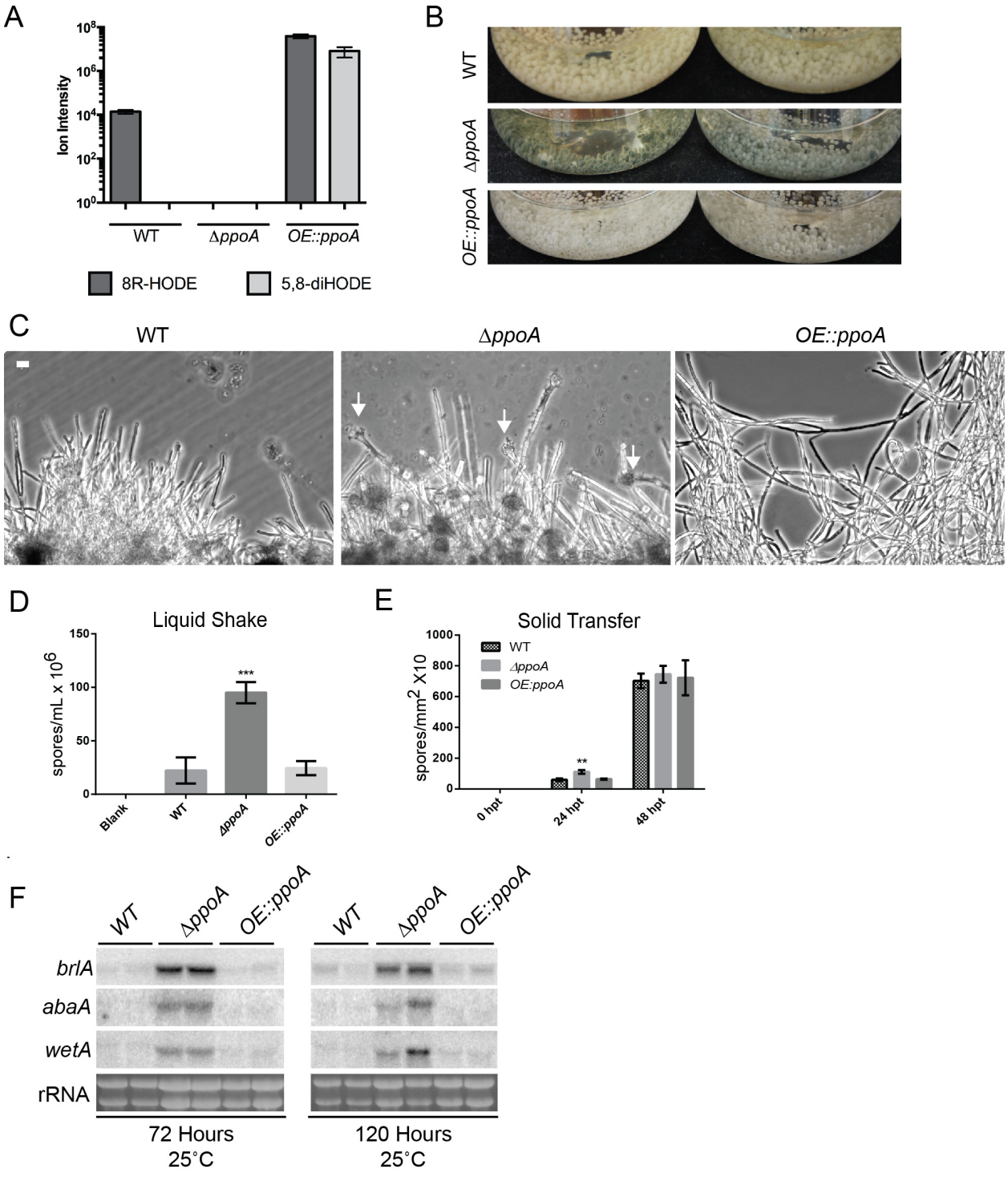

Figure 1. Characterization of *ppoA* disruption and overexpression mutants in *Aspergillus fumigatus.*

(A) Quantification of the known PpoA oxylipin metabolites 8R-hydroxyoctadecadienoic acid (8R-HODE) and 5,8-dihydroxyoctadecadienoic acid (5,8-diHODE) based on characteristic MS2 ions extracted from culture supernatants of wild type, *ppoA* disruption, and *ppoA* overexpression mutants. **(B)** Disruption of *ppoA* significantly accelerates asexual development after growth at 25˚C for 120 hours. Fungal balls of the Δ*ppoA* strain have a green appearance due to the accelerated production of conidiophores (white arrows) and conidia on the fungal balls. Scale bar represents 10 μm **(C).** The number of conidia present in culture supernatant of strains grown for 120 hours at 25˚C are significantly higher in the Δ*ppoA* strain compared to wild type or the overexpression *ppoA* (*OE::ppoA)* strains **(D)**. **(E)** Quantification of conidia derived from the transfer of vegetative hyphae to solid media also revealed an elevated number of spores in the Δ*ppoA* strain compared to wild type or the *OE::ppoA* strains 24 hours post transfer (hpt). However, this phenotype was no longer observed 48 hpt. **(F)** The accelerated asexual development phenotype correlates with maintained up-regulation of *brlA*. At both 72 and 120 hours post inoculation, *brlA* is up-regulated compared to the wild type or *OE::ppoA* strains. The members of the conidiation suite downstream of *brlA* (*abaA* and *wetA*) are also up-regulated in the Δ*ppoA* strain. Bars represent average values from 3 biological replicates ± SEM. * $p<0.05$, ** $p< 0.01$, *** $p< 0.001$.

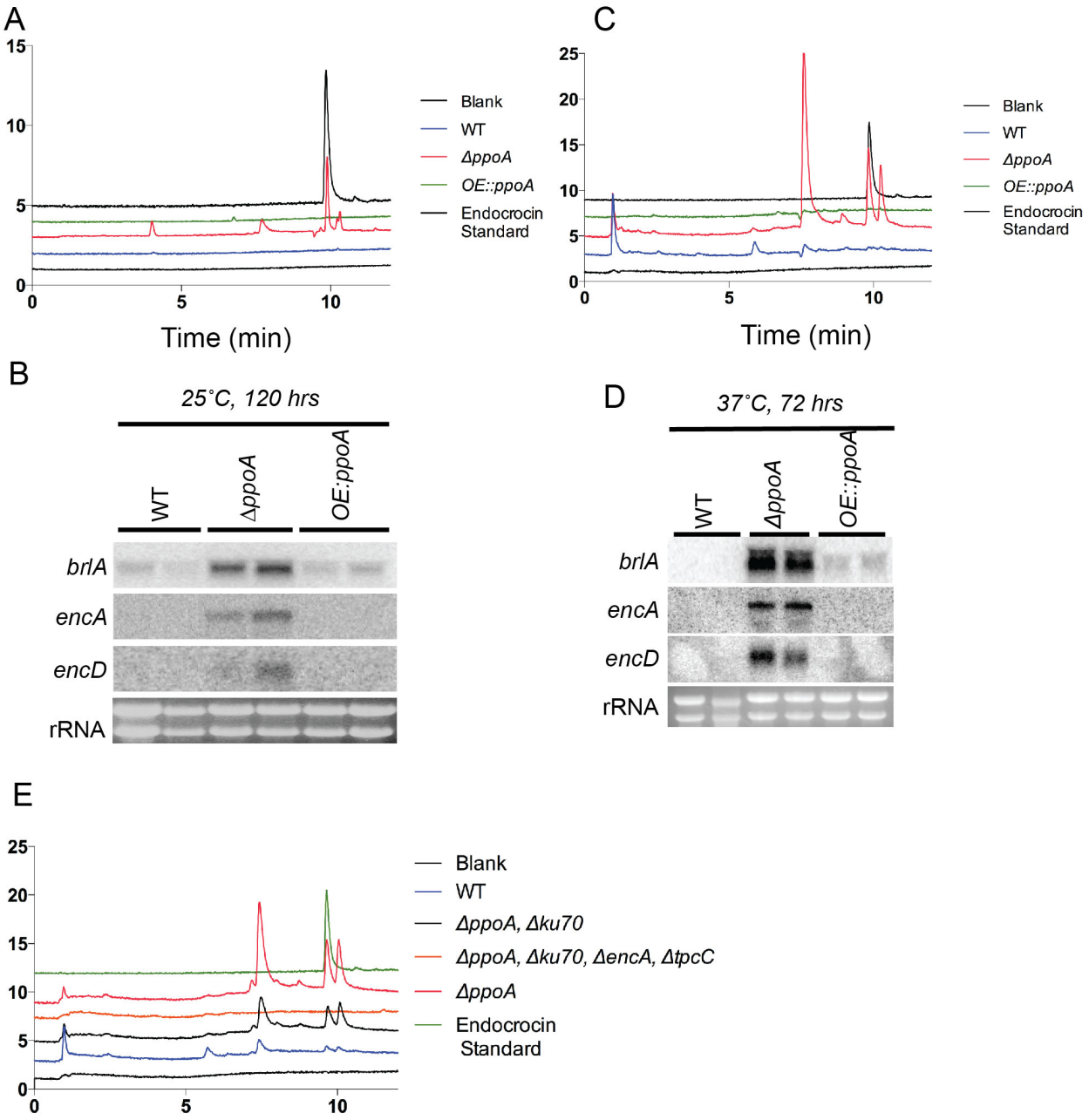

Figure 2. HPLC analysis of endocrocin production in various *ppoA* mutants grown at either 25 or 37˚C.

(A) HPLC chromatogram of metabolites detected at 441 nm identifies endocrocin as a metabolite product from cultures grown at 25˚C for 120 hours. Purified endocrocin has

an identical retention time to that of a major peak identified only in extracts derived from the Δ*ppoA* strain. **(B)** Expression studies of tissue extracted from the same growth condition reveals that *brlA,* the endocrocin polyketide synthase *encA*, and the endocrocin oxidoreductase *encD* are up-regulated only in the Δ*ppoA* strain. **(C)** HPLC chromatograms of extracts from the various strains grown 72 hours at 37˚C. Previous studies have identified that endocrocin is a spore-associated metabolite detected at temperatures below 32˚C (24). However, in supernatant from vegetative hyphae derived from the Δ*ppoA* strain, a significant peak corresponding with purified endocrocin is observed. Furthermore, expression analysis of tissue derived from this growth condition reveals up-regulation of *brlA, encA,* and *encD* **(D).** **(E)** To conclusively show this metabolite was indeed endocrocin, disruption of the known endocrocin PKS (*encA)* and the trypacidin PKS (*tpcC)* capable of also producing endocrocin as an intermediate (39) were disrupted in a Δ*ppoA* Δ*akuA* background. A peak corresponding to endocrocin was identified in extracts derived from the Δ*ppoA* Δ*akuA* strain grown at 37˚C*,* similar to that observed in the Δ*ppoA* wild type background strain. However, in the Δ*ppoA* Δ*encA* Δ*tpcC* Δ*akuA* mutant, the endocrocin-associated peak (as well as several others) are no longer observed.

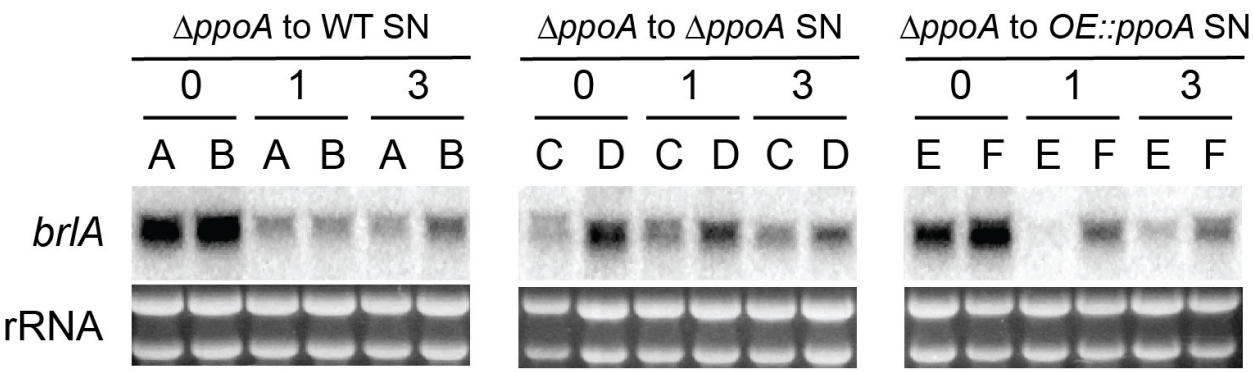

Figure 3. Transfer of Δ*ppoA* tissue into conditioned media containing the oxylipin products of PpoA results in the down-regulation of *brlA* transcript.

Tissue derived from the Δ*ppoA* strain was grown for 72 hours at 37˚C. Tissue was then removed from culture supernatant (SN) and transferred to conditioned media from the wild type (WT), Δ*ppoA*, or overexpression *ppoA* (*OE::ppoA)* strains grown in identical conditions for oxylipin analysis analyzed in Figure 1A (see Material and Methods). Each treatment was carried out in biological duplicate and the letters above each well correspond to tissue derived from the same biological sample over 3 hours. In treatments where Δ*ppoA* tissue was transferred to either WT or *OE::ppoA* conditioned media, *brlA* transcript levels decreased as quickly as 1 hour post transfer. However, Δ*ppoA* tissue transferred to Δ*ppoA* conditioned supernatant maintained an equivalent level of *brlA* expression to the 0 hr timepoint in both replicates.

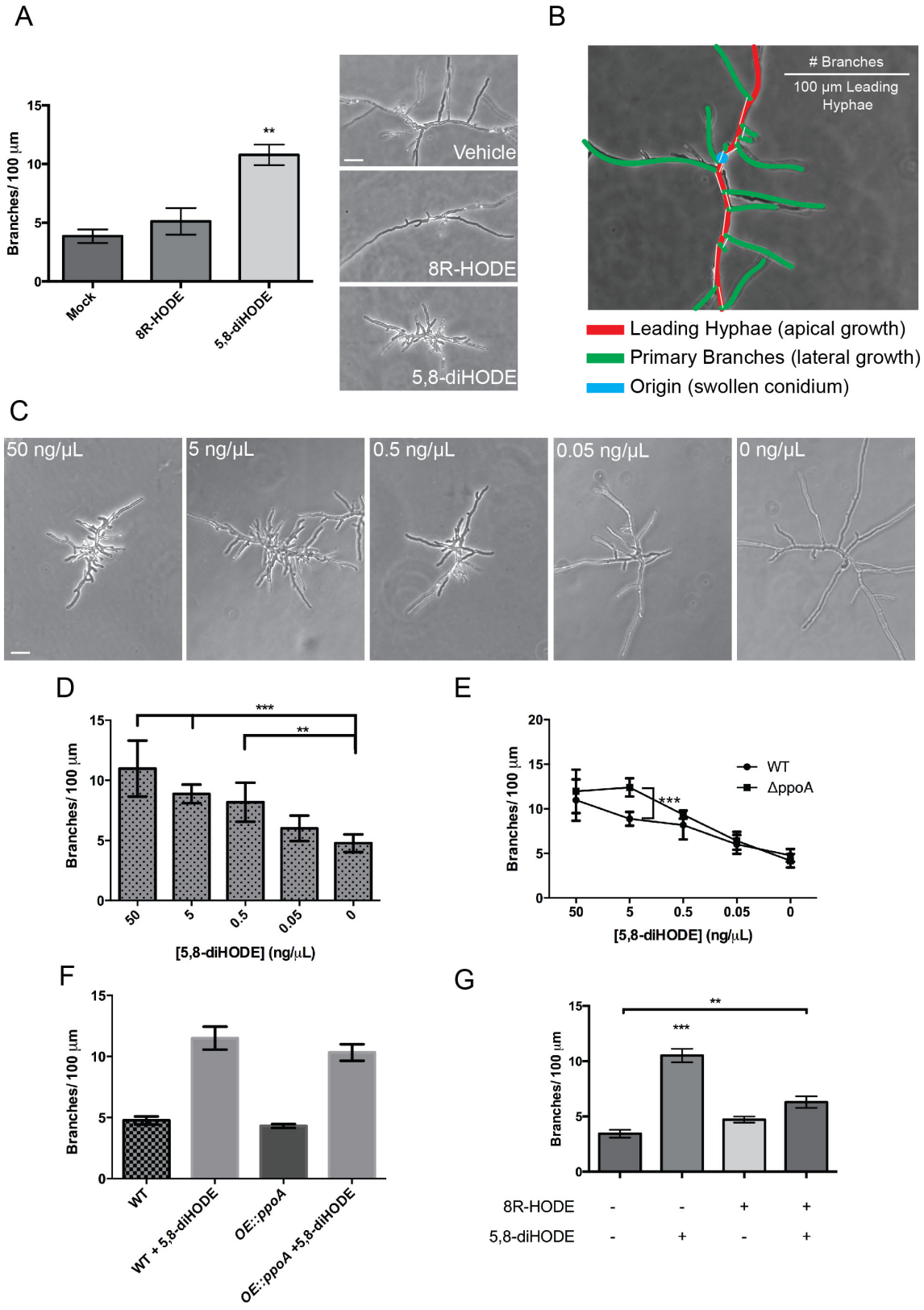
A
Branches/ 100 µm
15
10
5
0
**
Mock
8R-HODE
5,8-diHODE
Vehicle
8R-HODE
5,8-diHODE
B
Branches
100 µm Leading Hyphae
Leading Hyphae (apical growth)
Primary Branches (lateral growth)
Origin (swollen conidium)
C
50 ng/µL
5 ng/µL
0.5 ng/µL
0.05 ng/µL
0 ng/µL
D
Branches/ 100 µm
***
**
50
5
0.5
0.05
0
[5,8-diHODE] (ng/µL)
E
Branches/ 100 µm
WT
ΔppoA
***
50
5
0.5
0.05
0
[5,8-diHODE] (ng/µL)
F
Branches/ 100 µm
WT
WT + 5,8-diHODE
OE::ppoA
OE::ppoA +5,8-diHODE
G
Branches/ 100 µm
**
***
8R-HODE - - + +
5,8-diHODE - + - +

Figure 4. 5,8-diHODE but not 8R-HODE induces hyperbranching in a dose-dependent fashion in *A. fumigatus.*

(**A)** Addition of 5,8-diHODE induced hyperbranching of wild type hyphae. Quantification of the degree of branching revealed a significant increase in the number of branches / 100 μm leading hyphae in colonies treated with 50 ng/μL 5,8-diHODE: 50 ng/μL 8R-HODE did not affect branching compared to the mock treatment. **(B)** To quantify the degree of hyperbranching, a measurement scheme was developed based on one previously described (42). The number of primary branches (green) originating from the leading hypha (red) are determined and the distance between each branch recorded. The number of branches are then divided by the sum of the total distance recorded between each branch for that colony and standardized to 100 μm. The origin (blue) demarks the initial swollen spore from which the hypha emerged. (**C)** Ten-fold serial dilutions of 5,8-diHODE revealed the hyperbranching behavior was dose-dependent, and was statistically different from no treatment at concentrations as low as 0.5 ng/μL **(D). (E)** The Δ*ppoA* strain has a dose-dependent response equivalent to wild type except at 5 ng/μL, at which the degree of branching was greater. Branching of the *OE::ppoA* strain was tested at the same concentration of 5,8-diHODE (5 ng/μL), but no statistical difference in branching was observed compared to wild type in the mock condition or with 5 ng/μL 5,8-diHODE **(F),** even though *OE::ppoA* produces more 8R-HODE and 5,8-diHODE. **(G)**. Co-incubation of 5 ng/μL 8R-HODE and 5,8-diHODE suppresses the hyperbranching phenotype. Values represent average branches / 100 μm (n=6) ± SEM. * $p<0.05$, ** $p< 0.01$, ***$p<0.001$.

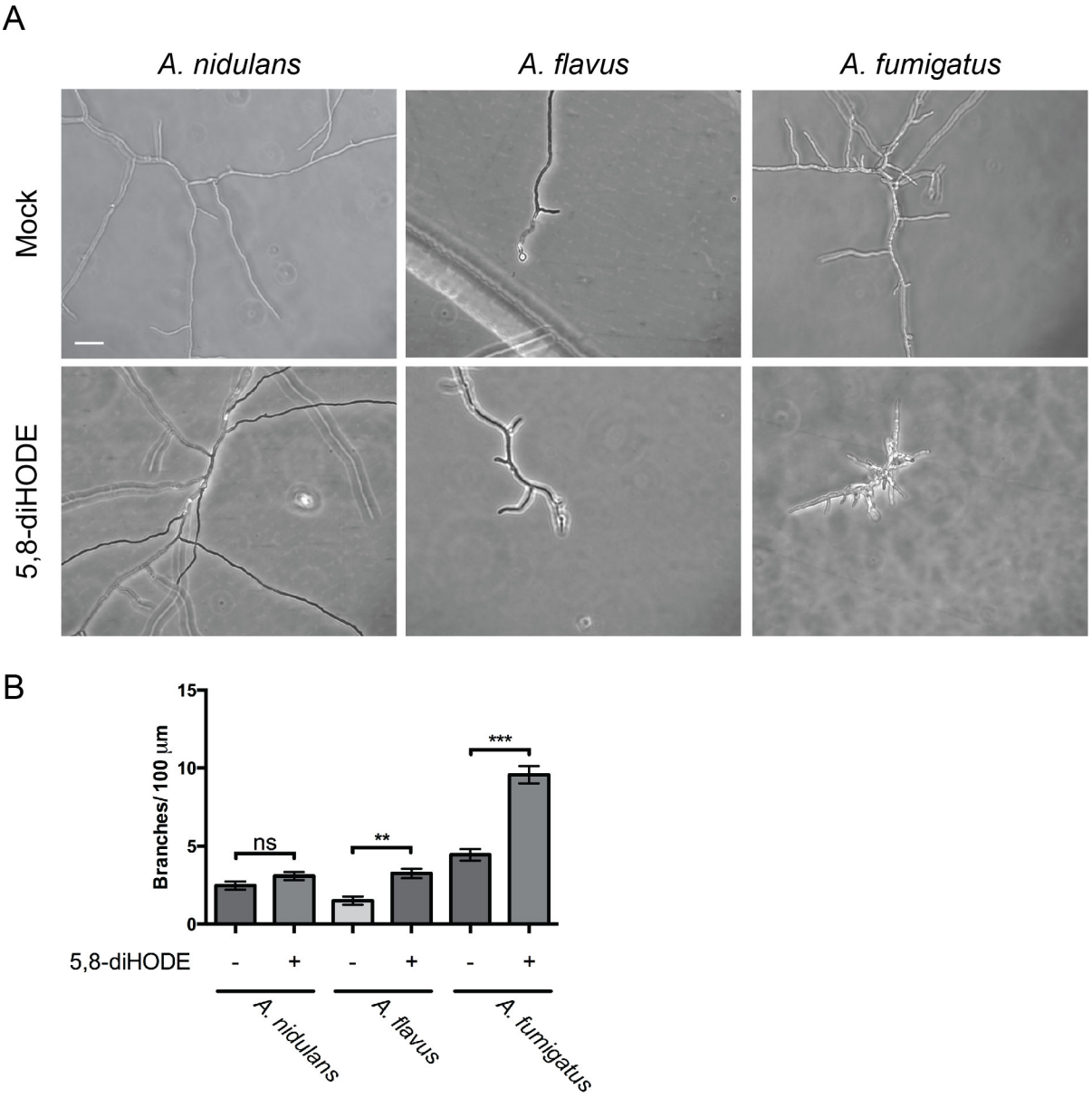

Figure 5: *Aspergillus fumigatus*, *Aspergillus flavus*, but not *Aspergillus nidulans* hyperbranch upon exposure to 5,8-diHODE.

To determine whether the hyperbranching phenomenon was conserved in other aspergilli, wild type *A. nidulans* and *A. flavus* spores were treated with 5 ng/µL 5,8-diHODE. **(A).** Only *A. flavus* hyperbranched to a higher degree than the mock treatment

in 5,8-diHODE, but to a much less extent than that observed in *A. fumigatus* **(B)**. Values represent average branches / 100 μm (n=6) ± SEM. * $p<0.05$, ** $p< 0.01$, ***$p<0.001$.

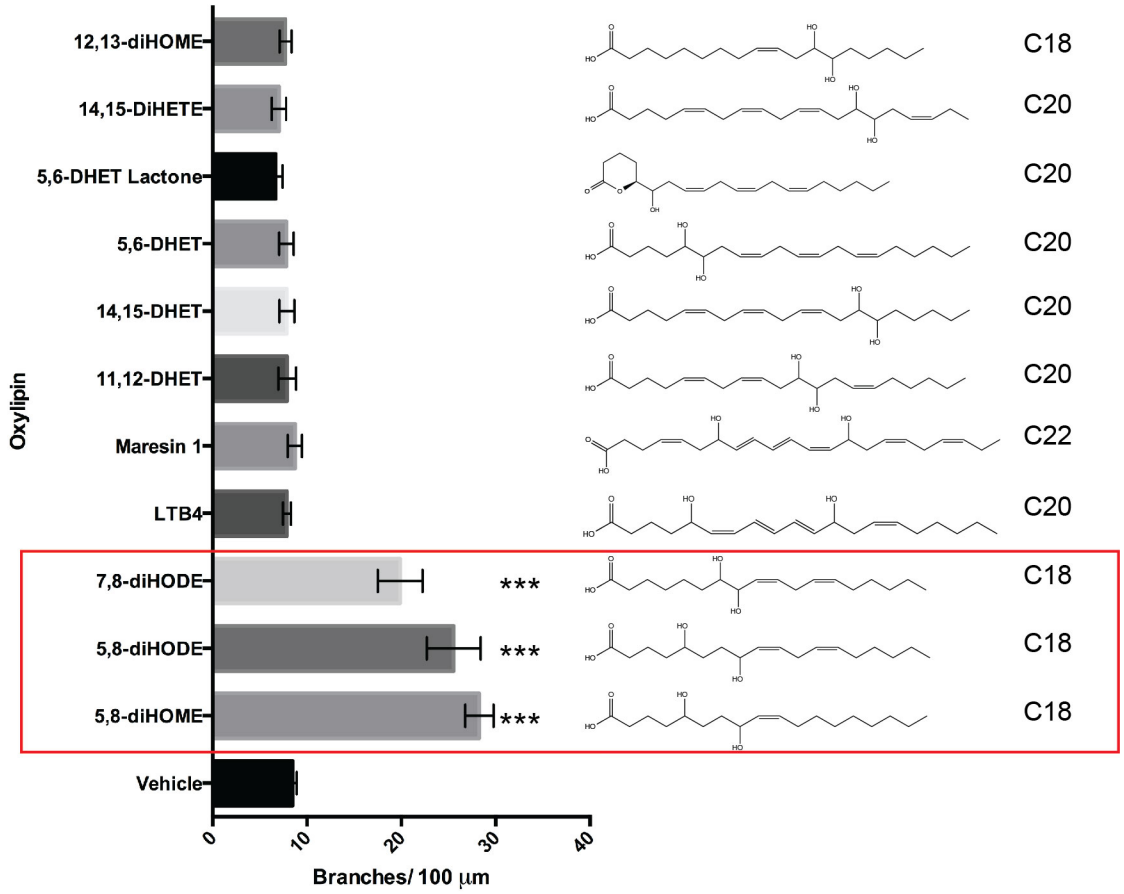

Figure 6: Hyperbranching behavior is induced by specific diol-oxylipins.

Commercially available and purified oxylipin compounds from *Magnaporthe oryzae* (formally *Magnaporthe grisea*, 7,8-diHODE) and the oleic acid-derived PpoA product 5,8-diHOME were tested for their ability to induce hyperbranching in *A. fumigatus* (5 ng/μL). Only 7,8-diHODE (not produced by *A. fumigatus)* and 5,8-diHOME could induce hyperbranching similar to 5,8-diHODE, suggesting the response is specific to particular diol-oxylipins. Values represent average branches / 100 μm (n=6) ± SEM. * $p<0.05$, ** $p< 0.01$, ***$p<0.001$.

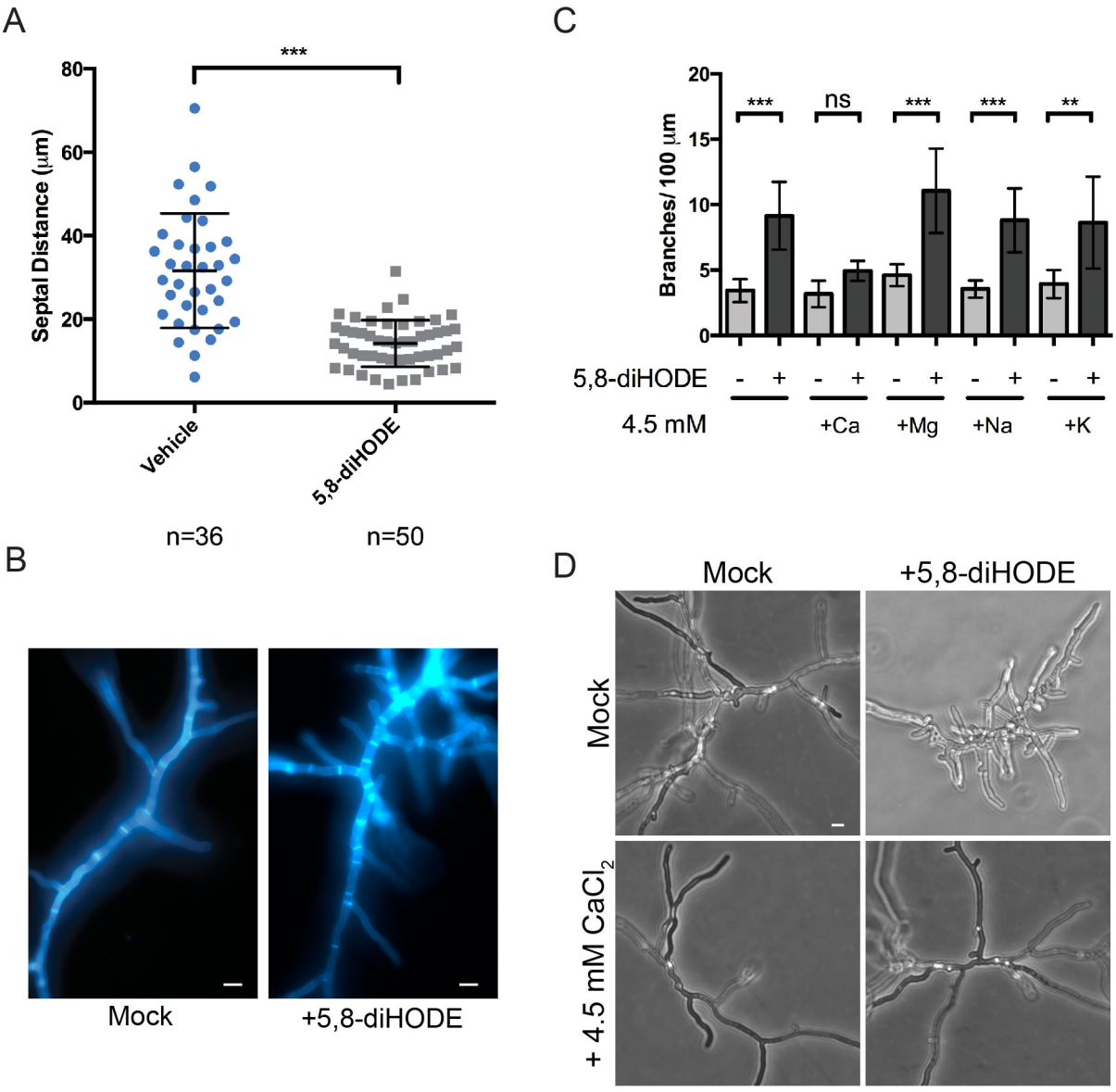

Figure 7: 5,8-diHODE reduces the septal distance of hyphae and induces hyperbranching through calcium-dependent mechanisms.

(A). Septal distances in hyphae stained with calcofluor white (CFW) are reduced in tissue treated with 5,8-diHODE. **(B).** Representative image of both mock and 5,8-diHODE CFW-stained tissue. **(C)**. Addition of 4.5 mM $CaCl_2$ but not $MgCl_2$, NaCl, or KCl suppress hyperbranching in the presence of 5 ng/μL 5,8-diHODE. Representative images of

hyphae treated with 5,8-diHODE and/or 4.5 mM $CaCl_2$. Values represent average branches / 100 μm (n=6), with the exception of Figure 7A, where n=36 and n=50, respectively (average septal distance), ± SEM. * $p<0.05$, ** $p< 0.01$, ***$p<0.001$.

4.8 TABLES

Table 1. Strains used in this study

Strain	Genotype	Source
AF293	wild type	
TDWC1.13	*pyrG1*, Δ*ppoA*::*A. parasiticus pyrG*	(38)
TJMP143.28	*pyrG1*, *pyrG::gpdA(p)::ppoA*	This study
TFYL72.1	Δ*encA::parapyrG;* Δ*tpcC::fumiargB;* Δ*akuA::mluc; pyrG1; argB1*	(39)
TFYL45.1	Δ*akuA::mluc; pyrG1; argB1*	(39)
TFYL80.1	Δ*akuA::mluc; A. fumi argB; pyrG1; argB1*	This study
TFYL110.1	Δ*encA;* Δ*tpcC::fumiargB;* Δ*akuA::mluc; pyrG1; argB1*	This study
TGJF40.9	Δ*akuA::mluc; A. fumi argB;* Δ*ppoA::parapyrG; pyrG1; argB1*	This study
TGJF41.1	Δ*encA;* Δ*tpcC::fumiargB;* Δ*akuA::mluc;* Δ*ppoA::parapyrG; pyrG1; argB1*	This study

Table 2. Primers used in this study

Name	Sequence (5'-3')	Purpose
JP OE Af ppoA 5' F For	TGGGGACACACTAATTGGGC	*OE::ppoA* Up Flank
JP OE Af ppoA 5' F Rev	CAATTCGCCCTATAGTGAGTCGTATTACGGGC GGATATAGCTTGCAGAAC	*OE::ppoA* Up Flank
JP modified T7 promoter For	CGTAATACGACTCACTATAGGG	*pyrG-gpdA(p)*
JP gpdA(p) Fusion Rev	CATGGTGATGTCTGCTCAAG	*pyrG-gpdA(p)*
JP OE Af ppoA 3' F For	CTACCCCGCTTGAGCAGACATCACCATGTCTG AGAAGCAAACCGGTTC	*OE::ppoA* Down Flank
JP OE Af ppoA 3' F Rev	TCGTCGTACGATCCATCTGC	*OE::ppoA* Down Flank
JP OE Af ppoA Nest For	GCCTTCTCCGTTGCGTATCG	Fusion cassette

JP OE Af ppoA Nest Rev	GCAAGAAGTCCTGCAGGGAG	Fusion cassette
GF abaA Probe F	CCTCCTGGCATGACTGATGC	*abaA* Probe
GF abaA Probe R	CCATGCGCTCTGGCTATTTCC	*abaA* Probe
GF wetA Probe F	TCACCCCCTCCATCTGATATCC	*wetA* Probe
GF wetA Probe R	CGCGTCTTGCTTTAGTCTTGG	*wetA* Probe
brlA INT FOR	TCTTGCCGGTCCATTGGGG	*brlA* Probe
brlA INT REV	AGCTGGAGCCCATAGACGG	*brlA* Probe
FY 4G00210 INTB FOR	CAAGAGTTGGAACCATACCTC	*encA* Probe
FY 4G00210 INTB REV	GCTGCAGATTGATGATGTCAG	*encA* Probe
FY 4G00230 INT FOR	GACCAAGCCACAGCCACC	*encD* Probe
FY 4G00230 INT REV	CTCTCTCGACGGTGCCTC	*encD* Probe
GF ppoA 5' Probe F	GAGAAGCAAACCGGTTCAGCC	*ppoA* Probe
GF ppoA 5' Probe R	CCAACGTCCGGAGGGAATCC	*ppoA* Probe
GF tpcC Probe F	GCAGGAGAACACCAAGTCACC	*tpcC* Probe
GF tpcC Probe R	CGTCTCCCGGAACTTCTCGG	*tpcC* Probe
GF ppoA del Cassette F	CGCGCGTAATACGACTCACTATAGG	*ppoA* deletion cassette
GF ppoA del Cassette R	AACAAAAGCTGGAGCTCCACC	*ppoA* deletion cassette
4G00210 5'F FOR	CGCTGAACTCAGGCCATAGAC	PCR amplification of *encA* 5-FOA *pyrG* recycling 5' flank

5-FOA encA 5'F REV	GAGATCACCAATGGTGGGACAGGGTCAACTC AATGAATGCCCATCC	PCR amplification of *encA* 5-FOA *pyrG* recycling 5' flank
5-FOA encA 3'F FOR	GGATGGGCATTCATTGAGTTGACCCTGTCCCA CCATTGGTGATCTC	PCR amplification of *encA* 5-FOA *pyrG* recycling 3' flank
4G00210 3'F REV	CCAAATGTGCAAAGCGCGG	PCR amplification of *encA* 5-FOA *pyrG* recycling 3' flank
4G00210 NEST FOR	CGAAGATTACCTCGGCGC	PCR amplification of *encA-5-FOA pyrG recycling* construct
4G00210 NEST REV	GGATGACAGAGCGTCCAG	PCR amplification of *encA-5-FOA pyrG recycling* construct

4.9 SUPPLEMENTAL FIGURES AND LEGENDS

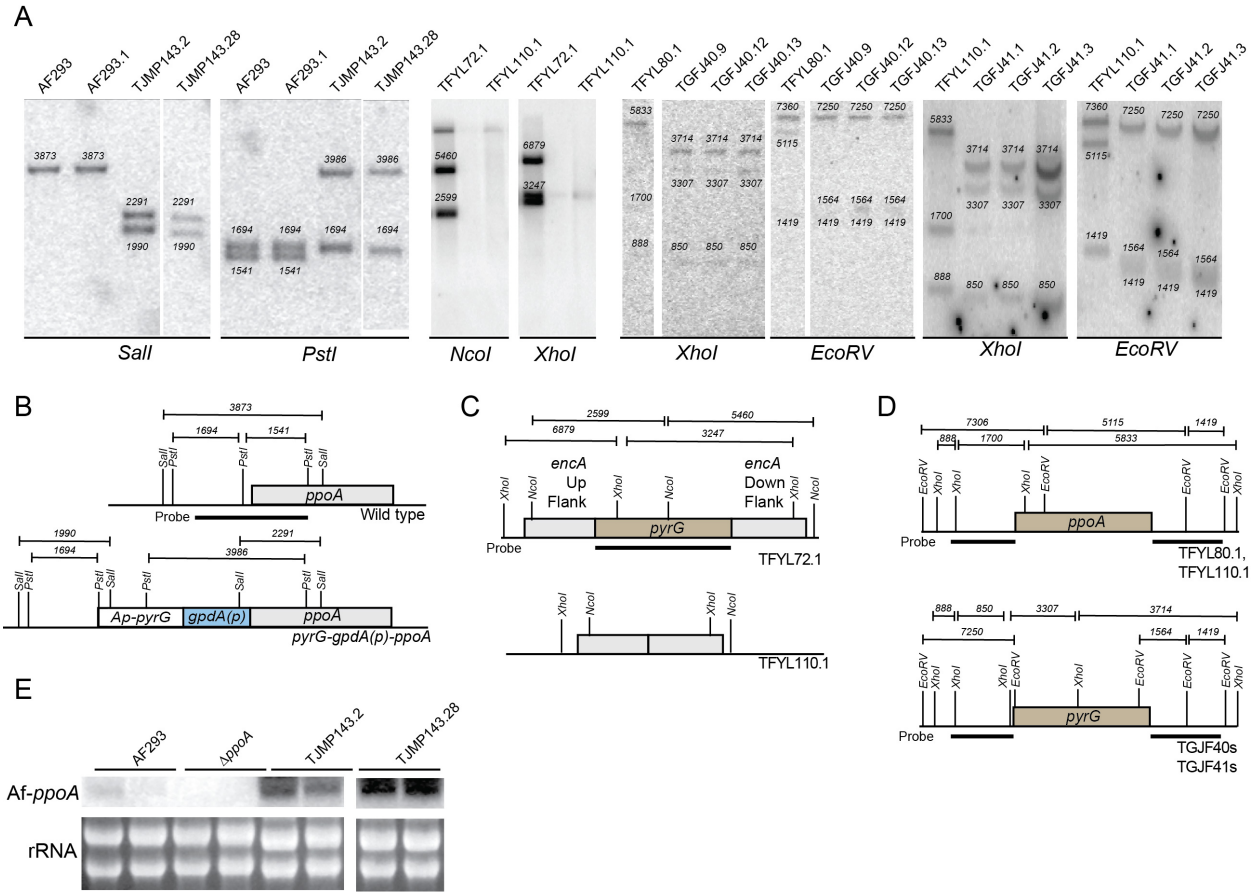

Supplemental Figure 1. Confirmation of *A. fumigatus ppoA* mutants.

(A) Southern blot analysis of the various mutants developed for this study. The restriction digest and expected bands for the various constructs are depicted below **(B-D)** with PCR primers for probes listed in Table 2. **(E)** Northern blot analysis was used to verify disruption and overexpression of the various *ppoA* mutants.

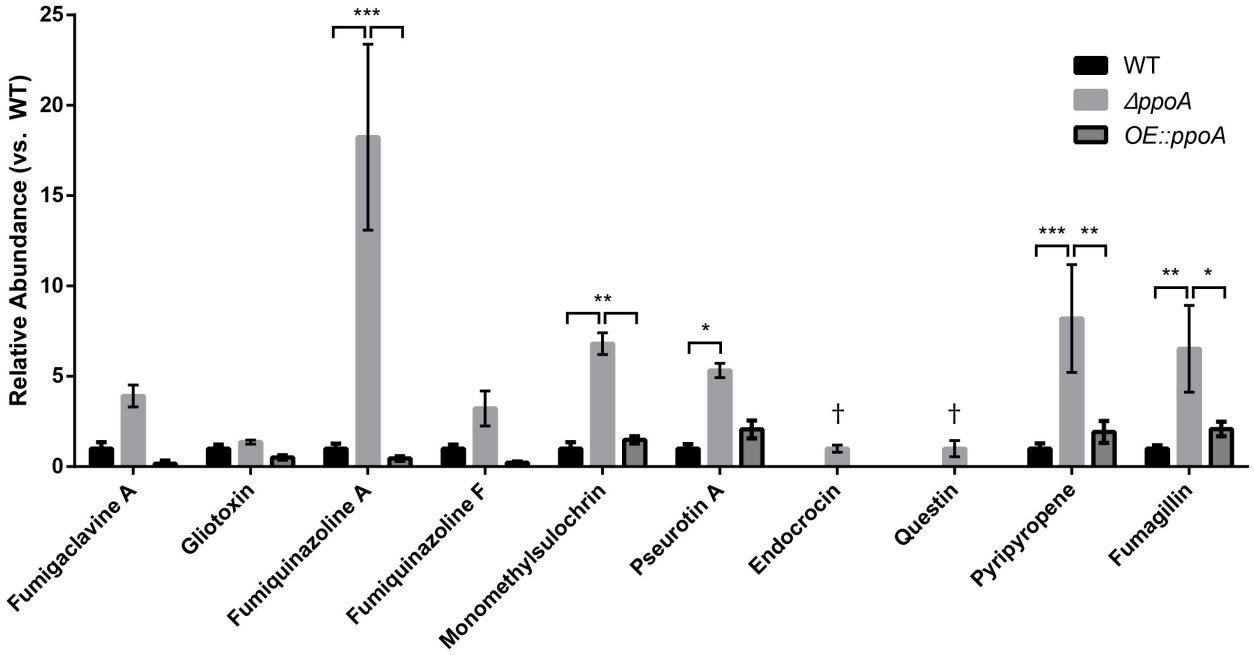

Supplemental Figure 2. Standardized metabolite profile of *ppoA* mutants compared to wild type.

A collection of compounds for which standards were available were used to assess difference in metabolite production after 120 hours at 25˚C in 50 mL GMM (10^7 spores/mL). For each metabolite, the relative abundance is standardized to the corresponding amount observed in the wild type. Neither endocrocin or questin were observed in the wild type, thus values were standardized to the amount in the Δ*ppoA* strain (†). Value represents average abundance (n=3) ± SEM. * $p < 0.05$, ** $p < 0.01$, *** $p < 0.001$.

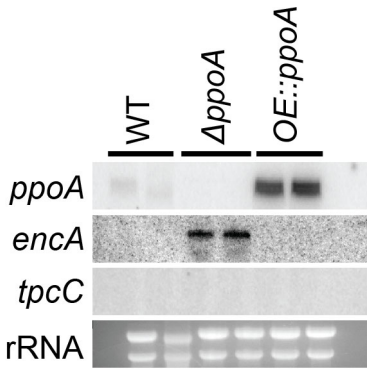

Supplemental Figure 3. Expression of the PKS *encA* but not *tpcC* is observed in the Δ*ppoA* strain.

While both an endocrocin and trypacidin cluster in *A. fumigatus* are capable of producing endocrocin (39), only the PKS within the endocrocin cluster is up-regulated in the Δ*ppoA* strain. Tissue was extracted from cultures grown 72 hours at 37˚C in 50 mL GMM (10^6 spores/mL).

4.10 REFERENCES

1. **Champe SP**, **Rao P**, **Chang A**. 1987. An endogenous inducer of sexual development in *Aspergillus nidulans*. J Gen Microbiol1987/05/01. **133**:1383–1387.

2. **Fischer GJ**, **Keller NP**. 2016. Production of cross-kingdom oxylipins by pathogenic fungi: An update on their role in development and pathogenicity. J Microbiol **54**:254–264.

3. **Champe SP**, **El-Zayat AA**. 1989. Isolation of a sexual sporulation hormone from *Aspergillus nidulans*. J Bacteriol **171**:3982–3988.

4. **Tsitsigiannis DI**, **Kowieski TM**, **Zarnowski R**, **Keller NP**. 2004. Endogenous lipogenic regulators of spore balance in *Aspergillus nidulans*. Eukaryot Cell **3**:1398–1411.

5. **Tsitsigiannis D**, **Kowieski T**, **Zarnowski R**, **Keller N**. 2005. Three putative oxylipin biosynthetic genes integrate sexual and asexual development in *Aspergillus nidulans*. Microbiology **151**:1809–1821.

6. **Tsitsigiannis DI**, **Zarnowski R**, **Keller NP**. 2004. The lipid body protein, PpoA, coordinates sexual and asexual sporulation in *Aspergillus nidulans*. J Biol Chem **279**:11344–11353.

7. **Tsitsigiannis DI**, **Kunze S**, **Willis DK**, **Feussner L**, **Keller NP**. 2005. *Aspergillus* infection inhibits the expression of peanut 13S-HPODE-forming seed lipoxygenases. Mol Plant Microbe Interact **18**:1081–1089.

8. **Brodhagen M**, **Tsitsigiannis DI**, **Hornung E**, **Goebel C**, **Feussner I**, **Keller NP**. 2008. Reciprocal oxylipin-mediated cross-talk in the *Aspergillus*-seed pathosystem. Mol Microbiol **67**:378–391.

9. **Calvo A**, **Hinze L**, **Gardner H**, **Keller N**. 1999. Sporogenic effect of polyunsaturated fatty acids on development of *Aspergillus* spp . Appl Env Microbiol **65**:3668–3673.

10. **Tsitsigiannis D**, **Bok J**, **Andes D**, **Nielsen K**, **Frisvad J**, **Keller N**. 2005. *Aspergillus* cyclooxygenase-like enzymes are associated with prostaglandin production and virulence. Infect Immun **73**:4548–4559.

11. **Brown SH**, **Scott JB**, **Bhaheetharan J**, **Sharpee WC**, **Milde L**, **Wilson RA**, **Keller NP**. 2009. Oxygenase coordination is required for morphological transition and the host-fungus interaction of *Aspergillus flavus*. Mol Plant Microbe Interact **22**:882–894.

12. **Calvo A**, **Gardner H**, **Keller N**. 2001. Genetic connection between fatty acid metabolism and sporulation in *Aspergillus nidulans*. J Biol Chem **276**:25766–25774.

13. **Mazur P**, **Meyers H**, **Nakanishi K**, **Elzayat A**, **Champe S**. 1990. Structural elucidation of sporogenic fatty-acid metabolies from *Aspergillus nidulans*. Tetrahedron Lett **31**:3837–3840.

14. **Brodhun F**, **Gobel C**, **Hornung E**, **Feussner I**. 2009. Identification of PpoA from *Aspergillus nidulans* as a fusion protein of a fatty acid heme dioxygenase/peroxidase and a cytochrome P450. J Biol Chem **284**:11792–11805.

15. **Fielding AJ**, **Brodhun F**, **Koch C**, **Pievo R**, **Denysenkov V**, **Feussner I**, **Bennati M**. 2011. Multifrequency electron paramagnetic resonance characterization of PpoA, a CYP450 fusion protein that catalyzes fatty acid dioxygenation. J Am Chem Soc **133**:9052–9062.

16. **Garscha U**, **Jerneren F**, **Chung D**, **Keller NP**, **Hamberg M**, **Oliw EH**. 2007. Identification of dioxygenases required for *Aspergillus* development. Studies of products,

stereochemistry, and the reaction mechanism. J Biol Chem **282**:34707–34718.

17. **Jernerén F**, **Garscha U**, **Hoffmann I**, **Hamberg M**, **Oliw E**. 2010. Reaction mechanism of 5,8-linoleate diol synthase, 10R-dioxygenase, and 8,11-hydroperoxide isomerase of *Aspergillus clavatus*. Biochim Biophys Acta **1801**:503–507.

18. **Jerneren F**, **Sesma A**, **Francheschetti M**, **Hamberg M**, **Oliw EH**. 2010. Gene deletion of 7,8-linoleate diol synthase of the rice blast fungus: studies on pathogenicity, stereochemistry, and oxygenation mechanisms. J Biol Chem **285**:5308–5316.

19. **Tsitsigiannis DI**, **Keller NP**. 2006. Oxylipins act as determinants of natural product biosynthesis and seed colonization in *Aspergillus nidulans*. Mol Microbiol **59**:882–892.

20. **Prade RA**, **Timberlake WE**. 1993. The *Aspergillus nidulans brlA* regulatory locus consists of overlapping transcription units that are individually required for conidiophore development. Embo **12**:2439–2447.

21. **Kang EH**, **Kim JA**, **Oh HW**, **Park HM**. 2013. LAMMER Kinase LkhA plays multiple roles in the vegetative growth and asexual and sexual development of *Aspergillus nidulans*. PLoS One **8**:e58762.

22. **Nahlik K**, **Dumkow M**, **Bayram O**, **Helmstaedt K**, **Busch S**, **Valerius O**, **Gerke J**, **Hoppert M**, **Schwier E**, **Opitz L**, **Westermann M**, **Grond S**, **Feussner K**, **Goebel C**, **Kaever A**, **Meinicke P**, **Feussner I**, **Braus GH**. 2010. The COP9 signalosome mediates transcriptional and metabolic response to hormones, oxidative stress protection and cell wall rearrangement during fungal development. Mol Microbiol **78**:964–979.

23. **Lim FY**, **Ames B**, **Walsh CT**, **Keller NP**. 2014. Co-ordination between BrlA regulation and secretion of the oxidoreductase FmqD directs selective accumulation of

fumiquinazoline C to conidial tissues in *Aspergillus fumigatus*. Cell Microbiol **16**:1267–83.

24. **Berthier E**, **Lim FY**, **Deng Q**, **Guo CJ**, **Kontoyiannis DP**, **Wang CC**, **Rindy J**, **Beebe DJ**, **Huttenlocher A**, **Keller NP**. 2013. Low-volume toolbox for the discovery of immunosuppressive fungal secondary metabolites. PLoS Pathog **9**:e1003289.

25. **Coyle CM**, **Kenaley SC**, **Rittenour WR**, **Panaccione DG**. 2007. Association of ergot alkaloids with conidiation in *Aspergillus fumigatus*. Mycologia **99**:804–811.

26. **Gauthier T**, **Wang X**, **Sifuentes Dos Santos J**, **Fysikopoulos A**, **Tadrist S**, **Canlet C**, **Artigot MP**, **Loiseau N**, **Oswald IP**, **Puel O**. 2012. Trypacidin, a spore-borne toxin from *Aspergillus fumigatus*, is cytotoxic to lung cells. PLoS One **7**:e29906.

27. **Harris SD**. 2008. Branching of fungal hyphae: regulation, mechanisms and comparison with other branching systems. Mycologia **100**:823–832.

28. **Virag A**, **Lee MP**, **Si H**, **Harris SD**. 2007. Regulation of hyphal morphogenesis by *cdc42* and *rac1* homologues in *Aspergillus nidulans*. Mol Microbiol **66**:1579-1596.

29. **Brand A**, **Shanks S**, **Duncan VMS**, **Yang M**, **Mackenzie K**, **Gow NAR**. 2007. Hyphal orientation of *Candida albicans* is regulated by a calcium-dependent mechanism. Curr Biol **17**:347–352.

30. **Kumamoto CA**. 2008. Molecular mechanisms of mechanosensing and their roles in fungal contact sensing. Nat Rev Microbiol **6**:667–673.

31. **Akiyama K**, **Matsuzaki K**, **Hayashi H**. 2005. Plant sesquiterpenes induce hyphal branching in arbuscular mycorrhizal fungi. Nature **435**:824–827.

32. **Kankanala P**, **Czymmek K**, **Valent B**. 2007. Roles for rice membrane dynamics

and plasmodesmata during biotrophic invasion by the blast fungus. Plant Cell **19**:706–724.

33. **Shimizu K**, **Keller NP**. 2001. Genetic involvement of a cAMP-dependent protein kinase in a G protein signaling pathway regulating morphological and chemical transitions in *Aspergillus nidulans*. Genetics **157**:591–600.

34. **Sambrook J**, **Russell DW**. 2001. Molecular Cloning: A Laboratory Manual. Book, Cold Spring Harbor Laboratory Press, New York.

35. **Yu JH**, **Hamari Z**, **Han KH**, **Seo JA**, **Reyes-Dominguez Y**, **Scazzocchio C**. 2004. Double-joint PCR: a PCR-based molecular tool for gene manipulations in filamentous fungi. Fungal Genet Biol2004/10/07. **41**:973–981.

36. **Soukup AA**, **Farnoodian M**, **Berthier E**, **Keller NP**. 2012. NosA, a transcription factor important in *Aspergillus fumigatus* stress and developmental response, rescues the germination defect of a *laeA* deletion. Fungal Genet Biol **49**:857–865.

37. **Szewczyk E**, **Nayak T**, **Oakley CE**, **Edgerton H**, **Xiong Y**, **Taheri-Talesh N**, **Osmani S a**, **Oakley BR**. 2006. Fusion PCR and gene targeting in *Aspergillus nidulans*. Nat Protoc **1**:3111–3120.

38. **Dagenais TR**, **Chung D**, **Giles SS**, **Hull CM**, **Andes D**, **Keller NP**. 2008. Defects in conidiophore development and conidium-macrophage interactions in a dioxygenase mutant of *Aspergillus fumigatus*. Infect Immun **76**:3214–3220.

39. **Throckmorton K**, **Lim FY**, **Kontoyiannis DP**, **Zheng W**, **Keller NP**. 2016. Redundant synthesis of a conidial polyketide by two distinct secondary metabolite clusters in *Aspergillus fumigatus*. Environ Microbiol **18**:246–259.

40. **Albright JC**, **Henke MT**, **Soukup AA**, **McClure RA**, **Thomson RJ**, **Keller NP**, **Kelleher NL**. 2015. Large-scale metabolomics reveals a complex response of *Aspergillus nidulans* to epigenetic perturbation. ACS Chem Biol **10**:1535–1541.

41. **Wiemann P**, **Lechner BE**, **Baccile JA**, **Velk TA**, **Yin W-B**, **Bok JW**, **Pakala S**, **Losada L**, **Nierman WC**, **Schroeder FC**, **Haas H**, **Keller NP**. 2014. Perturbations in small molecule synthesis uncovers an iron-responsive secondary metabolite network in *Aspergillus fumigatus*. Front Microbiol **5**:530.

42. **Simonin A**, **Palma-Guerrero J**, **Fricker M**, **Glass NL**. 2012. Physiological significance of network organization in fungi. Eukaryot Cell **11**:1345–1352.

43. **Lee I**, **Oh J-H**, **Shwab EK**, **Dagenais TRT**, **Andes D**, **Keller NP**. 2009. HdaA, a class 2 histone deacetylase of *Aspergillus fumigatus*, affects germination and secondary metabolite production. Fungal Genet Biol **46**:782–790.

44. **Seo JA**, **Guan Y**, **Yu JH**. 2006. FluG-dependent asexual development in *Aspergillus nidulans* occurs via derepression. Genetics **172**:1535–1544.

45. **Lim FY**, **Hou Y**, **Chen Y**, **Oh JH**, **Lee I**, **Bugni TS**, **Keller NP**. 2012. Genome-based cluster deletion reveals an endocrocin biosynthetic pathway in *Aspergillus fumigatus*. Appl Env Microbiol **78**:4117–4125.

46. **Jerneren F**, **Sesma A**, **Franceschetti M**, **Hamberg M**, **Oliw EH**. 2010. Gene deletion of 7,8-linoleate diol synthase of the rice blast fungus: studies on pathogenicity, stereochemistry, and oxygenation mechanisms. J Biol Chem **285**:5308–5316.

47. **Seo M-J**, **Shin K-C**, **Jeong Y-J**, **Oh D-K**. 2015. Production of 5,8-dihydroxy-9(Z)-octadecenoic acid from oleic acid by whole recombinant cells of *Aspergillus nidulans* expressing diol synthase. Biotechnol Lett **37**:131–137.

48. **Semighini CP**, **Harris SD**. 2008. Regulation of apical dominance in *Aspergillus nidulans* hyphae by reactive oxygen species. Genetics **179**:1919–1932.

49. **Li H**, **Barker BM**, **Grahl N**, **Puttikamonkul S**, **Bell JD**, **Craven KD**, **Cramer RAJ**. 2011. The small GTPase RacA mediates intracellular reactive oxygen species production, polarized growth, and virulence in the human fungal pat*hogen Aspergillus fumigatus*. Eukaryot Cell **10**:174–186.

50. **Willger SD**, **Puttikamonkul S**, **Kim K-H**, **Burritt JB**, **Grahl N**, **Metzler LJ**, **Barbuch R**, **Bard M**, **Lawrence CB**, **Cramer RAJ**. 2008. A sterol-regulatory element binding protein is required for cell polarity, hypoxia adaptation, azole drug resistance, and virulence in *Aspergillus fumigatus*. PLoS Pathog **4**:e1000200.

51. **Kurtz MB**, **Heath IB**, **Marrinan J**, **Dreikorn S**, **Onishi J**, **Douglas C**. 1994. Morphological effects of lipopeptides against *Aspergillus fumigatus* correlate with activities against (1,3)-beta-D-glucan synthase. Antimicrob Agents Chemother **38**:1480–1489.

52. **Mellado E**, **Dubreucq G**, **Mol P**, **Sarfati J**, **Paris S**, **Diaquin M**, **Holden DW**, **Rodriguez-Tudela JL**, **Latge JP**. 2003. Cell wall biogenesis in a double chitin synthase mutant (*chsG-*/*chsE-*) of *Aspergillus fumigatus*. Fungal Genet Biol **38**:98–109.

53. **da Silva Ferreira ME**, **Heinekamp T**, **Hartl A**, **Brakhage AA**, **Semighini CP**, **Harris SD**, **Savoldi M**, **de Gouvea PF**, **de Souza Goldman MH**, **Goldman GH**. 2007. Functional characterization of the *Aspergillus fumigatus* calcineurin. Fungal Genet Biol **44**:219–230.

54. **Steinbach WJ**, **Cramer RAJ**, **Perfect BZ**, **Asfaw YG**, **Sauer TC**, **Najvar LK**, **Kirkpatrick WR**, **Patterson TF**, **Benjamin DKJ**, **Heitman J**, **Perfect JR**. 2006.

Calcineurin controls growth, morphology, and pathogenicity in *Aspergillus fumigatus*. Eukaryot Cell **5**:1091–1103.

55. **Juvvadi PR**, **Fortwendel JR**, **Rogg LE**, **Burns KA**, **Randell SH**, **Steinbach WJ**. 2011. Localization and activity of the calcineurin catalytic and regulatory subunit complex at the septum is essential for hyphal elongation and proper septation in *Aspergillus fumigatus*. Mol Microbiol **82**:1235–1259.

56. **Mazur P**, **Nakanishi K**, **Elzayat AAE**, **Champe SP**. 1991. Structure and synthesis of sporogenic psi factors from *Aspergillus nidulans*. Chem Soc Chem Commun 1486–1487.

57. **O'Gorman CM**, **Fuller H**, **Dyer PS**. 2009. Discovery of a sexual cycle in the opportunistic fungal pathogen Aspergillus fumigatus. Nature **457**:471–474.

58. **McDonald T**, **Devil T**, **Shimizu K**, **Sim S**, **Keller N**. 2003. Signaling events connecting mycotoxin biosynthesis and sporulation in *Aspergillus* and *Fusarium* spp. Mycotoxins **2003**:139–147.

59. **Shim WB**, **Dunkle LD**. 2002. Identification of genes expressed during cercosporin biosynthesis in *Cercospora zeae-maydis*. Physiol Mol Plant Pathol **61**:237–248.

60. **Lim FY**, **Keller NP**. 2014. Spatial and temporal control of fungal natural product synthesis. Nat Prod Rep **31**:1277–1286.

61. **Jahn B**, **Koch A**, **Schmidt A**, **Wanner G**, **Gehringer H**, **Bhakdi S**, **Brakhage AA**. 1997. Isolation and characterization of a pigmentless-conidium mutant of *Aspergillus fumigatus* with altered conidial surface and reduced virulence. Infect Immun **65**:5110–5117.

62. **Sugui JA**, **Pardo J**, **Chang YC**, **Mullbacher A**, **Zarember KA**, **Galvez EM**, **Brinster L**, **Zerfas P**, **Gallin JI**, **Simon MM**, **Kwon-Chung KJ**. 2007. Role of *laeA* in the regulation of *alb1*, *gliP*, conidial morphology, and virulence in *Aspergillus fumigatus*. Eukaryot Cell **6**:1552–1561.

63. **Bayry J**, **Beaussart A**, **Dufrene YF**, **Sharma M**, **Bansal K**, **Kniemeyer O**, **Aimanianda V**, **Brakhage AA**, **Kaveri S V**, **Kwon-Chung KJ**, **Latge JP**, **Beauvais A**. 2014. Surface structure characterization of *Aspergillus fumigatus* conidia mutated in the melanin synthesis pathway and their human cellular immune response. Infect Immun **82**:3141–3153.

64. **Nagahashi G**, **Douds DD**. 2011. The effects of hydroxy fatty acids on the hyphal branching of germinated spores of AM fungi. Fungal Biol **115**:351–358.

65. **Riquelme M**, **Bartnicki-Garcia S**. 2004. Key differences between lateral and apical branching in hyphae of *Neurospora crassa*. Fungal Genet Biol **41**:842–851.

66. **Virag A**, **Lee MP**, **Si H**, **Harris SD**. 2007. Regulation of hyphal morphogenesis by *cdc42* and *rac1* homologues in *Aspergillus nidulans*. Mol Microbiol **66**:1579–1596.

67. **Ganem S**, **Lu S-W**, **Lee B-N**, **Chou DY-T**, **Hadar R**, **Turgeon BG**, **Horwitz BA**. 2004. G-protein beta subunit of *Cochliobolus heterostrophus* involved in virulence, asexual and sexual reproductive ability, and morphogenesis. Eukaryot Cell **3**:1653–1663.

68. **Delgado-Jarana J**, **Martinez-Rocha AL**, **Roldan-Rodriguez R**, **Roncero MIG**, **Di Pietro A**. 2005. *Fusarium oxysporum* G-protein beta subunit Fgb1 regulates hyphal growth, development, and virulence through multiple signalling pathways. Fungal Genet Biol **42**:61–72.

69. **Yamagishi D**, **Otani H**, **Kodama M**. 2006. G protein signaling mediates

developmental processes and pathogenesis of *Alternaria alternata*. Mol Plant Microbe Interact **19**:1280–1288.

70. **Fortwendel JR**, **Fuller KK**, **Stephens TJ**, **Bacon WC**, **Askew DS**, **Rhodes JC**. 2008. *Aspergillus fumigatus* RasA regulates asexual development and cell wall integrity. Eukaryot Cell **7**:1530–1539.

71. **Rispail N**, **Soanes DM**, **Ant C**, **Czajkowski R**, **Grunler A**, **Huguet R**, **Perez-Nadales E**, **Poli A**, **Sartorel E**, **Valiante V**, **Yang M**, **Beffa R**, **Brakhage AA**, **Gow NAR**, **Kahmann R**, **Lebrun M-H**, **Lenasi H**, **Perez-Martin J**, **Talbot NJ**, **Wendland J**, **Di Pietro A**. 2009. Comparative genomics of MAP kinase and calcium-calcineurin signalling components in plant and human pathogenic fungi. Fungal Genet Biol **46**:287–298.

72. **Liebmann B**, **Muller M**, **Braun A**, **Brakhage AA**. 2004. The cyclic AMP-dependent protein kinase a network regulates development and virulence in *Aspergillus fumigatus*. Infect Immun **72**:5193–5203.

73. **Gehrke A**, **Heinekamp T**, **Jacobsen ID**, **Brakhage AA**. 2010. Heptahelical receptors GprC and GprD of *Aspergillus fumigatus* are essential regulators of colony growth, hyphal morphogenesis, and virulence. Appl Environ Microbiol **76**:3989–3998.

74. **Silverman-Gavrila LB**, **Lew RR**. 2003. Calcium gradient dependence of *Neurospora crassa* hyphal growth. Microbiology **149**:2475–2485.

75. **Suresh K**, **Subramanyam C**. 1997. A putative role for calmodulin in the activation of *Neurospora crassa* chitin synthase. FEMS Microbiol Lett **150**:95–100.

76. **Tellez-Inon MT**, **Ulloa RM**, **Glikin GC**, **Torres HN**. 1985. Characterization of *Neurospora crassa* cyclic AMP phosphodiesterase activated by calmodulin. Biochem J **232**:425–430.

77. **Ortega Perez R**, **Irminger-Finger I**, **Arrighi JF**, **Capelli N**, **van Tuinen D**, **Turian G**. 1994. Identification and partial purification of calmodulin-binding microtubule-associated proteins from *Neurospora crassa*. Eur J Biochem **226**:303–310.

78. **Silverman-Gavrila LB**, **Lew RR**. 2000. Calcium and tip growth in *Neurospora crassa*. Protoplasma **213**:203–217.

79. **Stathopoulos-Gerontides A**, **Guo JJ**, **Cyert MS**. 1999. Yeast calcineurin regulates nuclear localization of the Crz1p transcription factor through dephosphorylation. Genes Dev **13**:798–803.

80. **Rusnak F**, **Mertz P**. 2000. Calcineurin: form and function. Physiol Rev **80**:1483–1521.

81. **Hemenway CS**, **Heitman J**. 1999. Calcineurin. Structure, function, and inhibition. Cell Biochem Biophys **30**:115–151.

82. **Aramburu J**, **Rao A**, **Klee CB**. 2000. Calcineurin: from structure to function. Curr Top Cell Regul **36**:237–295.

83. **Juvvadi P**, **Steinbach W**. 2015. Calcineurin orchestrates hyphal growth, septation, drug resistance and pathogenesis of *Aspergillus fumigatus*: Where do we go from here? Pathogens **4**:883–893.

84. **de Castro PA**, **Chiaratto J**, **Winkelstroter LK**, **Bom VLP**, **Ramalho LNZ**, **Goldman MHS**, **Brown NA**, **Goldman GH**. 2014. The involvement of the Mid1/Cch1/Yvc1 calcium channels in *Aspergillus fumigatus* virulence. PLoS One **9**:e103957.

CONCLUDING REMARKS

Among organisms, variations of common biological themes are observed in almost every aspect of their biology. Conserved signaling pathways like MAPK cascades, signaling molecules such as calcium, epigenetic regulation of gene expression, and developmental programs are only a few examples that are observed and regulated in mammals, plants, and fungi. This thesis set out to investigate a common class of signaling molecules (oxylipins) and their role in development of a ubiquitous opportunistic pathogen, *A. fumigatus*. I've provided strong evidence that both *A. fumigatus* and the mammalian host produce shared lipid signals that influence fungal development, but may also affect disease outcomes.

Oxylipins and the enzymes that produce them are well-characterized in mammals. Interestingly lipoxygenases were first described in plants and fungi, but thought to be absent in animals until 1974 (1, 2). The extent to which *fungal* oxylipins (both endogenous and exogenous) influence fungal development and host responses is not well-understood. The best examples to date consist of the work done with Ppo enzymes in *Aspergillus* spp. and their influence on asexual/sexual development and prostaglandin production (3, 4). Recently a global analysis of fungal lipoxygenases was carried out, but only a few studies comment on the biological roles of these fungal enzymes (5–8).

This thesis work ascribes several new functions of *A. fumigatus* oxylipins and oxygenase activity to fungal development and host responses. Chapter 3 investigates an otherwise unknown function of fungal lipoxygenases: their ability to influence spore germinations.

We initially hypothesized that the lipoxygenase activity of LoxB may contribute to allergenic disease, and indeed we observed that *loxB* overexpression yielded a more allergenic strain. This supports the hypothesis that increased fungal LoxB activity correlates with heightened immune responses. Unexpectedly, my observations revealed that LoxB promotes germination in environments where arachidonic acid (which is inhibitory to germination) is high, while the mammalian leukotriene intermediate 5-HETE promotes spore germination. This is an excellent example by which two different organisms utilize the same molecule in different ways: the host to bring about inflammatory responses through 5-HETE modification into leukotrienes, and the fungus an environmental germination cue.

Chapter 4 describes a novel hyperbrancing phenomenon from an oxylipin previously characterized. 5,8-diHODE has not been identified in mammals and its hyperbranching activity is the first of its kind described for *A. fumigatus.* These observations lead to a new set of interesting questions with respect to host interactions. For example, does transient PpoA activity from interactions with immune cells intensify branching and subsequently invasive growth? Are hyperbranched *A. fumigatus* mycelia more susceptible to antifungal agents? It remains to be determined whether hyperbranching is desirable or undesirable in the context of invasive disease.

Aspergillus fumigatus hyperbranching behavior appears unique to specific symbiotic relationships, as oxylipins produced by *Magnaporthe oryzae* could elicit the same behavior. With the development of micro-scale growth platforms, oxylipin-specific growth

phenotypes can continue to be used to answer these questions. Oxylipins are commercially available, but at low quantities and high cost. Microfluidic platforms are a cost-effective way to investigate developmental phenotypes on a large scale with numerous compounds or immune cell types.

What other classes of signaling molecules are part of a shared language between mammals, fungi, plants, or even bacteria? While this work has only considered oxylipins, other signals have been described which contribute to the developmental program of fungi. For example, the bacteria *Ralstonia solenaciarum* produces a lipopeptide (ralsolamycin) that induces production of survival structures (chlamydospores) in 34 species of fungi among ascomycetes, basidiomycetes, and zygomycetes (9). This suggests that responses from shared signaling molecules are abundant among organisms, and even more when considering that microbial diversity is orders of magnitude greater than that of plants or multicellular organisms (10). Any ion, peptide, lipid, oxygenated lipid, sugar, secondary metabolite, or host factor could serve as a signaling molecule for inter-species cross-talk.

Now that simultaneous profiling of various oxylipin compounds via mass spectrometry has become a reality (11), the scientific community should develop detailed oxylipin profiles for mammals, plants, and fungi, or an “oxylipome” signature. Most studies focusing on fungal infection have looked at physical and chemical interactions between cell types, the pathogen, and host tissue. My thesis work contributes to this area of research with the FleA-fucose interactions described in Chapter 2. However, perturbation

of the *A. fumigatus* oxylipome open up a whole new area of research for host-pathogen interactions, unveiling ways to combat primary aspects of fungal disease such as spore germination and invasive growth. Future studies investigating the mechanisms by which oxylipins (or any signaling molecular for that matter) are perceived in fungi (previous work in *A. flavus* suggests G-Protein Coupled Receptors as intriguing candidates, 11) could lead to novel antifungal compounds. Individual oxylipome profiling could also shed light on any deficiencies that predispose individuals to microbial infection. While our interactions with microbial pathogens have existed for thousands of years and likely will continue for a thousand more, it is critical that we understand the interpretation of these signaling molecules by pathogens, particularly the oxylipome, if we want to improve disease outcomes.

REFERENCES

1. **Satoh T**, **Matsuda Y**, **Takashio M**, **Satoh K**, **Arima K**. 1975. Isolation of lipoxygenase-like enzyme from *Fusarium oxysporum*. Agr Biol Chem **40**:953–961.

2. **Hamberg M**, **Samuelsson B**. 1974. Prostaglandin endoperoxides. Novel transformations of arachidonic acid in human platelets. Proc Natl Acad Sci U S A **71**:3400–3404.

3. **Tsitsigiannis D**, **Bok J**, **Andes D**, **Nielsen K**, **Frisvad J**, **Keller N**. 2005. *Aspergillus* cyclooxygenase-like enzymes are associated with prostaglandin production and virulence. Infect Immun **73**:4548–4559.

4. **Tsitsigiannis DI**, **Kowieski TM**, **Zarnowski R**, **Keller NP**. 2004. Endogenous lipogenic regulators of spore balance in *Aspergillus nidulans*. Eukaryot Cell **3**:1398–1411.

5. **Burow GB**, **Nesbitt TC**. 1997. Seed lipoxygenase products modulate *Aspergillus* mycotoxin biosynthesis. Mol Plant-Microbe Interact **10**:380–387.

6. **Burow G**, **Gardner H**, **Keller N**. 2000. A peanut seed lipoxygenase responsive to *Aspergillus* colonization. Plant Mol Biol **42**:689–701.

7. **Wennman A**, **Magnuson A**, **Hamberg M**, **Oliw EH**. 2015. Manganese lipoxygenase of *F. oxysporum* and the structural basis for biosynthesis of distinct 11-hydroperoxy stereoisomers. J Lipid Res **56**:1606–1615.

8. **Andreou A**, **Brodhun F**, **Feussner I**. 2009. Biosynthesis of oxylipins in non-mammals. Prog Lipid Res **48**:148–170.

9. **Spraker JE**, **Sanchez LM**, **Lowe TM**, **Dorrestein PC**, **Keller NP**. 2016. *Ralstonia solanacearum* lipopeptide induces chlamydospore development in fungi and facilitates

bacterial entry into fungal tissues. ISME J. Epub ahead of print.

10. **Cragg GM**, **Newman DJ**. 2013. Natural products: a continuing source of novel drug leads. Biochim Biophys Acta **1830**:3670–3695.

11. **Yang J**, **Schmelzer K**, **Georgi K**, **Hammock BD**. 2009. Quantitative profiling method for oxylipin metabolome by liquid chromatography electrospray ionization tandem mass spectrometry. Anal Chem **81**:8085–8093.

12. **Affeldt K**, **Carrig J**, **Amare M**, **Keller NP**. 2014. Global survey of canonical *Aspergillus flavus* G protein-coupled receptors. MBio **5**:1501–14.

APPENDIX 1: LIST OF PUBLICATIONS

1. **Tyler BM**, **Kale SD**, **Wang QQ**, **Tao K**, **Clark HR**, **Drews K**, **Antignani V**, **Rumore A**, **Hayes T**, **Plett JM**, **Fudal I**, **Gu B**, **Chen QH**, **Affeldt KJ**, **Berthier E**, **Fischer GJ**, **Dou DL**, **Shan WX**, **Keller NP**, **Martin F**, **Rouxel T**, **Lawrence CB**. 2013. Microbe-independent entry of oomycete RxLR effectors and fungal RxLR-like effectors into plant and animal cells is specific and reproducible. Mol Plant-Microbe Interact **26**:611–616.

2. **Fischer GJ**, **Keller NP**. 2016. Production of cross-kingdom oxylipins by pathogenic fungi: An update on their role in development and pathogenicity. J Microbiol **54**:254–264.

3. **Kerr SC**, **Fischer GJ**, **Sinha M**, **McCabe O**, **Palmer JM**, **Choera T**, **Yun Lim F**, **Wimmerova M**, **Carrington SD**, **Yuan S**, **Lowell CA**, **Oscarson S**, **Keller NP**, **Fahy J V**. 2016. FleA expression in *Aspergillus fumigatus* Is recognized by fucosylated structures on mucins and macrophages to prevent lung infection. PLoS Pathog **12**:e1005555.

4. **Fischer GJ**, **Yang J**, **Bacon W**, **Palmer JM**, **Dagenais T**, **Huang X**, **Hammock BD**, **Keller NP**. 2016. Programmed spore germination and allergenic responses in a murine model of asthma are mediated by lipoxygenase activity in *Aspergillus fumigatus*. Environ Microbiol **Resubmitted**.

5. **Bok J**, **Fischer GJ**, **Pisithkul T**, **Amador-Noguez D**, **James SW**, **Keller NP**. 2016. LaeA involvement in DNA replication and cell cycle dynamics of *Aspergillus nidulans*. Genetics **Submitted**.

6. **Fischer GJ**, **Palmer JM, Henke M**, **Lim FY**, **Berthier E, Kelleher NL**, **Oliw EH**, **Keller NP**. 2016. *Aspergillus fumigatus* PpoA-derived 5,8-diHODE induces hyperbranching while disruption influences asexual development and endocrocin production. ***In Prep.***